

# Introduction to **Centrifugal Compressors**

*for Oil and Gas Applications*

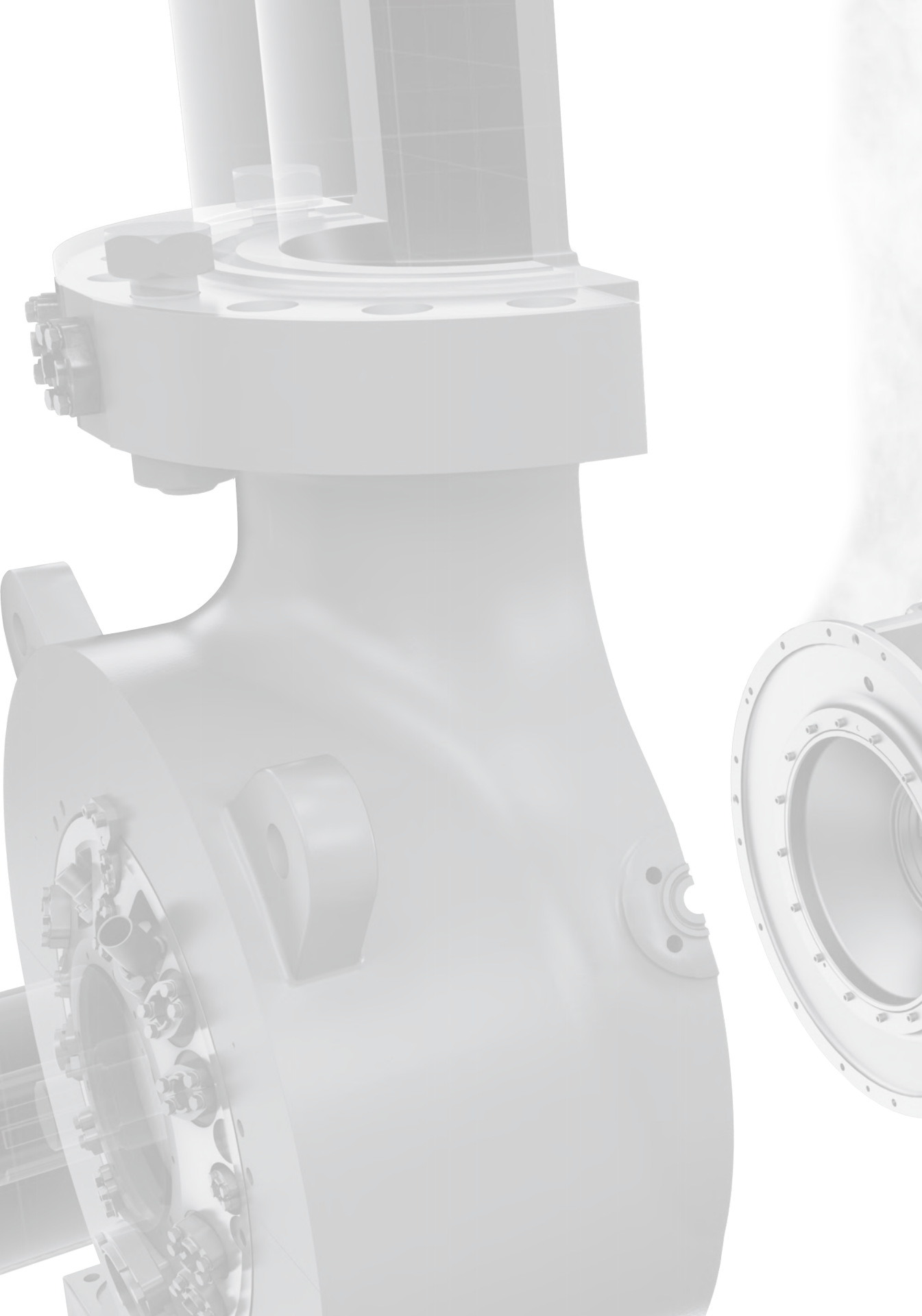
Rainer Kurz

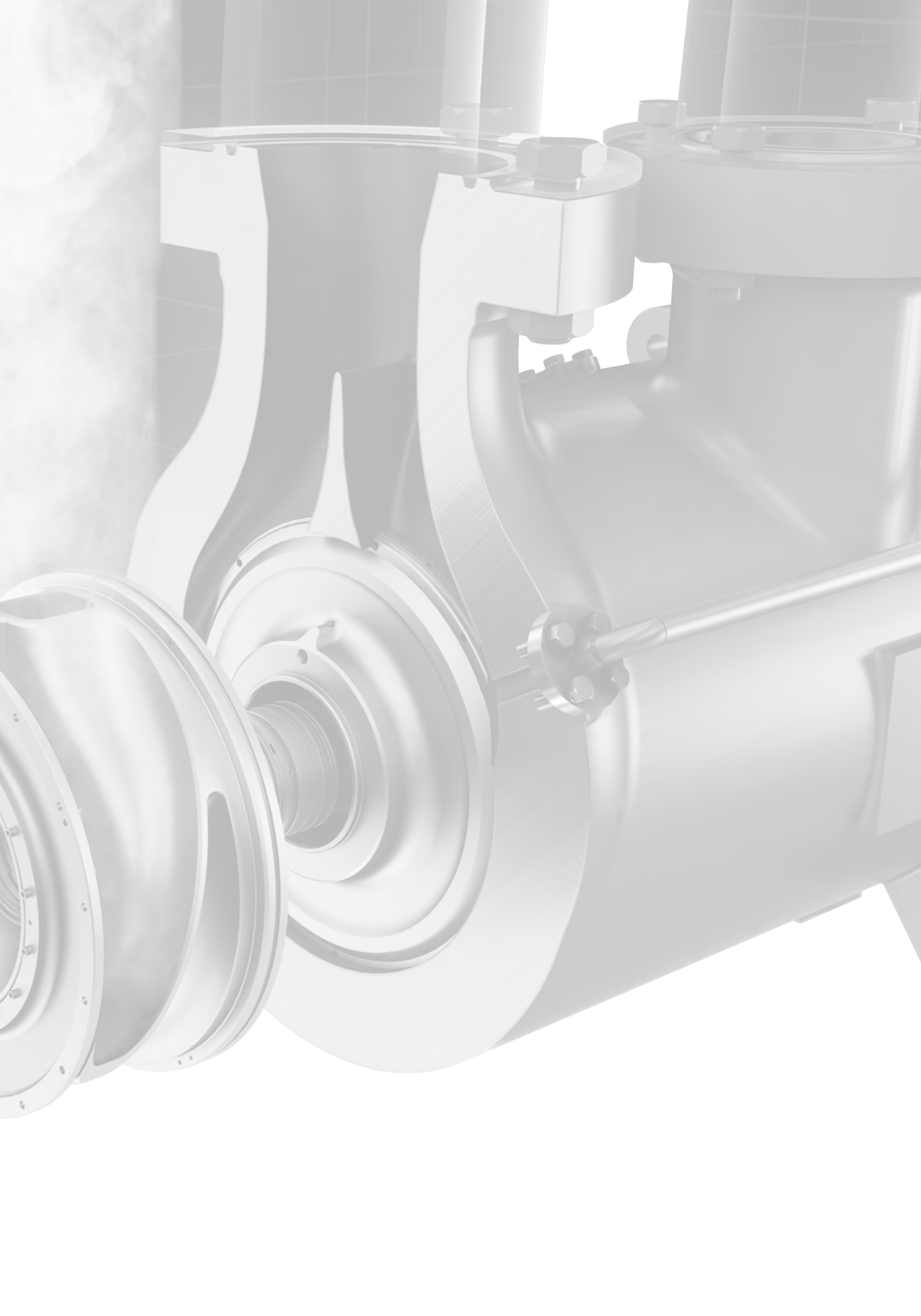
**Solar® Turbines**

*A Caterpillar Company*

Introduction to **Centrifugal Compressors** for Oil and Gas Applications

Rainer Kurz







Introduction to

# Centrifugal Compressors

*for Oil and Gas Applications*

Rainer Kurz

*Introduction to Centrifugal Compressors for Oil & Gas Applications* is published by Solar Turbines Incorporated. Cat® and Caterpillar® are registered trademarks of Caterpillar Inc. Solar, Saturn, Centaur, Taurus, Mars and Titan are trademarks of Solar Turbines Incorporated. All contents of this publication are protected under U.S. and international copyright laws, and may not be reproduced without permission. Featured equipment may include options offered by Solar Turbines and/or modifications not offered by Solar Turbines for specialized customer applications. Because information and specifications are subject to change without notice, check with Solar Turbines Incorporated for the latest equipment information.

Introduction to Centrifugal Compressors for Oil & Gas Applications, 1<sup>st</sup> Edition, 2022

© 2022 Solar Turbines Incorporated - All rights reserved.

Printed in the U.S.A.

ISBN: 979-8-3507-0164-7

# CONTENTS

	Introduction	12
<b>Chapter 1:</b>	<b>Thermodynamics of Gas Compression</b>	<b>18</b>
<b>Chapter 2:</b>	<b>Components of Gas Compressors</b>	<b>30</b>
<b>Chapter 3:</b>	<b>Aerodynamics of Centrifugal Compressors</b>	<b>42</b>
<b>Chapter 4:</b>	<b>Rotordynamics</b>	<b>84</b>
<b>Chapter 5:</b>	<b>Mechanical Design</b>	<b>112</b>
<b>Chapter 6:</b>	<b>Controls of Centrifugal Compressors</b>	<b>132</b>
<b>Chapter 7:</b>	<b>Compressor Drivers</b>	<b>180</b>
<b>Chapter 8:</b>	<b>Centrifugal Compressors in Oil &amp; Gas Applications</b>	<b>190</b>
<b>Chapter 9:</b>	<b>Optimizing Compressor Stations</b>	<b>218</b>
<b>Chapter 10:</b>	<b>Importance of Testing</b>	<b>236</b>
<b>Chapter 11:</b>	<b>Restage: Centrifugal Gas Compressors</b>	<b>266</b>
	References	286

# ABOUT THE AUTHOR

**Rainer Kurz** – Dr. Kurz is the Manager, Gas Compressor Engineering, at Solar Turbines Incorporated in San Diego, California. His organization is responsible for the design, research and development of Solar's Centrifugal Gas Compressors, including aerodynamic, rotordynamic, and mechanical design.

Dr. Kurz attended the University of the Federal Armed Forces in Hamburg, Germany where he received the degree of a Dipl.-Ing. And, in 1991, the degree of a Dr.-Ing. He has authored more than 100 publications in the field of turbomachinery and fluid dynamics, holds two patents, and was named an ASME Fellow in 2003. He is a member and former chair of the ASME Oil and Gas Applications Committee, a member of the Turbomachinery Symposium Advisory Committee, the Gas Machinery Conference Organizing Committee, the GMRC Project Supervisory Committee, and the SDSU Aerospace Engineering Advisory Committee. Many of his publications are recognized as being of archival quality, and he received numerous Best Paper awards, as well as the ASME Industrial Gas Turbine Award in 2013.

# DEDICATION AND ACKNOWLEDGMENTS

This book is dedicated to the more than 8,000 professionals who design, engineer, manufacture, install, test, service, repair, retrofit and finance Solar Turbines products for thousands of satisfied customers in more than 100 countries around the world. A “one-team” mentality assures that everyone is working towards the same goal: making customers more successful. With decades of experience, the Solar Turbines’ global teams are committed to exceeding customer expectations in every operational discipline. Solar Turbines provides best-in-class energy solutions with turbomachinery for power generation and motor-driven compression applications. Technology and innovation focused on the entire ecosystem and customer experience are hallmarks of Solar Digital’s InSight Platform™.

Special thanks go to the people at Solar who supported and encouraged the creation of this book: Gil Amengual, Janet Barnett, Dan Campion, Mike Cave, Tim David, Kevin Davis, Peter Davis, Vinnie Delaney, Hans Drenth, Edrees Faizi, Ed Fowler, Aziz Fozi, Sara Goucher, Min Ji, Klaus Jordan, Roland Kaiser, Matt Lubomirsky, Christina Macatee, Mike McCune, Greg McLorg, Jay Mistry, Richard Mundy, Daniel Sanchez, Mike Shimek, Avneet Singh, Marco Vagani, Balaji Venkataraman, Wade Willden, Roman Zamotorin, Lei Zhu and many others.

I also want to express my special appreciation to the contributors of several chapters: Daniel Sanchez (Chapter 2), Mike Cave and Min Ji (Chapter 3), Balaji Venkataraman and Marco Vagani (Chapter 4), Roman Zamotorin and Matt Lubomirsky (Chapter 9), and Avneet Singh (Chapters 9 and 11).

# PREFACE

Centrifugal gas compressors are vital for the transportation and processing of gas in the oil and gas industry. The compressors operate in harsh environments, providing compression with high availability and reliability. This book was developed directly from a series of Solar Turbines Incorporated internal short courses and reference documents that were presented to audiences with wide-ranging backgrounds. It expands on the applicable thought processes that were introduced in the companion *Introduction to Gas Turbine Theory* book and brings basic concepts into the realm of practical applications.

The book is intended to provide a basic understanding of the thermodynamics, aerodynamics and rotordynamics that specifically apply to compressors used in the oil and gas industry. It is not intended as a text book or a design guideline. The book is, however, intended as a summary and overview, covering the many different subjects and underlying theories pertaining to the subject matter. In the chapters, explanations on the components, the design and the function of centrifugal compressors are followed by more theoretical subjects. Then, practical application issues such as the controls, drivers, testing, optimization and restaging are covered, as well as a description of typical applications for these machines.

Throughout the text, the intent is to make relatively complex concepts understandable. Hopefully you, the reader, will develop an understanding of the many engineering concepts and disciplines that apply to the gas compression and distribution industries.

# NOMENCLATURE

A area

$c, u, w$  velocity

$c_p$  heat capacity

$\rho$  density

D diameter

$\phi$  flow coefficient

F force

$\omega$  frequency

g gravity acceleration

h enthalpy

k isentropic exponent

m mass

$\dot{m}$  mass flow

M momentum

M Mach number

N speed

P power

p pressure

Q volumetric flow

q heat

R gas constant

s entropy

T temperature

v specific volume

$W_t$  work

Z compressibility factor

z elevation coordinate

$\eta$  efficiency



# INTRODUCTION

A large number of technical papers, articles and presentations prepared by their respective authors during the last 25 years served as the basis for developing this book. It is not a classical textbook, nor is it a product brochure. The primary goal is to help readers understand basic concepts on how a centrifugal compressor works, how it is built, how it is controlled, and how it is integrated into the process. All this is discussed with the background of the oil and gas upstream and midstream industry.

The book is intended as a summary and overview of the many different topics and disciplines pertaining to centrifugal gas compressors, and an overview of the concepts and theories involved (*Figure 0-1*). Throughout the text, readers are provided with simplified explanations of complex concepts. By following this text, readers will hopefully develop an appreciation of the many engineering disciplines that are involved in the design, analysis and operation of centrifugal gas compressors as they are used in the oil and gas industry.

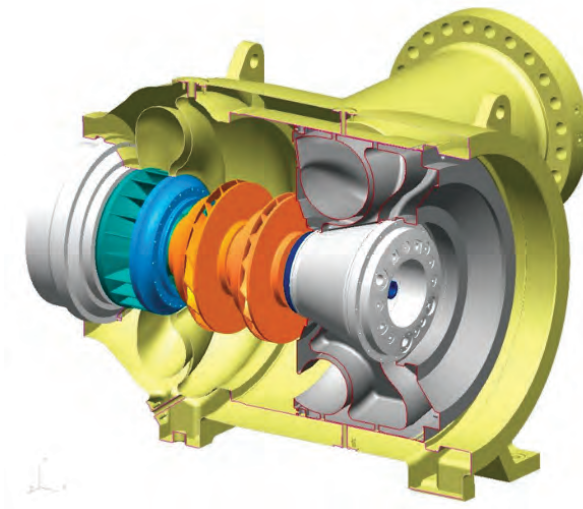


**Figure 0-1.** Centrifugal Gas Compressor

As mentioned earlier, this is not a product brochure. All authors work for Solar Turbines, a major manufacturer of centrifugal gas compressors, but every effort has been made to discuss topics in an objective, technical fashion. Many of the illustrations will show Solar products, for the simple reason that they are the most accessible. The book will also focus on compressors used in oil and gas upstream and midstream applications. While the general concepts of thermodynamics, aerodynamics and rotordynamics apply to any centrifugal compressor, the other chapters are focused on a discussion related to oil and gas applications.

The topics addressed by the book are organized in chapters.

To start, Solar Turbines team members will explain the **thermodynamic principles** of gas compression, introducing the concepts of enthalpy, work, and entropy, as well as methods to describe gas behavior.

In the next chapter, the **major components** of a centrifugal compressor will be introduced. This is an overview of components, following the gas flow through the compressor, and will serve as a reference for the subsequent chapters.

Next, the **aerodynamics** of centrifugal compressors will be covered in great detail, starting with fundamental principles, and developing the concepts that facilitate understanding the operation of a compressor at design and off-design conditions. In addition, an overview of computational methods will be provided.

The chapter on **rotordynamics** attempts to explain the principle ideas used to understand the rotordynamic behavior of compressors. Both lateral and torsional vibrations are addressed.

The previous chapters were used to cover the major theoretical concepts needed to understand centrifugal compressors. With the chapter on **mechanical design**, we look into more detailed issues are discussed. This chapter will pick up topics from an earlier chapter on compressor components, providing more in-depth descriptions. It also will show the implementation of concepts that are relevant to improving the rotordynamic stability of the machine.

The next chapter deals with methods to **control** compressors; in other words how compressors are integrated with the process they are supposed to support. The discussion will cover process control, but will also address methods to protect the compressor from surge.

A discussion of compressor would be incomplete without introducing the different types and characteristics of **drivers** frequently used to provide power for these compressors. The characteristics of the main drivers, gas turbines and electric motors are explained in detail.

The chapter on **Oil and Gas Applications** provides a description of the major applications, and the related process conditions, for which centrifugal compressors are used.

Related to the chapter on applications, the concepts of optimizing the operation of centrifugal compressors and their drivers for a given process will be explained. This chapter draws heavily from the previous three chapters.

A major topic for users and designers of compressors is methods to **test** them, in order to verify the predicted performance of a machine or a train. Concepts developed in earlier chapters, like aerodynamics and thermodynamics, are used to describe test methods, and test evaluation methods, and also discusses concepts like test uncertainties.

While centrifugal compressors are extremely flexible in their capability to adapt to changes in operating conditions, the economics of the application may require **restaging** the machines. The process of restaging is described, and guidelines and examples are provided.

These chapters provide you with an overview of the key topics and theories essential to understanding the design and application of centrifugal compressors in the oil and gas industry. Throughout the text, you'll be provided with simplified explanations of complex concepts.

## THE HISTORY OF GAS COMPRESSORS

The earliest mention of a turbomachine dates back to 150 B.C.E., when Heron of Alexandria described the *Aeolipile* (*Figure 0-2*), using steam, expanded through nozzles, to create power.

Early turbomachines were essentially turbines, that is devices that produced power. In 1705, Denis Papin in France originated the idea of a turbopump, and a turbo blower. Around 1750, Leonard Euler derived the Euler equations that describe the energy transfer in turbomachines, and Bernoulli explained the relationship between kinetic energy and pressure energy in a flow. By the mid 1800's, several turbo pump designs were offered—empirical designs for relatively low head and modest efficiencies. Further improvements were introduced by Osborne Reynolds, and the first turbopumps based on his designs were built in 1887. By the early 1900's, several companies (Mather and Platt, Sulzer Bros., Rateau, Byron Jackson, DeLaval, Allis-Chalmers and Worthington) were building turbopumps.



**Figure 0-2.** *Aeolipile, Heron of Alexandria 150 B.C.E.*

Gas compression in the early days was the domain of positive displacement machines (reciprocating compressors, roots blowers). The credit for the invention of the centrifugal impeller goes to Denis Papin in 1869. Initially, no diffuser was used, but Reynolds patented a vaned diffuser in 1875. Parsons designed and marketed a 3-stage centrifugal compressor as early as 1887. Rateau, around 1900 commercialized turbo compressors for ventilation, especially for mine ventilation. He also realized that his turbo compressors matched the speed of steam turbines quite well, and thus could be directly coupled.

Early centrifugal compressors were superior to axial compressors, as blade aerodynamics were not well understood at the time. Aerodynamic developments for propellers and airfoils during World War 1, that had their roots in research by Otto Lilienthal in Germany and the Wright Brothers in the US, and research work by Prandtl in Germany, leading to a better understanding of boundary layer behavior became beneficial in the development

of turbocompressors. In the 1930s, the development of gas turbines (Whittle in England, v. Ohain in Germany), using centrifugal compressors (*Figure 0-3*), and the use of turbochargers for aircraft engines (the first flight of an airplane using a turbine powered turbocharger, designed by S. Moss, occurred in 1919) intensified the research in centrifugal compressors.

The treatment of the rotordynamics of high-speed shafts goes back to a publication by Rankine in 1869, who examined the behavior of a frictionless uniform shaft. Initially it was assumed that operation above the first critical speed would not be possible, but in 1892, Gustaf de Laval and Charles Parsons proved the possibility for operation above the first critical speed. Not until 1919, H.H. Jeffcott laid a comprehensive groundwork for the treatment of high-speed rotors. In the 1920s, several manufacturers offered turbomachinery running at speeds above the first critical speed. In 1924, B.L. Newkirk described the critical influence of bearing behavior on rotordynamics.

In the 1950s and 1960s centrifugal compressors became popular in the oil and gas industry, for example, as pipeline boost compressors. These compressors were usually driven by industrial gas turbines. In the late 1950s, Solar developed a 1000 hp two-shaft gas turbine (the Saturn) for marine applications (*Figure 0-4*). There was also interest in using this gas turbine for pipeline applications, but a compressor to match the power and the power turbine speed of this gas turbine was not available. Therefore, Solar engineers used their expertise with the design of gas turbines, including the design of centrifugal air compressors for gas turbines, to design a centrifugal compressor for these applications. Many design features, for example the modular rotor design, have their origins in the design of gas turbines, but later became very beneficial in applications for the oil and gas upstream and midstream industry.

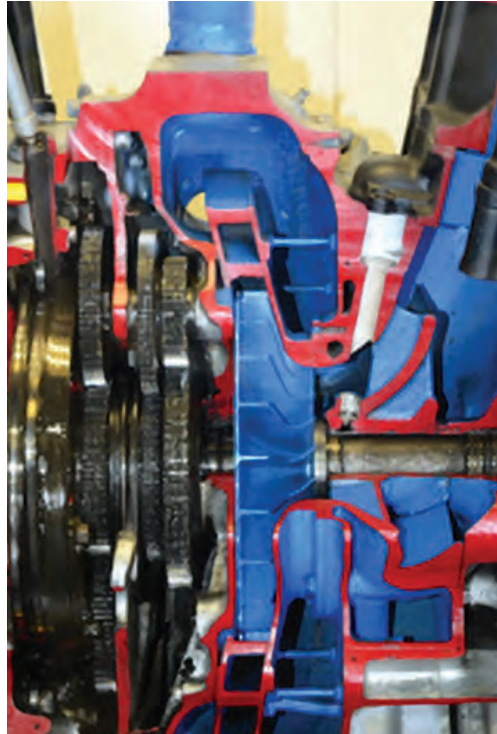


**Figure 0-3.** Centrifugal compressor as supercharger for an aircraft engine, late 1930s.

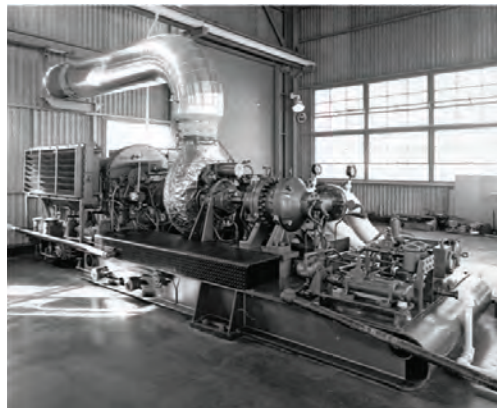


**Figure 0-4.** Solar Saturn gas turbine driving a C16 compressor (ca. 1961).

Over time, Solar Turbines expanded its portfolio of 2-shaft gas turbines to gas turbines with over 30,000 hp output, gas compressors to match the power and speed of these gas turbines were developed parallel to the new gas turbine models (Figure 0-5). Based on customer demands, Solar Turbines also developed the capability to drive these compressors with electric motors (Figure 0-6).



**Figure 0-5.** Titan 130 2-shaft gas turbine driving a Solar compressor.

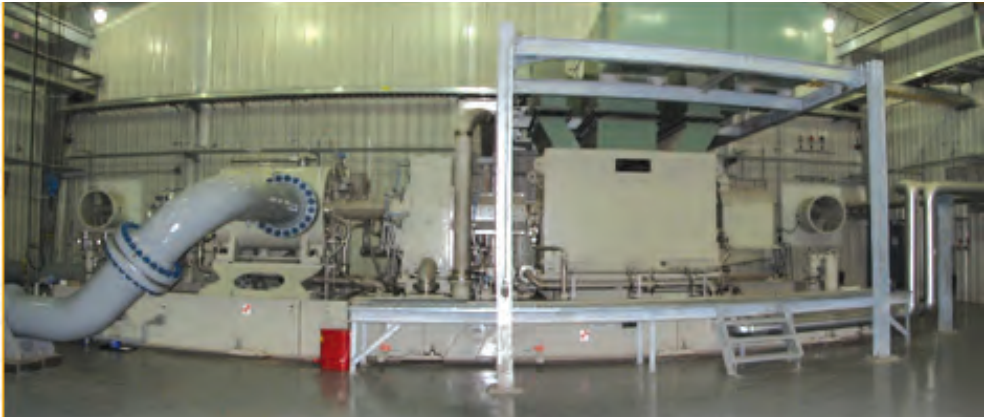


**Figure 0-6.** Solar compressor driven by a variable speed electric motor.





## CHAPTER 1

# THERMODYNAMICS OF GAS COMPRESSION

Understanding the working principles of centrifugal gas compressors can be enhanced by applying some basic laws of physics. Using the first and second laws of thermodynamics together with basic laws of fluid dynamics, such as Bernoulli's law and Euler's law, the fundamental working principles of gas compression are readily apparent. By extension, the operational behavior of centrifugal gas compressors can also be explained. The thermodynamics of gas compression will be discussed in this chapter, followed by a discussion of fluid dynamics in the next chapter.

This general description of gas-compression thermodynamics applies to any type of compressor, independent of its detailed working principles. Compression fundamentally involves the use of mechanical energy, to increase the energy of a gas that has flowed through a compressor. The increased energy of the compressed gas is accompanied by increased temperature, and if the compression process is done properly, increased pressure and density as well.

### GAS BEHAVIOR AND EQUATIONS OF STATE

Gases have properties that can be observed, such as pressure and temperature, plus the mass and volume that contain the gas. Key features of a gas are that pressure, temperature and density (the mass of gas contained in a given volume) are related (Boyle's law): An increase in pressure (at constant temperature) leads to an increase in density, while an increase in temperature (at constant pressure) leads to a reduction in density. For any consideration of temperature changes, the possibility of heat loss across the system boundaries must also be discussed. Most compressors are considered adiabatic, which means that no heat is lost through the cylinder walls.

As used in reciprocating compressors, the simplest compression process utilizes positive-displacement, typical of a basic bicycle air pump. The idea is to trap an amount of gas in a cylinder with a piston able to move inside the cylinder (*Figure 1-1*). By pushing a piston into the gas, effort or work is required. Because the mass of gas is trapped inside the pump's walls, the mass of gas remains constant, while the volume is reduced. Therefore, the density of the gas (mass divided by volume) is increased.

To describe the compression process, the first and second laws of thermodynamics apply. The first law says that when transferring one form of energy into another form of energy, no energy is lost. The second law says that most of these energy transfers are not reversible. For example, converting a motor's electrical energy creates mechanical energy, which can then be used to convert it back to electricity in a generator.

However, the electricity generated in this manner is less than the electricity originally fed into the motor. Because of these losses, heat is created. This is also referred to as an increase in entropy. The concept of enthalpy, which describes the total heat content of a gas, must also be considered.

Consider a flow process, with a flow entering the system at point 1, leaving at point 2 (Figure 1-1). Mechanical energy, work (W) is also fed into the system, and the system exchanges heat (q) with the environment.

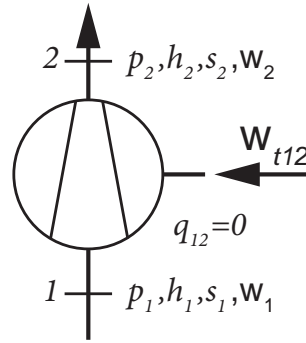


**Figure 1-1. Compression process**

Then, the first law of thermodynamics, defining the conservation of Energy, can be written for a steady-state, flow process:

$$\left( h_2 + \frac{w_2^2}{2} + gz_2 \right) - \left( h_1 + \frac{w_1^2}{2} + gz_1 \right) = q_{12} + W_{t,12}$$

with  $q=0$  for adiabatic processes, and  $gz=0$  because changes in elevation are not significant for gas compressors. Enthalpy and velocity can be combined into a total enthalpy by:

$$h_t = h + \frac{w^2}{2}$$

$W_{t,12}$  is the amount of work<sup>1</sup> that must be applied to affect the change in enthalpy of the gas. The work  $W_{t,12}$  is related to the required power, (P), by multiplying it with the mass flow.

$$P = \dot{m}W_{t,12}$$

The power and enthalpy difference is thus related by:

$$P = \dot{m}(h_{t,2} - h_{t,1})$$

If a relationship that combines enthalpy with the pressure and temperature of a gas can be found, the necessary tools to describe the gas compression process have been identified.

The quality of a compressor’s performance can be assessed by comparing the actual head (which directly relates to the amount of power required to achieve compression) with the

<sup>1</sup>Physically, there is no difference between work, head, and enthalpy. In systems with consistent units (such as the SI system), work, head and enthalpy difference utilize the same unit (e.g. kJ/kg in SI units). Only in inconsistent systems (such as US customary units), you need to consider that the enthalpy difference (e.g. in BTU/lbm) is related to head and work (e.g. in ft lbf/lbm) by the mechanical equivalent of heat (e.g. in ft lbf/BTU).

head that the ideal, isentropic compression would require. This defines the isentropic efficiency:

$$\eta_s = \frac{\Delta h_s}{\Delta h}$$

(Figure 1-2) For a compressor receiving gas at a certain suction pressure and temperature, and delivering the gas at a certain output pressure, the isentropic head represents the energy input required by a reversible, adiabatic (thus isentropic) compression. The actual compressor will require a higher amount of energy input than needed for the ideal (isentropic) compression.

### IDEAL GAS

At this point, some additional explanation is required to discuss this behavior of gases, because it's fundamental to the understanding of gas compression. A simple way to understand the behavior of gas is to consider an ideal gas. Any gas can be considered ideal at low pressure and elevated temperature.

Unfortunately, the pressures and temperatures relevant to the focus of this book require consideration of real gas behavior. However, to understand some general relationships, the ideal gas behavior will be discussed. In a second step, how real gas deviates from ideal gas behavior will be described.

Understanding gas compression requires an understanding of the relationships between pressure, temperature and density of a gas. An ideal gas exhibits the following behavior:

$$\frac{p}{\rho} = RT$$

where R is the gas constant, and as such is constant as long as the gas composition is not changed. Any gas at very low pressures ( $p \rightarrow 0$ ) can be described by this equation.

Enthalpy is not a property that can be measured directly. It is a value that can be calculated once the temperature and pressure of a given gas composition are known. This is important. The enthalpy of any gas (ideal or real) is completely defined by the pressure and temperature of the gas. Enthalpies are defined as differences.

For a perfect gas, with constant heat capacity, the relationship between enthalpy and temperatures is:

$$\Delta h = c_p(T_2 - T_1)$$

The heat capacity,  $c_p$ , in this equation is the amount of heat energy needed to raise the temperature by one degree, while the pressure of the gas is kept constant. A second heat capacity,  $c_v$ , is defined by the amount of heat needed to increase the gas temperature

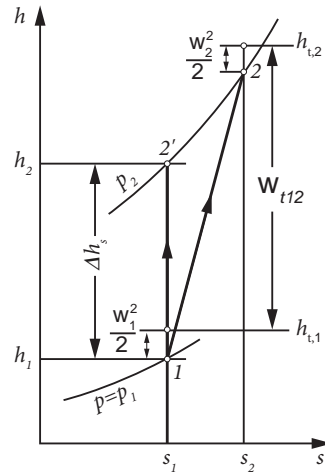


**Figure 1-2. Enthalpy and Entropy for the compression process**

by one degree, while the volume of the gas is kept constant. For the gas compression requirements,  $c_p$  is a function of only the temperature for an ideal gas:

$$\Delta h = c_p(T) \cdot \Delta T = \int_{T_1}^{T_2} c_p dT$$

This relationship is valid for any type of compression involving an ideal gas. Now, consider a specific type of compression such as the isentropic compression in an adiabatic system.

Before doing that, consider the concept of entropy: The second law of thermodynamics says:

$$\dot{m}(s_2 - s_1) = \int_1^2 \frac{dq}{T} + s_{irr}$$

A change in entropy is either due to irreversible losses, or because heat crosses the system boundaries at a certain temperature (the first temperature in the equation above). For adiabatic flows, where no heat,  $q$  enters or leaves, the change in entropy simply describes the losses generated in the compression process. These losses come from the friction of gas with solid surfaces and the mixing of gas having different energy levels.

An adiabatic, reversible compression process ( $dq=0$ ,  $s_{irr}=0$ ) therefore does not change the entropy of the system. It is isentropic. This is an ideal process. This isentropic compression process assumes that no entropy is generated during the compression process. Because the system is adiabatic (that is, no heat can enter or leave the system except with the flowing gas), the only change in entropy can come from losses, which are irreversible.

For an isentropic compression, the discharge temperature for this process,  $T_{2s}$ , is determined by the pressure ratio (with  $k = c_p/c_v$ ). The ratio of specific heats is strictly only a constant for a perfect gas. For an ideal gas, a suitable average value is usually selected.

$$T_{2s} = T_1 \left( \frac{p_2}{p_1} \right)^{\frac{k-1}{k}} + T_1$$

So for an isentropic compression of a perfect gas, the isentropic head, temperature and pressures can be related by:

$$\Delta h_s = c_p T_1 \left[ \left( \frac{p_2}{p_1} \right)^{\frac{k-1}{k}} - 1 \right]$$

This means, in particular, that the isentropic head is fully defined by typical process requirements. If the gas, the inlet temperature and pressure are known, as well as the desired discharge pressure, the isentropic head or isentropic work can be defined.

Once the compressor is built and installed on the test stand (and the gas composition is known), the suction and discharge pressures and temperatures can be measured. Then, the actual amount of work,  $\Delta h$ , (the actual head) that this compressor has absorbed can be

calculated from the suction and discharge temperature. If the mass flow of gas had been measured, the power consumption is derived directly from:

$$P = \dot{m} \Delta h$$

To determine the quality of the aerodynamic performance of the compressor, efficiency can be defined by comparing the work,  $\Delta h$ , the compressor requires with the work a perfect compressor that does not create any losses,  $\Delta h_s$ , would require:

$$\eta_s = \frac{\Delta h_s}{\Delta h}$$

## REAL GAS

The Mollier diagram for Methane at low pressures and temperatures (Figure 1-3) demonstrates that the gas behaves as an ideal gas. Note the change in enthalpy is only a function of temperature.

For the elevated pressures found in natural gas compression, this equation becomes inaccurate, and an additional variable, the compressibility factor  $Z$ , has to be added:

$$\frac{p}{\rho} = ZRT$$

Unfortunately, the compressibility factor  $Z$  itself is a function of pressure, temperature and gas composition.

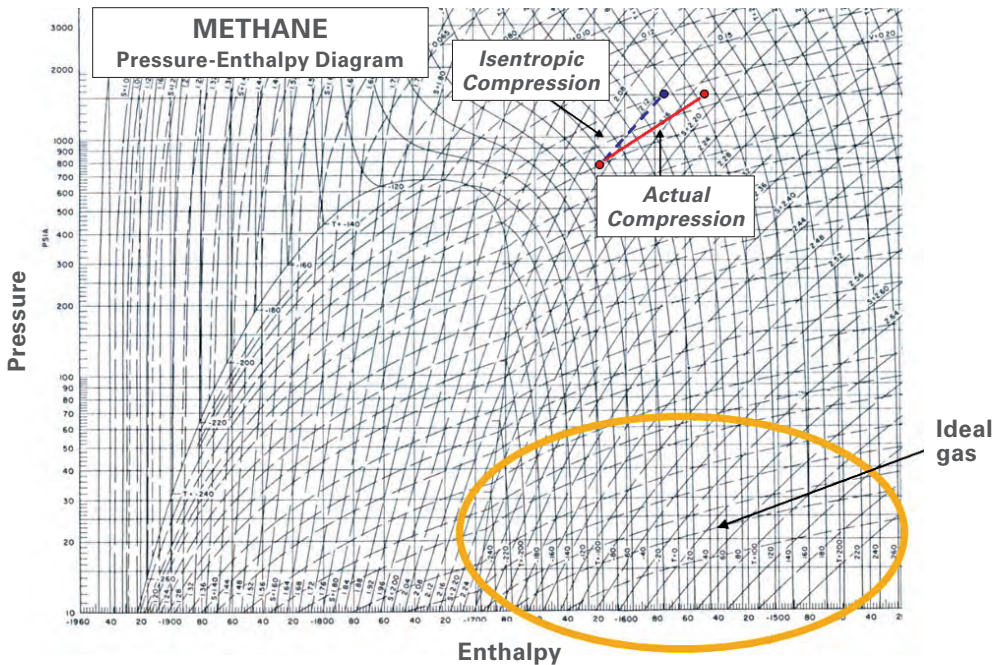


**Figure 1-3.** Mollier Diagram for a gas (Methane): enthalpy versus pressure is shown, with lines of constant temperature, density, and entropy.

To calculate enthalpy in a real gas, additional terms for the deviation between real gas behavior and ideal gas behavior are evident. (Poling et al, 2001):

$$\Delta h = (h^0 - h(p_1))_{T_1} + \int_{T_1}^{T_2} c_p dT - (h^0 - h(p_2))_{T_2}$$

The terms  $(h^0 - h(p_1))_{T_1}$  and  $(h^0 - h(p_2))_{T_2}$  are called departure functions, because they describe the deviation of the real gas behavior from the ideal gas behavior. They relate the enthalpy at some pressure and temperature to a reference state at low pressure, but at the same temperature. The departure functions can be calculated solely from an equation of state, while the term  $\int c_p dT$  is evaluated in the ideal gas state. (Figure 1-4) shows the path of a calculation using an equation of state.

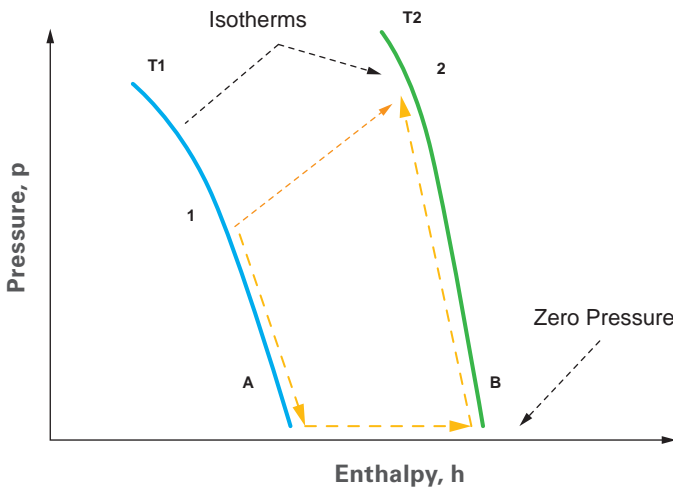


**Figure 1-4.** Calculation path for equations of state.

While a Mollier diagram is perfectly suited for pure gases, working with gas mixtures is much more common in typical applications. For gas mixtures, so called Equations of State (EoS) are used. Equations of state are semi-empirical relationships that enable calculation of the compressibility factor, as well as the departure functions, for a given set of pressures and temperatures, or pressures and entropies. Equations of state also consider how the components of gas mixtures influence each other, thereby providing mixing rules for that purpose.

For gas compression applications, the most frequently used equations of state are Redlich-Kwong, Soave-Redlich-Kwong, Benedict-Webb-Rubin, Benedict-Webb-Rubin-Starling and Lee-Kessler-Ploecker (Poling et al, 2001). More recently, AGA 8 and GERG are frequently considered.

In general, all of these equations provide accurate results for typical applications in pipelines, i.e. for gases with a high methane content, and at pressures less than approximately 3500 psia. Kumar et al. (1999) and Beinecke et al. (1983) have compared these equations of state regarding their accuracy for compression applications. It should

be noted that the Redlich Kwong equation of state is the most effective equation from a computational point of view (because the solution is found directly rather than through an iteration).

Beinecke and Luedtke (1983) have conducted thorough evaluations on the accuracy of the Lee-Kesler-Ploecker (LKP) method, the Benedict-Webb-Rubin-Starling (BWRS) method and the Soave-Redlich-Kwong (SRK) method. All of the EOS mentioned can predict the properties of hydrocarbon mixtures quite accurately over a wide range of pressures. Still, deviations of 0.5 to 2.5% and greater in the values for gas density are common.

Even more important than the compressibility factor is the calculation of the enthalpy and entropy using the EOS. Because derivatives of the EOS have to be used to perform these calculations (Poling et al, 2001), the deviations can be even larger than those for the compressibility factor.

EOS may differ from program to program because different mixing rules are sometimes used, different interaction parameters between the gases are assumed, and/or a different treatment of the ideal gas portion in the EOS is used. Poling et al (2001) provide an overview of the theory behind equation-of-state procedures.

For real gases (where  $k$ , and  $c_p$  in the equations above become functions of temperature and pressure), the enthalpy of a gas  $h(p,T)$  is thus calculated in a more complicated way, using equations of state (Poling et al., 2001). For a gas of known composition, these calculations represent relationships that enable determination of enthalpy, if any two of its variables—pressure, temperature, and entropy—are known.

The actual head for the compression can then be calculated by:

$$\Delta h = h(p_2, T_2) - h(p_1, T_1)$$

and the isentropic head by:

$$\begin{aligned} \Delta h &= h(p_2, s_1) - h(p_1, T_1) \\ s_1 &= s(p_1, T_1) \end{aligned}$$

The equation for the actual head implicitly includes the entropy rise(s), because:

$$\Delta h = h(p_2, T_2) - h(p_1, T_1) = h(p_2, s_1 + \Delta s) - h(p_1, s_1)$$

(Figure 1-3) shows the compression process in a Mollier diagram. Because the above enthalpy definition is on a per-mass-flow basis, the absorbed gas power  $P_g$  (that is, the power that the compressor transferred into the gas), can be calculated as:

$$P_g = \dot{m} \cdot \Delta h$$

The mechanical power ( $P$ ) necessary to drive the compressor is the gas absorbed power increased by all mechanical losses (friction in the seals and bearings), expressed by a mechanical efficiency  $\eta_m$  (typically on the order of 1 or 2% of the total absorbed power):

$$P = \frac{1}{\eta_m} \dot{m} \cdot \Delta h = \frac{\dot{m} \cdot \Delta h_s}{\eta_m \eta_s}$$

Energy conservation is also encountered on a different level in turbomachines. As discussed in a subsequent section, its aerodynamic function relies on the capability to trade two forms of energy: kinetic energy (velocity energy) and potential energy (pressure energy).

If cooling is applied during the compression process, for example, with intercoolers between two compressors in series), then the increase in entropy is smaller than for an uncooled process. Therefore, the power requirement is reduced (*Figure 1-4*).

Bringing gas from a certain suction pressure to a higher discharge pressure by means of mechanical work is the task of compression. The actual compression process is often compared to one of two ideal processes:

The compression process is isentropic, if the process is frictionless and no heat is added to or removed from the gas during compression. With these assumptions, the entropy of the gas does not change during the compression process, and it is reversible. Because no heat transfer occurs across the system boundaries, the process is often referred to as reversible adiabatic.

Like the isentropic cycle, the polytropic compression process is reversible, but is not adiabatic. It can be described as an infinite number of isentropic steps, each interrupted by isobaric heat transfer, such that the efficiency in each step is the same. The heat addition enables the process to yield the same discharge temperature as the real process.

While the compressor's path from inlet to outlet in the isentropic process is defined by following a constant entropy, the isentropic path is defined by infinitesimal steps of constant polytropic efficiency ( $\eta_p$ ). This means that the actual compression process consists of an infinite number of steps (for practical purposes, a large number, such as 20 is sufficient). Each step consists of an isentropic compression step, followed by an isobaric heat addition:

$$\Delta h = \frac{1}{\eta_p} \int_{p_1}^{p_2} v dp = \frac{\Delta h_p}{\eta_p}$$

and:

$$\Delta h_p = \int_{p_1}^{p_2} v dp$$

The polytropic efficiency ( $\eta_p$ ) is defined as:

$$\eta_p = \frac{\Delta h_p}{\Delta h}$$

Using the polytropic process (Beinecke and Luedtke, 1983) for comparison reasons works fundamentally the same way as using the isentropic process for comparison reasons. The difference lies in the fact that the polytropic process uses the same discharge temperature as the actual process, while the isentropic process has a different (lower) discharge temperature than the actual process for the same compression task. In particular, both the

isentropic and the polytropic processes are reversible and adiabatic. In order to fully define the isentropic compression process for a given gas, suction pressure, suction temperature and discharge pressure must be known. To define the polytropic process, either the polytropic compression efficiency or the discharge temperature must also be known.

For designers of compressors, the polytropic efficiency has an important advantage. If a compressor has five stages and each stage has the same isentropic efficiency ( $\eta_s$ ), then the overall compressor efficiency will be lower than ( $\eta_s$ ). If, for the same example, it's assumed that each stage has the same polytropic efficiency ( $\eta_p$ ), then the polytropic efficiency of the entire machine is also ( $\eta_p$ ).

Either process can be used for the definition of the operating point and the efficiency of the compressor. It should be noted that the absorbed compressor power is not impacted by this choice, because it solely depends on the actual head. Since the site test will be performed at conditions very similar to the design point in many instances, the isentropic definition has an inherent advantage. The isentropic head (and thus the operating point) are fully defined by the process conditions (gas, suction and discharge pressure and suction temperature). Additionally, the polytropic head depends on the compressor efficiency which—in itself—is the subject of the test.

The actual polytropic process compared to an isentropic process has the advantage because the efficiency for an aerodynamically similar point is less dependent on the actual pressure ratio. However, a disadvantage for the polytropic process is the head for a given set of operating conditions depends on the efficiency of the compressor, while the isentropic head does not.

## DEWPOINT

When a gas is cooled at constant pressure (assuming the pressure is below the critical pressure), liquids will eventually form (*Figure 1-3*). The pressure and temperature at which the first liquids form defines the dewpoint. At pressures above the critical pressure, there is no phase change. In general, gas compressors are designed to compress gas. Installing a separator upstream of the compressor to remove liquids in the gas is common.

## DEFINITIONS

### 1. Pressure

**Absolute Pressure** is the pressure measured relative to an absolute vacuum. It equals the algebraic sum of barometric pressure and gage pressure.

**Static Pressure** is the pressure in the gas measured in such a manner that no effect is produced by the velocity of the gas stream. It is the pressure that would be shown by a measuring instrument moving at the same velocity as the moving stream and is the pressure used as a property in defining the thermodynamic state of the fluid. Pressure tabs in a pipeline measure static pressure.

**Stagnation (Total) Pressure** is the pressure which would be measured at the stagnation point when a moving gas stream is brought to rest and its kinetic energy is converted to an enthalpy rise by an isentropic compression from the flow condition to the stagnation condition. It is the pressure usually measured by an impact tube. In a stationary body of gas, the static and stagnation pressures are numerically equal.

**Velocity Pressure (Dynamic Pressure)** is the stagnation pressure minus the static pressure in a gas stream. It is the pressure generally measured by the differential pressure reading of a Pitot tube.

## 2. Temperature

**Absolute Temperature** is the temperature above absolute zero. It is equal to the degrees Fahrenheit plus 459.69 and is stated as degrees Rankine. In SI units, it is equal to the degrees Celsius plus 273.15, and is stated as Kelvin.

**Static Temperature** is the temperature that would be shown by a measuring instrument moving at the same velocity as the fluid stream. It is the temperature used as a property in defining the thermodynamic state of the gas.

**Stagnation (Total) Temperature** is that temperature which would be measured at the stagnation point if a gas stream were brought to rest and its kinetic energy converted to an enthalpy rise by an isentropic compression process from the flow condition to the stagnation condition.

## 3. Flow

**Capacity (Actual Flow)** of a compressor is the volume rate of flow of gas compressed and delivered referred to conditions of pressure, temperature and gas composition prevailing at the compressor inlet.

**Standard or Normal Flow** is the rate of flow under certain 'standard' conditions, for example 60°F and 30" Hg (US Standard) or 0°C and 101.325 kPa (SI Normal).





## CHAPTER 2

# COMPONENTS OF GAS COMPRESSORS

*Daniel Sanchez, Rainer Kurz*

The thermodynamic considerations in the previous chapter treat the compressor as a black box. These considerations apply to any type of compression device. In this chapter, the essential components of a centrifugal compressor (*Figures 2-1a-b*) that accomplish the task of compressing a gas are discussed.

The gas enters the compressor at the suction flange, and is then directed axially into the impeller with the help of inlet guide vanes. After each impeller, the flow enters a diffuser, followed by a crossover bend. The subsequent turn vane conditions the flow to enter the next impeller approximately in an axial direction. After the last diffuser, the gas is gathered using a volute and leaves the compressor at the discharge flange, now at a higher pressure.

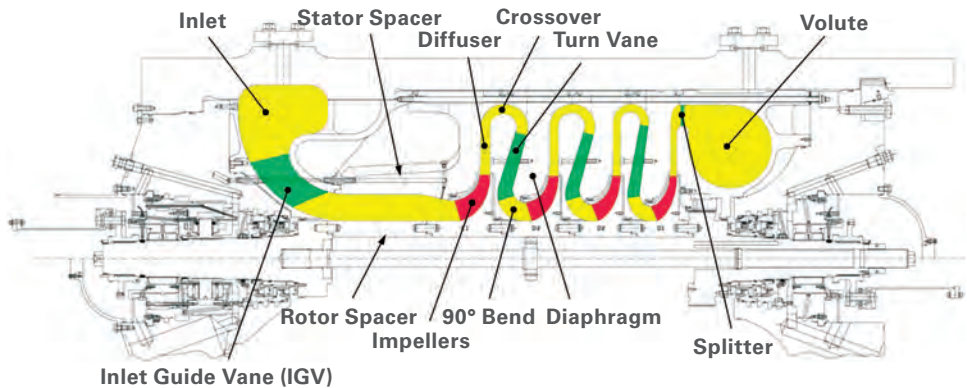


**Figure 2-1a.** Compressor cross section showing the aerodynamic components.

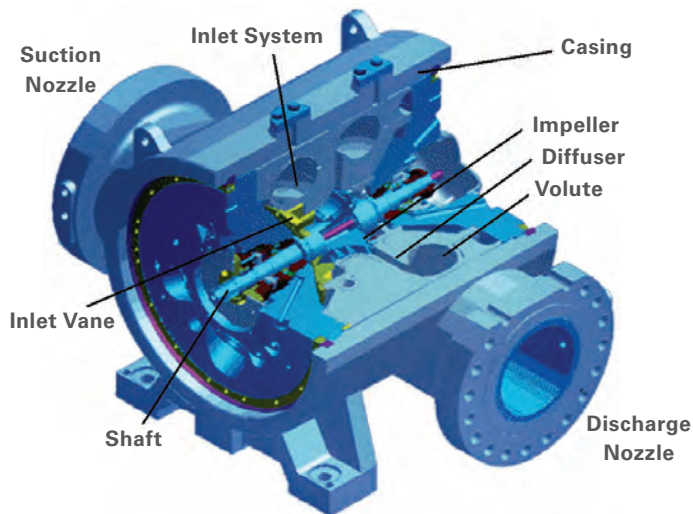


**Figure 2-1b.** Compressor components cutaway view.

The only rotating parts of the compressor are the shaft with the impellers, the balance piston, the thrust bearing collar, and the rotating portion of the dry gas seal.

Compressors are typically composed of a module (bundle), casing, end caps, and bearing and seal assemblies. The bundle is composed of the rotor, stators, inlet housing and discharge volute. The bundle holds all the essential aerodynamic components needed to perform the required functions. The casing is a pressure vessel containing a vertically or horizontally split barrel whose main purpose is to contain the bundle. Suction and discharge endcaps contain the bearings and seal assemblies along with service ports for oil and gas. *Figure 2-1a* shows a typical centrifugal compressor cross section. *Figures 2-1b and 2-2* show the major compressor components.

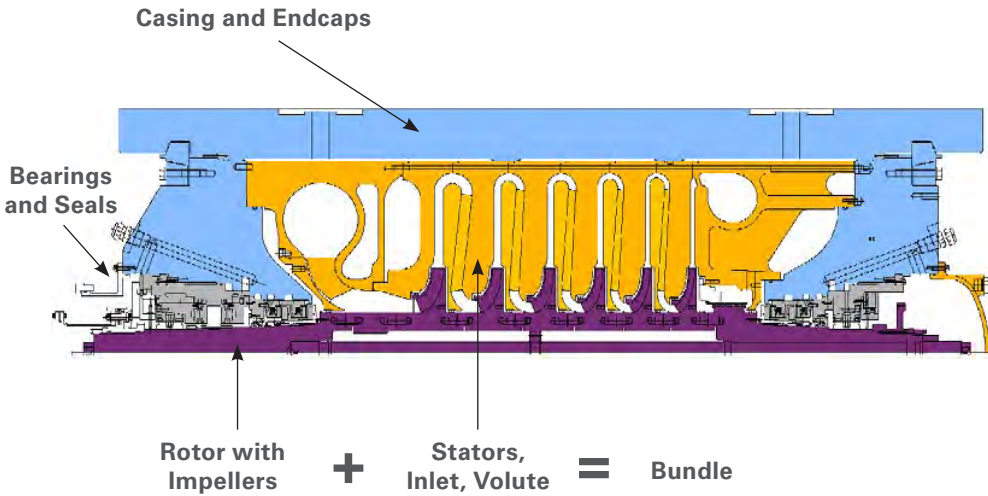


**Figure 2-2.** Major compressor components.

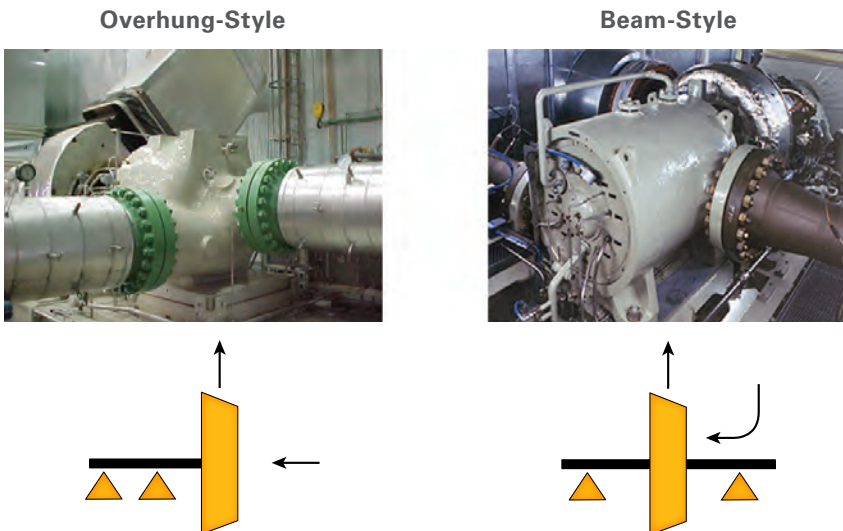


**Figure 2-3.** Overhung- and Beam-Style designs.

Depending on the arrangement of the journal bearings, you can easily identify beam-style compressors and overhung-style compressors. (*Figure 2-3*) In a beam-style compressor, all impellers sit between the bearings, while in an overhung design, the impeller sits outside the bearing span. Designs with overhung impellers are typically limited to a single impeller (2 impellers, if each impeller is positioned on either end of the shaft), but allow the gas to flow axially into the compressor.

## COMPRESSOR CASING

The casing is the pressure-containing part of the compressor, and must withstand the pressure differential between the ambient pressure and the process gas pressure, without deflection.

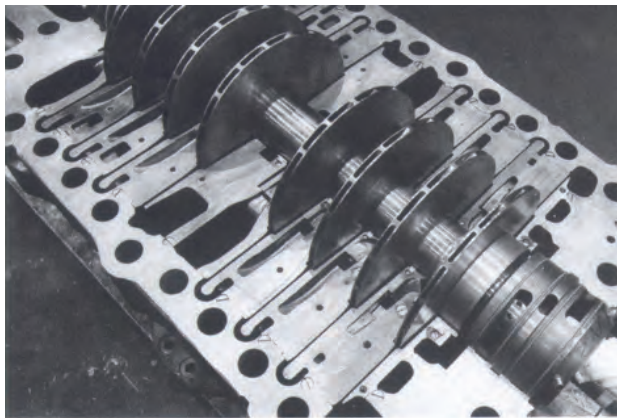


**Figure 2-4a.** *Horizontally split casing*

While lower pressure applications may allow a horizontally split casing (*Figure 2-4b*), high-pressure applications always require a barrel type design (sometimes also called vertically split). A barrel-type design consists of the center body, which together with two endcaps, forms the pressure-containing barrel. The bundle can also be vertically or horizontally split (*Figure 2-4a*).



**Barrel Type Casing -**  
Horizontally or vertically split bundle

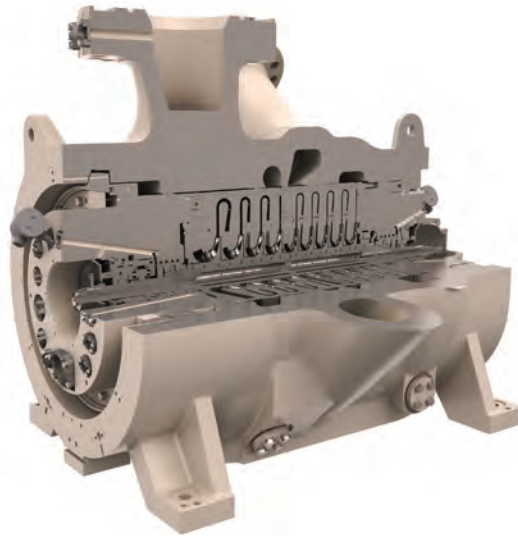


**Figure 2-4b.** Barrel-type casing.

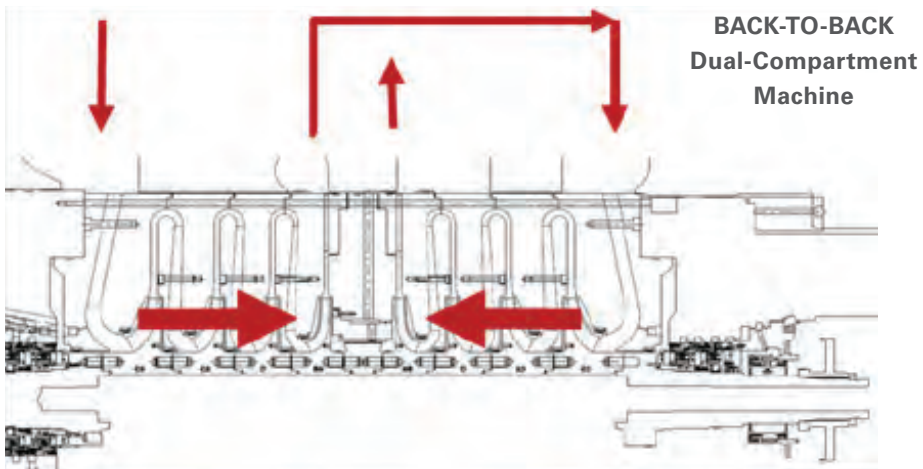
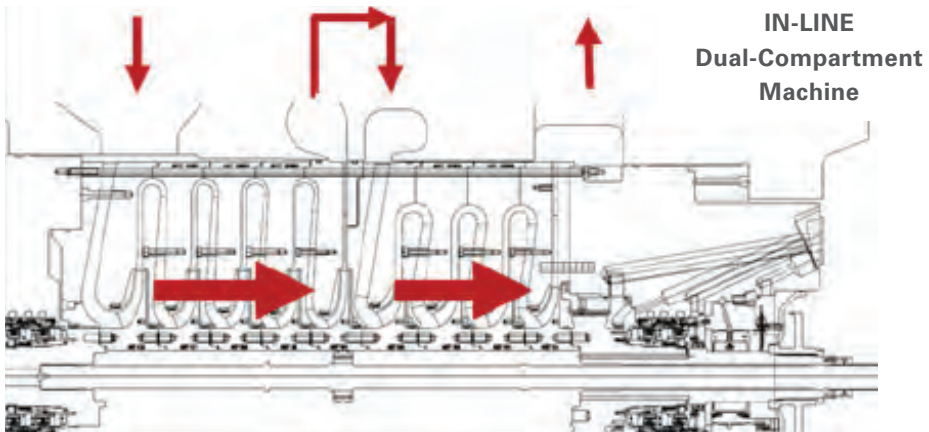


**Figure 2-5.** Centrifugal compressors with two compartments.

A specific type of compressor is a compressor with two compartments in the same casing (*Figure 2-6*). The compressor shown in *Figure 2-5* has four nozzles. The gas enters the first section via the first nozzle, and leaves this section via the second nozzle. Now, the gas can be cooled by an external heat exchanger. The cooled gas is fed back into the second section via the third nozzle, and leaves this section and the compressor through the fourth nozzle. This configuration leads to lower power consumption and allows higher pressure ratios. This will be discussed in greater detail in the rotodynamic section.



**Figure 2-6.** *Compartment compressor with four nozzles on the test stand, showing the compressor casing with the flanges for process piping (top), and the end cap (facing) with service connections.*

## FLOW PATH

A centrifugal compressor is essentially a series of one or more impellers rotating on a shaft within a pressure vessel. The gas enters at the compressor inlet flange and flows through the suction piping to the inlet system. Since the gas enters the compressor from the side or the top, the inlet system guides the gas (often with the help of guide vanes) to the inlet of the first stage impeller. The flow at this point is more or less in an axial direction, but it may have a swirl component. After each impeller, stationary parts such as guide-return vanes and vane/vaneless diffusers are positioned. The combination of one rotating section and a stationary section is considered a “stage” of the compressor (*Figure 2-7*). Between the inlet flange and outlet flange, a series of stages can be installed. *Figure 2-1a* shows a typical compressor with labeled parts.

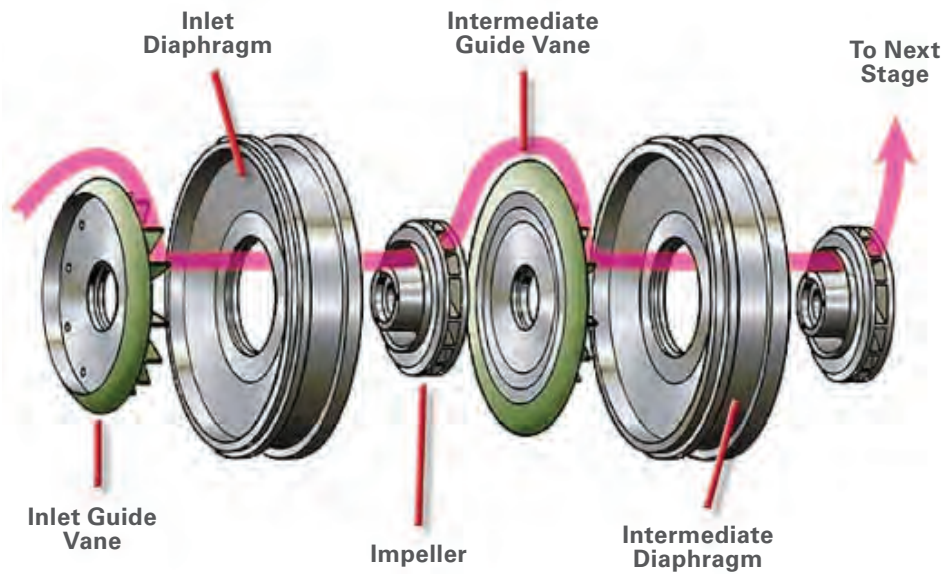


**Figure 2-7.** Flow path.

To compress gas, the centrifugal compressor adds energy to the gas by rotating the shaft and thus rotating the impellers. The rotating impellers increase the velocity and static pressure of the gas. Once the gas passes to the diffuser, the flow is slowed down, transforming most of the kinetic energy of the impeller into an increased static pressure. After the last stage, the flow is directed out of the discharge flange through a volute (Figure 2-8).

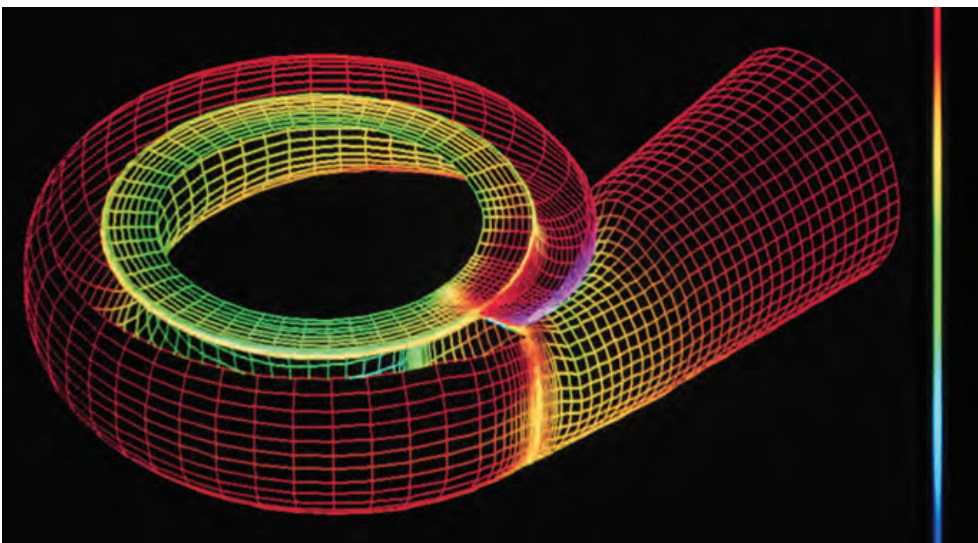


**Figure 2-8.** Discharge volute.

An impeller consists of a number of rotating vanes, enclosed on the back of a disk (back face), that impart mechanical energy to the gas (Figure 2-9). As discussed in greater detail later, the gas leaves the impeller with increased velocity and increased static pressure. For oil and gas applications, mostly shrouded impellers (front-face cover) are used. Open-faced impellers are not common. The impeller hub is the surface of the disk (back face) touched by the fluid. The entry into the impeller is called 'impeller eye' (Figure 2-9).

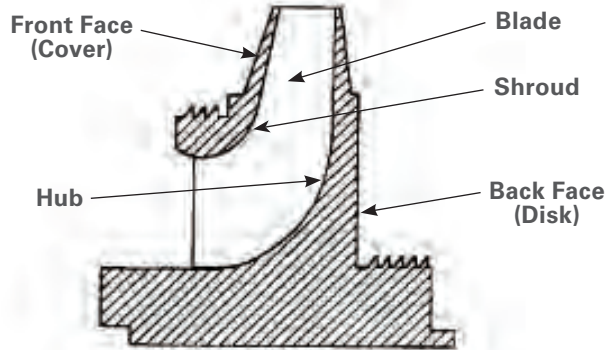


**Figure 2-9.** Impeller cross section.

Impellers are typically manufactured using one of three methods: 1. machining from a single piece ('hog out'), 2. precision casting, or 3. machining the vanes and brazing or welding the shroud onto the vanes. Other methods include additive manufacturing, erosion, and three-piece impellers where the vanes are welded or riveted to both the back face and the shroud.

Lastly, impellers are typically categorized based on their respective flow ranges in two primary applications: multistage or pipeline. Impellers will be discussed in greater detail in the following aerodynamic section (Figure 2-10).

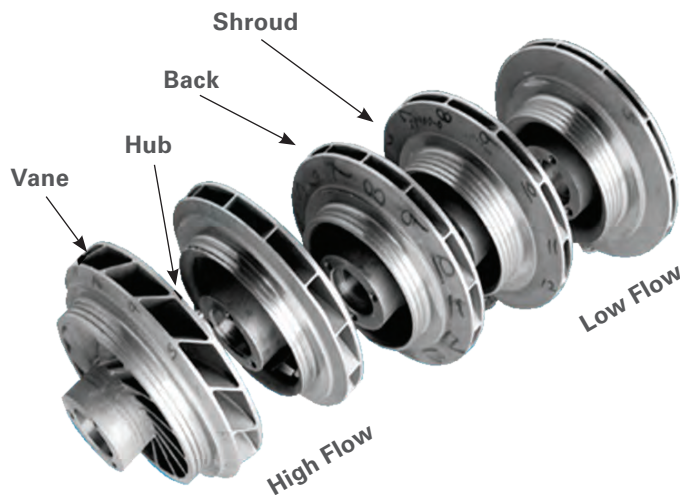


**Figure 2-10.** Impellers

## ROTOR

When designing a centrifugal compressor, one of two rotor designs is typically used. A modular design or a solid-shaft design. A solid-shaft design uses a solid rotor with interference-fit impellers, while a modular rotor uses a tie-bolt (center bolt) pulled in tension attached to impellers with a suction and discharge stub shaft at the respective ends.

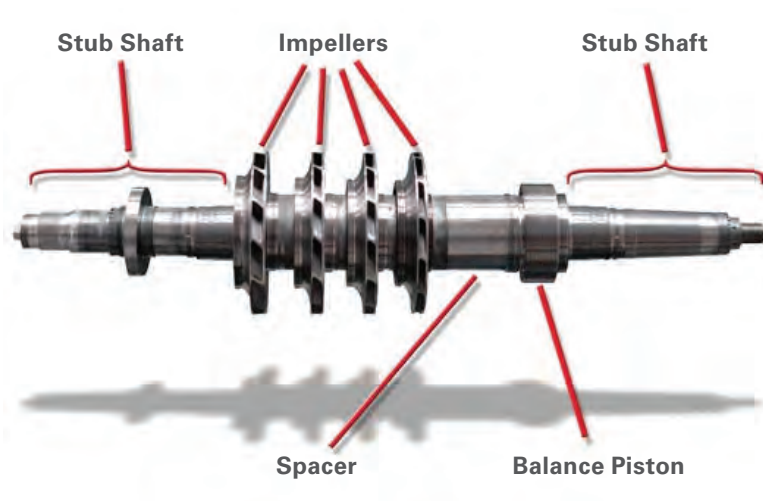


**Figure 2-11.** Compressor shaft with impellers, spacers and balance piston.

The rotating part of the compressor consists of all the impellers. The rotor runs on two radial bearings. On all modern compressors, hydrodynamic tilt-pad bearings are used, while the axial thrust generated by the impellers is balanced by a balance piston. The resulting force is balanced by a hydrodynamic tilt pad thrust bearing. Each impeller has its own labyrinth seal on the backside of the impeller to help prevent leakage (*Figure 2-11*). The balance piston is exposed to the compressor discharge pressure on its inboard side, and via a balancing line (i.e. piping that connects to the suction side of the compressor), to the suction pressure of the compressor on the outboard side. This also has the effect that the dry gas seals on both the suction and the discharge ends of the compressor are exposed to the compressor suction pressure.

To keep the gas from escaping at the shaft ends, dry gas seals are used on both shaft ends (*Figure 2-12 and 2-13*). Other seal types have been used in the past, but virtually all modern centrifugal compressors in pipeline applications use dry gas seals (*Figure 2-13*). Sealing is accomplished by a stationary and a rotating disk, with a very small gap (about  $5\mu\text{m}$ ) between them. At standstill, springs press the movable seal disc onto the stationary disc. Once the compressor shaft starts to rotate, the groove pattern on one of the discs causes a separating force, making the seals run without mechanically contacting the sealing surfaces. This is one of the most critical components in a gas compressor and will be discussed in more detail later.

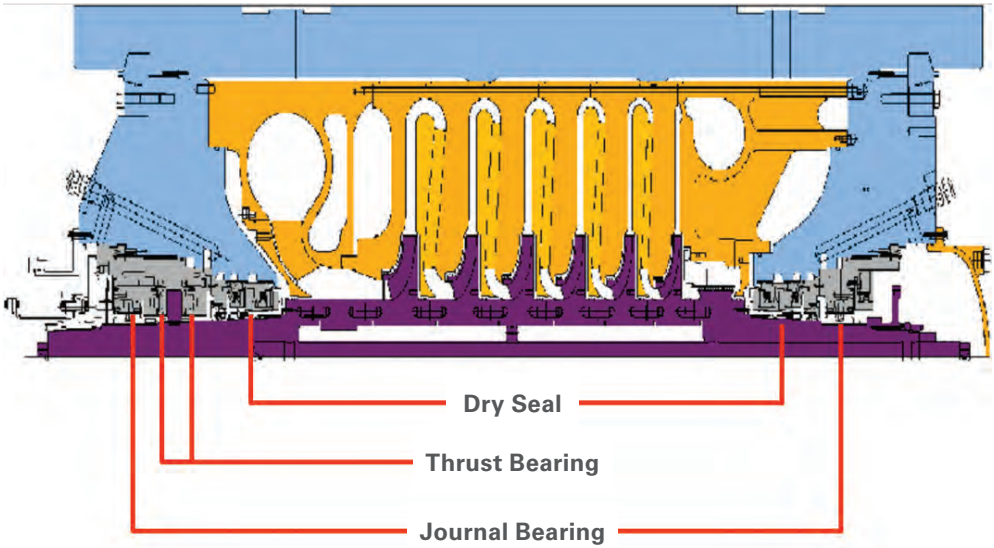


Figure 2-12. Bearings and seals.

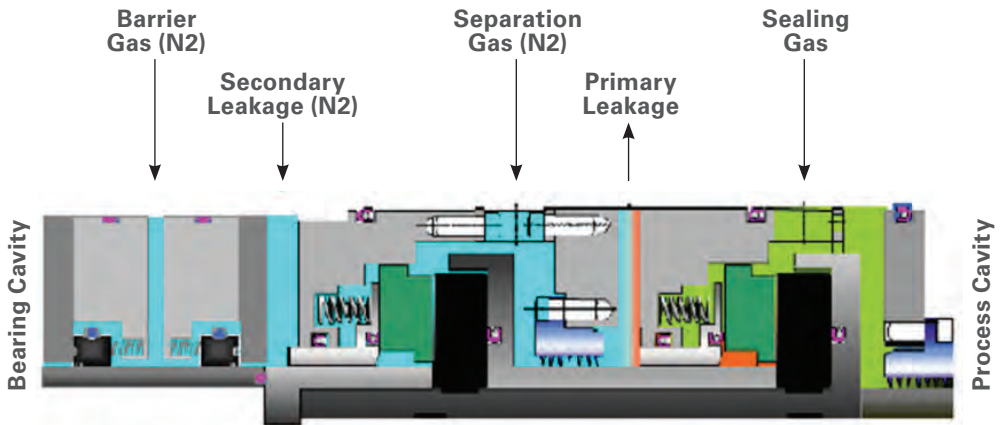
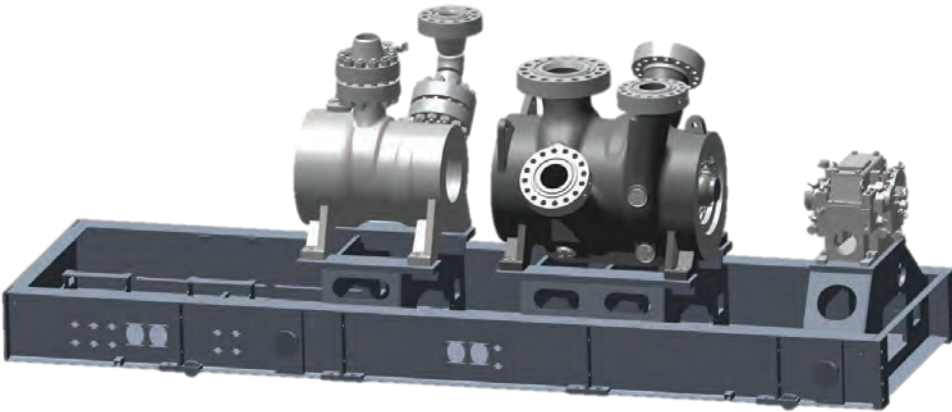


Figure 2-13. Dry gas seals.

## MULTI-BODY TRAINS

If the required pressure ratio exceeds the capability of a single-casing machine, or if side streams have to be accommodated, multiple-casing trains are employed. This involves multiple compressor bodies (some of them can have multiple sections), all driven by the same driver. A gearbox, either between the driver and the compressor, or between compressors can be used to adapt compressor and driver speeds (*Figure 2-14*).



**Figure 2-14.** Designs for high pressure ratios showing a train with a gearbox, a two-compartment compressor and a single-compartment compressor.





## CHAPTER 3

# AERODYNAMICS OF CENTRIFUGAL COMPRESSORS

Rainer Kurz, Michel J. Cave, Min Ji

In the last chapter, the discussion focused on the impeller, which imparts mechanical energy to the gas and the diffuser, where part of the kinetic energy (velocity) is converted into internal energy (static pressure). In this chapter, how this works is described in greater detail.

If you hold your hand, palm down, out the window of a moving vehicle and angle your hand somewhat upward against the horizontal, you'll feel the air pushing your hand upwards.

**(CAUTION: This is a thought experiment; please do not attempt this in real life).**

Why does this happen? It happens because your hand is pushing a portion of the flowing air downward, and (as Newton's law about action and reaction states), your hand is pushed upward. This is the same principle the wings of an aircraft use to keep an airplane in the air (*Figure 3-1*). Similarly, if a garden hose is let loose, you'll see that the same principle also works for flow channels, pipes and hoses. If you want to change the direction of a flowing fluid, you have to apply a force.

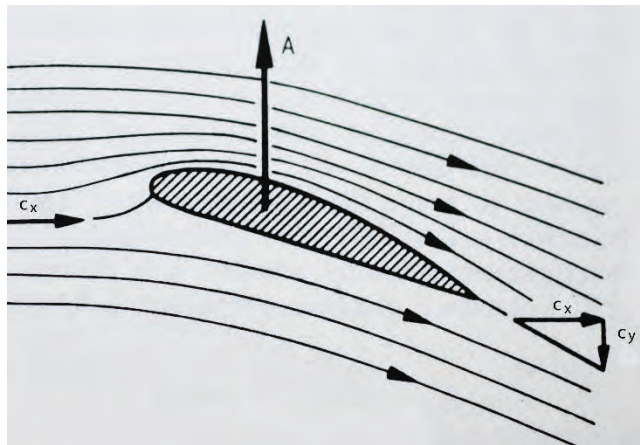


**Figure 3-1.** Airfoil creates lift ( $A$ ) by deflecting air downward.

A force applied does not yet relate to a portion of work applied. Work is done, if a force is applied over a distance. So, to apply work, it's not sufficient to simply apply a force. It must be a force that's applied to a moving object, such that the force (or at least part of the force) is applied in the direction of the movement. So, if a force is applied (by changing the direction of a fluid or gas) in a rotating (i.e. moving) system, work can be transferred. This is the basic working principle for any type of turbomachinery.

In the following text, this concept will be described in more detail. The fact that a gas is compressible must also be considered, specifically that its volume changes with pressure and temperature.

But first, consider what happens to a gas if it flows in a channel that increases or reduces its flow area. Bernoulli's law (which is strictly true only for incompressible flows, but which can be modified for the subsonic compressible flows found in gas compressors) describes the interchangeability of two forms of energy: static pressure and velocity. Consider the flow of a gas in a duct (*Figure 3-2*):

The incompressible formulation of Bernoulli's law for a frictionless, stationary, adiabatic flow without any work input is:

$$p_t = p + \frac{\rho}{2}c^2 = \text{const}$$

For compressible flows, the equation becomes, using the concept of enthalpy discussed earlier:

$$h_t = h + \frac{c^2}{2} = \text{const}$$

Another requirement is that mass cannot appear or disappear, thus for any flow from point 1 to point 2:

$$\dot{m}_1 = \rho_1 Q_1 = \dot{m}_2 = \rho_2 Q_2$$

$$\rho \cdot Q = \rho \cdot c \cdot A$$

This requirement is valid for compressible and incompressible flows, with the caveat that for compressible flows, the density is a function of pressure and temperature, and thus ultimately a function of the velocity.

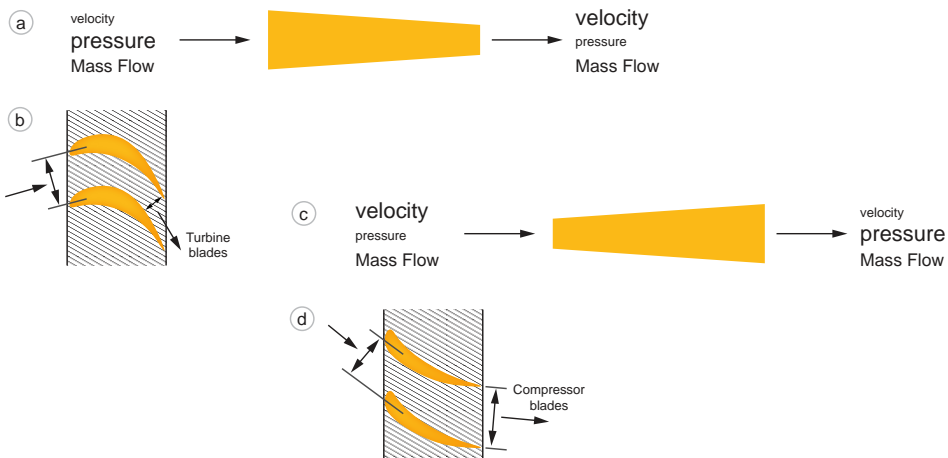


**Figure 3-2a-d. Bernoulli's law.**

These two concepts explain the working principles of the vanes and diffusers used in turbomachines (*Figure 3-2*). Due to the requirement for mass conservation, any flow channel that has a wider flow area at its inlet and a smaller flow area at its exit will require

a velocity increase from inlet to exit. If no energy is introduced to the system, Bernoulli's law requires a drop in static pressure (*Figure 3-2a*). Examples for flow channels like this are turbine blades and nozzles, inlet vanes in compressors and others (*Figure 3-2b*). Conversely, any flow channel that has a smaller flow area ( $A$ ) at its inlet and a larger flow area at its exit will require a velocity decrease from inlet to exit. If no energy is introduced to the system, Bernoulli's law requires an increase in static pressure (*Figure 3-2c*). Examples for flow channels like this are diffusers with or without vanes, impeller flow channels, rotor and stator blades of axial compressor volutes, and others (*Figure 3-2d*).

If these flow channels are in a rotating system (for example, in an impeller), mechanical energy is added to or removed from the system. Nevertheless, if the velocities are considered in a rotating system of coordinates, the above principles are applicable as well.

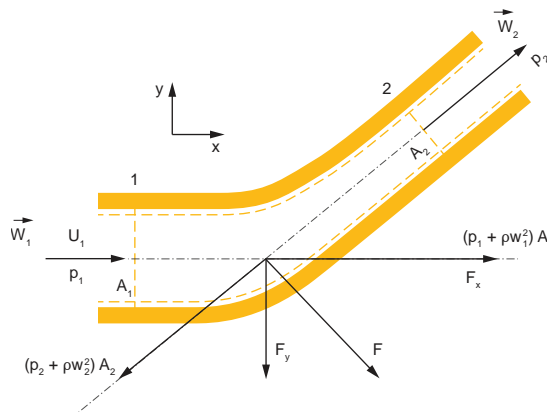


**Figure 3-3.** Conservation of momentum.

Another important concept is the conservation of momentum (*Figure 3-3*). The change in momentum ( $M$ ) of gas flowing from a point 1 to a point 2 is its mass times its velocity ( $m c$ ), and is also the sum of all forces ( $F$ ) acting. The change in momentum is:

$$\frac{d\vec{M}}{dt} = \dot{m}(\vec{c}_2 - \vec{c}_1) = \vec{F}$$

To change the momentum of this gas, either by changing the velocity or the direction of the gas (or both), a force is necessary. *Figure 3-3* outlines this concept for the case of a bent, conical pipe. The gas flows in through the area  $A_1$  with  $w_1$ ,  $p_1$ , and out through the flow area  $A_2$  with  $w_2$ ,  $p_2$ . The differences in the force due to the pressure ( $p_1A_1$  and  $p_2A_2$ ), respectively), and the fact that a certain mass flow of gas is forced to change its direction generates a reaction force ( $F_R$ ). Split into  $x$  and  $y$  coordinates, and considering that:

$$\dot{m} = \rho_1 A_1 w_1 = \rho_2 A_2 w_2$$

yields ( $w_{1y}=0$ ) due to the choice of coordinates.

$$\begin{aligned} x: & \quad \rho A_1 w_1 (w_{2x} - w_1) = p_1 A_1 - (p_2 A_2)_x + F_{Rx} \\ y: & \quad \rho A_1 w_1 (w_{2y}) = -(p_2 A_2)_y + F_{Ry} \end{aligned}$$

It should be noted that this formulation is also valid for viscous flows, because the friction forces become internal forces. So, force is created by deflecting the fluid flow. Now, if the channel spins around an axis in x-direction, at a certain radius  $r$ , a force that moves at a certain speed is created. In other words, power is either extracted (if the flow channel drives some load connected to the shaft), or power is absorbed (if the shaft is driven with a motor or even a hand crank). This works, with rotating blades or flow channels that are capable of changing the direction of the flow. For a rotating row of vanes (no matter if considered individual airfoils, or as in previous discussions, flow channels) in order to change the velocity of the gas, the vanes have to exert a force upon the gas. This is fundamentally the same force ( $F_{Ry}$ ) that acts in the previous example for the pipe. This force has to act in the direction of the circumferential rotation of the vanes in order to work on the gas. According to the conservation of momentum, the force that the blades exert is balanced by the change in circumferential velocity times the associated mass of the gas.

*Figure 3-4* shows a compressor stage that uses the principles outlined above. Since the blades on the rotor move, while the blades in the stator are stationary, a way must be found to describe velocities in a rotating system and in a stationary system. This works by simply adding velocity vectors: The vanes of the rotating blades 'see' the gas in a coordinate system that rotates with the rotor. The transformation of velocity coordinates from an absolute frame of reference ( $c$ ) to a frame of reference rotating with a velocity ( $u$ ) is by:

$$\vec{w} = \vec{c} - \vec{u}$$

The velocities here are vectors, describing both the magnitude of the velocity, as well as its direction.

*Figure 3-4* also shows this vector addition in the form of a velocity triangle. If rotated with the rotor, the velocity  $c_1$  (in a stationary system) entering the rotor, as the velocity  $w_1$ , which is determined by subtracting the vector  $u_1$  from the vector  $c_1$  would result. This is called a velocity triangle. Similarly, at the exit from the rotor, the air leaving with the velocity  $w_2$  is observed (while still rotating with the rotor), and the velocity  $c_2$  entering the stator by adding  $u_2$  is derived. In axial machines, where the air flows more or less parallel to the axis of rotation, this can essentially be treated for every constant diameter as a two dimensional problem. This means, that  $u_1$  and  $u_2$  are about the same, and the third spatial coordinate is nothing to worry about.

What can be seen in *Figure 3-4* is, that the rotor blade deflects the air from  $w_1$  to  $w_2$ , and since it rotates, it adds work to the air. It also reduced the velocity, thus increasing the pressure according to Bernoulli's law (*also see Figure 3-2d*). The velocity  $c_2$  entering the stator is higher than  $c_1$ , but the stator which also has a shape to increase the flow passage (*Figure 3-2d*). Therefore, the pressure is further increased. The exit velocity  $c_3$  becomes the inlet velocity  $c_1$  for the next stage. The important step is, that the change in the circumferential velocity ( $c_{u2}-c_{u1}$ ), multiplied by the speed at which the blade rotates ( $u_2$  and  $u_1$  respectively) yields the entire amount of work that was transferred to the air, which is also the power per mass flow of air absorbed by this compressor:

$$P = \dot{m} \cdot \Delta h = \dot{m} \cdot (u_2 c_{u2} - u_1 c_{u1})$$

This relationship is usually referred to as Euler's Law, after Leonard Euler, who formulated it in the 18<sup>th</sup> century. It describes the conservation of angular momentum at the inlet and

outlet of a stage. As mentioned earlier, the only place where work is added is in the rotating part of the machine. All the stator does is convert some of the kinetic energy (velocity) to additional pressure. *Figure 3-5* illustrates this. The impeller adds energy (expressed as total pressure), but both in the form of more pressure and more velocity. The diffuser converts velocity into pressure, but does not add energy to the flow. The important contribution of Euler's law is that it connects thermodynamic properties (like enthalpy, or therefore pressures and temperatures) with aerodynamic properties (velocities).

The axial velocity  $c_{z1} = c_{z2}$  in this example stays approximately constant. This is a good assumption for axial machines.

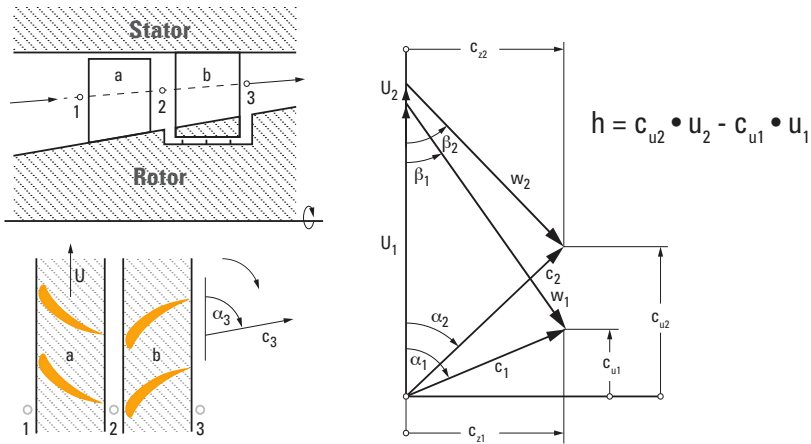


**Figure 3-4.** Velocities in a typical compressor stage. Mechanical Work ( $h$ ) transferred to the air is determined by the change in circumferential momentum of the air.

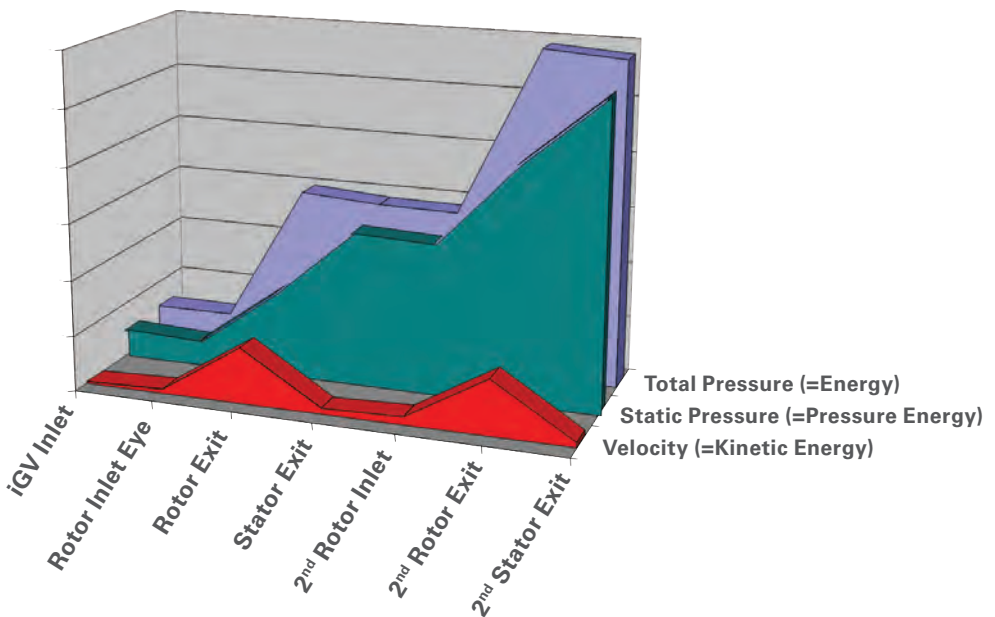


**Figure 3-5.** Energy transfer in compressors.

The work input  $h$  (also known as actual head) in the equations above does not identify anything about the pressure increase of the stage. Only when the efficiency of the stage is known can the amount of pressure rise be gauged.

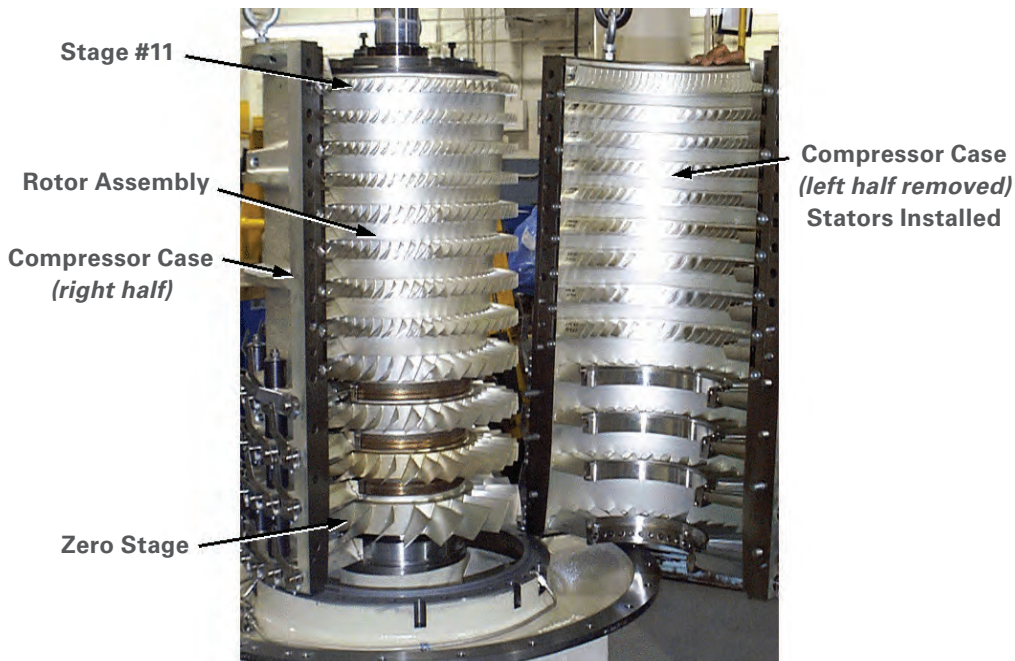


**Figure 3-6.** Axial compressor rotor and stator with multiple stages and alternating rows of stationary and rotating blades.

## CENTRIFUGAL COMPRESSORS

In general, the flow of an axial compressor is typically parallel to the axis of the turbomachine, while in a centrifugal compressor, each stage has a more or less axial flow into the stage. The gas leaves each stage with a significant radial component. In axial machines, two dimensional considerations have merit. In a centrifugal machine, all three dimensions must be considered. However, just as with the axial machines, the important feature is the force in the direction of the rotational speed, and thus the changes in velocities in the circumferential direction. While in an axial machine the blade speeds ( $u$ ) at the inlet and exit are almost the same, they are quite different in a centrifugal machine. *Figures 3-7 and 3-8* show the impeller (i.e. the rotating blades), and the diffuser of a centrifugal compressor.



**Figure 3-7.** Centrifugal compressor stage, showing the spinning impeller feeding the gas into a diffuser.

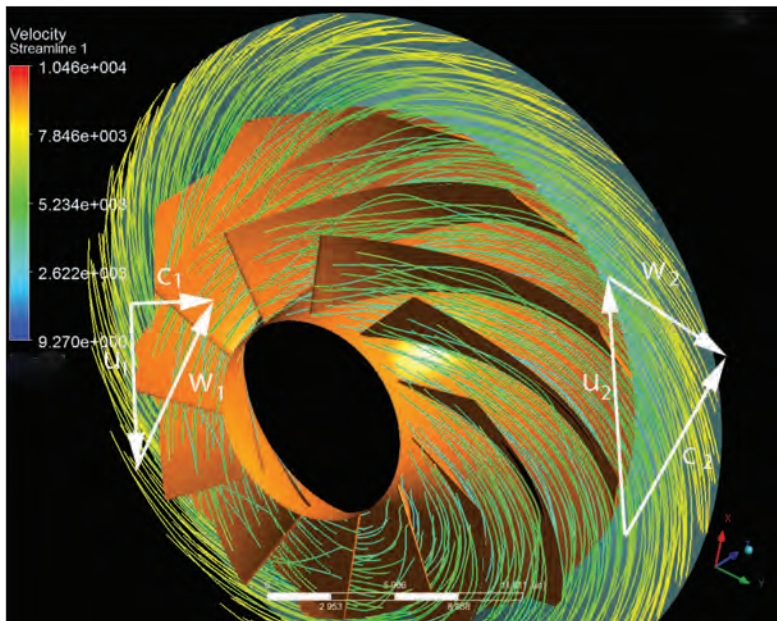


**Figure 3-8.** Centrifugal impeller, showing the velocity triangles at inlet (1) and exit (2).

Figure 3-8 shows the velocity triangles at the impeller, where ( $u$ ) is the circumferential blade velocity at the inlet (1) and exit (2). The  $c_1$ - $w_1$  plane has to be imagined perpendicular to the  $c_2$ - $w_2$  plane, because the inlet flow is more or less axial, while the exit flow is more or less radial. However, the circumferential components of ( $c_1$ ) and ( $c_2$ ), respectively, are in the same plane.

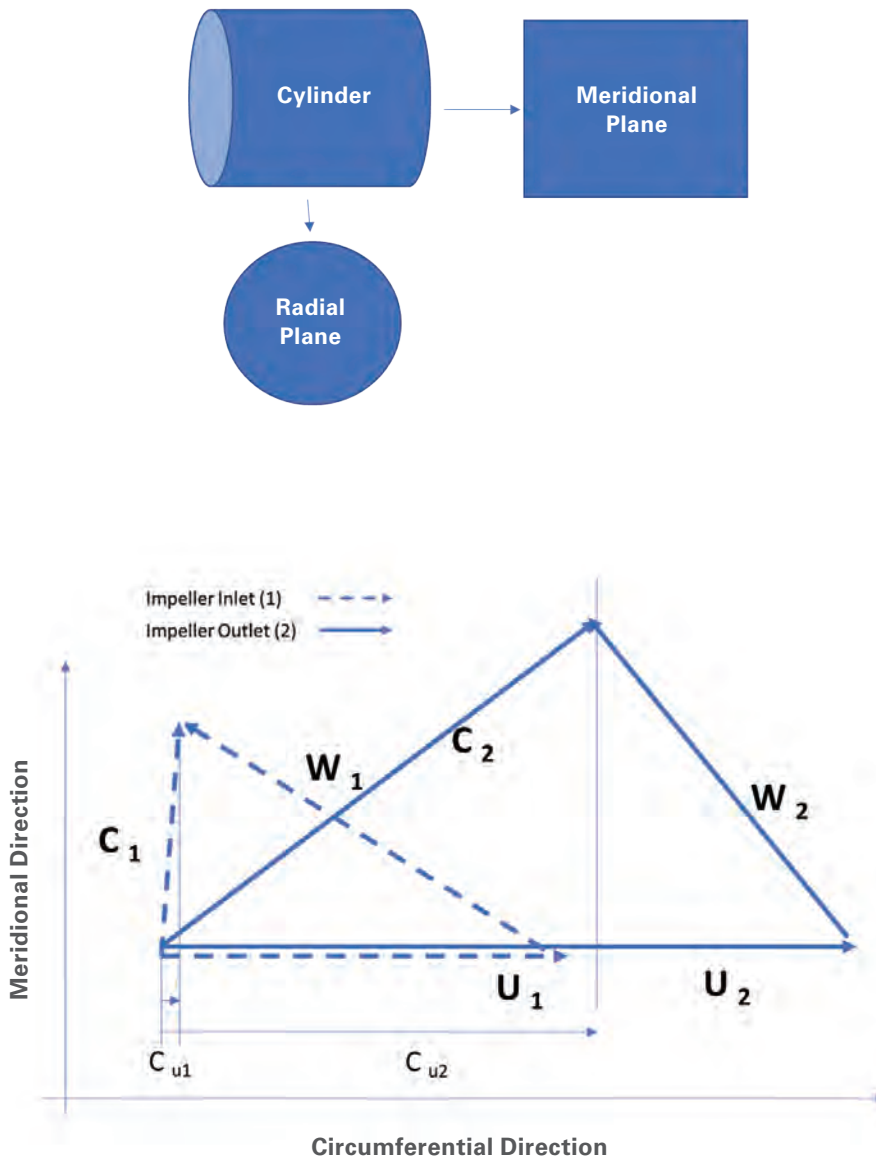


**Figure 3-9.** Velocity triangles for a centrifugal compressor.

Figure 3-9 shows these velocity triangles. Just like for the axial compressor, the relative velocities are found by subtracting the vector of blade velocity ( $u$ ) from the gas velocity in the stationary reference frame. The velocity ( $c_1$ ) is the absolute velocity at the inlet to the impeller, and ( $c_2$ ) is the velocity of the gas entering the diffuser. The relative velocity ( $w_1$ ) is often the machine's highest velocity, if the velocity is taken at the tip of the impeller. The relative velocity ( $w_2$ ) is largely determined by the direction of the blades at the exit of the impeller. If ( $w_2$ ) points against the direction of rotation (as in Figures 3-8 and 3-9), the blades are called backwards bent, as opposed to forward bent blades and radial blades. Most compressor impellers in oil and gas applications utilize the backwards bent design,

because as discussed later, this favors a wider operating range. Rather than using cartesian coordinates for impellers, cylindrical coordinates are used here.

The radial plane and the meridional plane are described as follows:

- Meridional coordinate (m), which increases from the inlet to the outlet of the impeller.
- Span-wise coordinate (s), which increases from impeller hub to the shroud.
- Circumferential coordinate (u), which increases from the blade pressure side to the suction side of the next blade.

Additionally, ( $c_u$ ) is the circumferential component of the gas velocity, taken in an absolute reference frame at the inlet (1) and exit (2) as shown in *Figure 3-8*. At this point, one of the advantages of centrifugal compressors over axial compressors becomes apparent. In the axial compressor, the entire energy transfer has to come from the turning of the flow imposed by the blade ( $c_{u2}-c_{u1}$ ), while the centrifugal compressor has added support from the centrifugal forces on the gas flowing from the diameter at the impeller inlet ( $u_1=\pi D_iN$ ) to the larger diameter at the impeller exit ( $u_2=\pi D_{tip} N$ ). But, just as for the axial machines, Euler’s law also applies to centrifugal machines.

$$P = \dot{m} \cdot \Delta h = \dot{m} \cdot (u_2 c_{u2} - u_1 c_{u1})$$

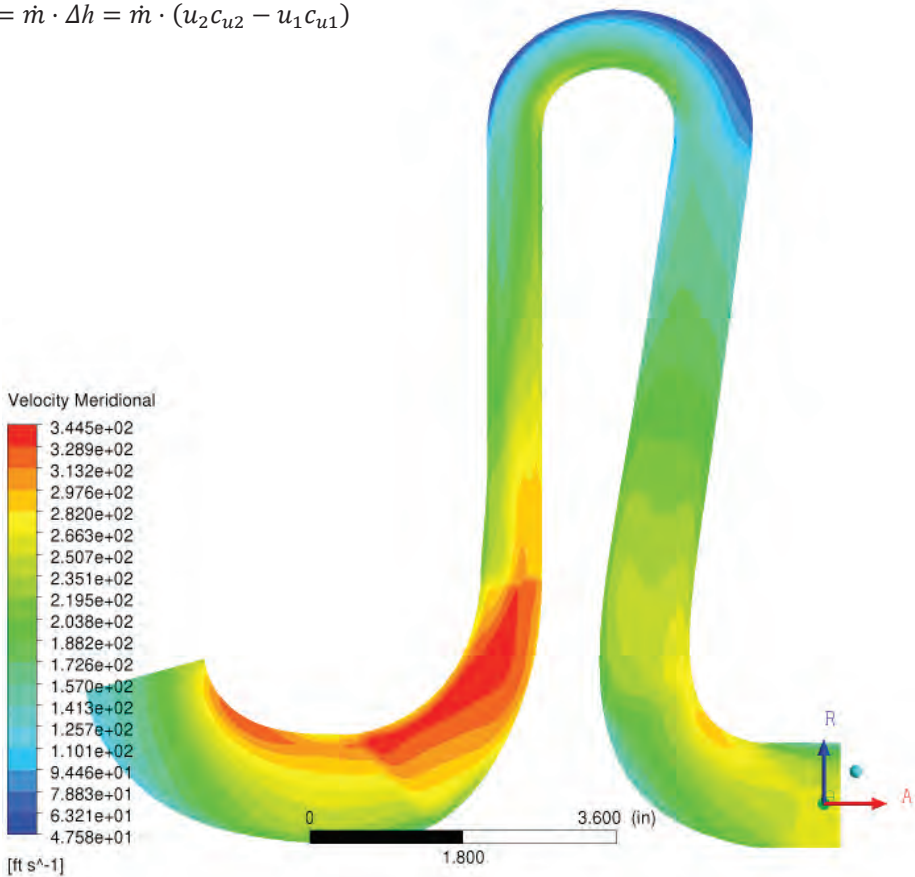


**Figure 3-10.** Illustrates the velocity buildup in the meridional section of the compressor.

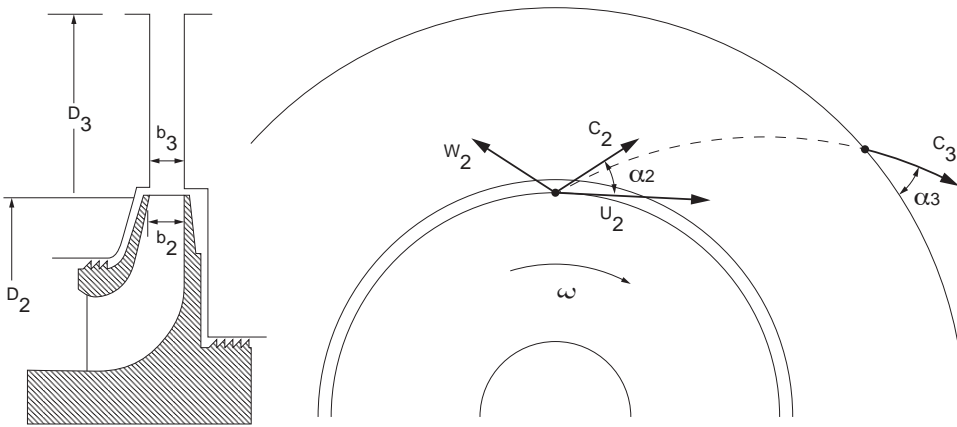


**Figure 3-11.** The diffuser.

As mentioned in the previous chapter, most centrifugal compressors utilized in the applications discussed in this book have so called vaneless diffusers, due to their advantages in operating range. In *Figure 3-11*, the aerodynamics of such a diffuser are explained. The absolute velocity at the impeller exit ( $c_2$ ) has meridional and circumferential components. Because the diffuser has no vanes, the circumferential component has to maintain its momentum, which enforces  $(c_u \text{ times } r) = \text{const}$ . In other words,  $(c_u)$  is reduced when the flow moves from diffuser inlet to diffuser exit. The meridional component is reduced proportionally to the increase in the diffuser when the radius is increased. The two effects together mean that the flow path becomes a logarithmic spiral. The more  $(c_2)$  leans towards the tangential direction, the longer the flow path through the diffuser becomes. The shorter flow path applies to situations when  $(c_2)$  is entirely in the radial direction. In the absence of flow separation in the diffuser, the velocity energy difference between inlet and exit from the diffuser is converted into pressure.

## OPERATION

Based on the general principles for the operation of a centrifugal compressor introduced here, the discussion advances to how a compressor operates when operating conditions change. Understanding the behavior of a compressor stage, running at constant speed, is a good place to start.

Impeller exit geometry ('backsweep') determines the direction of the relative exit velocity ( $w_2$ ). The basic 'ideal' slope of head vs. flow is dictated by the kinematic flow relationship of the compressor, in particular the amount of impeller backsweep.

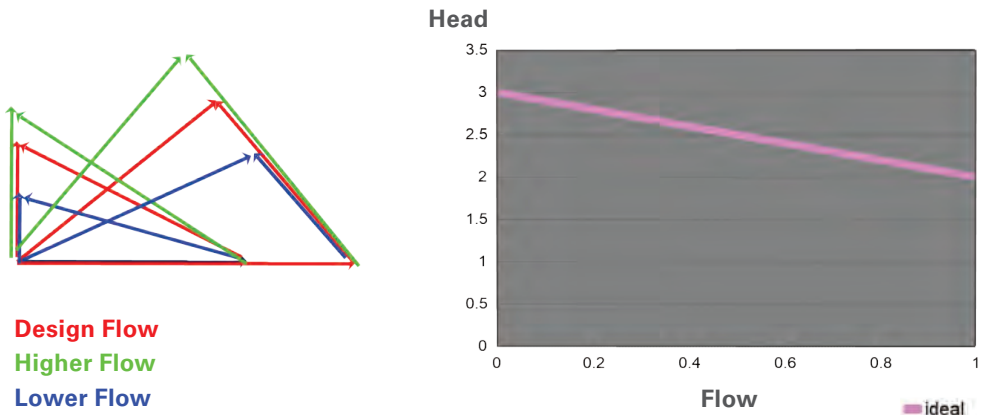


**Figure 3-12.** Constant-speed operation at changing flow.

Any increase in flow at constant speed causes a reduction of the circumferential component of the absolute exit velocity ( $c_{u2}$ ), as seen in *Figure 3-12*. The meridional velocity ( $c_m$ ) is also impacted. As flow increases, the meridional velocity also increases. The compressor speed is fixed, thus ( $u_1$ ) and ( $u_2$ ) don't change. The inlet flow is assumed to be strictly axial, so only the magnitude, but not the direction of ( $c_1$ ) changes. The example is valid even for inlet flow that is not axial, as long as the flow direction stays the same. Further, the direction of the impeller exit flow in the relative frame, which is dictated by the blade geometry, will not change. You can see that the change in circumferential velocity ( $c_{u2}-c_{u1}$ ) is impacted by the change in inlet flow. It's reduced when the inlet flow is increased.

It follows from Euler's equation above, that this causes a reduction in head. This is shown on the right of *Figure 3-11*. The impeller geometry causes a reduction in head with an increased flow, and vice versa.

So far, losses in the compressor haven't been discussed. The losses are lowest at the design point of the compressor, and two types of losses must be considered. First, the incidence loss (*Figure 3-13*). The impeller inlet, as well as other components such as the diffuser, are sized assuming the gas comes from a specified direction. From *Figure 3-11*, you can see that ( $w_1$ ) for impeller direction, changes when the flow is increased or reduced from the design point. This causes additional aerodynamic losses in the compressor.

*Figure 3-13* further illustrates this, using an airfoil as an example. At the 'design flow, the air follows the contours of the airfoil. If the direction of the incoming air changes, increasing zones where the airflow ceases to follow the contours of the airfoil, creation of increasing losses is evident.

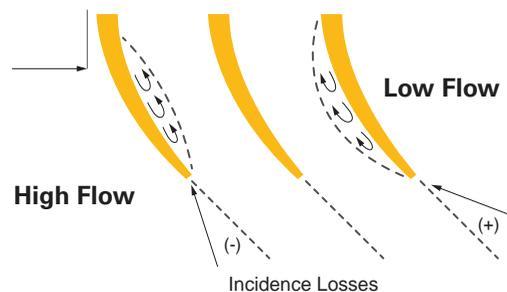


**Figure 3-13.** Incidence of loss at the impeller inlet.

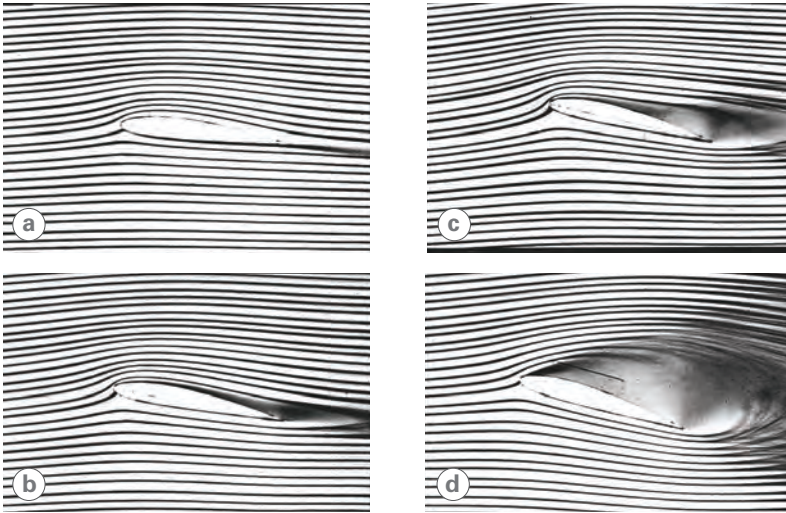


**Figure 3-14a-d.** Unseparated (a, b), partially separated (c), and fully separated (d) flow over an airfoil at increasing angle of attack (Nakajima, 1988).

The second type is related to the flow velocity. Increasing the velocity's magnitude increases the friction losses in the impeller channels and the diffuser. Adding the influence of various losses to the basic relationship developed earlier (Figure 3-11) shapes a compressor's head-flow-efficiency characteristic (Figure 3-15). Whenever the flow deviates from the flow for which the stage was designed, the components of the stage operate less efficiently. This is the reason for incidence losses. Furthermore, the higher the flow, the higher the velocities, and thus the increased friction losses.

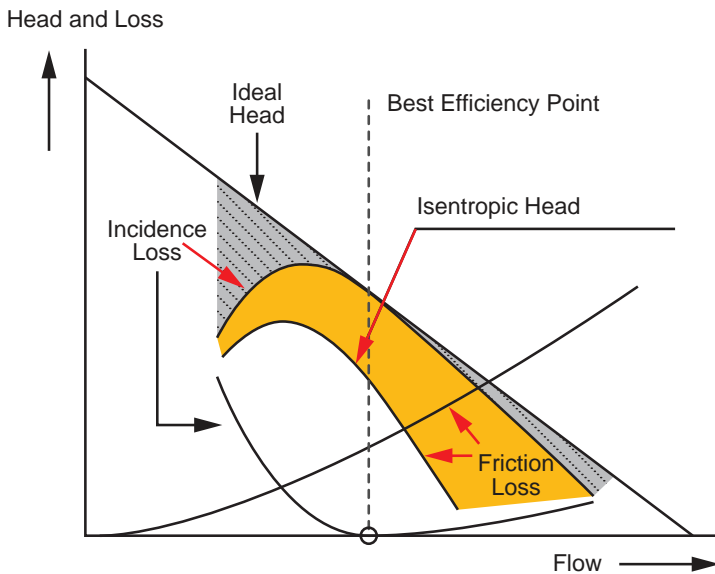


**Figure 3-15.** Head versus flow relationship at constant speed.

Centrifugal compressor behavior can be described by its head-flow-efficiency relationships. The basic relationship, for a compressor at constant speed is shown in *Figure 3-15*. The compressor shows a distinct relationship between head and flow. In the case of machines with backwards bent impellers (the type generally used in upstream and midstream compression applications), the head of the compressor increases with reduced flow. Due to the increase in losses when the compressor is operated away from its design point, the curve eventually becomes horizontal, and subsequently starts to drop again. The curve section with positive slope is usually not available for stable operation. When the flow is increased beyond the design flow, the losses also increase, and increase the slope of the curve, sometimes to a vertical line.

A compressor operated at constant speed is at its best efficiency point. If the flow through is reduced, the compressor's efficiency will be gradually reduced because, for example, the discharge pressure that the compressor has to overcome is increased. At a certain flow, stall will occur, probably in the form of a rotating stall in one or more of the compressor components. As flow is further reduced, the compressor will eventually reach its stability limit, and go into surge.

Again starting from the best efficiency point, if flow is increased, then you'll also see a reduction in efficiency, accompanied by a reduction in head. Eventually the head and efficiency will drop steeply, until the compressor will not produce any head at all. This operating scenario is called "choke." For practical applications, the compressor is usually considered to be in choke when the head falls below a certain percentage of the head at its best efficiency point).

You'll also see that the resulting curve has a negative slope for the higher flow, but at some point, reaches a maximum, followed by a positive slope. The horizontal slope marks the stability limit of the compressor, and operating it at lower flows than this point usually leads to surge.

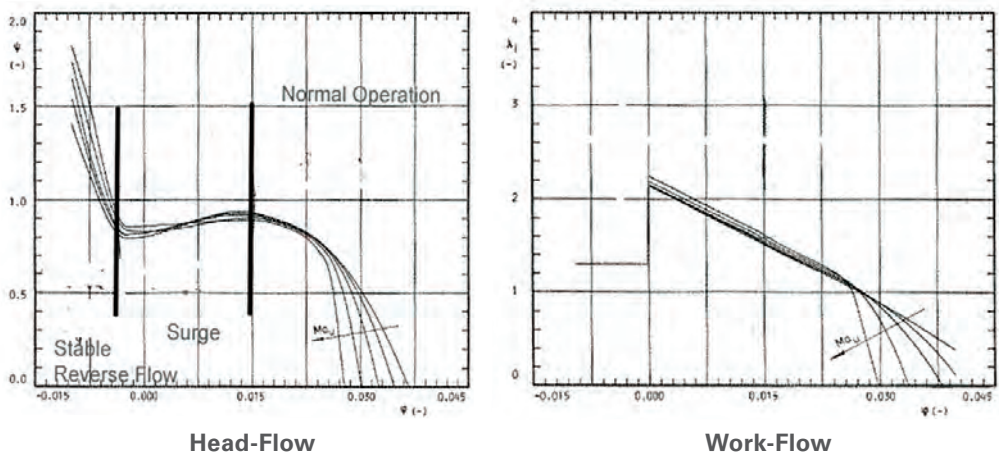


**Figure 3-16.** Compressor map showing head vs. flow and work vs. flow, including operation in surge.

## SURGE

For flows lower than the flow at the stability limit, practical operation of the compressor is not possible. At flows to the left of the stability limit, the compressor cannot produce the same head as at the stability limit. It is therefore no longer able to overcome the pressure differential between the suction and discharge sides. Because the gas volume upstream (at discharge pressure) is now at a higher pressure than the compressor can achieve, the gas will follow its natural tendency to flow from the higher to the lower pressure. The flow through the compressor is reversed. Due to the flow reversal, the system pressure at the discharge side will be reduced over time, and eventually the compressor will be able to overcome the pressure on the discharge side again. If no corrective action is taken, the compressor will again operate to the left of the stability limit, and the above described cycle will repeat. The compressor is in surge. The observer will detect strong oscillations of pressure and flow in the compression system. It must be noted that the violence and the onset of surge are a function of the interaction between the compressor and the piping system.

## STALL

If the flow through of a compressor at constant speed is reduced, the losses in all aerodynamic components will increase, because their operating conditions will move away from the design point. Eventually, the flow in one of the aerodynamic components, usually in the diffuser or the impeller inlet, will separate. The last picture (*d*) in *Figure 3-14* shows such a flow separation for an airfoil. It should be noted that stall usually appears in one stage of a compressor first. The separation can be stationary, or of a propagating, and therefore rotating nature. Stall and surge are not directly related. If the flow at constant speed is reduced, stall can appear before the compressor actually reaches its maximum head or before it actually surges.

Flow separation and stall in a vaneless diffuser means that all or parts of the flow will not exit the diffuser on its discharge end, but will form areas where the flow stagnates or reverses its direction back to the inlet of the diffuser (*i.e. the impeller exit, Figure 3-15*). This is due to either boundary layer separation or insufficient kinetic energy to overcome the diffuser pressure gradient.

Stall in the impeller inlet or a vaned diffuser is due to the incoming flow (relative to the rotating impeller) changing with the flow rate through the compressor. Therefore, a reduction in flow will lead to an increased mismatch between the direction of the incoming flow the impeller was designed for and the actual direction of the incoming flow. At one point, this mismatch will become so significant that the flow through the impeller breaks down. Similarly, vanes in the diffuser will reduce the operating range of a stage compared to a vaneless diffuser.

Flow separation can take on the characteristics of a rotating stall. When the flow through the compressor stage is reduced, parts of the diffuser may experience flow separations. Rotating stall occurs if the regions of flow separation are not stationary, but move in the direction of the rotating impeller (typically at 15-30% of the impeller speed). Rotating stall can often be detected by the increasing vibration signatures in the sub-synchronous region, but with distinct frequencies. This is different from the ubiquitous increase in flow noise when the

compressor operates close to stall, in stationary stall, or in choke, as this noise generally has no distinct frequencies. Another type of noise is generated by the interaction of the impellers with a vaned diffuser. This noise is not the result of aerodynamic off-design conditions, but rather due to the interaction between the impeller and the diffuser. Onset of stall does not necessarily constitute a compressor's operating limit. In fact, in many cases, the flow can be reduced further before the actual stability limit is reached, and surge may occur.

## CHOKE

At high flow, the head and efficiency will drop steeply, until the compressor will not produce any head at all. This operating scenario is called choke. However, for practical purposes, the compressor is usually considered to be in choke when the head falls below a certain percentage of the head at its best efficiency point. Some compressor manufacturers do not allow operation of their machines in deep choke. In these cases, the compressor map has a distinct high flow limit for each speed line.

The efficiency starts to drop off at higher flows, because a higher flow causes higher internal velocities, and thus higher friction losses. The head reduction is a result of both the increased losses and the basic kinematic relationships in a centrifugal compressor. Even without any losses, a compressor with backwards bent blades (as used in virtually every industrial centrifugal compressor) will experience a reduction in head with increased flow (*Figure 3-11*). 'Choke' and 'Stonewall' are different terms for the same phenomenon. You can observe two distinctly different behaviors in choke.

For compressors at low Mach numbers, and in particular single- and two-stage machines, you'll observe a gradual decline in head. This is mainly due to the increasing losses in the machine. Other machines, especially multi-stage machines, and machines at higher Mach numbers show an almost vertical drop in head at a certain flow. This is due to a true choke event, where at some component, often the inlet of an impeller, the flow in the narrowest flow path reaches the speed of sound, and thus prevents any increase in flow, regardless how low the discharge pressure is set. *Figure 3-17* shows both of these behaviors. At low Mach numbers, increased losses show a gradual reduction of head and efficiency, while at a higher machine Mach number, true choke causes an almost vertical drop in head and efficiency.

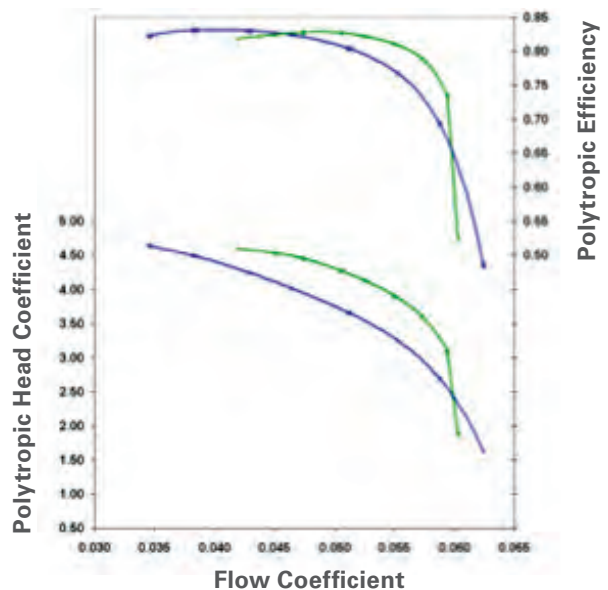


**Figure 3-17.** Stage map for  $Mn=0.56$  (blue) and  $Mn=0.76$  (green).

## MACH NUMBER

Previously, the Mach number was mentioned several times in the text. To make things more complicated, the density of the gas flowing over airfoils or through channels is not constant. In other words, the gas is compressible, and the density changes with pressure and temperature. Both pressure and temperature are in turn dependent on the flow velocity. From the above explanation, you can understand that when the mass flow is conserved, then the volumetric flow, and with it all velocities, will change, if the density changes. An indicator of the severity for the impact of these density changes is the Mach number ( $Ma$ ) which compares flow velocities ( $c$ ) to the speed of sound ( $a$ ).

$$Ma = c/a$$

If the flow velocities through the entire section are below the speed of sound, commonly referred to as subsonic flow, and for really low Mach numbers, the flow can actually be considered incompressible. In other words, you don't need to consider the density changes. Flow velocities above the speed of sound are called supersonic. If the flow changes within a component from subsonic to supersonic or vice versa, the flow is called transonic. An example for a transonic compressor stage is shown in *Figure 3-18*, where the flow enters at speeds above the speed of sound and is decelerated through a shock to subsonic velocities.

For centrifugal compressors, a machine's Mach number ( $M_n$ ) is often defined as:

$$Mn = u/a_{\text{inlet}}$$

This is not a true Mach number, since it compares a blade velocity ( $u$ ) at the impeller exit with the speed of sound based on the inlet conditions into the impeller (or the machine). It is, however, very practical for comparing operating conditions for a given machine. The machine Mach number for a given compressor will increase with increased speed, but also with a reduction in inlet temperature. It will also change when the process gas changes. For example, an increase in  $\text{CO}_2$  (with a low speed of sound) in a natural gas mixture will increase the machine Mach number. It must be noted that the machine Mach number does not indicate the highest Mach number anywhere in the machine. That is usually found at the inlet tip (or shroud) side of the first impeller.

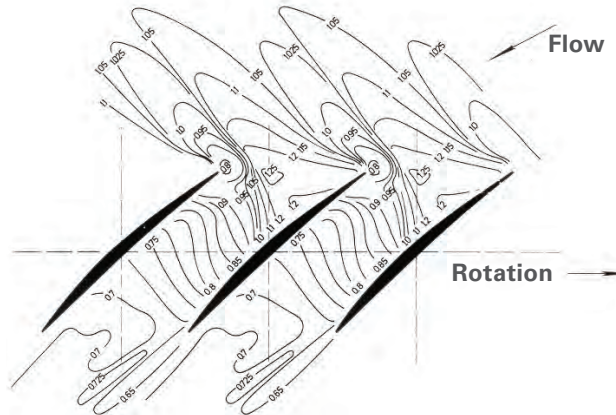


**Figure 3-18.** Mach number distribution for typical transonic compressor blades. The flow enters at supersonic speeds. It is decelerated to subsonic speeds at the exit (Schodl, 1977). The shock is clearly visible, where the supersonic flow is decelerated to subsonic speeds immediately upstream of the leading edge.

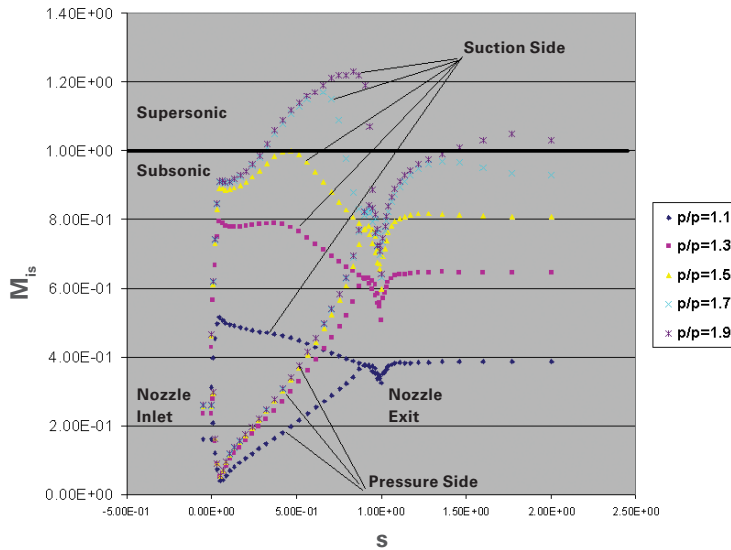


**Figure 3-19.** Velocity distribution (isentropic Mach Number  $M_{is}$  along the surface coordinates) in a turbine nozzle at different pressure ratios. As soon as the maximum local flow velocity exceeds Mach 1 (at a pressure ratio of 1.5 in this example), the inlet flow can no longer be increased (Kurz, 1991).

Figure 3-19 shows the situation of a turbine nozzle that is operated at different pressure ratios. Not only do you see the levels of velocity increase with increased pressure ratios, but you see the velocity distribution actually changes its shape. This is an example of the profound changes in aerodynamic behavior that occur with changes in the Mach number. At a certain pressure ratio (in this case 1.5) the velocity at the suction side of the nozzle just reaches the speed of sound. For higher pressure ratios, the flow is actually accelerated beyond the speed of sound. A further increase of the pressure ratio yields higher velocities downstream of the throat, but the flow, which is proportional to the velocity at the inlet into the nozzle, can no longer be increased.

When looking at the volumetric flow represented by the flow velocity entering the nozzle (Figure 3-19) you'll find that once the pressure ratio reaches the point where the speed of sound was first exceeded, the flow cannot be increased any more. The nozzle is choked. In other words, even an increase in pressure ratio does not yield more flow.

Performance of any aerodynamic component will change, if the characteristic Mach numbers are changed. Figure 3-20 shows the flow through a centrifugal impeller at two different Mach numbers, in both cases within the choke region. For the lower Mach number, you'll see flow separation in the impeller inlet, causing the efficiency and the isentropic head to drop rapidly. For the higher Mach number, you'll see a transonic shock at the impeller inlet, thus setting a limit for the flow that cannot be exceeded even if the compressor backpressure drops further.

Not surprisingly, the Mach number has a strong influence on losses and enthalpy rise or decrease for a given blade row. Figure 3-15 shows how efficiently isentropic head and flow range for a compressor stage change with a rising machine Mach number, while Figure 3-21 shows the changes for a six-stage compressor. The practical conclusion is that the performance of any aerodynamic component will change, if the characteristic Mach

number changes. On the other hand, if characteristic Mach numbers of a component are held constant, then the performance of said component will remain the same (except for changes in Reynolds number, gas composition, etc.). The aerodynamic behavior of a turbine or compressor is thus significantly influenced by the Mach number of the flow. The same turbine or compressor will show significant differences in operating range (flow range between stall and choke), pressure ratio and efficiency. Component performance maps show a significant sensitivity to changes in Mach numbers. There is a strong dependency of losses, enthalpy rise or decrease, and flow range for a given blade row on the characteristic Mach number.

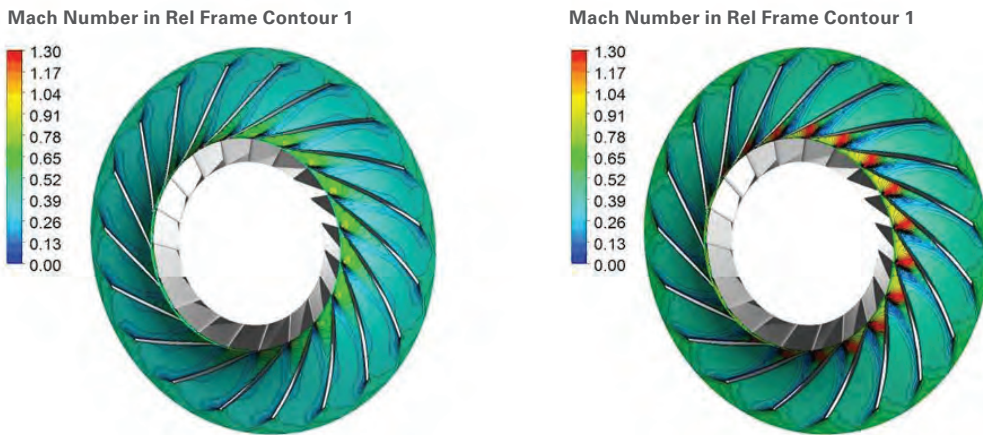


**Figure 3-20.** Mach number contours (relative frame) for impeller operating at  $M_n = 0.56$  (left) and  $M_n = 0.76$  and slightly lower flow coefficient (right). At the lower Mach number, stall due to negative incidence has developed. At the higher Mach number, shock has formed at the pressure surface. Refer to Figure 3-12.

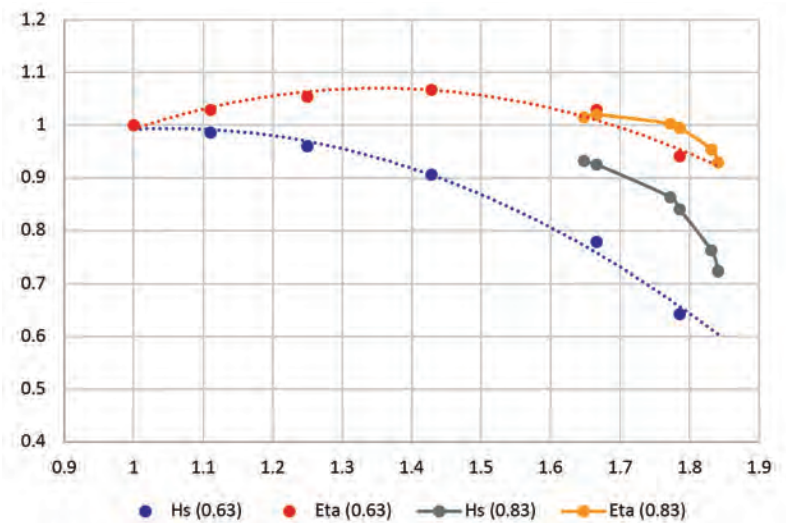


**Figure 3-21.** Head, flow and efficiency for a six-stage compressor for two different machine Mach numbers.

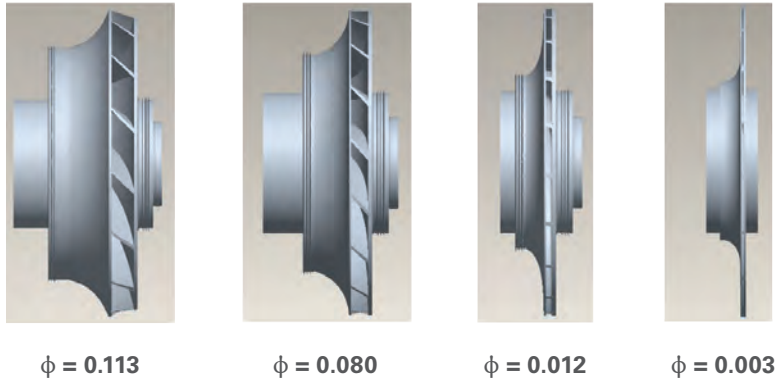


**Figure 3-22.** Impellers for different flows, from low flow (right) to high flow (left)

**OPERATING SPEED**

Until now, the discussion has been limited to compressors operating at constant speed. If the driver of the compressors varies the speed, within the mechanical capabilities of the machine, a rather significant increase in operating range is achieved. (Figure 3-22). For each possible speed of the compressor, a head flow characteristic as seen in Figures 3-14 is determined.

Under certain simplifying conditions, operating points of a compressor at different speeds can be directly compared. This fact is captured in the fan law, which strictly is only true

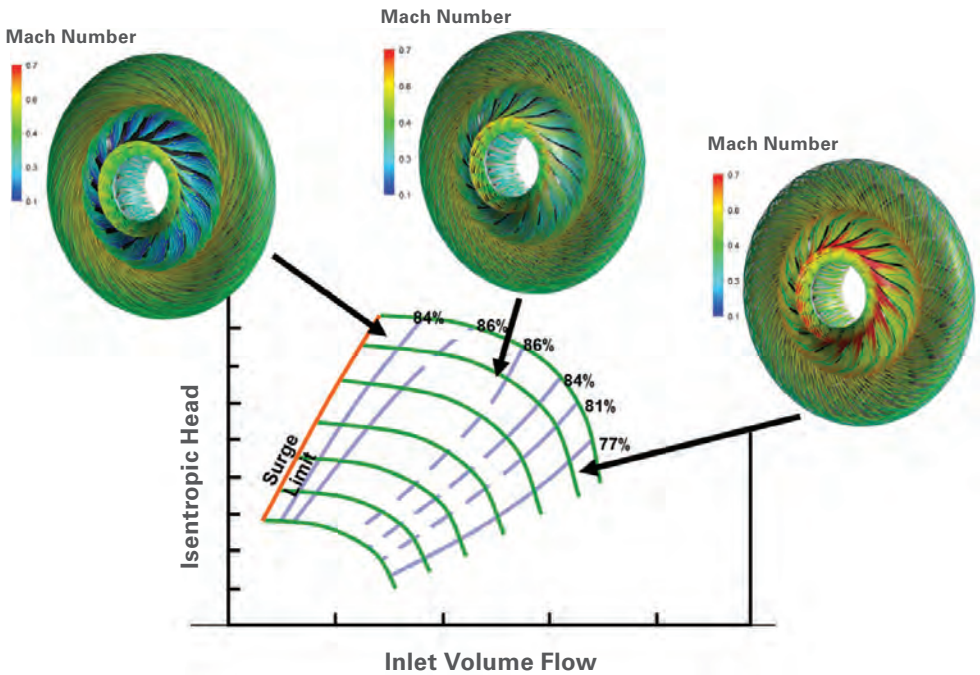


**Figure 3-23.** The highest efficiency is achieved at the center of the map, with reduced efficiencies at higher and lower flows.

for identical Mach numbers in all stages, but which is still a good approximation for cases where the machine Mach number changes by less than 10% (for single and two-stage compressors). The more stages the compressor has, the less deviation is acceptable. The fan law is based on the fact that if for two operating points A and B, all velocities change by the same factor (which in particular means that none of the flow angles change), then the compressor will show the following relationships between two different operating points.

$$\frac{Q_A}{N_A} = \frac{Q_B}{N_B}$$

$$\frac{H_{SA}}{N_A^2} = \frac{H_{SB}}{N_B^2}$$

$$\eta_A = \eta_B$$

These relationships are also used to define non-dimensional flow and head values, thus allowing comparisons for machines of different sizes and speeds.

Flow coefficient is designed as follows:

$$\varphi = \frac{Q_s}{\frac{\pi}{4} D_{1,tip}^2 u} = \frac{Q_s}{\frac{\pi^2}{4} D_{1,tip}^3 N}$$

And a head coefficient (isentropic or polytropic) is defined as:

$$\psi^* = \frac{H^*}{\frac{u^2}{2}} = \frac{2H^*}{(\pi D_{1,tip} N)^2} \quad \psi^p = \frac{H^p}{\frac{u^2}{2}} = \frac{2H^p}{(\pi D_{1,tip} N)^2}$$

For operation of a compressor, the distance of the actual operating point from the surge or stability limit is important. Any operating point A can be characterized by its distance from the onset of surge. Two definitions are widely used to define the margin.

$$SM(\%) = \frac{Q_A - Q_B}{Q_A} \cdot 100$$

This is based on the flow margin between the operating point and the surge point at constant speed and the turndown percentage.

$$Turndown(\%) = \frac{Q_A - Q_C}{Q_A} \cdot 100$$

It is based on the flow margin between the operating point and the surge point at constant head. For the test on a machine, which is usually conducted for various points at constant speed, as well as for machines that are operated at constant speed, the surge margin is a very useful parameter. For machines operated with variable speeds, it is more common to define the distance from surge by turndown.

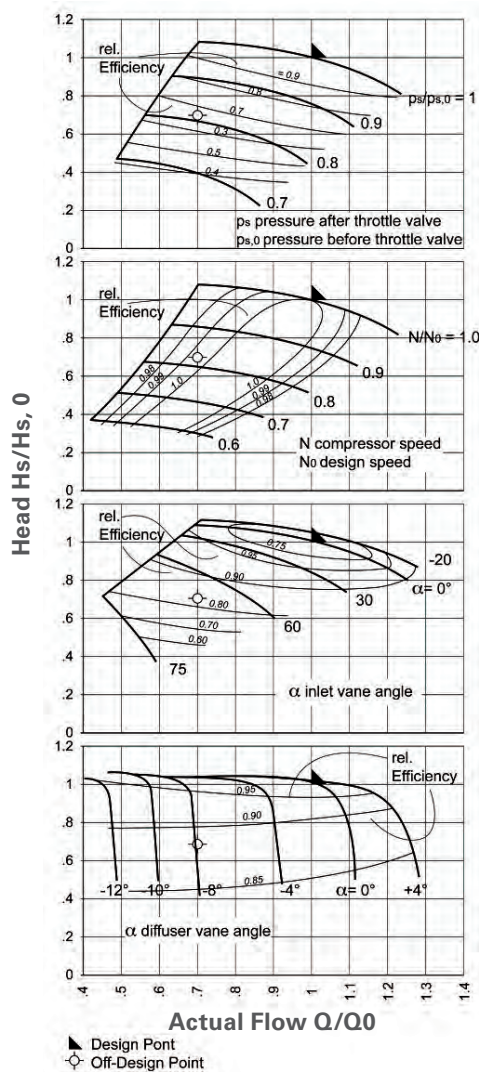
Variable speed has been introduced as a method to increase the operating range of a compressor, and thus as a means to adapt the compressor to varying process demands.

The following methods are available:

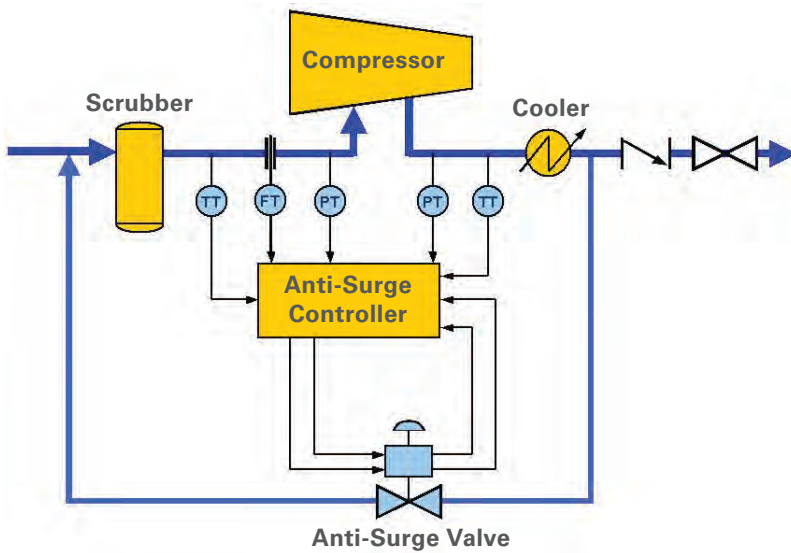
- Speed variation
- Adjustable inlet vanes
- Adjustable diffuser vanes enable the compressor to operate on a family of curves, as seen in *Figure 3-24*

Additionally, compressors can be controlled by:

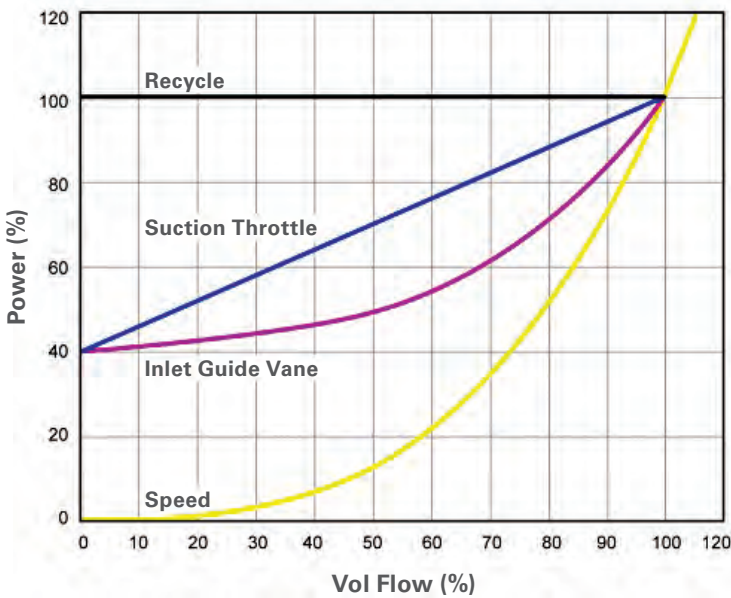
- Suction or discharge throttling (*Figure 3-24*)
- Recycling (*Figure 3-25*)



**Figure 3-24.** Control methods for centrifugal compressors (from top): suction throttling, variable speed, adjustable inlet guide vanes, and adjustable diffuser guide vanes (Rasmussen et al.).



**Figure 3-25.** Recycle System



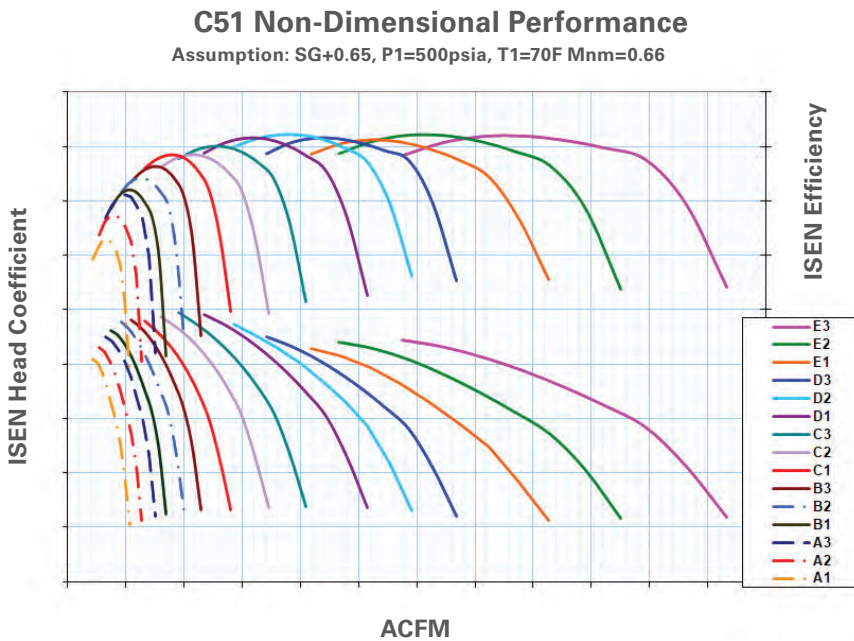
**Figure 3-26.** Power consumption for different control methods.

Figure 3-26 indicates the effectiveness and efficiency of different control methods. A compressor that can be operated at varying speeds in upstream and midstream applications is particularly important, since it is the most effective and efficient control method. Using a throttle, recycling or adjustable inlet vanes are very effective in reducing the volumetric flow, but they're not very efficient, because the power consumption is not reduced at the same rate as a speed-controlled machine.

## MULTISTAGE COMPRESSOR

So far, the focus has been on an individual compressor stage. Since the amount of head and pressure ratio of a single-stage are limited, multiple stages are often used in a single compressor, and all stages operate at the same speed. The stages operate in series, so the inlet conditions for each stage are defined by the discharge conditions of the previous stage.

If the head-flow-efficiency characteristics of a number of stages that were designed for different flows are known, the overall performance of a multistage compressor can be easily determined, and vice versa. Thus, a compressor for a given set of process requirements can be designed.



**Figure 3-27.** Head-flow-efficiency characteristics for 15 different stages.

For example, if the compressor speed and the inlet flow (together with a gas composition and the inlet temperature) are known, the flow coefficient for the first stage can be calculated. Say, this works out to be a flow coefficient of 0.11. Therefore, using *Figure 3-27*, the 'E1' first stage, which will have an efficiency of 87% and a head coefficient of 0.95, is determined. Knowing the head created by that stage, the pressure, temperature and density of the flow for the next stage can be calculated. This leads to determination of the actual flow, and the flow coefficient for the next stage, which may be 0.10. This then leads to selection of the next stage, the 'E1' stage, with a head coefficient of 1.0 and an efficiency of 86%. This information enables calculation of the inlet conditions for the next stage, and so forth until the last stage is reached. Table 3-1 shows an example for a compressor. Using this method to design a new compressor uses the described procedure in an iterative process, since initially, only the inlet conditions and the discharge pressure are known, but not the compressor speed, or the number of stages needed.

STAGES	D1	C3	C2	C2	C1	B3	Discharge
stage diam (in)	19.83	19.83	19.83	19.83	19.83	19.83	
phi	0.0590	0.0500	0.0430	0.0374	0.0325	0.0286	
psi isen	1.0533	1.0341	1.0138	1.0870	1.0351	0.9904	
eff isen	0.8667	0.8499	0.8312	0.8382	0.8358	0.7946	
Flow (ACFM)	6109.9	5181.0	4451.5	3871.8	3360.6	2959.6	2643.8
Press (psia)	500.00	626.36	771.68	936.49	1139.82	1361.14	1600.00
Temp (°F)	91.1	124.8	157.6	189.5	222.7	253.5	283.4

**Table 3-1.** Worked out example for a compressor design. The stage designations indicate the stage selections from the available stages for the compressor model (Figure 3-27), showing flow coefficient ( $\phi$ ), head coefficient ( $\psi$ ) and the efficiency of successive stages. Flow reduction, pressure build-up and temperature increase from suction to discharge are also shown.

## COMPUTATIONAL FLUID DYNAMICS (CFD)

While axial compressors successfully used two-dimensional (2D) CFD codes, the flow in a centrifugal compressor is inherently three-dimensional (3D). The rotating flow channel of the impeller plus a change in flow direction from axial inflow to radial outflow are the source of massive secondary flow regions that are dominated by large vortices. Another difficult task is the transition from the flow in the rotating reference frame, (i.e. in the impeller) to the flow into the stationary diffuser). 2D codes were used during the 1980s and early 1990s, known as the so-called streamline curvature methods. They were often used to create impellers that followed some prescribed velocity distributions known to the user as being advantageous to impeller performance. Most of the earlier codes also were so called inviscid codes, (i.e. they did not consider the impact of friction and turbulence). Using these codes as a basis for designing impellers and predicting their performance was difficult and not very accurate.

Similarly, calculating flows through seals on a rotating shaft was also challenging, because the shaft in a real machine does not rotate in concentric fashion. This leads to a continuous change in flow geometry. Particularly difficult are problems where aerodynamic forces impact the position and movement of the rotor, which in turn changes the geometry for the aerodynamic calculations. In addition, these changes are time dependent.

Over the last 30 years as computers became more sophisticated, gas turbine designers were able to perform some limited theoretical performance and efficiency calculations. Hundreds of different numerical methods have been developed, but in principle, most of them can be separated into two classes: streamline balance and computational fluid dynamics.

Developed in the early 1960s, streamline balance methods were employed until the mid-1970s. These methods were based on the concept that the streamline locations in a gas turbine's internal flow field can be determined from the interactions of the centrifugal, Coriolis and inertial forces on the fluid (air). However, experience showed that results from

the streamline balance method were not very accurate. These methods did not provide correct performance predictions utilizing new gas turbine component designs.

Since the early 1970s, significant efforts have been made by a large number of researchers to develop numerical methods for solving theoretical equations that describe the actual behavior and dynamics of a fluid. These equations are called the Navier-Stokes equations and, generally, are applicable to any fluid and boundary condition (*Figure 3-28*). The Navier-Stokes equation set consists of: continuity equation - conservation of mass; x,y,z equations of motion -  $F = m \cdot a$  (Newton's Second Law for a fluid); and an energy equation – first law of thermodynamics (energy is conserved).

The Navier-Stokes equations were originally derived by M. Navier in 1827 and S.D. Poisson in 1831. Historically, however, useful analysis of the equations is mostly associated with the work of L. Prandtl, T. v. Karman, H. Blasius, and H. Schlichting of the University of Gottingen in Germany between 1900 and 1930. Solutions to these equations are difficult since they are non-linear, non-homogenous numerical, rather than an analytical approach. They also coupled partial differential equations. Only for a limited number of very simple cases can exact analytic solutions be found. Thus, until modern computers became available in the 1970s, the Navier-Stokes equations were of very limited practical use for engineering applications. However, with the advent of high-speed computers, more complicated mathematical equations became solvable using the following:

$$\begin{aligned}
 \text{Continuity Equation: } & \frac{\partial \rho}{\partial t} + \frac{\partial(\rho u_i)}{\partial x_i} = 0 \\
 \text{Momentum Equation: } & \underbrace{\frac{\partial(\rho u_i)}{\partial t}} + \underbrace{\rho u_j \frac{\partial u_i}{\partial x_j}} = \underbrace{\frac{\partial P}{\partial x_i}} + \underbrace{\frac{\partial}{\partial x_j} \left( \mu \frac{\partial u_i}{\partial x_j} - \overline{\rho u'_i u'_j} \right)} + \underbrace{S} \\
 & \qquad \qquad \qquad \text{Unsteady} \quad \text{Convection} \quad \text{Pressure} \quad \text{Viscous/Turbulence} \quad \text{Source} \\
 \text{Scalar Transport: } & \frac{\partial(\rho \phi)}{\partial t} + \rho u_j \frac{\partial \phi}{\partial x_j} = \frac{\partial}{\partial x_j} \left( \gamma \frac{\partial \phi}{\partial x_j} - \overline{\rho u'_j \phi'} \right) + S
 \end{aligned}$$

**Figure 3-28.** Navier-Stokes equations in differential form.

Analytical solutions of the Navier-Stokes equations cannot be found for complex turbomachinery geometries and inlet/outlet boundary conditions. However, analytic solutions for simple geometries, such as cubes or wedges, if they have simple, uniform boundary conditions can be calculated. Thus, a complex-turbomachinery geometry is divided into thousands of simple geometries (cubes, bricks, wedges or tetrahedrals) that are individually solvable. *Figure 3-30* shows this for the complex geometry of a condenser fan. By matching the boundary conditions of each geometry in a sophisticated iterative-stepping process, a solution of the complete complex-geometry flow field can be found.

$$\begin{aligned}
& \iiint_{\forall} \frac{\partial \vec{U}}{\partial t} d\forall + \iint_{\sigma} [(\vec{E}_{inv}) dA_z + (\vec{F}_{inv}) dA_r + (\vec{G}_{inv}) dA_{\theta}] \\
&= \iint_{\sigma} [(\vec{E}_{vis}) dA_z + (\vec{F}_{vis}) dA_r + (\vec{G}_{vis}) dA_{\theta}] + \iiint_{\forall} H(\vec{U}) d\forall + D(\vec{U})
\end{aligned}$$

$$\vec{U} = \begin{Bmatrix} \rho \\ \rho V_z \\ \rho V_r \\ \rho r V_{\theta} \\ e_t \end{Bmatrix} \quad \vec{H} = \begin{Bmatrix} 0 \\ 0 \\ \frac{\rho V_{\theta}^2 + p}{r} - \frac{\tau_{\theta\theta}}{r} \\ 0 \\ 0 \end{Bmatrix} \quad \vec{E}_{inv} = \begin{Bmatrix} \rho V_z \\ \rho V_z^2 + p \\ \rho V_z V_r \\ (\rho + p) V_z \end{Bmatrix} \quad \vec{E}_{vis} = \begin{Bmatrix} 0 \\ \tau_{zz} \\ \tau_{zr} \\ r \tau_{z\theta} \\ q_z \end{Bmatrix} \quad D(\vec{U}) = \text{Scalar Artificial Dissipation}$$

$$\vec{F}_{inv} = \begin{Bmatrix} \rho V_r \\ \rho V_r V_z \\ \rho V_r^2 + p \\ \rho V_r r V_{\theta} \\ (e_t + p) V_r \end{Bmatrix} \quad \vec{F}_{vis} = \begin{Bmatrix} 0 \\ \tau_{rz} \\ \tau_{rr} \\ r \tau_{r\theta} \\ q_r \end{Bmatrix} \quad \vec{G}_{inv} = \begin{Bmatrix} \rho W_{\theta} \\ \rho V_z W_{\theta} \\ \rho V_r W_{\theta} \\ r(\rho V_{\theta} W_{\theta} + p) \\ (e_t + p) W_{\theta} \end{Bmatrix} \quad \vec{G}_{vis} = \begin{Bmatrix} 0 \\ \tau_{\theta z} \\ \tau_{\theta r} \\ r \tau_{\theta\theta} \\ q_{\theta} \end{Bmatrix}$$

**Figure 3-29.** Integral form of the Navier-Stokes equations in cylindrical coordinates.

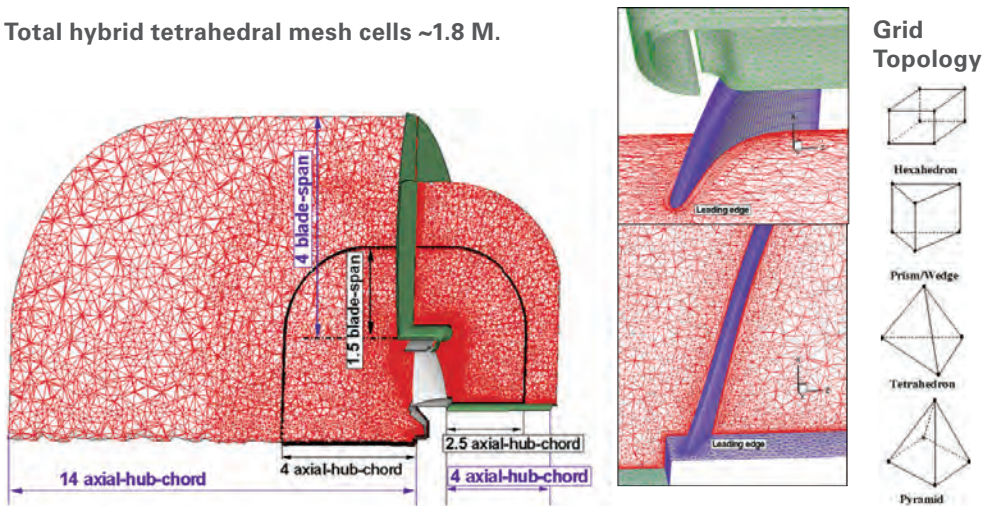


**Figure 3-30.** Computational mesh for a condenser fan.

This is a computationally very intensive method that enables the analysis of the internal flow field of many complicated turbomachinery component geometries. Accurately modeling the gas compressor as a whole is still many developmental years away, particularly because the interaction between fluid forces and the rotor, as well as heat transfer effects, and the behavior of real gases have to be included. Nonetheless, once the internal flow field of a turbomachinery component is known, the component's efficiency and pressure drop can be calculated, and the results can be easily integrated into the model for multi-stage compressors. Similar numerical methods exist for the analysis of rotordynamic and vibration applications.

Following is a brief discussion of three commonly employed CFD methods, their assumptions, limitations and applicability. Any type of CFD analysis approximates the real world. The real flow is approximated by more-or-less accurate mathematical models, which usually don't lend themselves to analytical solutions, but have to be solved by approximately accurate numerical methods.

**Potential Flow Method (1930-1965):** Potential flow assumes that the fluid is irrotational, inviscid and incompressible. Turbulence, boundary layers or flow unsteadiness cannot be directly modeled. This type of method is limited to large Reynold's number gas flows, typically external flows such as subsonic flow around an airplane wing or propeller. Frequently, to account for the boundary layer losses, the method is coupled with a simple, empirical boundary displacement function. Since the method assumes incompressible flow, no density changes can be modeled, which makes it useless for compressor or turbine applications. For internal gas turbine component flow analysis, this method is not adequate.

**Euler Method (1970-1985):** CFD programs using the Euler method solve the Navier-Stokes equations, but neglect the terms that account for viscosity, i.e. the fluid is inviscid. Since turbulence and boundary layer are both viscosity functions, the Euler method cannot account for either. However, since the Euler code does not assume irrotational flow and allows for density changes, it is significantly more accurate than the Potential Flow Method for compressible flow. Euler codes are often employed to analyze internal turbomachinery flows, however, because viscosity is not modeled, it can be inaccurate, especially for turbulent flows with fluid separation and recirculation. This is particularly an issue for centrifugal compressors, because many flow structures inside of an impeller (so called secondary flow) are caused by viscous flow interactions.

**Full Navier-Stokes Solvers (1980-Present):** The Navier-Stokes solver evaluates the full set of equations for fluid dynamics. Since the length and time scales of turbulence are too small to be properly modeled, Navier-Stokes solvers still typically employ simplified methods to account for the effects of turbulence (so called turbulence models). Navier-Stokes solvers can be very accurate, but are extremely computationally intensive. In recent years, Navier-Stokes solvers have become a standard tool in the turbomachinery industry. Nonetheless, because of the many assumptions for boundary conditions and turbulence modeling that must be made, even with the full Navier-Stokes solver, computational results need to be carefully vetted with actual tests.

Today, it is possible to model the aerodynamic behavior of entire compressors, thereby resolving unsteady flow (*Figure 3-30*). Modeling entire turbomachines creates the difficulty that some components rotate, while others are stationary. For the rotating components, the flow from the stationary components appears unsteady, and for the stationary components, the flow from the rotating components appears unsteady. In other words, the code must compute unsteady flow.

The capability to model the interaction between aerodynamic forces and the rotordynamic allow for more precise determination of destabilizing forces on a rotor. Other classes of problems are also solvable with great accuracy, including flows where real gas behavior becomes important, or gas flows with solid or liquid particles.

Many techniques are available to model the flow inside a gas compressor. In the future, the Solar team expects to completely design gas compressors and optimize them solely using a computer, without ever having to build a prototype. Currently, however, the state of the art for CFD technology lags behind. Computational results are often inaccurate and need test validation.

CFD modeling and analysis can be expensive and time intensive, depending on the number of components that have to be analyzed, and the accuracy of the results required. Transient, non-steady-state calculations exponentially increase the effort. Typically, CFD models provide good insights into flow structures, but may encounter problems supplying accurate predictions for bulk characteristics such as stage mass flow or stage efficiency. It also must be stressed that in order to achieve correct results, the user has to be quite experienced in using the code and interpreting the results. Ubiquitous inaccuracies are caused by modeling errors (i.e., the numerical model is not identical with the physical reality), numerical errors (the solution of the programmed equations is not accurate), convergence errors (calculations are stopped after too few iterations to save time), application uncertainties (inlet or exit conditions, or geometry are not precisely known),

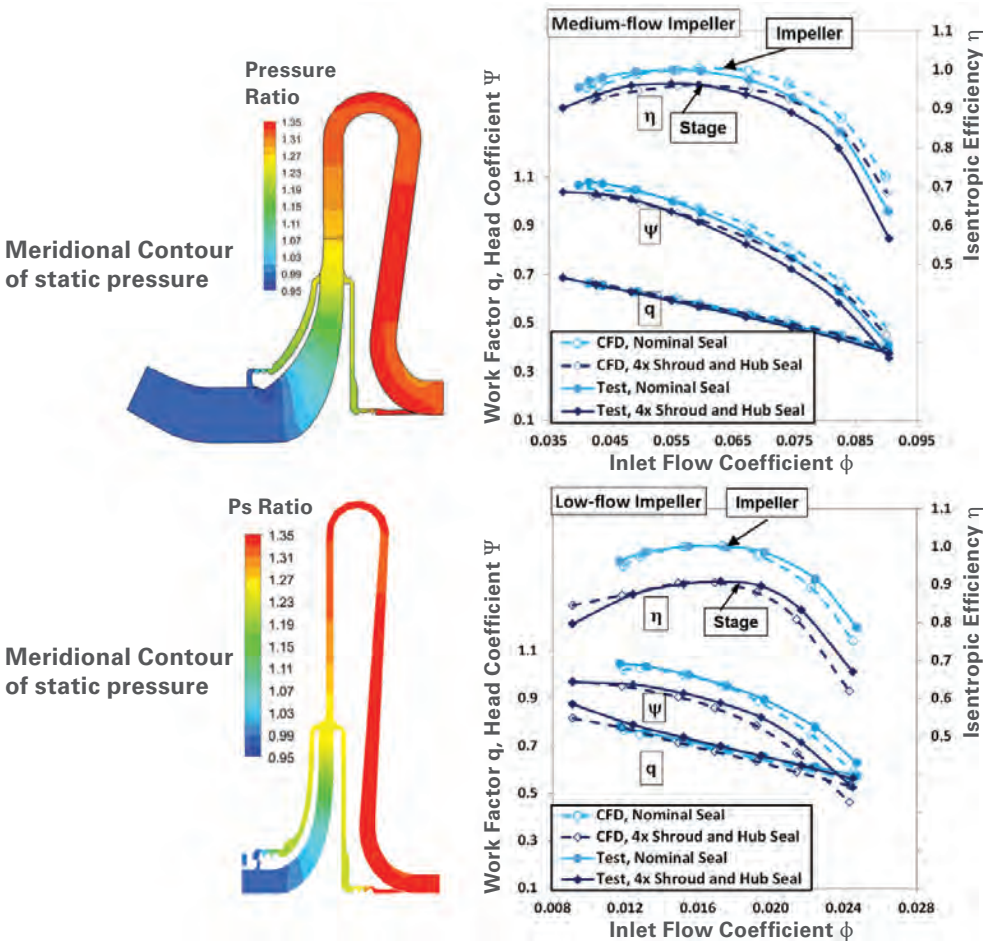


**Figure 3-31.** Performance validation for medium-flow and low-flow stages, including the simulation of different hub and shroud seal clearances.

user errors (use of the wrong model, neglect of structures that influence the flow, etc.), and code errors (“bugs”). Detail problems, such as the transition from laminar to turbulent flow, are still not entirely resolved. All calculations, therefore, need to be calibrated against reliable test data. However, the detailed insight in flow structures has yielded numerous detail improvements, leading to higher compressor efficiencies, and improved reliability. Thus, a combination of experimental results with CFD is currently the most sensible design approach for gas turbines. The compressor engineer should never base a design decision solely on CFD results.

Today, CFD can be used for inverse calculations (i.e., a favorable flow field is defined, and the blade shapes to match the flow field are calculated), or to calculate the interaction of liquid droplets in Dry Gas Seal gaps. The interaction between aerodynamic forces and the lateral rotor or seal movement can be modelled, thus allowing a more precise determination of de stabilizing forces.

CFD calculation can also be used to optimize the manufacturing process for the impeller, for example, by combining the CFD calculations with the model of machining tools, thus enabling single-piece impellers to be machined. In general, CAD models of geometries can be used to define these geometries in the CFD tool (Figures 3-31 to 3-34).

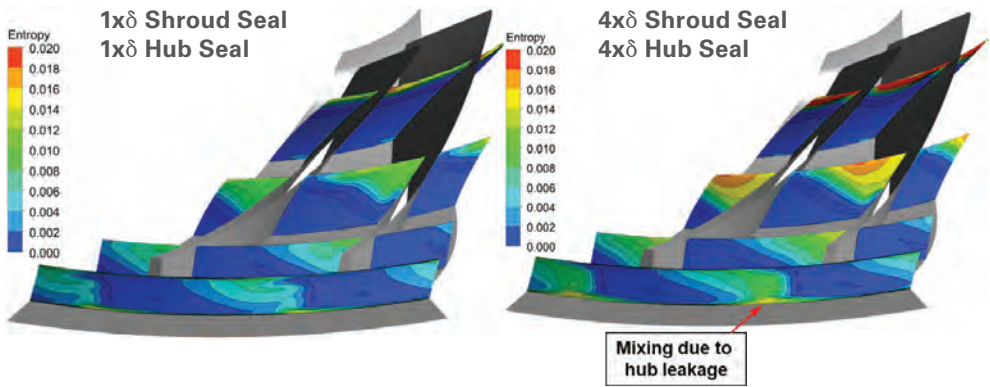


**Figure 3-32.** Detailed CFD analysis of the passage flow in an impeller, and the impact of increased seal clearance.

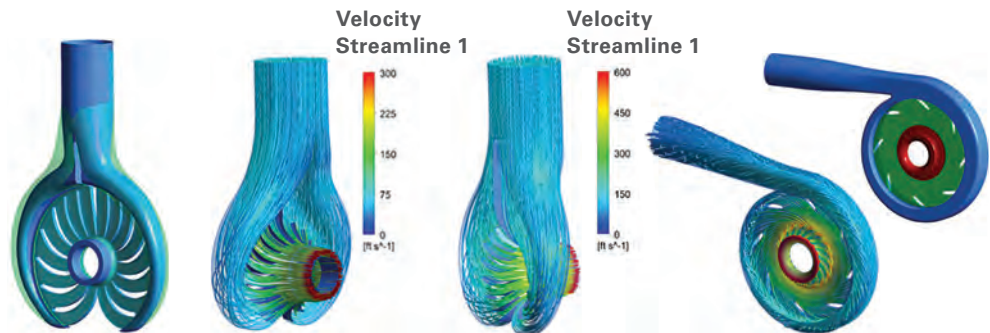


**Figure 3-33.** Flow simulations for complex inlet and discharge geometries.

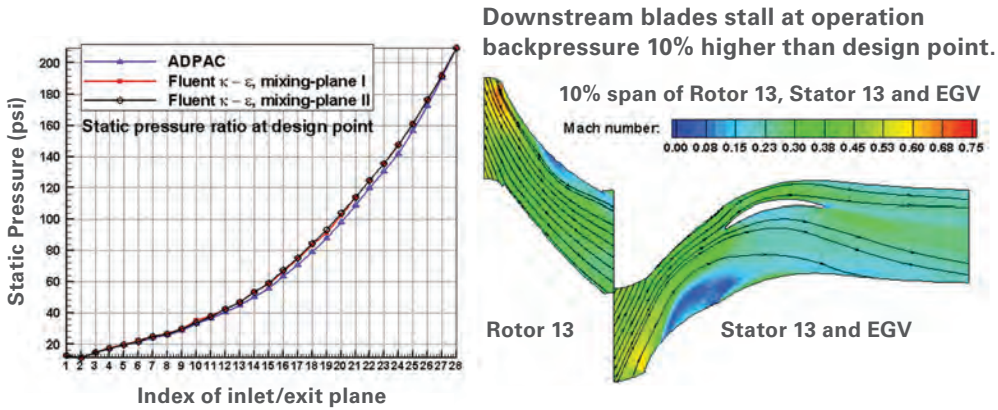


**Figure 3-34.** Simulation of a 13-stage axial compressor, showing stall on the last stages when the backpressure is increased to 10% above design pressure.

### FROM CONCEPT TO FINAL STAGE

During the preliminary design, trade-offs between performance, mechanical rigidity and rotor dynamic behavior are made. Some of the design trade-offs made during the preliminary design phase are listed in Table 3-2.

Design Feature	Disciplines Impacted
Impeller tip speed	Aero, structural
Impeller blade thickness	Aero, structural, and castability
Impeller blade angles and shape	Aero, structural
Impeller blade height	Aero, structural
Impeller blade fillet size	Aero, structural, and castability
Impeller shroud thickness	Structural, vibration, and castability
Stage length, bearing span	Aero, structural, and rotor dynamic
Impeller hub diameter	Aero, rotor dynamic, and structural
Diffuser diameter	Aero, cost, and weight

**Table 3-2.** Design trade-offs during preliminary design phase.

During the preliminary design phase, impellers are sized to develop the head identified during the conceptual phase. Impeller head-making capability is controlled by two basic geometric parameters: blade turning and tip diameter. Tall impellers can generate large amounts of head but at the expense of high tip speeds, which increases blade stresses. In addition, this high head can decrease specific speeds, lowering the efficiency potential of the stage. Short impellers are limited by the amount of turning they can efficiently impart

on the flow. Optimization studies are conducted to determine proper amounts of turning and tip diameter to meet the required head, while maintaining acceptable impeller tip speeds.

For a gas pipeline compressor, overall head requirements are lower, typically below 90 kJ/kg, and can be met with one or two stages of compression. This stage count requirement helps to determine overall shaft length which influences rotor dynamic behavior. Since rotational speeds of the compressor are established by the turbine engine, rotor dynamic tools can be used to set axial lengths. To maximize efficiency, impellers with long axial lengths are used to minimize curvature effects on the flow stream. Rapid increases in curvature increase local gas velocities inside the blade passages, which must later be diffused. Diffusion always incurs loss and decreases efficiency. Minimizing curvature throughout the machine maximizes the efficiency potential of the compressor.

For the production compressor, head requirements are much higher, thus stage counts can range from two to 10 stages, and intercooling may be required. This leads to longer shafts. To maintain rotor dynamic stability, larger shaft diameters are required. This increases the hub diameter. The high stage counts require axially shorter stages than those used in a gas pipeline compressor. The combination of shorter stages and a larger hub diameter increases flow path curvature, thus decreasing the efficiency potential for the production compressor relative to the gas pipeline compressor.

To help during the preliminary aerodynamic design, a one-dimensional code is used to design the basic dimensions of the stage and predict its performance. Using a built-in database of compressor test data augmented by Solar's own experience, a 1D-Code can quickly size a compressor and predict its performance. This allows for many iterations and "what-if" scenarios to be performed in arriving at an optimum design. Trade-offs between tip speed and turning can be quickly determined.

## **DETAILED DESIGN**

Detailed design is where the engineering sketches become detailed drawings. Further optimization occurs at the component level to ensure mechanical integrity, rotor dynamic rigidity, manufacturability, and aerodynamic performance goals are met.

**Aerodynamic Design Tools** - For detailed blade design, a CAD based tool allows for rapid geometric modifications of impellers, flow paths and return channels. Intuitive screens provide the designer with tools to easily change blade angle distributions through the blade passage, as well as blade thickness and flow path shape. Plots of curvature and slope help to guide the engineer to quickly optimize component shapes.

Computational Fluid Dynamics (CFD) has now reached a maturity level in both accuracy and speed, making it an effective design tool. Using proprietary tools, blade geometry and fluid information, or boundary conditions are quickly defined and analyzed. Solutions that required eight to 10 hours to obtain a decade ago now take 20 minutes. Improved GUI based software enables engineers to quickly process the solutions and visually display areas of high loss, which can be addressed on the next iteration. CFD is also used for complex geometries such as radial inlets and volutes. Using solid models, unstructured

meshes can be quickly generated and analyzed for extremely complex geometries. The CFD results help to identify regions of high loss generated by the geometry, and the software then facilitates easy geometrical modifications to reduce or eliminate these regions.

**Structural Analysis Tools** - Finite element analysis (FEA) has also become an integral part of the structural design process, resulting from vast improvements in computer hardware and software. More rapid finite element analysis is made possible by the ability to quickly input detailed information, develop a solution and interpret the results. These new tools do not necessarily replace classic manual calculations that have and will continue to be used, but are a supplement to them. The new tools have the capability to analyze and design components that previously were sized by either iterative testing or conservative scaling from earlier designs. The benefit is that complicated parts are no longer needlessly oversized. Oversized structural components, such as casings, drive up the weight and cost of the compressor, and in the case of aero components, can significantly degrade compressor performance.

The compressor component most significantly affected by improvements in structural analysis is the impeller. The aero requirements of high head, high efficiency and wide operating range, when combined with the need to have a shroud on the impeller produce blade shapes subject to high stress. Prior to FEA, accurate analytical predictions of stress in the impeller's shroud and blades were very difficult. Normal practice was to design the impeller for aero performance, and then conduct destructive structural testing that was expensive, time consuming, and provided minimal opportunity for optimization.

Return channels are designed with the same tools and methodology as the impellers. The only structural concerns for the return channels are assembly bolts that hold the return vane to the diaphragm and must penetrate through the vane itself. Deflections caused by pressure loads are also a concern. Evaluating the return vane at the case maximum operating pressure checks these deflection loads.

By using the modular rotor design approach, mechanical and rotor dynamic advantages can be realized by incorporating solid stator diaphragms. With the elimination of a split-line in the stator diaphragm, less axial length is needed to maintain the same deflection levels. This decreased axial length results in shorter shaft lengths for an equivalent split-stator compressor with the same number of stages. Combined with the larger hub diameter for the modular rotor design (see Compressor Design Objectives), Solar multi-stage compressors have a stiffer, shorter shaft than those using solid shafts with interference-fit impellers and split-stator diaphragms.

FEA validates one of the advantages of the modular rotor design. Centrifugal stiffening can be seen in *Figure 3-35* that compares a modular rotor to an interference fit impeller. For the modular rotor, centrifugal forces work advantageously on the pilots and interlocking surfaces, tightening with speed. For the interference fit impeller, centrifugal forces work to pull the impeller away from the shaft. To offset this force, higher levels of interference are needed, affecting the balance of the assembly.

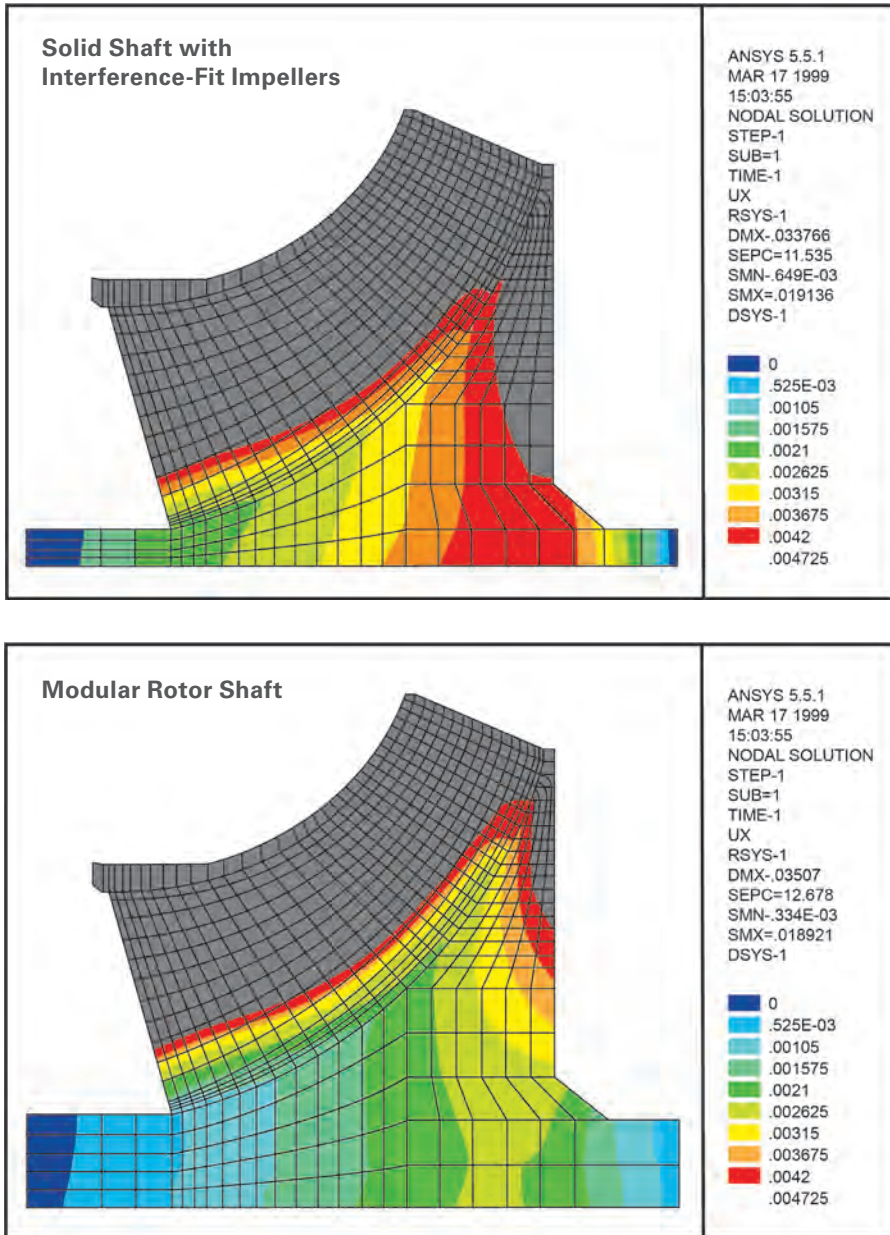


**Figure 3-35.** FEA showing modular shaft design has increased stiffness from centrifugal forces relative to the solid shaft.

### AXIAL THRUST

Thrust loads of centrifugal impellers are the result of a pressure imbalance between the front face and the rear face of the impeller. The sum of these forces over all impellers and the forces created by the balance piston constitute the resulting load on the compressor thrust bearing (*Figure 3-36*).

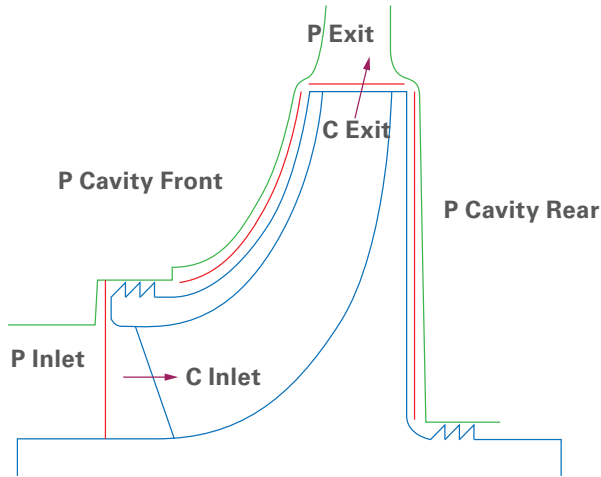


**Figure 3-36.** Forces on the impeller.

From the axial momentum equation that considers the change of the axial momentum of the gas, and the forces due to the static gas pressure in the axial direction:

$$\oint \rho \vec{C} (\vec{C} \cdot d\vec{A}) = \oint p \cdot d\vec{A} + \vec{F}$$

The forces on the impeller as shown in (Figure 3-36) result.

$$\vec{F}_{impeller} = \vec{F}_{momentum} (c_{exit} \cdot c_{inlet}) - \vec{F}_{pressure} (P_{cavity, front} \cdot P_{cavity, rear} \cdot P_{inlet} \cdot P_{exit})$$

The front and rear cavities are formed between the impeller tip and the labyrinth seals at the impeller inlet and the impeller hub seals.

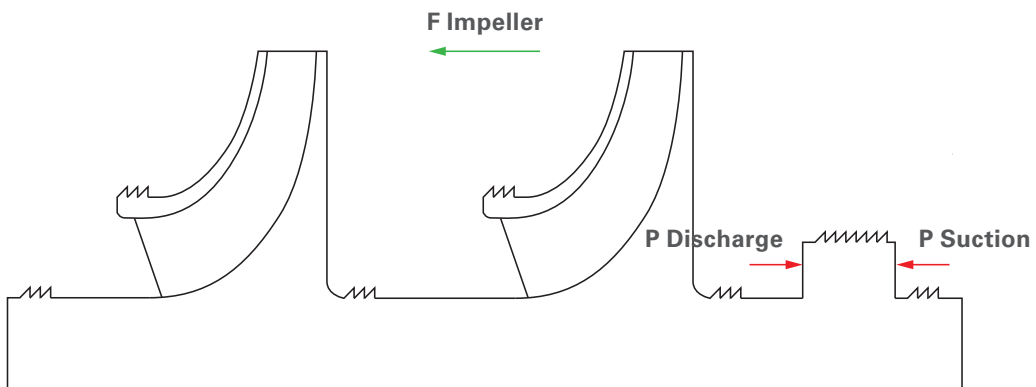


**Figure 3-37.** Balance piston.

The force on the thrust bearing is shown in (Figure 3-37).

$$\bar{F}_{thrustbearing} = \bar{F}_{impeller} - \bar{F}_{balancepiston} (P_{discharge} \cdot P_{suction})$$

In the simplest approach to calculating the forces on the impeller, one would assume the pressure in the front and rear cavities to be equal to the pressure at the impeller tip. In a shrouded impeller, however, the gas in the cavity is subject to swirl, and as a result, the static pressure at lower radii is lower than at the tip. The amount of swirl is a function of the cavity geometry, and the leakage flows through the labyrinths.

The cavity static pressure distribution can be calculated by:

$$p(r) = p_{tip} - \frac{1}{2} \rho (q\omega)^2 (r_{tip}^2 - r^2)$$

accounting for the cavity characteristics by introducing a cavity swirl coefficient (q).

A simple approach would assume constant swirl coefficients for front and rear cavities. This approach is frequently used in the industry, but high pressure compressors require more accurate estimates. Correlations and CFD analysis (Figure 3-38a) are utilized for these, along with subscale test measurements for validation.

The fact that the swirl coefficient changes when the impeller is operated away from its design point (Figure 38b) is of particular importance for off-design operation. Also, the magnitude of the swirl coefficient on the impeller backside changes in the opposite direction from the swirl coefficient on the impeller frontside. This means that the thrust imbalance (for a given pressure level and a given speed) changes not just due to the pressure difference between the impeller eye and the corresponding backside, but also due to different cavity swirl factors at the front and back of the impeller. This imbalance, in particular, changes when the compressor moves from the design point to choke. In general, the shroud side swirl is higher than the backside swirl, a result also reported by Koenig et al, 2009.

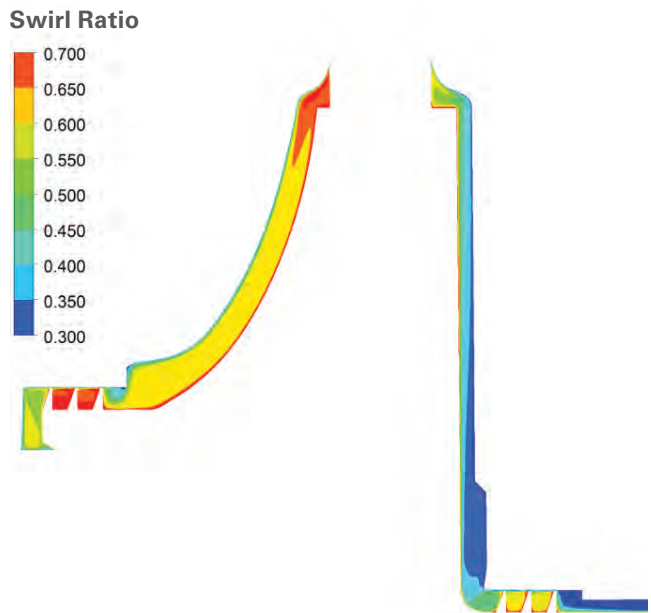


**Figure 3-38a.** Swirl ratio in the shroud and the backside cavity.

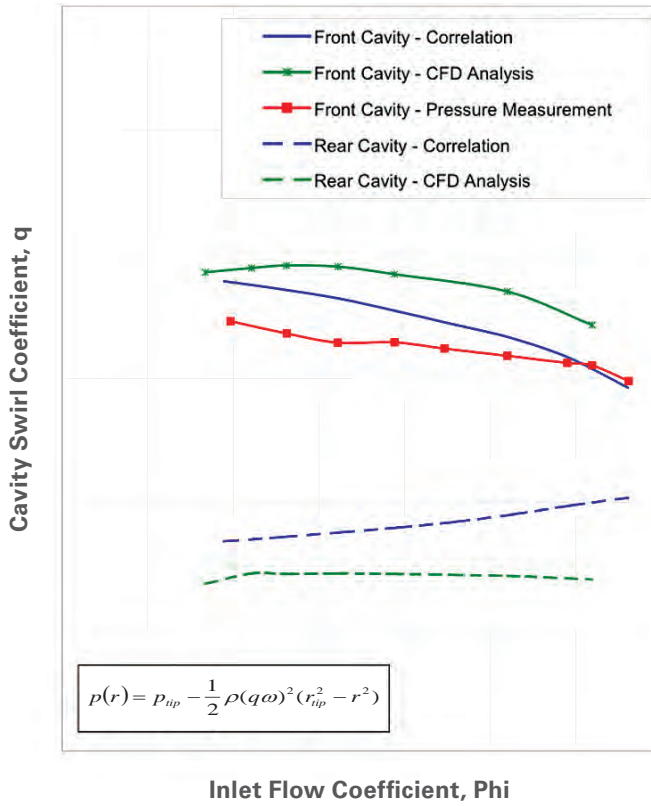


Figure 3-38b. Cavity swirl coefficient for a medium-flow stage at different operating points.

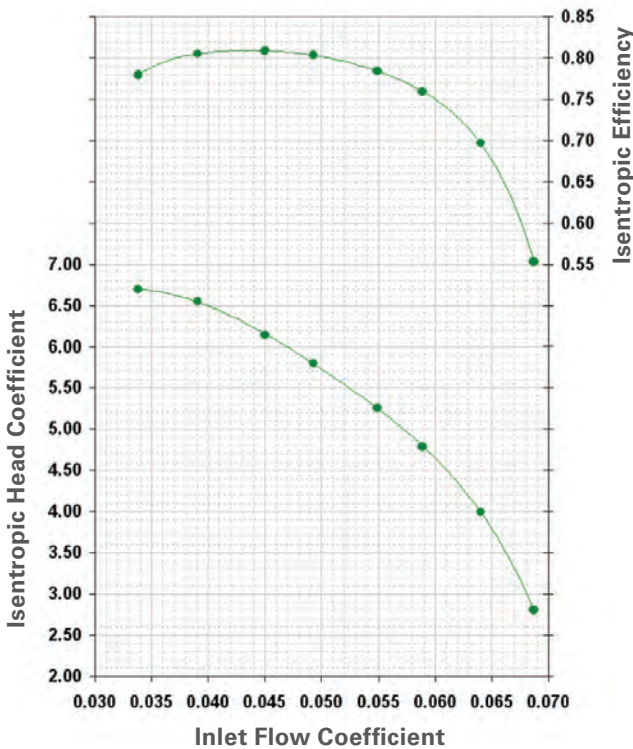


Figure 3-39a. Non-dimensional map for a multistage compressor.

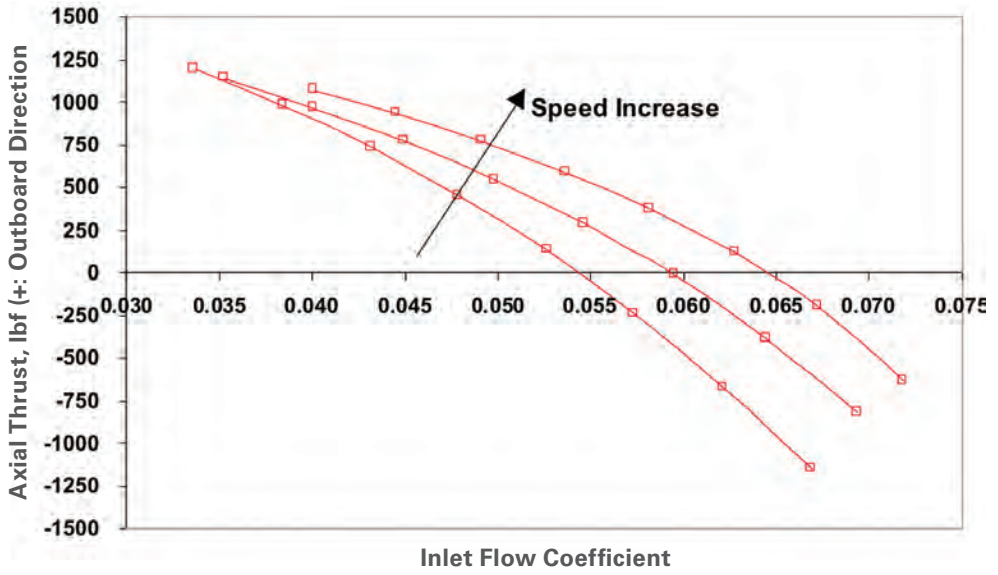


Figure 3-39b. Change of axial thrust with operating point.

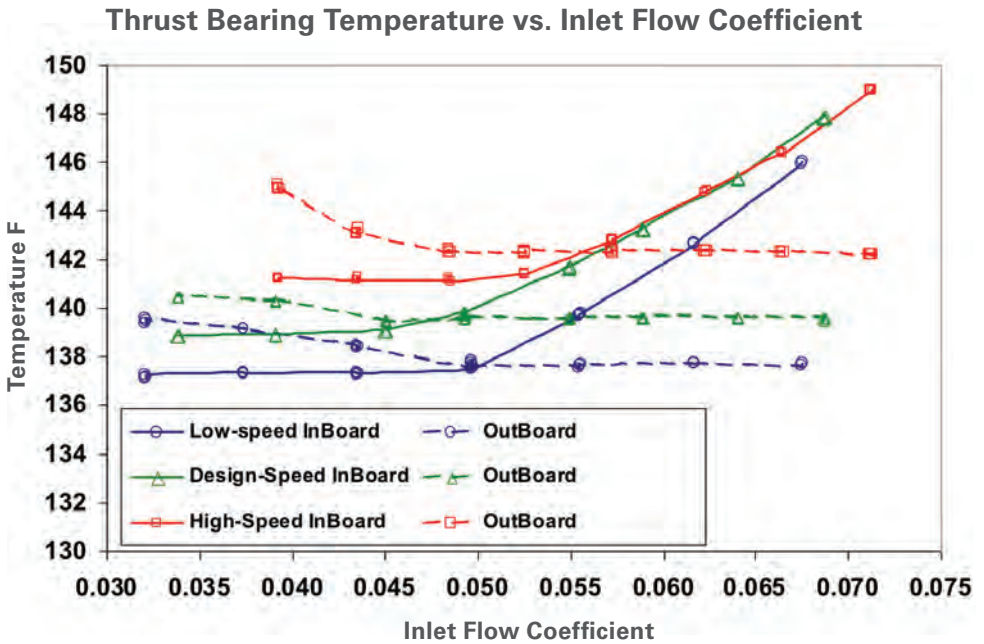
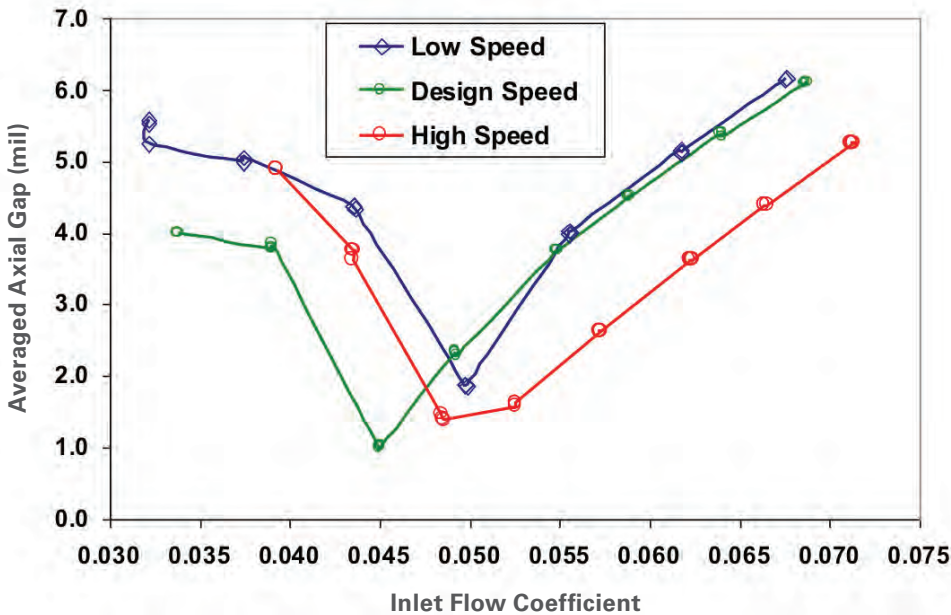


Figure 3-39c. Thrust bearing temperature as a function of operating point.

### Axial Gap vs. Inlet Flow Coefficient



**Figure 3-39d.** Axial position of the rotor as a function of the operating point.

Because the thrust load has a direct impact on the thrust bearing temperature, which can be conveniently measured, *Figures 3-39a-d* establish the correlation between non-dimensional operating point (*Figure 3-39a*), thrust load at different speeds (*Figure 3-40b*), the resulting bearing temperature of the loaded and unloaded pads of the thrust bearing (*Figure 3-39c*), as well as the axial position of the rotor as a result (*Figure 3-39d*). The inboard bearing shows a significant increase in temperature (albeit not to a level that would cause concern) when the compressor enters the choke region. The outboard bearing shows a much lower increase in temperature when the operating point moves towards surge. For this particular application, with the particular selection of the balance position size, the thrust load reverses direction, which explains the behavior of the inboard and outboard bearing temperatures. Of course, the bearing temperature also increases with speed. As a result of the thrust load changes and the changing load capacity of the thrust bearing with speed, the axial gaps for all speeds are fairly close together, but change significantly when the compressor is operated from design point to surge or into choke.

When comparing the magnitude of the forces acting on the impeller (*Figure 3-40*), the pressure from the inlet eye and the pressures in the cavities are usually dominant, but act in opposite directions. In general, they generate a resulting force, but much smaller than the pressure forces, in the direction of the compressor inlet, this is not always the case. The momentum force, generated by deflecting the gas from more or less axial to more or less radial direction, is usually much smaller than the pressure forces. At very high discharge pressures near choke, when the pressure differential over the impeller is rather small, the momentum force can become dominant, and create a net force towards the discharge end of the compressor.

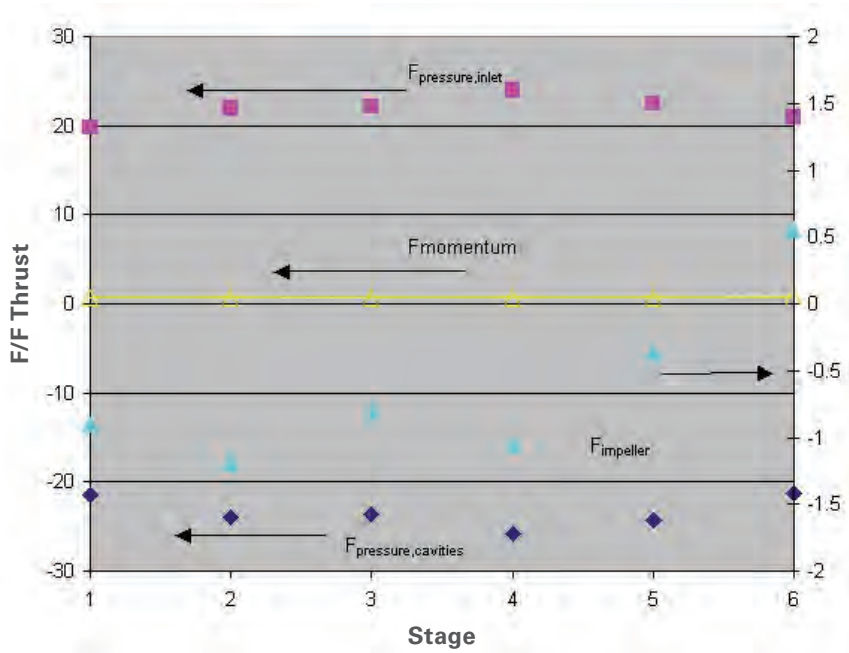


Figure 3-40. Contributing forces to the impeller thrust in a 6-stage compressor.

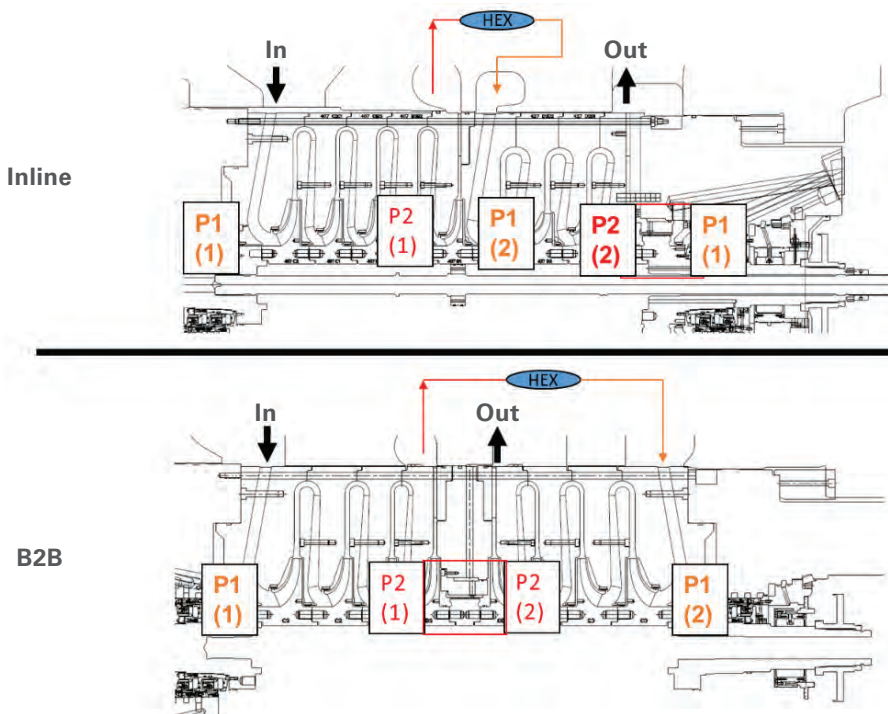
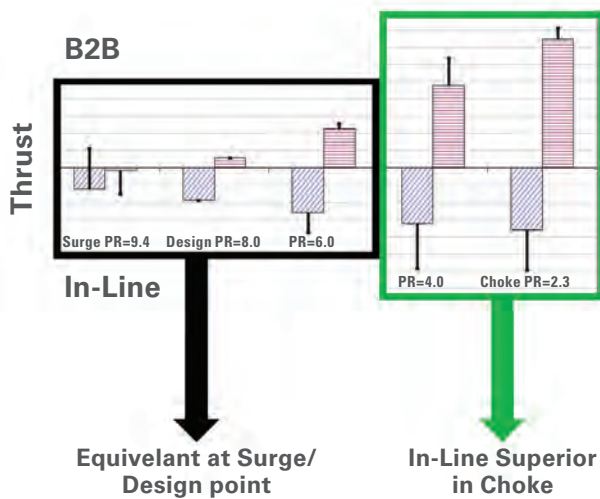


Figure 3-41. Inline and back-to-back arrangements.

The descriptions in this section are based on shrouded impellers. As opposed to open faced impellers that have free standing blades, the blades in shrouded impellers are covered. Therefore, the pressure distribution on the front face of the impeller is governed by the impeller discharge pressure and the impact of swirl flow. In an open-faced impeller, the pressure distribution would be governed by the pressure build up in the impeller flow passages.

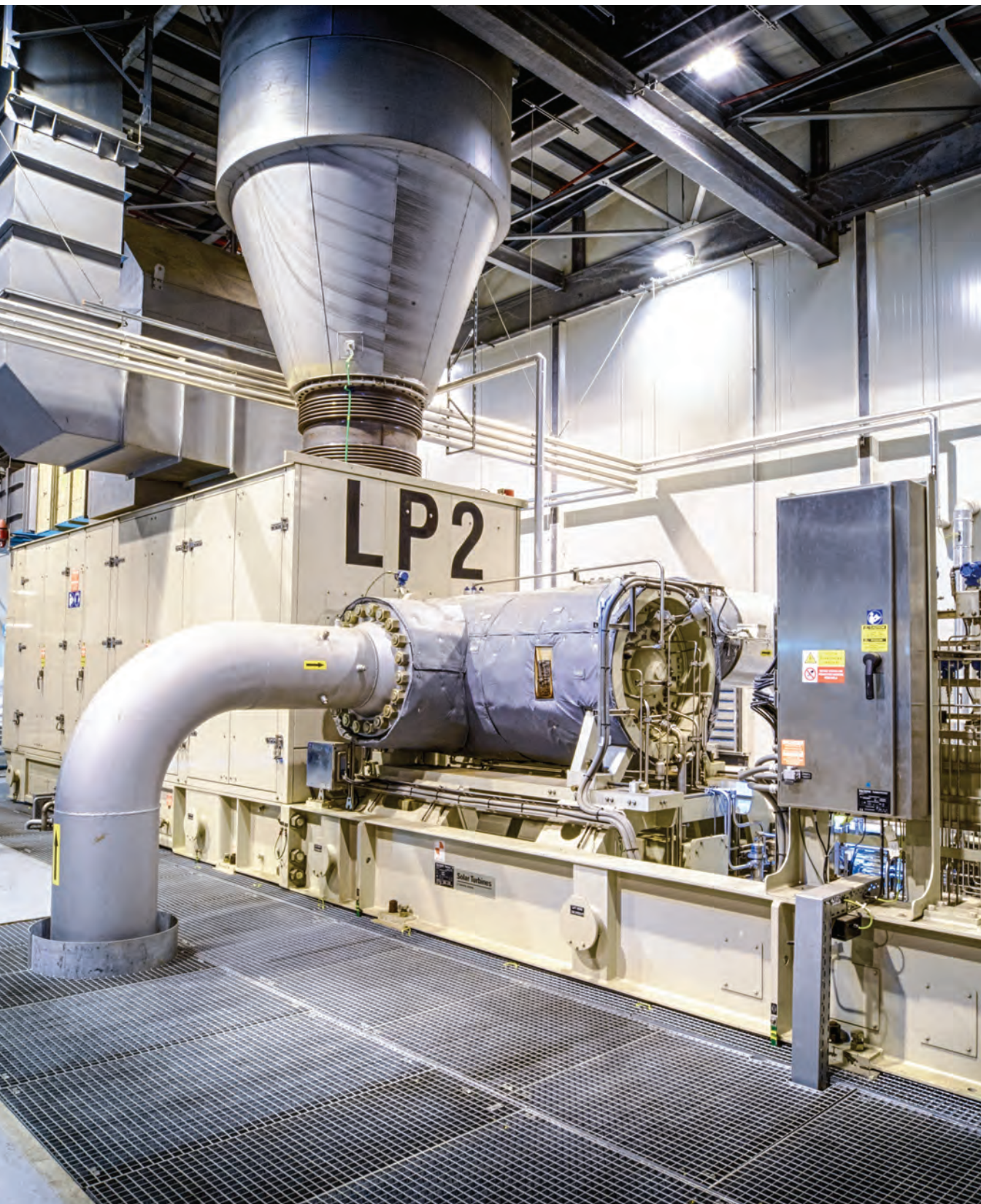
Considerations as described above can be used to determine the relative benefits of back-to-back versus inline arrangements for compressors with two sections (*Figures 3-41 and 3-42*). They show that back-to-back arrangements have a larger change in thrust load from surge to choke than in-line arrangements. This is especially evident if the operating conditions for the individual sections can change independently. They are also more sensitive to asymmetrically worn seals.

Another finding is the impact of thrust variations due to tolerances in seal clearances, but also due to compressor deterioration from fouling or erosion, especially for compressors operating at very-high-pressures.



**Figure 3-42.** Variation of axial thrust from surge to choke, for inline arrangements versus back-to-back arrangements.





## CHAPTER 4

# ROTOR DYNAMICS

*Balaji Venkataraman, Marco Vagani, Rainer Kurz*

The principal moving mechanical components (*Figure 4-1*) of any gas compressor are the shaft, and with it the impellers, bearings and various seals. The shaft in a centrifugal compressor may rotate at speeds between 3,000 and 25,000 revolutions per minute, with the impeller tips reaching over 1100 ft/s (350 m/s). The shaft is supported by two journal bearings. These are typically hydrodynamic, tilting pad-bearings, but they can also be magnetic bearings. The impellers of the compressor are either arranged between the bearings, or, for so-called overhung designs, outside the bearing span.

In addition, an axial thrust bearing compensates for the residual axial thrust load.

Fluid film bearings utilize petroleum-based or synthetic oil to act as a lubricant and coolant between the moving shaft and the stationary bearing surfaces. Bearings function to transmit the static loads and dynamic vibration forces.

When the compressor shaft rotates at high angular speeds, small imbalances or eccentricities in the shafts due to manufacturing imperfections or mechanical/thermal stresses are amplified and can create significant forces on the compressor bearings and cause shaft deflection. In addition, especially for high gas pressures and high gas densities, aerodynamic forces acting on the impellers and seals can create destabilization effects. These concerns are covered in the discussion of lateral rotordynamics.

In addition, the drive train (driver, couplings, gearboxes, compressors) are also subject to torsional excitation, and the resulting torsional vibrations.

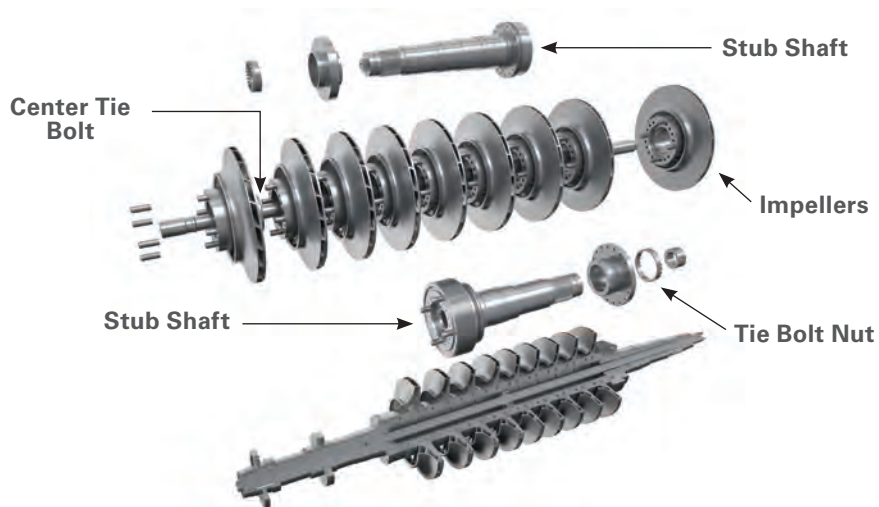


**Figure 4-1.** Rotor design

If any of these forces are not adequately controlled, catastrophic failure may be the consequence. Hence, you can see the importance for the compressor designer to understand and predict the shaft and bearing rotordynamic forces.

The primary design goal of rotordynamics is to assure that the compressor is stable under the required operating conditions. One of the most critical aspects of compressor design is the ability to predict the behavior of the rotor. The quality of the prediction depends on the modeling accuracy of the rotor and its support system, including bearings, pedestals and casing into a computer model. Ultimately, actual test data determine the accuracy of predictions, and the capability of the compressor to operate reliably and in a stable fashion.

A benchmark is defined by meeting or exceeding American Petroleum Institute 617 [1] requirements for centrifugal gas compressors. The following design requirements were established in order to achieve this goal:

- Insensitive to unbalance
- Operating below bending mode
- Critically dampened lower modes
- High stability margin

The primary rotordynamic considerations are the vibration level at operating speeds and the location of the resonant frequencies. The compressor rotor should be insensitive to unbalance throughout the operating speed range. Inevitably, rotors will have residual unbalance that appears as speed-synchronous vibration during operation. The rotor system should be able to accommodate the API residual unbalance limit without exceeding the vibration limit.

Finite element-based rotordynamic analyses, coupled with advanced fluid-film bearing analysis, form the base of the tools for rotordynamic analysis. Other component analyses, such as for labyrinth and oil seals, must be considered. Major advances in recent years came from improvements in the areas of bearing-rotor interaction, seal-rotor interaction, impeller-rotor interaction and modeling of bearings. The improvements in bearing models, for example, result from a better understanding of the behavior of the lubrication oil once it enters the bearing. Obviously, the local temperature of the lubrication oil has a significant influence on the local viscosity of the oil and, thus, of the damping characteristics of the bearing. Proven tools and a large number of tested configurations combined with pre-engineered rotor systems provide a high degree of confidence in predictions.

Over the next pages, you'll be presented with a basic explanation of mechanic and dynamic theory for compressor rotordynamics. The discussion starts with lateral rotordynamics, and the torsional behavior will be covered in the second part.

### **Vibrations of a Simple Mass-Spring Damper System (Single Degree of Freedom)**

Analyzing a significantly simplified mechanical model is a good place to start. The assumption is that shaft vibrations can be simulated by modeling the shaft as a single stationary mass ( $m$ ) with one fixed support (bearing). Naturally, this single support bearing would possess a certain physical stiffness ( $k$ ) and damping ( $c$ ) characteristic. *Figure 4-2* shows a schematic of this simple mass-spring damper system.

After applying Newton's second law ( $f=ma$ ), the following equation of motion for this single-degree-of-freedom system is derived:

$$ma + cv + kx = f$$

where (a) is the acceleration, (v) is velocity, (x) is the displacement, and (f) is an external force. The above equation can easily be rewritten as an ordinary differential equation:

$$m \frac{d^2 x}{dt^2} + c \frac{dx}{dt} + kx = f$$

For now, the damping ( $c = 0$ ) and the external force ( $f = 0$ ) will be ignored. Thus, the ordinary differential equation simplifies to:

$$m \frac{d^2 x}{dt^2} + kx = 0$$

It is beyond the scope of this text to demonstrate the solution for this equation, which can be found in most differential-equation textbooks. But the general solution of this equation is:

$$x = A \sin \sqrt{\frac{k}{m}}t + B \cos \sqrt{\frac{k}{m}}t$$

where (A) and (B) are constants that are evaluated from the initial conditions. This solution is also sometimes called the Eigenvalue analysis. The above solution shows that if the system is allowed to vibrate freely, the frequency at which it would vibrate is:

$$\omega_N = \sqrt{\frac{k}{m}}$$

( $\omega_N$ ) is called the natural frequency or Eigenvalue of the system. This natural frequency is very important in rotordynamics, since it also corresponds to the resonance frequency of a system; namely:

**If an excitation force is applied to a system at its natural frequency, the system will resonate.**

Now assume that a regular periodic force (excitation) is applied to the mass in the form of a sinusoidal function,

$$f = F \sin(\omega t)$$

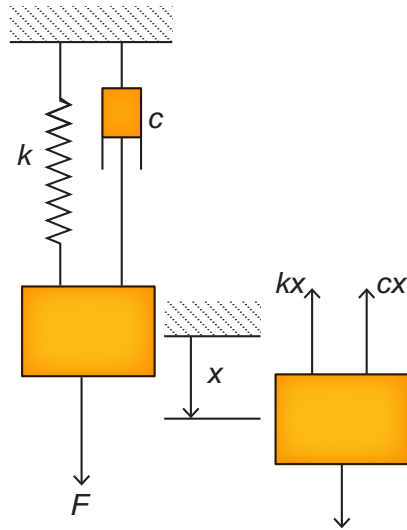


**Figure 4-2. Simple mass-spring-damper system**

where ( $\omega$ ) is the excitation frequency, and ( $F$ ) is the amplitude of the excitation force. To generalize further, the damping ( $c$ ) will not be neglected. The equation of motion thus becomes:

$$m \frac{dx^2}{dt^2} + c \frac{dx}{dt} + kx = F \sin(\omega t)$$

The steady-state “particular” solution to the above ordinary differential equation is:

$$x = X \sin(\omega t - \varphi)$$

where

$$X = \frac{F}{\sqrt{(k - m\omega^2)^2 + (c\omega)^2}}$$

**NOTE:** There is also a “complementary” transient term of the functional form  $x = Ce^{-Dt} \sin(Et + \alpha)$ , which is part of the complete solution to the above ordinary differential equation. However, because of the exponential multiplication factor, this transient term decreases with time and will approach zero for most real systems. Thus, for a steady-state rotordynamic analysis the complementary term can often be neglected.

$$\varphi = \tan^{-1} \left( \frac{c\omega}{k - m\omega^2} \right)$$

The above steady-state solution shows that the system vibrates at the excitation frequency ( $\omega$ ) but experiences a certain lag ( $\varphi$ ). This lag is called the phase lag or phase angle of the system. We can non-dimensionalize the above equation and rewrite it as follows:

$$Z = \frac{Xk}{F} = \frac{1}{\sqrt{\left(1 - \left(\frac{\omega}{\omega_N}\right)^2\right)^2 + \left(2\zeta\left(\frac{\omega}{\omega_N}\right)\right)^2}}$$

$$\tan \varphi = \frac{2\zeta\left(\frac{\omega}{\omega_N}\right)}{1 - \left(\frac{\omega}{\omega_N}\right)^2}$$

where ( $\zeta$ ) is defined as the damping factor and ( $Z$ ) is called the force response.

Damping Factor:

$$\zeta = \frac{c}{2m\omega_N}$$

Force Response:

$$Z = \frac{Xk}{F}$$

The force response represents the non-dimensional vibration amplitude of the system. Hence, the peak vibration amplitude of the system is:

$$X = \frac{F}{2\zeta k} = \frac{F}{c\omega_N}$$

If  $Z$  is plotted versus  $\omega/\omega_N$  (non-dimensional excitation frequency), the result is shown in *Figure 4-3*. This type of plot, also called a force response plot, is commonly employed for vibration analysis, since it allows for the determination of the vibration peak amplitude for any frequency at which the system may be excited. The force response plot shows asymptotic behavior at  $\omega/\omega_N = 1.0$ ; i.e., when the forcing frequency reaches the system's natural frequency. Namely, as the frequency of the sinusoidal force approaches the system's natural frequency, there is a possibility that the system's resonance may become unstable if the system is not adequately dampened.

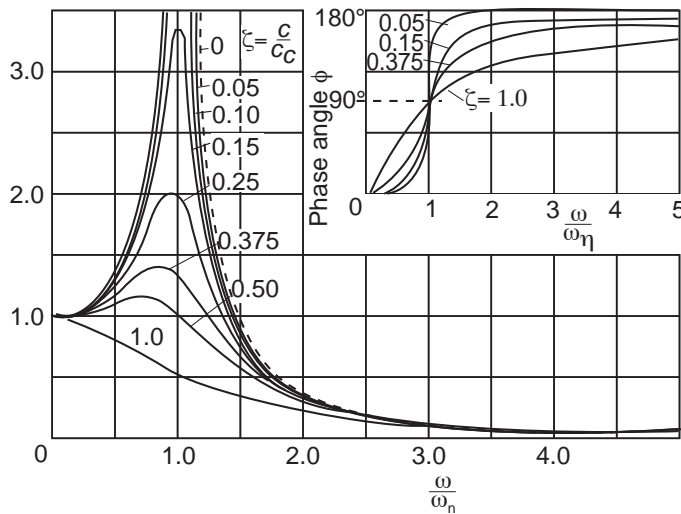


**Figure 4-3.** Force response plot utilized in vibration analysis.

As can be seen in *Figure 4-3*, the system's force response significantly depends on the level of system damping. For example, if the system is damped beyond unity ( $\zeta > 1.0$ ), the plot shows no peak response and the stable system is called overdamped. On the other hand, if the damping is below unity ( $\zeta < 1.0$ ), the system force response ( $Z$ ) will exceed unity at the natural frequency, and the system is called underdamped. The damping value at which the system is just in between over and underdamped ( $\zeta = 1.0$ ), is called the critical damping. It is important to realize that even systems that are underdamped ( $\zeta < 1.0$ ) may be considered to be stable and acceptable for a particular application as long as the force response stays within the systems allowable engineering design parameters.

## Lateral Rotordynamics Supported Rotor System (Two Degrees-of-Freedom)

So far the study focus has been on a single degree of freedom mass-spring-damper system. Now the focus shifts to a more realistic, but still somewhat simplified, mechanical model of an actual rotor. Consider a single rotor with a concentrated mass ( $m$ ), supported on two bearings, as shown in *Figure 4-4*. The bearings are considered infinitely stiff; i.e., they do not allow for any displacement. However, the shaft itself still has certain stiffness and damping characteristics; if the shaft experiences sufficiently unbalanced force at its mass center, it will bend or vibrate.

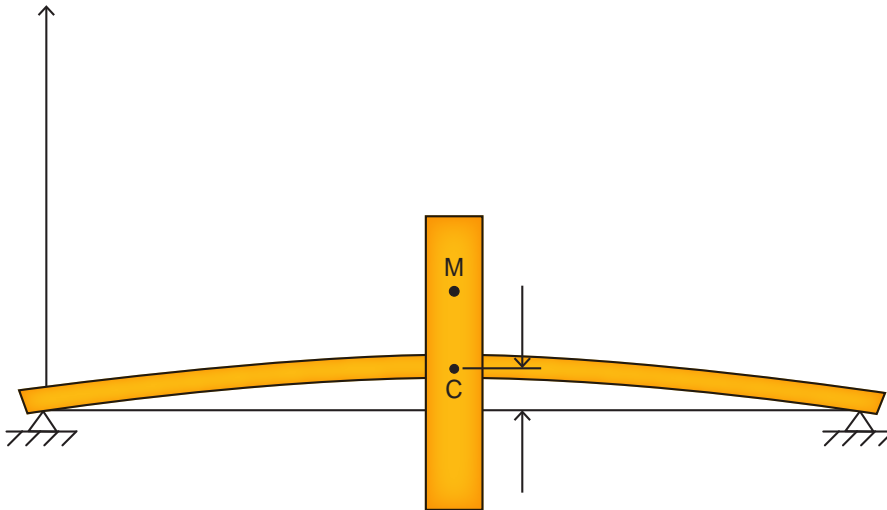


**Figure 4-4.** Simple rotor model.

**NOTE:** Clearly, a real rotor never has a mass concentrated at one single point. Thus, for a more advanced rotordynamic analysis, the modal mass—which accounts for the rotor’s weight distribution, rather than the actual mass of the rotor—is used. Typically, the modal mass of a rotor is between 50% and 80% of its actual mass.

An unbalance force occurs when the rotor’s center of gravity is not perfectly aligned with the rotor’s axis of rotation. This effect is called rotor mass unbalance (RMU) or shaft bow. The rotordynamic definition of rotor mass unbalance is:

$$RMU = W_u \cdot R_u$$

where  $W_u$  (unbalance weight) is a small weight located a distance  $R_u$  (unbalance radius) away from the axis of rotation. The eccentricity ( $e$ ) of a rotor is thus:

$$e = \frac{RMU}{W}$$

where  $W$  is the weight of the rotor. To determine the actual unbalanced force magnitude on a rotor, multiply the rotor’s unbalance mass by its centrifugal acceleration ( $f=ma$ ):

$$F = m_u \omega^2 = m e \omega^2$$

Since the rotor is spinning at a fixed angular speed, the unbalanced force acts on the shaft in the form of a periodic sinusoidal function:

$$f_u = F \sin(\omega t) = m e \omega^2 \sin(\omega t)$$

For example, if a small 1000-hp gas turbine shaft rotates at 20,000 rpm (=2094 rad/sec) and has an unbalanced weight of 100 grams located 5 mm away from the shaft center, the resulting unbalanced force is 2190 N (approximately 100 lbf).

The equations of motion for the two degrees-of-freedom supported rotor (as shown in Figure 4-4) are again derived using Newton's second law. When analyzing the model, you'll see that there are two degrees-of-freedom rather than one as in the previous example; namely, the system can vibrate in the x and y directions. The equations of motion for this system are:

$$m \frac{d^2 x}{dt^2} + c \frac{dx}{dt} + kx = m e \omega^2 \cos(\omega t)$$

$$m \frac{d^2 y}{dt^2} + c \frac{dy}{dt} + ky = m e \omega^2 \sin(\omega t)$$

For now, assume that the damping is very small and can be neglected. The stiffness of the shaft from basic material properties is:

$$k = -48 \frac{EI}{L^3}$$

where (E) is Young's Modulus, (I) is the area moment of inertia, and (L) is the rotor length. The natural frequencies of the system can be determined if the unbalance force is neglected, solving for the Eigenvalues:

$$m \frac{d^2 x}{dt^2} - 48 \frac{EI}{L^3} x = 0$$

$$m \frac{d^2 y}{dt^2} - 48 \frac{EI}{L^3} y = 0$$

Thus,

$$\omega_{Nx} = \sqrt{\frac{k}{m}} = \sqrt{48 \frac{EI}{mL^3}}$$

$$\omega_{Ny} = \sqrt{\frac{k}{m}} = \sqrt{48 \frac{EI}{mL^3}}$$

In rotordynamics, these natural frequencies are also called the undamped critical speeds. If the rotor operates at any undamped critical speed or a multiple thereof, the system is excited at one of its natural frequencies and may resonate.

Clearly, it is desirable to operate the gas turbine shafts away from these critical speeds. One criteria that is often employed to evaluate a gas turbine's rotordynamic adequacy is the critical speed margin, which is the difference between the shaft operating speed and the nearest critical speed:

Critical Speed Margin:

$$\omega_{margin} = \omega_{operating} - \omega_{critical}$$

The critical speed margin is also often expressed as the separation margin:

Separation Margin:

$$SM = \frac{\omega_{critical} - \omega_{operating}}{\omega_{critical}}$$

For rotordynamic design purposes, a 15% separation margin,  $SM = 15\%$ , is desirable and usually adequate. However, in some cases, a gas turbine shaft is required to pass a critical speed during startup and shutdown. In these cases, the rotor system must be sufficiently damped to prevent large vibrations while traversing the critical speeds. If the vibration amplitudes exceed the design clearances, rubbing between the gas turbine's rotor and housing or even catastrophic gas turbine failure may be the result.

The steady-state "particular" solution for the above shaft equations of motion is identical in form to the solution for the previously analyzed simple mass-spring-damper system, except that two degrees of freedom must now be considered and the excitation force is  $F = m e \omega^2$ . Thus, the solution is expressed in the form of:

$$x = X \sin(\omega t - \phi)$$

$$\phi = \tan^{-1} \left( \frac{c\omega}{k - m\omega^2} \right)$$

$$y = Y \cos(\omega t - \phi)$$

where:

$$X = \frac{m e \omega^2}{\sqrt{(k - m\omega^2)^2 + (c\omega)^2}}$$

$$Y = \frac{m e \omega^2}{\sqrt{(k - m\omega^2)^2 + (c\omega)^2}}$$

These equations are arranged to:

$$Z_x = \frac{Xk}{F} = \frac{m e \omega^2}{\sqrt{\left(1 - \left(\frac{\omega}{\omega_N}\right)^2\right)^2 + \left(2\zeta\left(\frac{\omega}{\omega_N}\right)^2\right)^2}}$$

$$Z_y = \frac{Yk}{F} = \frac{m e \omega^2}{\sqrt{\left(1 - \left(\frac{\omega}{\omega_N}\right)^2\right)^2 + \left(2\zeta\left(\frac{\omega}{\omega_N}\right)^2\right)^2}}$$

In rotordynamics, the force response ( $Z$ ) is also called unbalance response. The peak vibration amplitudes are:

$$X = \frac{m e \omega^2}{2\zeta k} = \frac{m e \omega^2}{c \omega_N}$$

Using the above results, an unbalance response plot ( $Z$  versus  $\omega/\omega_N$ ) as shown in *Figure 4-5* can be developed. An unbalance response plot is crucial for gas turbine design, since it defines and limits the speed ranges at which the gas turbine shaft may operate. Clearly, the unbalance response magnitude at the critical speed ( $\omega/\omega_N = 1.0$ ) is again seen to be strongly dependent on the damping factor.

The unbalance response plot (*Figure 4-5*) also shows that for increased damping ratios, the peak amplitude of vibration occurs at frequencies slightly above the undamped critical

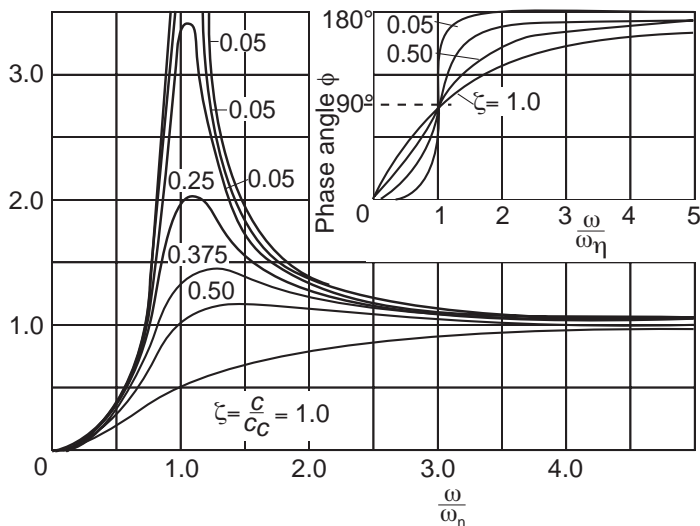


**Figure 4-5.** Unbalance Response Plot

speed. This small critical speed deviation from the natural frequency can easily be derived from the above unbalance response equation. Consequently, the frequency correction for the undamped critical speed is:

$$\omega_{ucr} = \frac{\omega_N}{\sqrt{1-2\zeta^2}}$$

The corrected undamped critical speed is usually called the unbalance critical speed. Although this appears to be only a quantitatively small deviation from the undamped critical speed, the unbalance critical speed correction is important for the accurate determination of a rotor's critical speeds, especially for well damped systems.

In some cases, if a rotor system is not adequately damped, the transient "complementary" solution to the equations of motion may also affect the rotordynamic performance and lead to rotor instability. Without going into too much detail, it should be stated that from the "complementary" solution, another set of Eigenvalues can be derived, which are called the damped critical speeds.

A transient analysis of the equations of motion shows that the damped critical speeds are related to the undamped critical speeds by:

$$\omega_{der} = \omega_N / \sqrt{1-2\zeta^2}$$

Theoretically, a rotor system remains stable at the damped critical frequency as long as the damping factor ( $\zeta$ ) is positive. However, in any real rotordynamic application, experience has shown that the damping factor at the damped critical speeds should exceed 0.1 ( $\zeta > 0.1$ ). Care must be taken when performing the damped critical speed analysis since bearing damping will significantly affect the overall system damping.

### Multi-Degrees of Freedom System

So far, a simple rotor has been analyzed by assuming that the rotor has a concentrated mass and bending movement in only two directions (x,y); i.e., a two degrees of freedom system. In reality, this is an over-simplification. Namely, a real rotor can bend in different shapes and the bearings allow for some limited vibration of the shaft. A real rotor thus has multiple degrees of freedom. Divided into three categories which are descriptive of the vibration types (modes) the rotor experiences: rigid body modes, lateral bending modes, and torsional modes.

**Rigid Body Modes:** Rigid body modes are the vibrations the rotor undergoes if it were perfectly stiff and not allowed to bend. A rigid rotor can move in one axial direction (z) and two radial directions (x,y).

**Lateral Bending Modes:** As previously shown, a typical rotor is not infinitely stiff and thus can bend laterally. Theoretically, an infinite number of possible bending shapes exist; however, for most gas turbine rotordynamic analysis, it is adequate to only study the first four bending modes. The actual shape of the bending modes is strongly dependent on the bearing locations, shaft bow, bearing and shaft stiffness.

It must be noted that the stiffness of the bearings utilized impacts the mode shapes (Figures 4-6 and 4-7). For example the first mode is a true rigid body mode if the bearings are not very stiff. Stiff bearings limit the movement of the shaft at the bearings, thus causing the shaft to bend.

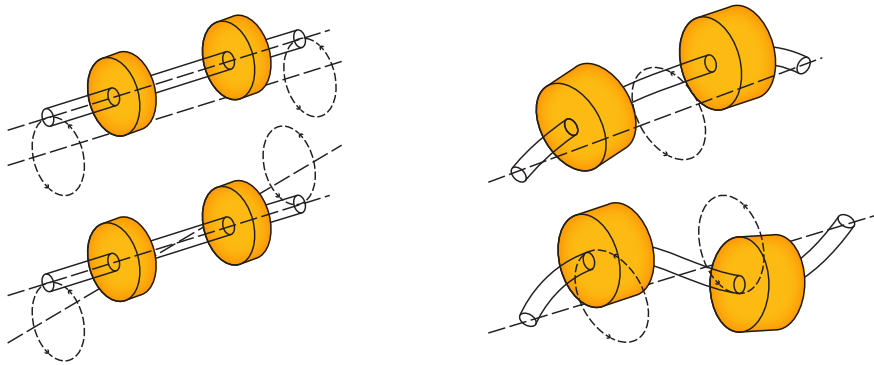


**Figure 4-6.** Rigid Body (left) and Bending Modes (right)

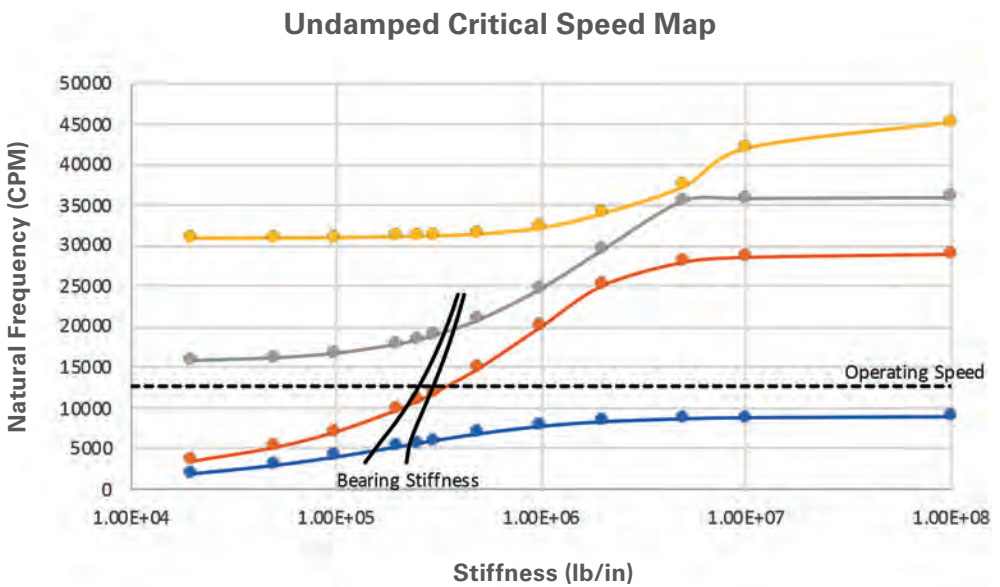


**Figure 4-7.** Undamped Critical Speed Map, showing critical speeds for the first modes of a rotor depending on the bearing stiffness. For a known bearing stiffness, the chart helps determine the undamped critical speed of the rotor system. Depending on the stiffness, the modes can be rigid body modes (low stiffness), or bending modes (high stiffness).

**Torsional Modes:** Due to the torque applied to the shaft, there also can be torsional twisting can also occur. On a single shaft, there is typically only one relevant torsional mode: simple rotor twist.

The equations of motion for a multi-degrees-of-freedom system are still derived from Newton's second law ( $f=ma$ ). However, one equation of motion is required for each degree of freedom. This results in a rather large system of equations, even for a simple shaft model. To simplify the mathematical syntax, this system of ordinary differential equations is usually expressed in matrix form:

$$\begin{bmatrix} m_{11} & m_{12} & m_{13} & \dots & m_{1n} \\ m_{21} & m_{22} & m_{23} & \dots & m_{2n} \\ m_{31} & m_{32} & m_{33} & \dots & m_{3n} \\ \cdot & \cdot & \cdot & \dots & \cdot \\ \cdot & \cdot & \cdot & \dots & \cdot \\ m_{n1} & m_{n2} & m_{n3} & \dots & m_{nn} \end{bmatrix} \begin{bmatrix} x_1'' \\ x_2'' \\ x_3'' \\ \cdot \\ \cdot \\ x_n'' \end{bmatrix} + \begin{bmatrix} c_{11} & c_{12} & c_{13} & \dots & c_{1n} \\ c_{11} & c_{12} & c_{13} & \dots & c_{1n} \\ c_{11} & c_{12} & c_{13} & \dots & c_{1n} \\ \cdot & \cdot & \cdot & \dots & \cdot \\ \cdot & \cdot & \cdot & \dots & \cdot \\ c_{11} & c_{12} & c_{13} & \dots & c_{nn} \end{bmatrix} \begin{bmatrix} x_1' \\ x_2' \\ x_3' \\ \cdot \\ \cdot \\ x_n' \end{bmatrix} + \begin{bmatrix} k_{11} & k_{12} & k_{13} & \dots & k_{1n} \\ k_{11} & k_{12} & k_{13} & \dots & k_{1n} \\ k_{11} & k_{12} & k_{13} & \dots & k_{1n} \\ \cdot & \cdot & \cdot & \dots & \cdot \\ \cdot & \cdot & \cdot & \dots & \cdot \\ k_{11} & k_{12} & k_{13} & \dots & k_{nn} \end{bmatrix} \begin{bmatrix} x_1 \\ x_2 \\ x_3 \\ \cdot \\ \cdot \\ x_n \end{bmatrix} = \begin{bmatrix} f_1 \\ f_2 \\ f_3 \\ \cdot \\ \cdot \\ f_n \end{bmatrix}$$

Here  $x_i$  is the displacement variable and  $n$  is the number of degrees of freedom. This can also be written as:

$$[M]x'' + [C]x' + [K]x = [F]$$

where  $M$  is the mass matrix,  $C$  is the damping matrix,  $K$  is the stiffness matrix, and  $F$  is the force vector. For more complicated systems, which may include multiple bearings, coupled shafts, and/or flexible support structures, the mathematical model may become very complex, with matrices easily reaching fifty or more degrees of freedom. The matrix equation can be solved for the Eigenvalues using a matrix solver, such as a Gauss-Seidel matrix inversion method. It is beyond this text to describe a detailed analysis, which can be found in most rotordynamics textbooks. However, it is important to note the following:

**Each degree of freedom can have a distinct undamped and damped critical rotor speed. Additional resonances can also occur at any multiple of the frequency of the original damped/undamped critical speed.**

**NOTE:** Since the equations of motion for the torsional vibrations are not coupled physically and mathematically with the lateral bending and rigid body equations of motion, the torsional critical speeds are typically calculated in a separate and independent Eigenvalue analysis.

### Rotordynamic Plots

It is often convenient to present a gas turbine's rotordynamic behavior in graphical form. The most common rotordynamic graph is called the frequency response plot, which is very similar to the unbalance response plot previously presented. The frequency response plot is generated by either experimentally or numerically determining the shaft unbalance response for a range of rotor running speeds and plotting the results in the form of vibration amplitude (mils) versus shaft speed (rpm or Hz). For example, *Figure 4-8* shows a typical compressor shaft speed response plot from 0 to 12,000 rpm. The first, second, and third critical speeds are easily identifiable by the asymptotic response behavior on the frequency response plot.

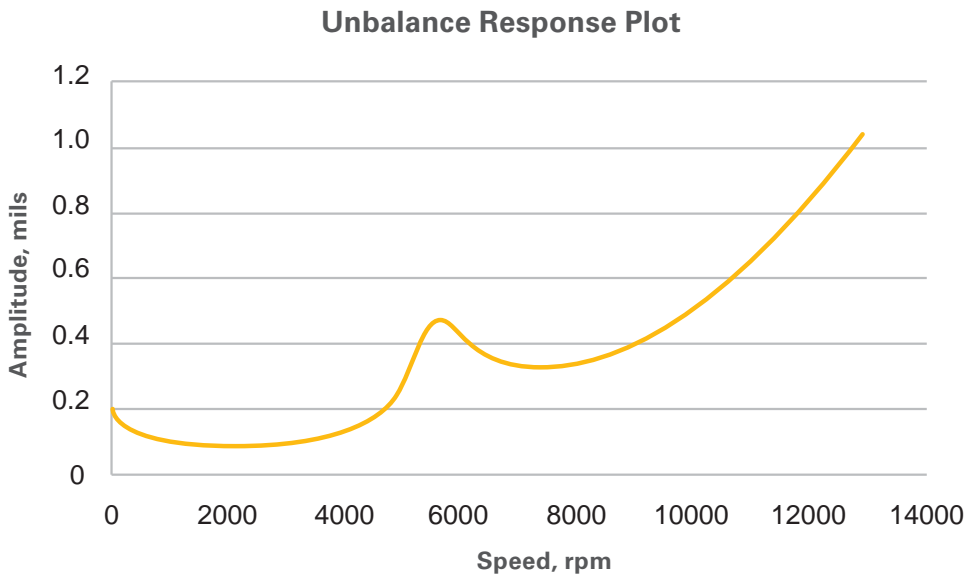


**Figure 4-8.** Response Plot

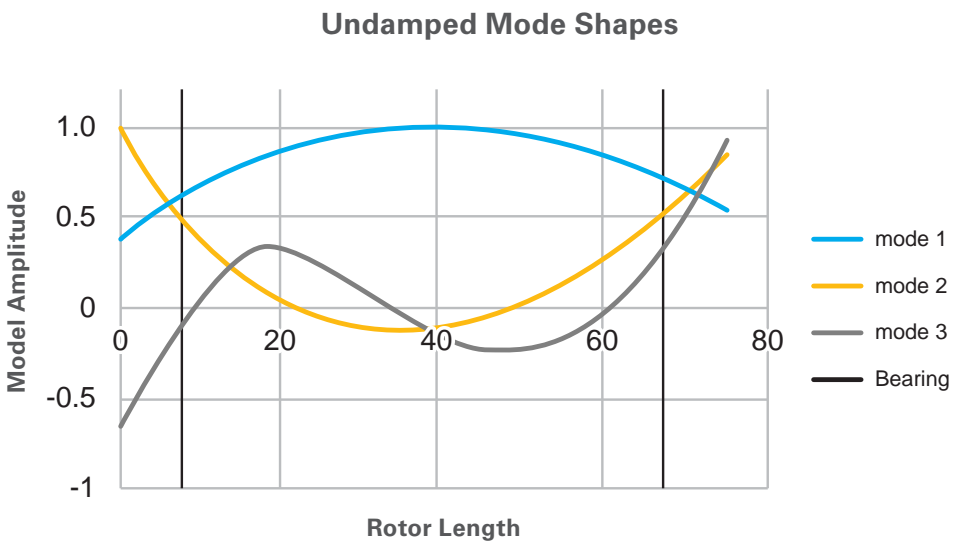


**Figure 4-9.** Mode Shapes

Figure 4-9 shows typical mode shapes that correspond to critical speeds. It is important to remember that the critical speed and mode shapes are system specific; i.e., they cannot easily be generalized to any system. Hence, to accurately determine the critical speeds and mode shapes of a given system, an Eigenvalue analysis must always be performed. In general, however, the following can be stated:

**Typically, the first two critical speeds (lowest frequencies) corresponds to rigid body mode, the next higher frequency critical speed is lateral bending mode.**

Critical speed analysis results are often plotted in the form of a Campbell diagram as shown in *Figure 4-10*. The Campbell diagram presents the individual critical speeds of a rotor as a function of the rotational speed. Rotor physical characteristics such as damping and stiffness are not system constants, but can vary with the angular speed and/or operating conditions of the system. Hence, a plot showing the locations of the critical speeds as a function of rotor speed is essential for the gas turbine designer to determine allowable shaft operating ranges.

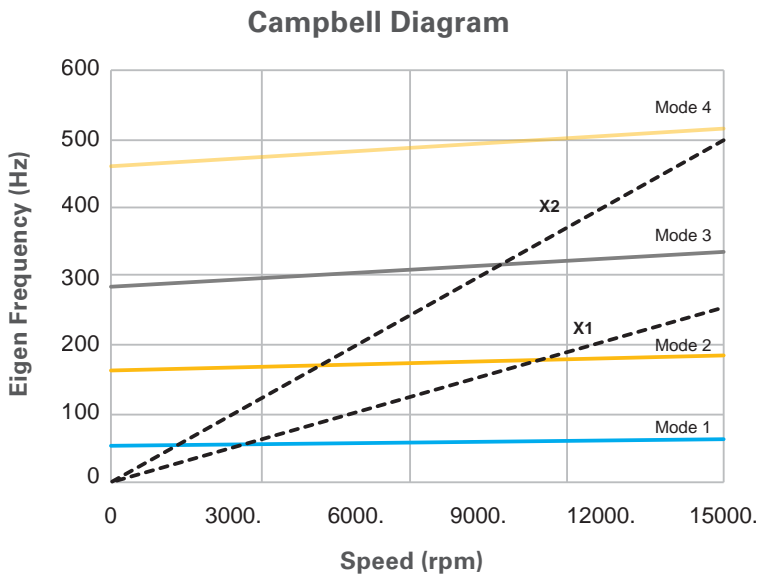


**Figure 4-10.** Results of critical speed analysis.

### Rotordynamics Testing and Instrumentation

To experimentally determine rotordynamic performance such as critical speeds and unbalanced response of a gas turbine, some standard tests can be performed. The two most common of these tests are the ping (or wrap) and the rundown test. For the ping test, the rotor is vibration isolated and then excited with an extremely short but high-amplitude impulse force. For example, the rotor is hung on a long, thin wire to mechanically isolate it and then hit with a metal hammer to apply the impulse. This short, high frequency impulse effectively excites the rotor simultaneously at all possible frequencies. By measuring the frequencies of the peak amplitudes of the resulting rotor vibrations, the natural frequencies and forced responses of the rotor can be identified. On the other hand, the rundown test is performed by simply accelerating a gas turbine shaft to its maximum operating speed, decoupling it and then carefully measuring its vibration amplitudes and frequencies as it decelerates. Clearly, a rundown test can only be performed if the gas turbine’s rotordynamic stability and safety are already well established.

Three types of transducers are commonly employed to measure rotordynamic vibrations on gas turbine packaging as follows:

**Proximity Probes:** Proximity probes measure the actual rotor displacement ( $x$ ) relative to a fixed position. Modern proximity probes are usually either magnetic reluctance, eddy

current, or optical pickups. Most gas turbines employ a set of orthogonal radial eddy current proximity probes for each radial bearing and two axial eddy current proximity probes to monitor shaft vibrations relative to the gas turbine casing. These proximity probes can typically measure vibration frequencies between 0 and 10 kHz.

**Velocity Transducers:** Velocity transducers measure the first derivative ( $dx/dt$ ) of the displacement (i.e., the actual free movement velocity) using a miniature piezo-electric or piezo-resistive mass-spring system. These transducers are typically employed to measure lower frequency free vibrations (100-1000 Hz) such as the gas turbine case, skid and other subsynchronous vibrations.

**Accelerometers:** Accelerometers typically employ a miniature piezo-electric or piezo-resistive, mass-spring system to measure the second derivative of the displacement ( $dx^2/dt^2$ ); i.e., the actual free movement acceleration. Accelerometers are most often used to measure high frequency vibrations (1-100 kHz) such as the gas turbine gear meshing and blade interaction frequencies.

Most gas turbines incorporate a combination of these three types of transducers to accurately monitor and diagnose the shaft's rotordynamic behavior. For safety reasons, no gas turbine should ever be operated without properly functioning vibration instrumentation and associated package alarm/shutdown switches.

Often, a transducer is combined with a spectrum analyzer to examine the rotordynamic behavior. A spectrum analyzer performs a mathematical transformation of the time/vibration signal into the frequency domain called a Laplace or Fourier transform (also sometimes referred to as an FFT or Fast Fourier Transform). The output from the spectrum analyzer FFT provides a plot of vibration amplitude versus frequency which is very similar to the previously described frequency response plot.

### **Shaft Balancing**

To minimize vibrations, a gas turbine's shaft must be mechanically balanced; i.e., eccentricities must be physically eliminated. This is typically achieved by applying counterweights and/or by removing material from the rotor at strategic radial locations. Rather than removing material from the rotor, which may permanently damage the shaft, compressors are typically balanced using counterweights. This method is also called trim balancing. Compressors usually have several special access points along the shaft to allow for easy application/removal of the balancing weights. Balancing weight, they range from fractions of one gram up to one hundred grams. Several mathematical procedures have been derived to determine the correct mass and radial location of the counterweights for proper trim balancing.

To maintain proper rotor balancing, the above trim balancing procedure must be repeated if any compressor shaft component and bearing elements are exchanged or repaired.

## **TORSIONAL VIBRATIONS**

The topic of train torsional integrity deals with the torsional natural resonances, their

interference with operating speeds, sources of torsional excitation, type of excitation and most importantly, the ability of individual components in the train to handle the peak static and dynamic stresses within appropriate safety margins [2], [6]. While the topic affects all types of compressor trains, it is particularly important for electric-motor-driven trains, due to potential high excitation forces at start and for line faults, and due to the excitation of multiples of the running speed if variable frequency drives are used. This section therefore primarily focuses on electric-motor-driven trains (*Figure 4-11*).

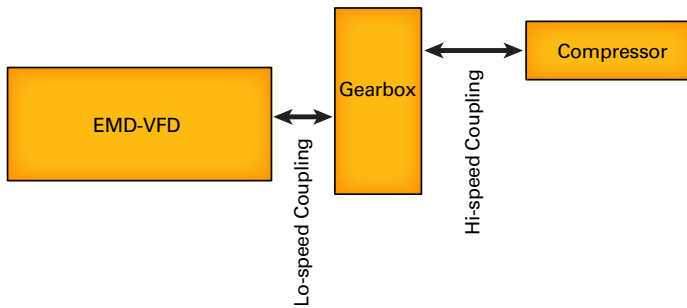


**Figure 4-11.** Typical configuration of a electric-motor-driven train.

Questions that need to be answered are:

1. Is all the train equipment adequately designed to handle the torsional vibrations?
2. Will the motor operation at rated conditions be acceptable to the driven equipment?
3. Will the high-speed couplings provide safe operation at all steady-state and transient conditions?
4. Given the air-gap torque pulsations, is all the train equipment designed to meet durability standards from an endurance standpoint?
5. Can the train handle high transient torque levels from motor fault events?

Ascertaining torsional integrity of EMD-GC packages involve a series of analysis:

1. Determining torsional natural frequencies (TNFs) and their interference on low-speed and high-speed shafts.
2. Steady-state harmonics from the VFD, subjecting the train to a forced response analysis and evaluating the resulting individual component stresses from a High Cycle Fatigue (HCF) standpoint. HCF is characterized by large cycles of small elastic deformations, while its counterpart Low Cycle Fatigue (LCF) refers to low cycles of large deformations (plastic/elastic).
3. Transient fault events (such as 2-Phase and 3-Phase short circuits), subjecting the train to transient torque through the fault time period, and confirming the resulting PU torque levels are within safety margins.

The American Petroleum Institute (API) and Gas Machinery Research Council (GMRC) have

long recognized the need for providing appropriate torsional information and have outlined this in guidelines [6], [7]. These guidelines are used extensively in the assumptions, analysis and data interpretation.

### TORSIONAL SOLUTION METHODS

Many references exist in the literature in the torsional formulation and solution methods [6], [8-10], so this section will focus on the aspects relevant for interpretation of analytical results presented in later sections. The torsional analysis is performed by a Finite Element formulation of the train as branched systems (Fig. 4-12), developed by one of the authors.

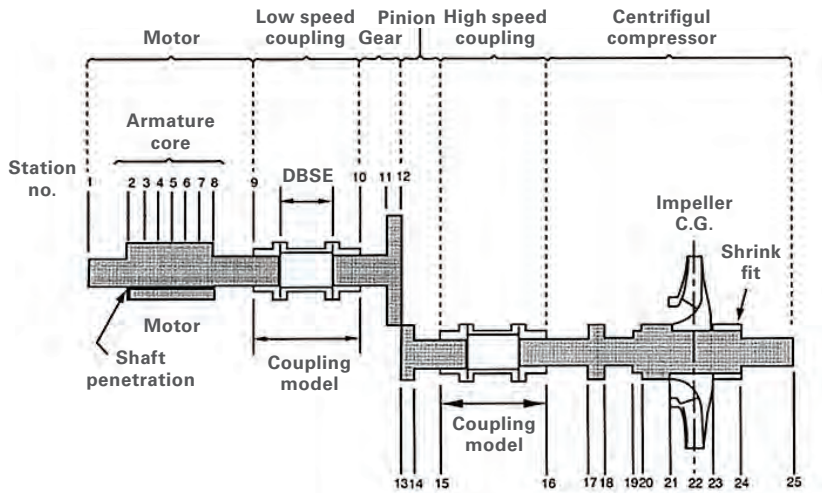


**Figure 4-12.** Torsional simulation model for a Finite Element Analysis

The twist in the shaft system ( $\theta$ ) can be represented as a harmonic function:

$$\theta = \theta_0 \cdot \sin(\omega t)$$

where,  $\theta_0$  = Amplitude of the harmonic excitation,  $\omega$  is the angular frequency and  $t$ , the time.

The equation of motions for the Finite Element formulation is written as:

$$[I]\{\ddot{\theta}\} + [C]\{\dot{\theta}\} + [K]\{\theta\} = \{f(t)\}$$

where

$[I]$  = Inertia matrix

$\{\dot{\theta}\}$  = angular velocity vector =  $\frac{\partial \theta}{\partial t}$

$[C]$  = damping matrix

$\{\ddot{\theta}\}$  = angular acceleration vector =  $\frac{\partial^2 \theta}{\partial t^2}$

$[K]$  = stiffness matrix

$\{\theta\}$  = angular displacement vector

$\{f(t)\}$  = Periodic or aperiodic forcing function vector

The element matrices are assembled into system inertia [I], damping [C] and stiffness [K] matrices.

The computer simulation tool accepts mass-elastic information of all the train components and the sources of torsional excitation. It then provides the solution to the second order partial differential equation in the form of:

**A. Steady-state solution:** torsional vibration modes and responses.

**B. Damped-response solution:** torsional amplitudes for specific harmonic excitations.

**C. Transient-response solution:** torsional amplitudes for time-varying forcing functions.

Time-marching methods, such as Runge-Kutta [8] or Newmark-Beta [9], are used to perform direct time integration of the 2<sup>nd</sup> order differential equation. The fault transients arising from electric-motor (2-phase or 3-phase short circuits etc.) are analyzed with transient solution. Forcing functions are provided by the motor vendors, based on their drive and motor design. With the transient solution, the peak torque levels (PU) and the shear stresses at various components are calculated across the train.

$$\text{Torque: } \{T\} = [K] \cdot \{\theta\}$$

$$\text{Shear stress: } \{\sigma\} = \frac{\{T\}r}{J}$$

Where, r = radius of the shaft element

J = polar moment of inertia of the element

## TORSIONAL INTERFERENCE STUDY

The primary task in a torsional integrity study is to determine the train torsional resonances and review them against the desired operating speed range of both low-speed and high-speed shaft systems. In general, the first few (1 to 3) torsional resonances are most important due to the energy content in those modes and mode shapes. For sources of excitations, certain harmonic multiples of a) the train speeds (mechanical) and b) the VFD-output frequencies (electrical) must be considered for interference. The goal is to keep most prominent torsional interference with necessary separation margins; where interference is not avoided, the modes are shown to be safe from a torsional standpoint.

To address the concern of torsional integrity of the drive train, a methodology to ensure torsional integrity of VFD-EMD driving Gas Compressors is shown. The train's ability to handle torsional interference, torque pulsation from VFDs and short-circuit fault events without impacting the durability of the equipment is critical to end-users. To this end, analytical torsional models are developed with API and GMRC guidelines, and used to standardize train equipment. Results are shown for a 45-Hz corner frequency, 4-pole 8700 HP motor driving a 10-stage compressor. Interference diagrams and forced excitation response analysis show that the train is safe from a torsional standpoint. Transient analysis shows the peak torques that can be handled by all of the equipment.

Figures 4-13 and 4-14 show the torsional interference charts (Campbell diagrams) with low-speed shaft as reference, for the train configuration mentioned earlier. One important source of excitation to consider with electric motors is the VFD harmonics transferred to the rotor through the air-gap. This information is provided by the motor vendor, and varies based on the VFD-type, inverter design and number of voltage-cells. Based on the drive design and topology, the fundamental VFD-induced excitation occurs at  $6f$ , where  $f$  is the frequency output of the VFD. Additional multiples of this fundamental occur at  $12f$ ,  $24f$  and  $48f$ . For a 4-pole motor, these harmonics translate to  $12\times$  motor ( $6f$ ),  $24\times$  motor ( $12f$ ),  $48\times$  motor ( $24f$ ) and so on, when plotted on the Campbell diagram. When the low-speed shaft is referenced, torsional interference occurs within the operating speed range (900-1890 rpm) between the following:

- 1<sup>st</sup> Torsional Resonance and 1X motor speed
- 2<sup>nd</sup> Torsional Resonance and 2X motor speed
- 2<sup>nd</sup> Torsional Resonance and 3X motor speed
- 3<sup>rd</sup> Torsional Resonance and 24X motor (12f VFD harmonic)
- 4<sup>th</sup> Torsional Resonance and 24X motor (12f VFD harmonic)

Figure 4-15 shows the torsional interference chart with high-speed shaft as reference. Note that there are no interferences between the lower-order torsional resonances and any significant excitation sources.

Altering train torsional frequencies to meet margins is not always possible, since any modifications to equipment must not violate other design norms. The softer stiffness elements in the train impact first few torsional modes strongly and hence, coupling designs are reconsidered whenever modifications are sought. However, coupling changes (length,

### EMD-STD; Motor 1 - 8.7kHP - 10Stg Compressor Map - LS

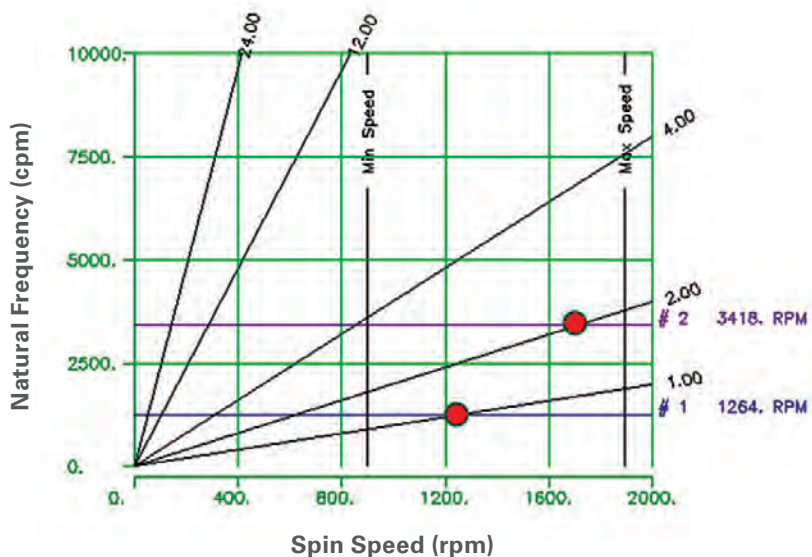
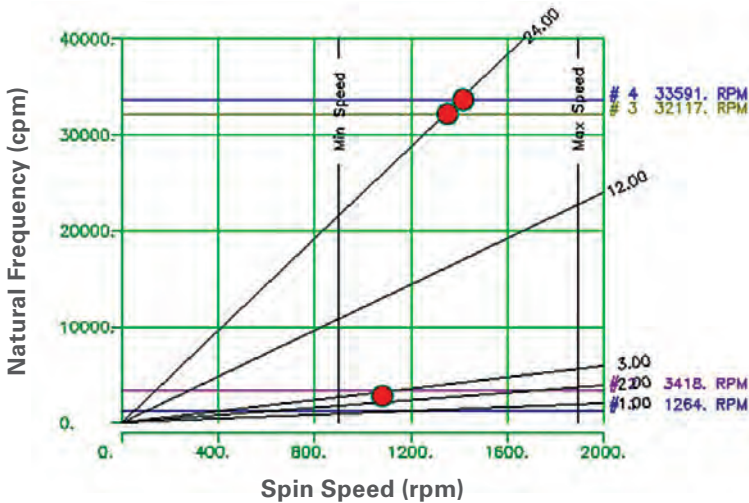


Figure 4-13. Torsional interference – low-speed shaft as reference.

type, weights, etc.) can significantly impact package design and footprint. Hence, it is best to incorporate coupling designs that can comfortably accommodate all technical requirements, as well as equipment-access capabilities.

Based on the interference charts shown in *Figures 4-13, 4-14 & 4-15*, the low-speed coupling design is optimized to provide the maximum separation margins and least torsional response at excitation (explained in the next section). Both the torsional stiffness (length and diameter) and inertia to a lesser extent were optimized.

### EMD-STD; Motor 1 - 8.7kHP - 10Stg Compressor Map - LS



**Figure 4-14.** Continuation of torsional interference chart – low-speed shaft as reference.

### STEADY-STATE HARMONICS AND TORQUE PULSATION

As explained earlier, when torsional interference cannot be avoided with operating speeds, analysis must be conducted to prove that the train has low torsional response to the excitation sources. This study also helps in choosing the optimum coupling parameters (in addition to other coupling safety factors).

Torque pulsation from the VFD harmonics is a natural excitation source in EMD-GC packages. *Figure 4-16* shows a typical spectrum chart provided by motor vendors, showing magnitudes of dynamic torque pulsation at various VFD-output frequencies.

### EMD-STD; Motor 1 - 8.7kHP - 10Stg Compressor Map - HS

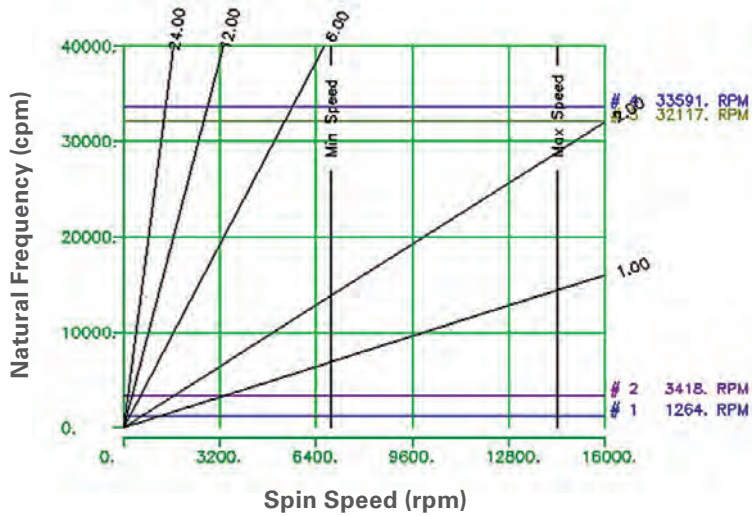


Figure 4-15. Torsional Interference – high-speed shaft as reference.

Air Gap Torque Amplitude  
(% of nominal motor torque)

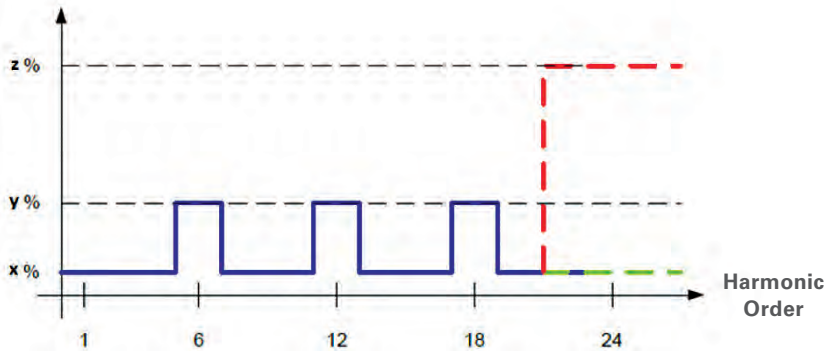


Figure 4-16. Motor air-gap torque harmonic envelope (pulsation torque), typically 0.5-2%.

### EWD-STD; Motor 1 - 8.7kHP - 10StgC Forced Resp - VFD Pulsation EWD

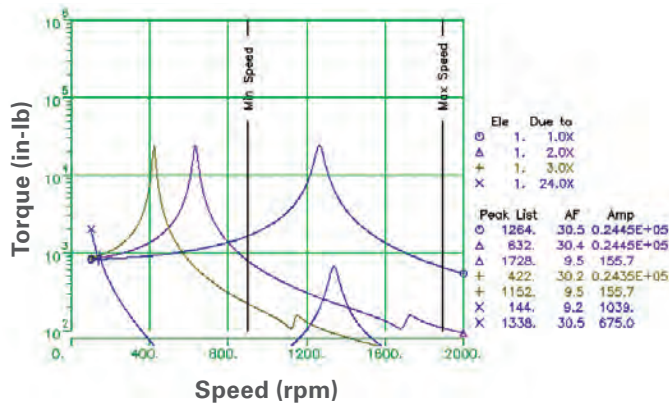


Figure 4-17. Results of forced response torsional analysis – at the motor location.

The motor’s rated torque at the rated frequency is a critical parameter for this analysis. A 45-Hz-corner-frequency motor drive, which implies that the motor can produce the rated torque up to 45 Hz, and then switches to constant power between 45 Hz and 60 Hz. The pulsation magnitudes are referenced to the nominal motor torque.

A steady-state, forced-response torsional analysis is performed with this pulsation data to determine the maximum dynamic torque for each of the train equipment. A damping ratio of 1.67% (AF=30) is used based on the API [6] and GMRC [7] guidelines. However, lower damping ratios are also considered, if the results show marginal safety factors.

Figure 4-17 shows the dynamic torque vs motor speed for all the torsional interferences identified in the earlier section - 1X, 2X, 3X and 24X (12f) – at the motor location.

Figure 4-18 shows the same at the compressor location. Peak dynamic torque amplitudes derived from the forced response analysis are then used to calculate the alternating stress. The rated torque is used to calculate the mean stress. A Goodman diagram is a graph of mean stress vs. alternating stress in a component, providing an idea of when the material fails at some given number of cycles. With those two parameters, an endurance study is constructed on the Goodman diagram [10] to confirm that the components have infinite life (alternating stress below the Goodman line) and sufficient safety factors (ratio of maximum allowable alternating stress on the line to the actual alternating stress) from a High-Cycle-Fatigue perspective. For the motor and compressor locations, the Factors of Safety to the limit line are 12.4 and 11.1 respectively. This is repeated for each of the train equipment. Based on these results, the train is considered safe from a torsional interference standpoint.

**EWD-STD; Motor 1 - 8.7kHP - 10StgC Forced Resp - VFD Pulsation EWD**

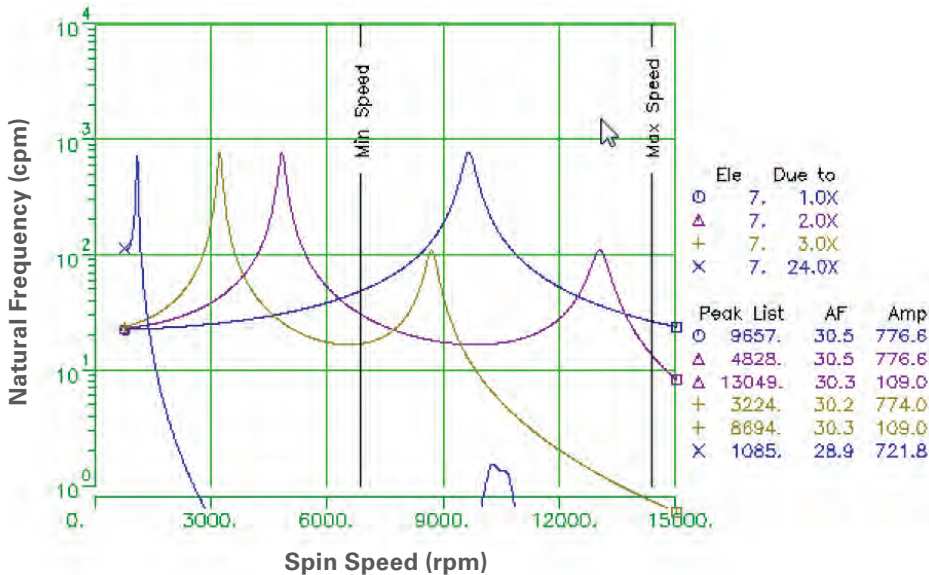


**Figure 4-18.** Results of forced response torsional analysis at the compressor shaft location.

Separate from the train endurance analysis, components in the individual machinery such as squirrel cage and fans in motors, are subject to fatigue analysis per API 516 and 517.

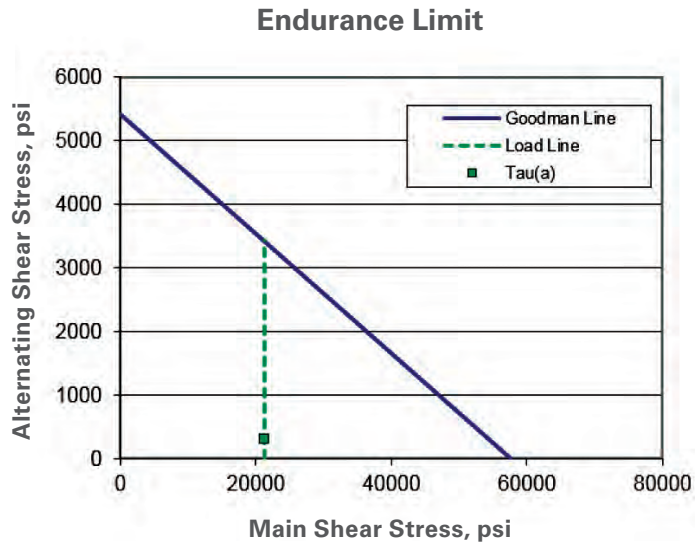


**Figure 4-19.** Endurance limit from torque pulsation – motor location – SF = 12.4.

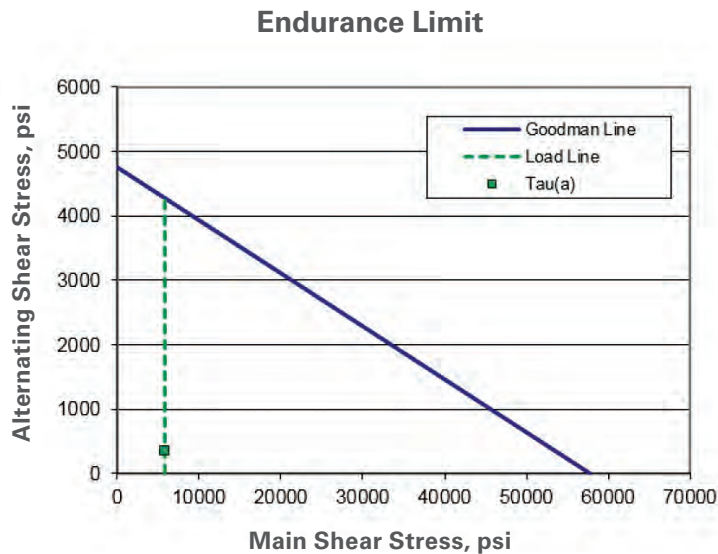


**Figure 4-20.** Endurance limit from torque pulsation – Compressor location – SF = 11.1.

## FAULT TRANSIENT ANALYSIS

Electric-motor drives can be subject to unexpected fault transients—such as phase-to-phase faults or phase-to-ground faults. They could either be 2-phase short circuits or 3-phase short circuits. The API guidelines require motor vendors and driven-equipment suppliers to consider these fault transients and ensure that the peak torques (expressed in terms of the PU (Per Unit rated torque) experienced by the train equipment do not exceed the component design limits.

Short-circuit information is provided by motor vendors. The faults shown are based on the cumulative effects of the electrical design and topology, inclusive of protective relays and breakers. In the event of a short-circuit, the motor shaft experiences an instantaneous peak torque as the energy stored in the stator coils dissipates through the air-gap, then decays over a small amount of time. The air-gap torques at fault conditions are shown in *Figures 4-21 and 4-22*.

### 2-Phase Short Circuit - Air-gap Torque vs Time

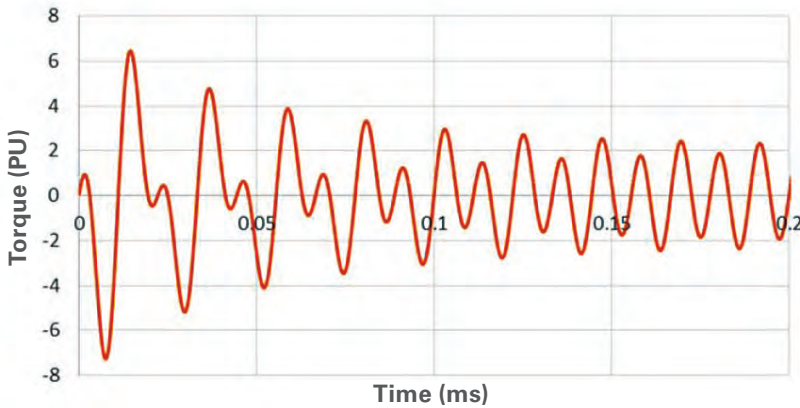


**Figure 4-21.** Fault transients - 2-Phase short circuit, Max PU = -7.3.

### 3-Phase Short Circuit - Air-gap Torque vs Time

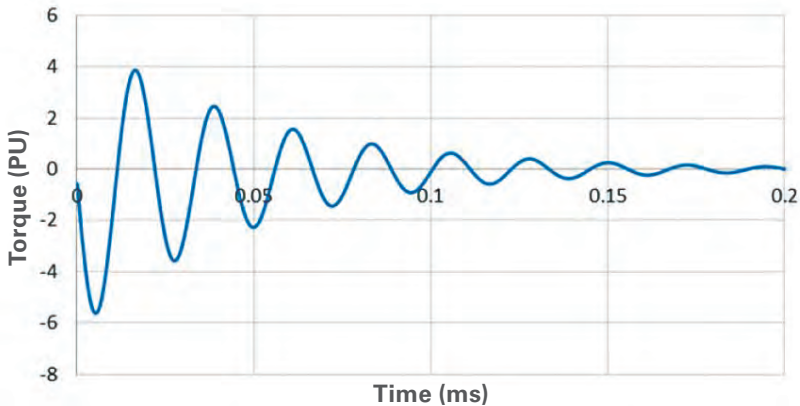


**Figure 4-22.** Fault transients - 3-Phase short circuit, Max PU = -5.6.

A transient torsional analysis is performed using the above fault transients as input to the equations of motion shown earlier. Time-marching is achieved using a Runge-Kutta method. The goal is to determine the propagation effect of the transient torque from the motor to other train equipment, their attenuation through the gearbox and the ability of the low-speed and high-speed couplings to handle the instantaneous torques.

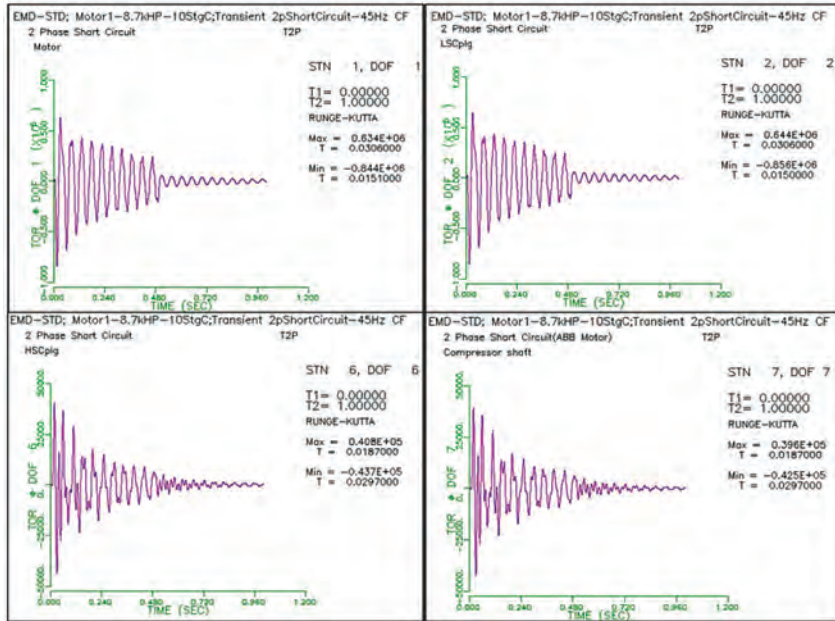


Figure 4-23. Results of transient torsional analysis from 2-phase short circuit fault event.

Figure 4-23 shows the results of transient torsional analysis from 2-phase short circuit fault event—peak torques at motor shaft, low-speed coupling, high-speed coupling and compressor shaft. Figure 4-24 shows the same for a 3-phase short circuit fault event. Based on the peak torques transmitted during the fault events, the maximum shear stress occurring in the components are calculated. These are compared with the shear

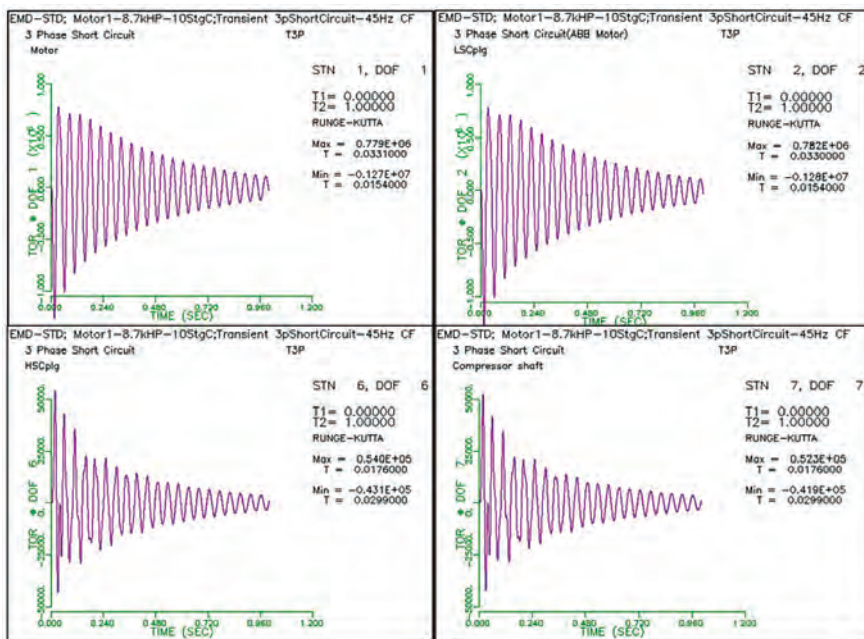


Figure 4-24. Results of transient torsional analysis from 3-phase short circuit fault event.

yield stress of the material to determine the safety factors. Also, the coupling designs are verified to be capable of transmitting the maximum momentary torque shown by this analysis.

Short-circuit events may be one-time unexpected events, however, it is imperative to design the train equipment to survive such events for safety purposes.

## CHAPTER 4 REFERENCES

[1] American Petroleum Institute, 2002, *Axial and Centrifugal Compressors and Expander-Compressors for Petroleum, Chemical and Gas Industry Services, API Standard 617, 7th Ed., 2002.*

[2] Corbo, M.A., and Malanowski, S.B., 1996, "Practical Design Against Torsional Vibrations", *Proc. 25<sup>th</sup> Turbomachinery Symposium*, pp. 189-223.

[3] Brun, K., Thorp, J., Meyenberg, C., Kurz, R. 2015, "Hydrodynamic Torque Converters for Oil & Gas Compression and Pumping Applications: Basic Principles, Performance Characteristics and Applications", 2015, *Turbomachinery & Pump Symposium, Houston.*

[4] Glasbrenner, M., Venkataraman, B., Kurz, R., Cole, G.J., Lee, C., 2017, *Electric Motor Driven Gas Compressor Packages, Proc. 48<sup>th</sup> Turbomachinery Symposium.*

[5] Kurz, R., White, R.C., Brun, K., 2012, "Upstream and Midstream Compression Applications- Part 2: Implications on Operation and Control of the Compression Equipment", *ASME Paper GT2012-68006.*

[6] *API 684: Standard Paragraphs Rotordynamic Tutorial: Lateral Critical Speeds, Unbalance Response, Stability, Train Torsionals, and Rotor Balancing.*

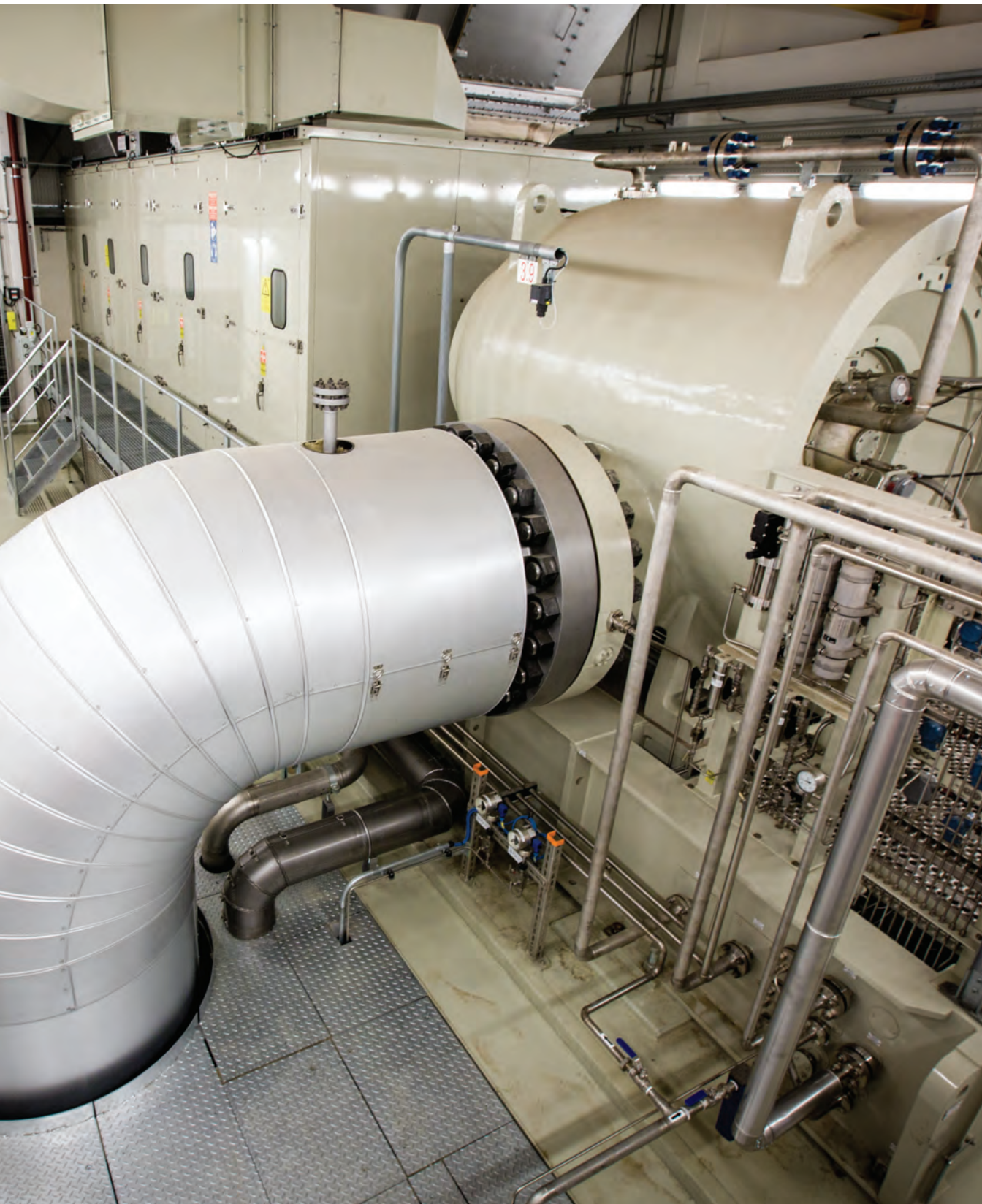
[7] *Application Guideline for Electric Motor Drive Equipment for Natural Gas Compressors, Version 4.0, May 2009, Gas Machinery Research Council and Southwest Research Institute.*

[8] Press, W.H., Vetterling, W.T., Teukolsky, S. A., Flannery, B. P., 1992, "Numerical Recipes in C", *The Art of Scientific Computing, 2nd Edition.*

[9] Newmark, N. M. ,1959 , "A method of computation for structural dynamics", *Journal of Engineering Mechanics, ASCE, 85 (EM3): 67-94.*

[10] Shigley, J. E., and Mischke, C. R., *Mechanical Engineering Design, New York: McGraw Hill, Inc. 1989.*







## CHAPTER 5

# MECHANICAL DESIGN

Centrifugal gas compressors are very versatile machines—used in vastly different industries—for all sorts of gases, pressures, temperatures, etc. Manufacturers must make hard decisions, if they choose to cater to focused industries and applications or if they want to pursue as many business opportunities as possible. Many suppliers have traditionally covered broad ranges of applications with their technologies, thereby promoting the use of centrifugal gas compressors that are custom designed for specific applications and operating conditions. This requires significant project-based engineering and testing, usually resulting in long lead times.

Solar Turbines designed gas compressors as a gas turbine accessory to meet the needs of the oil and gas industry (upstream and midstream) only. This focus enables pre-engineering and pre-testing of machine concepts that can be standardized to meet specific industry application requirements.

One of the basic concepts for standardized compressors is the requirement that all aerodynamic components within a common frame size must be mechanically interchangeable. This approach covers a very wide aerodynamic and mechanical design space (e.g. flow and head, pressure and temperature) within a fixed mechanical design. Other components such as the driver, coupling, bearings, seals, rotor length and support are common for that frame size—greatly reducing part count complexities. Extensive pre-testing of the compressor frame establishes application limits that can be presented to target customers with very high confidence levels.

Another side effect of this concept is the ability to re-stage the active components inside the machine to adjust performance and maintain optimum efficiency when onsite operating conditions change.

It is clear, however, that this methodology cannot cover all extreme operating conditions that a particular custom design might be able to satisfy through dedicated engineering efforts, extended lead times and higher product cost. Solar gas compressors have many components and technical solutions that are very common in the industry, but also have some design features that are unique. These special features have been developed and perfected over decades, helped greatly by the dedicated focus on upstream and midstream oil and gas applications.

Some typical features of modern centrifugal compressors utilized in upstream and midstream oil and gas applications are:

- Radial vibration monitoring
- Axial position monitoring
- Rotor trim balancing capabilities (at both shaft ends)
- Thrust bearing thermocouples or RTDs

- Journal bearing thermocouples or RTDs
- Dry-gas face seals with separation seals
- Tilt-pad journal bearings, integral body (non-split)
- Self-equalizing, tilt-pad, double-acting thrust bearing
- Thrust collar with elastic pilot-centered sleeve
- Flanges or ports (typically ring joint or raised-face type)
- Balance piston for thrust balance
- Dry flexible disk couplings, using spline couplings to shaft ends
- Vertically split, barrel-type construction
- Impellers manufactured as investment castings, machined from a solid forging, brazed or welded
- Impeller materials: stainless steel (eg. 15-5PH), titanium, inconel
- NACE H2S-resistant materials

Other features differ depending on individual manufacturer's design practices (Figure 5-1):

- Modular rotor construction (central tie bolt and stacked impellers / spacers / stub-shafts) or solid shafts (with the impellers keyed or shrunk on the shaft)
- Modular stator construction (stacked inlet and outlet system, diffusors, return channels, end caps), vertically split, or horizontally split stators
- Casings cast from carbon steel or stainless steel, forged or fabricated

**1<sup>st</sup> stage rotor and diaphragm being lowered into position**



**Completed rotor diaphragm assembly**

**Center body and endcap await module**



**Completed assembly with endcaps installed**

**Figure 5-1.** Assembly of a compressor utilizing modular design.

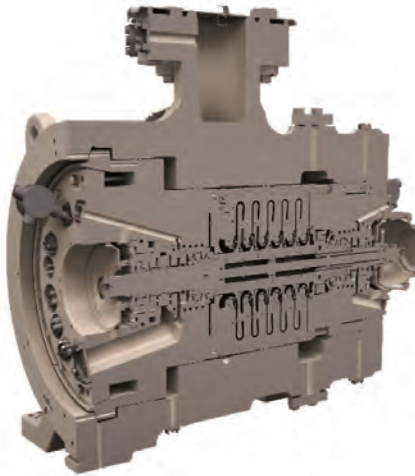


**Figure 5-2.** Cross section of a high-pressure compressor.

### CASING DESIGN

The compressor's pressure-containing body is a vertically split "barrel" assembly consisting of suction and discharge endcaps, which contain the bearing and seal assemblies, and a centerbody, which holds the rotor and stator assembly (*Figure 5-2*). The endcaps contain all the service ports for lube oil, dry gas seals, separation seals and instrumentation. The casings comply with the design requirements of API 617, which in turn uses many references from ASME Section VIII.

Finite-element-method computer codes are used to determine the stress levels and deflections in the centerbody and the endcaps (*Figure 5-3*). Endcaps and centerbody are connected using a lock-and-shear-ring arrangement. Drains are provided on both suction and discharge sides of the casing.

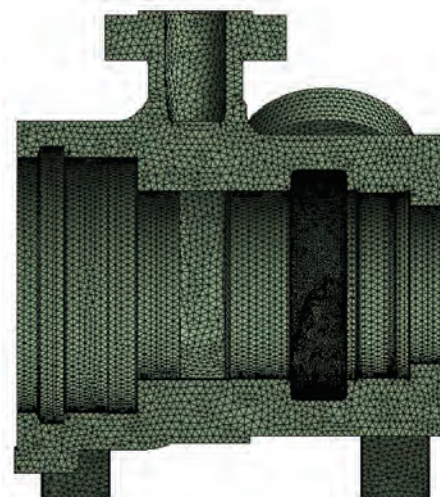
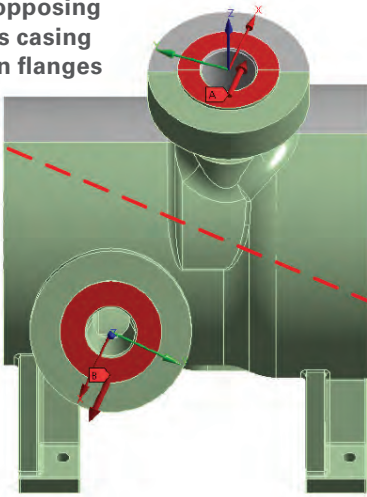


**Figure 5-3.** Finite element stress calculation for a cast centerbody.

**Forces opposing to stress casing between flanges**



**Moments opposing to stress casing between flanges**

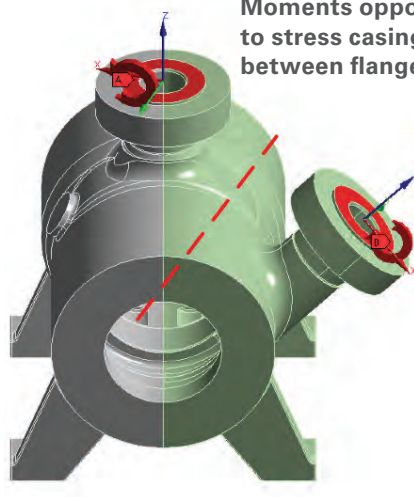


**Figure 5-4.** Calculation of allowable nozzle loads.

## CASING MANUFACTURE

Virtually all Solar gas compressors use cast steel centerbodies. The standardized design supports extensive optimization of the casting process to ensure consistent and sustained parts quality in the production phase. (Figure 5-4) Long-standing cooperation between foundries, machining houses and Solar provides for a continuous flow of centerbodies — the centerbody is not the long-lead item for a particular compressor build. After finish machining, hydrostatic pressure testing of all compressor casings and endcaps is performed at 1.5 times the maximum casing design pressure, independent of the particular application pressure.

The benefits of extensive special tooling for shop assembly and field maintenance are other positive outcomes resulting from the use of standardized products. Proper tooling permits quick removal of the (Figure 5-5) discharge endcap, the rotor/stator assembly, insertion of the restaged assembly ('module'), and closing of the endcap, all typically within one shift.



**Figure 5-5.** Bundle (Module) and centerbody.

## IMPELLER DESIGN

Each compressor family uses a set of standard impellers for various flow demands. The impeller geometry is fixed—only the tip diameter may be modified for special (and rare) applications. Tight tolerances during manufacture minimize any variance in aerodynamic geometry, thereby providing highly accurate performance estimates after extensive scaled and full-scale testing of impellers and their combinations with other aerodynamic components such as inlets, volutes, diffusers and return channels.

Compressor impellers are designed to conservative stress levels, making them suitable for sour gas applications (*Figure 5-6*). Careful design of blade leading and trailing edges avoids blade vibrations that might trigger fatigue failure.

## IMPELLER MANUFACTURE

Impellers are precision-cast stainless steel for strength and corrosion resistance. Precision casting involves final machining of critical interfaces. Alternatively, impellers are machined from solid forgings or machined as open blade impellers from a forging, with a separate, brazed shroud (*Figure 5-7*).

Impellers go through the following manufacturing procedures that are developed and fixed as part of the initial design effort:

- For cast impellers: wax check, casting, initial quality check and weld upgrades
- For machined impellers: forging quality checks (ultrasonic testing-UT), machining programs including cutting tool definition
- For brazed impellers: forging quality checks (UT), machining programs including cutting tool definition, shroud and impeller gap machining, brazing following defined heat treatment cycles, UT inspection of braze
- Heat treatment
- Magnetic particle inspection
- Visual inspection
- Machining of interface features and balance-for-spin test
- Dimensional inspection
- Spin test to 115% of maximum mechanical speed, dimensional inspection
- Fluorescent dye penetrant inspection
- Final component balance

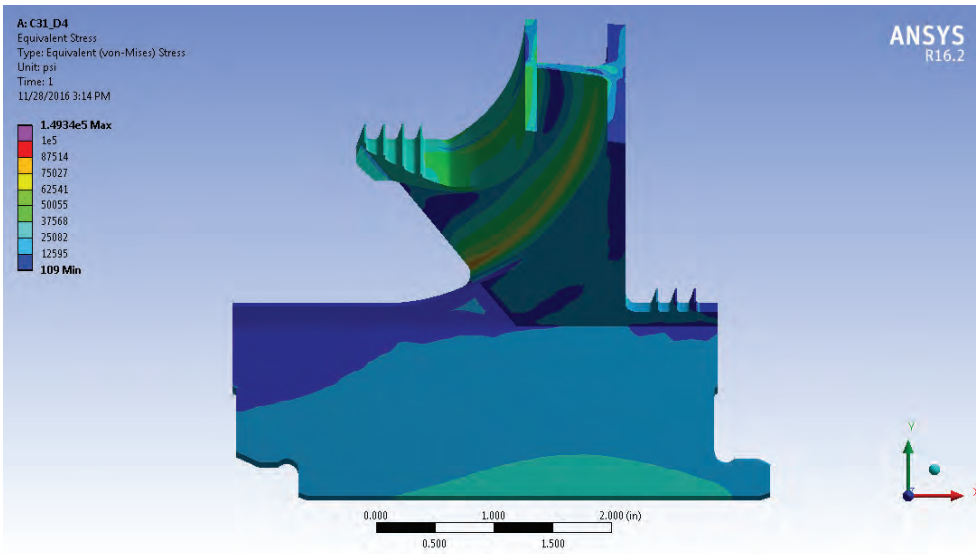


**Figure 5-6.** Stress calculation for an impeller. The picture also shows the labyrinth seals on the hub and the shroud.



**Figure 5-7.** Impeller manufacturing methods: (left) machined, (center) cast, (right) machined with brazed shroud.

## ROTORS

Industry practice has traditionally utilized solid-shaft rotor construction with impellers shrunk to the shaft. This results in a somewhat permanent rotor assembly that does not readily permit the substitution of different impellers on the shaft, in the event of a restage, due to the high cost and difficulty in removing and installing an impeller via the shrink-fit process. Standardized concepts take advantage of modular rotor assemblies, consisting of matching components like stub shafts, impellers, and (if required) rotor spacers (to maintain a constant bearing span) and a centerbolt (also called tie bolt) (Figure 5-8). These components are dynamically balanced individually and are rabbet-fit to each other for concentric alignment. Torque is transmitted through dowel pins, as well as through friction of the axial faces under high preload due to the tie bolt. The entire assembly is clamped together with the centerbolt. Assembly and disassembly are straightforward, using special tools. Special precautions are taken to ensure consistent balance quality throughout the manufacturing process.

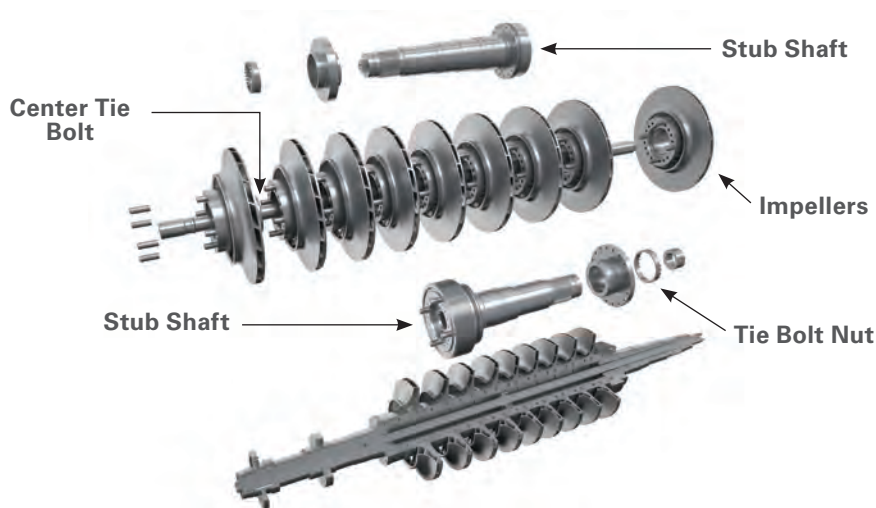


**Figure 5-8.** *Modular Rotor*

## BEARINGS

The high operating speeds of modern centrifugal gas compressors are made possible by use of tilt-pad journal bearings. Traditional oil-film sleeve journal bearings suffer from fluid-flow induced instabilities, commonly referred to as “oil whip” and “oil whirl,” which occur at operating speeds two to three times above the lowest critical speed of the compressor. The tilt-pad bearing is not prone to these problems because it does not generate forces on the rotor that destabilize the system.

Two types of thrust bearings are used in centrifugal gas compressors: fixed tapered land and self-equalizing tilt-pad thrust bearings. Both types perform well and have comparable load capacities for same-size bearings. Self-equalizing tilt-pad thrust bearings differ from the fixed tapered land bearings in two ways: Each thrust pad is an individual plate that is free to pivot. As the thrust collar rotates, each pad tilts, generating the optimum load-carrying oil film. Therefore, the bearing can accommodate slight misalignment between the bearing and thrust collar. Loads will be equally distributed among the pads through the movement of individual leveling links and disks. The self-equalizing tilt-pad thrust bearing has been adopted as the bearing of choice for all modern compressor designs, while older machines in the fleet are still supported with the fixed tapered land parts.

## INTERSTAGE SEALS

Solar gas compressors make extensive use of abradable seals on the rotor—every impeller has a shroud seal and a hub seal to reduce the backflow of pressurized gas after compression. The seal consists of rotating labyrinths, cut from the impeller body, running against a stationary ring that includes an abradable material: Babbitt, which is a sprayed powder component or honeycomb structures filled with again a powder material. The labyrinth tips of the impeller reduce the required clearance during the so-called break-in process as part of the manufacturing cycle.

## BALANCE PISTON

Depending upon the compressor configuration and application, the axial rotor thrust can become very large. The balance piston is installed at the discharge end of the compressor rotor to help counterbalance the axial forces of the impellers. The balance piston is a drum larger in diameter than the rotor shaft, with seals on the periphery, running against a replaceable seal ring (*Figure 5-9*). These seals can be abradable seals, similar to the interstage seals, or hole-pattern seals positioned against a smooth shaft. While one side of the balance piston is exposed to the discharge pressure from the last impeller, its other side is referenced back to suction pressure via a balance return line. The pressure difference multiplied by the balance piston area equals the balance piston thrust. The size of the balance piston (taken from a standardized set of geometries) is selected to provide optimum force balance to the rotor thrust. Depending on the actual operating point of the compressor on the compressor map, the thrust varies in magnitude and also direction. The balance piston selection ensures that the resultant axial force can be safely carried by the axial bearing. A restage operation as noted above might therefore also trigger a reselection of the balance piston and its associated seal from the standard set of components.

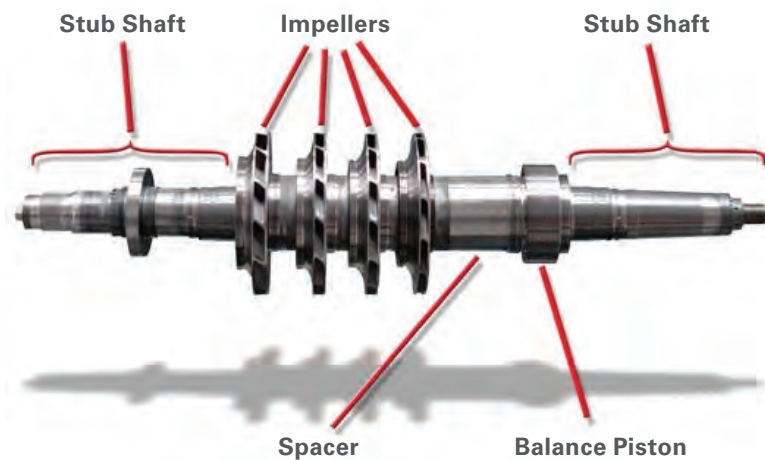


**Figure 5-9.** Shaft with stub shafts, impellers, spacer, and balance piston.

In Chapter 4 on Rotordynamics, the importance of controlling the excitation of the rotor, as well as the importance of creating sufficient damping were referenced.

Recent developments facilitate the direct measurement of the available rotor system damping, while operating at the speed, pressure and gas density of actual operating conditions. This method involving the use of a magnetic exciter, which is essentially a magnetic bearing mounted on the compressor rotor, allows the imposition of vibration forces on the running rotor (*Figure 5-10*). If the exciter is turned off, the damping forces lead to a decay in the vibrations. The ratio between two successive amplitudes is a direct measurement of the logarithmic decrement of the rotor system.

To increase the damping from conventional hydrodynamic bearings, so called damper bearings have been developed (*Figure 5-11*). These designs allow for additional damping from an oil film created between the outer bearing and the bearing capsule. The use of

these bearings facilitates operation of compressors at higher speeds and higher discharge pressures.

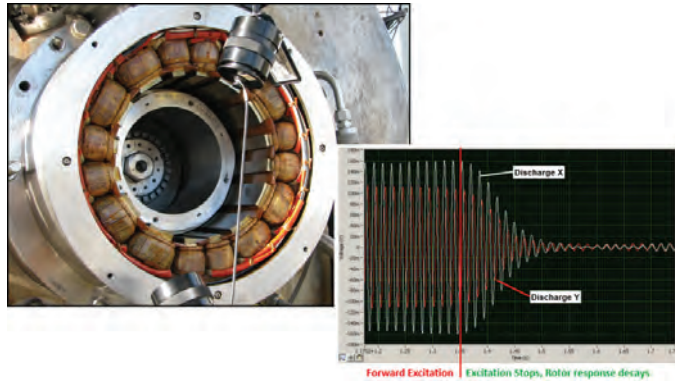


**Figure 5-10.** Measuring the actual damping of the rotor system in operation.

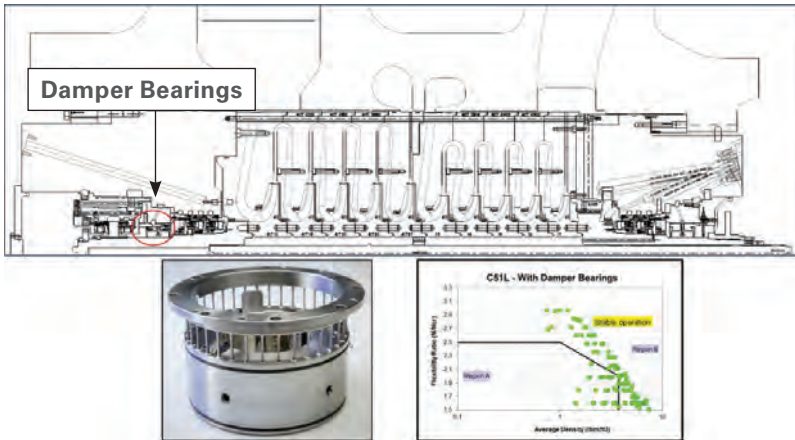


**Figure 5-11.** Damper bearings

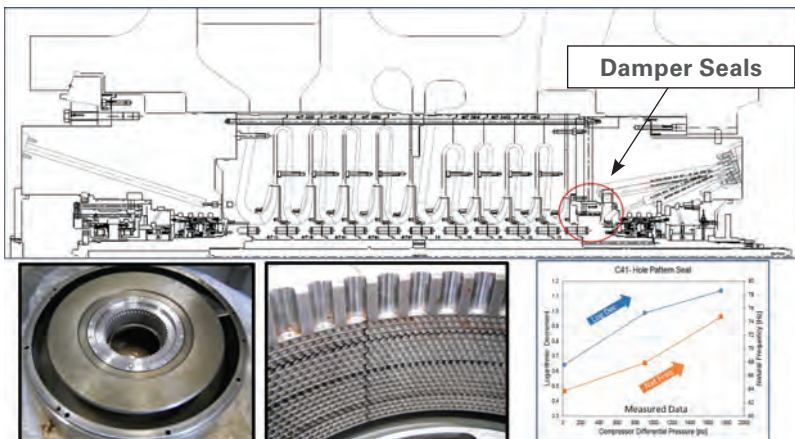


**Figure 5-12.** Damper seals (hole pattern seals)

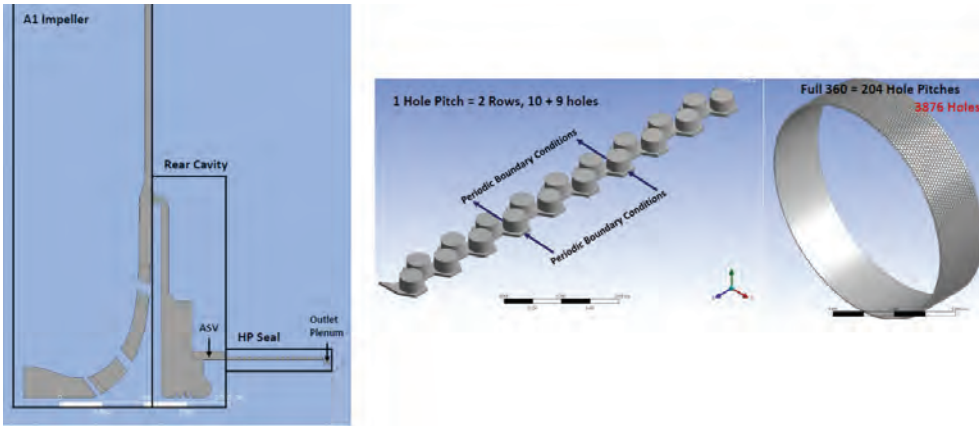


**Figure 5-13.** Modeling of a damper seal located on the balance piston.

Another method that increases damping is the use of damper seals. (Figure 5-12) The hole pattern of these seals—that can be used in lieu of conventional labyrinth or honeycomb seals, especially on the balance piston—create damping forces that increase with the pressure differential over the seal, thus improving the rotor’s logarithmic decrement (Figure 5-13).

Reducing the excitation forces on the rotor is another means of improving the compressor’s rotordynamic behavior. A major source of excitation forces can be the shroud seal on the impeller. The excitation results from instabilities caused by swirling flow entering the labyrinth. As discussed in the chapter on aerodynamics, the leakage flow along the shroud wall of the impeller accrues significant amounts of swirl, while travelling from the impeller tip to the impeller shroud seal at the impeller inlet. Anti-swirl vanes (Figure 5-14) reduce the amount of swirl in the flow when entering the labyrinth seal (Figure 5-15). Modelling the effect of these vanes and the excitation forces in the labyrinth requires complex CFD models that facilitate the capture of transient flow effects resulting from rotor eccentricity (Figure 5-16). Figures 5-17 and 5-18 shows the effect of using anti-swirl vanes (ASV) in a rotor showing high sub-synchronous vibrations that disappeared after the ASV were installed.

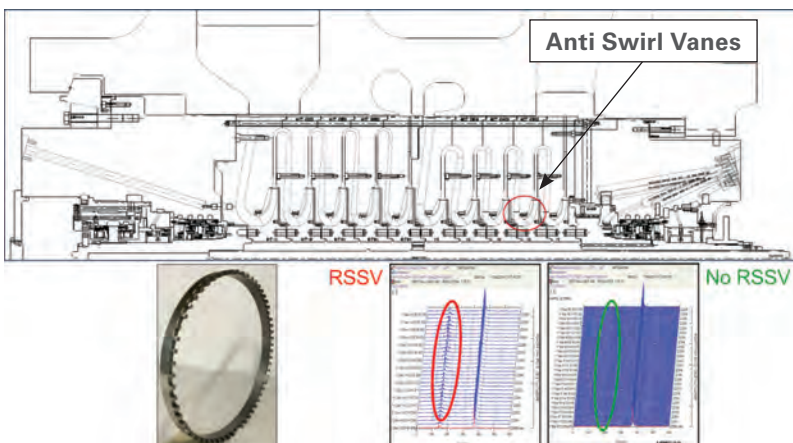


**Figure 5-14.** Anti-swirl vanes for the impeller shroud seals.

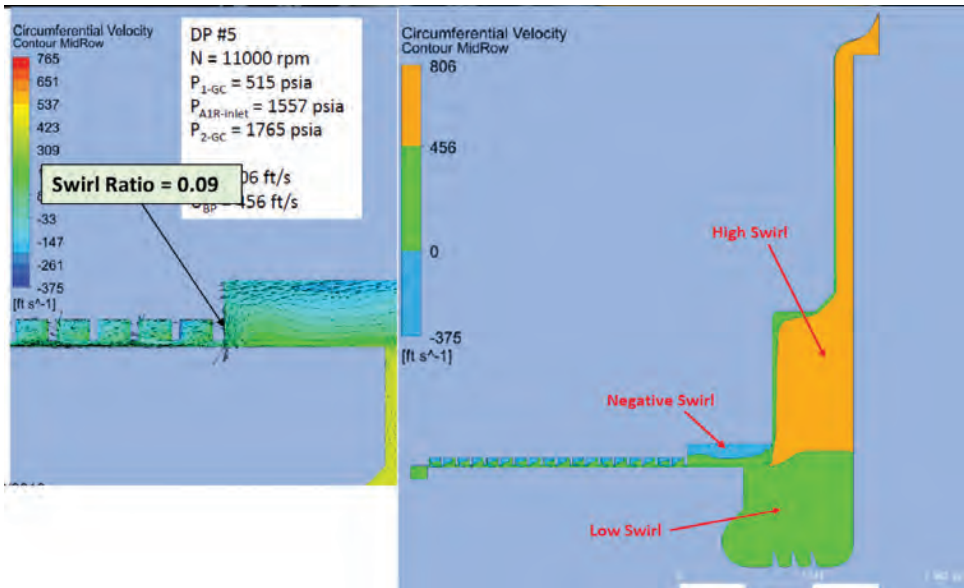


Figure 5-15. Swirl in the flow is reduced when entering the labyrinth seal.

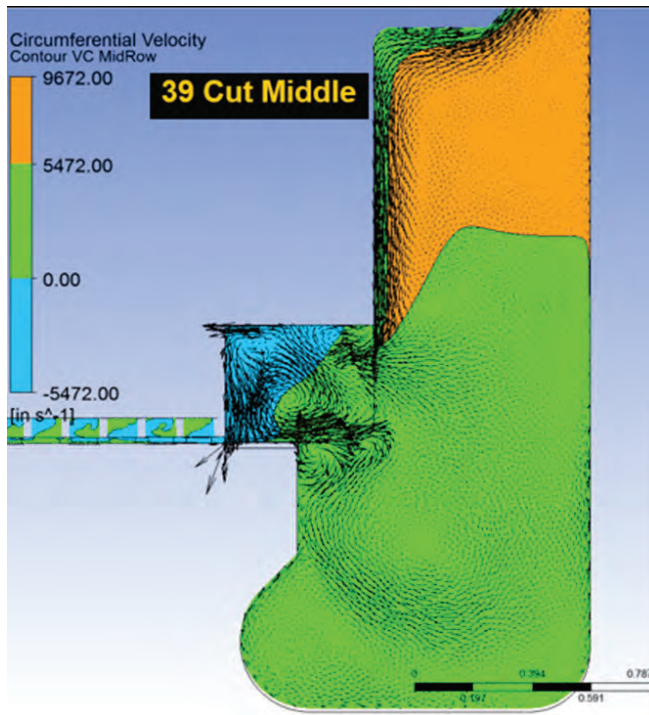
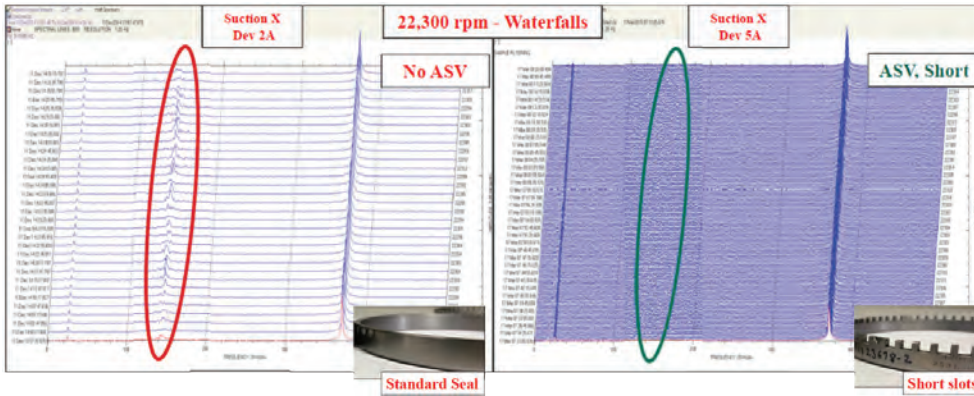
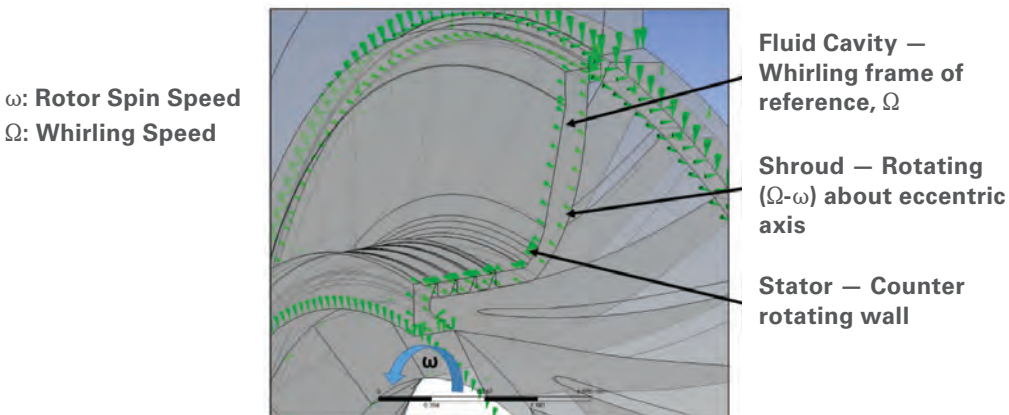


Figure 5-16. Modelling the effect of anti-swirl vanes.



**Figure 5-17.** Effect of utilizing anti-swirl vanes in a rotor showing high sub-synchronous vibrations that disappeared after the ASV were installed.

### Eccentric Cavity Model



**Figure 5-18.** Detailed numerical simulation.

## SHAFT END SEALS

Compressor shaft-end seals and their support systems prevent the escape of process gas along the shaft, as well as protecting the seal against oil ingress from the adjacent radial or axial bearings.

Most modern compressors in oil and gas applications use tandem dry-gas face seals (DGS) that are designed as self-contained cartridges (*Figure 5-19*). A rotating sleeve sits inside a stationary body. The seal function is created by the action of two rings: the stationary ring and the “mating” ring which rotates with the shaft via the shaft sleeve. The seal gas acts at the gap between the rotating and stationary rings and creates a gas film that provides the sealing effect, while at the same time ensuring frictionless operation. Since the gas film is very thin, only a small amount of gas is actually lost through the seal.

The stationary ring is held against the mating ring by springs located in the housing—during operation the gas seal pressure in the seal gap acts against this spring load. An O-ring seal ('dynamic O-ring') allows small axial movements of the stationary ring with a minimum of frictional forces, while maintaining full seal differential pressure across it. The shaft sleeve becomes a part of the rotor. Therefore, it is centered on the shaft by means of pilot surfaces and tolerance rings or O-rings.

For flammable and toxic gases, the above described seal system is effectively doubled, hence called the tandem DGS (*Figure 5-19*), with the total pressure drop taken across the primary seal and using the secondary seal as a backup seal in case of severe failure of the primary seal, providing temporary protection of the compressor train until safe shutdown. The space between the primary and the secondary seal can be routed to a flare in order to dispose of the small amount of process gas leaking through the primary seal.

When stationary (non-rotating), the seal dam area of the mating ring is in contact with the stationary ring, up to a differential pressure of about 689 kPa (100 psi). Above this pressure, or under rotation, the rings separate due to increasing hydrostatic pressure between the sealing faces. During dynamic operation, the rotating mating ring lift geometry, in conjunction with the sealing dam, creates a pressure distribution that causes the primary ring to move away from the mating ring. This very narrow gap allows a small leakage flow to pass through the seal. Different seal manufacturers use different patterns for lift augmentation.

For the DGS to perform satisfactorily, the amount, type, and size of contaminants—as well as the gas properties of the seal gas (e.g. dew point) entering the seal—must be controlled. Therefore, seal gas, which can be conditioned process gas, is brought between the inboard side of the DGS and the process gas at a pressure higher than the adjacent process to prevent ingress of contaminants.



**Figure 5-19.** Tandem dry gas seals.

To prevent lube oil from entering the DGS, a separation seal is installed between the outboard of the seal cartridge and the bearings. Solar gas compressors use pairs of segmented carbon rings with an air or nitrogen purge to create an effective dam against oil ingress.

Dry gas face seals consist primarily of a stationary ring that is attached to the housing and a mating ring that rotates with the compressor shaft. A spring keeps the face of the stationary ring against the rotating face of the mating ring when the shaft is not turning (Figure 5-20). Face separation is achieved when the seal pressure reaches 690 kPa (100 psid) across the seal. During operation, the groove pattern in the rotating seal face (Figure 5-21) pumps the seal gas inward toward the un-grooved portion, or sealing dam, creating a high-pressure area behind the sealing dam. This pressure distribution separates the rotating and static seals, forming a small, controlled gap between 0.0025 and 0.0050 mm (0.0001 and 0.0002 in.) wide. This very narrow gap allows a small leakage flow to pass through. Filtered seal gas, from either an external source or the compressor discharge, is supplied to the face seal. The extremely small gap clearances of face seals require clean and dry seal gas.

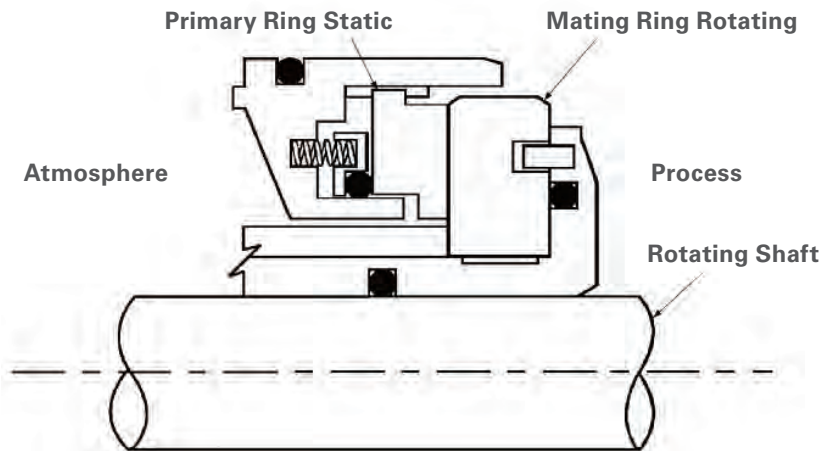


**Figure 5-20.** Gas face seal assembly.

In the event the faces approach each other, a rapid rise in pressure instantaneously causes separation. This automatic reversal is self-correcting, and the gap width stabilizes when the hydrostatic and hydrodynamic forces equalize.

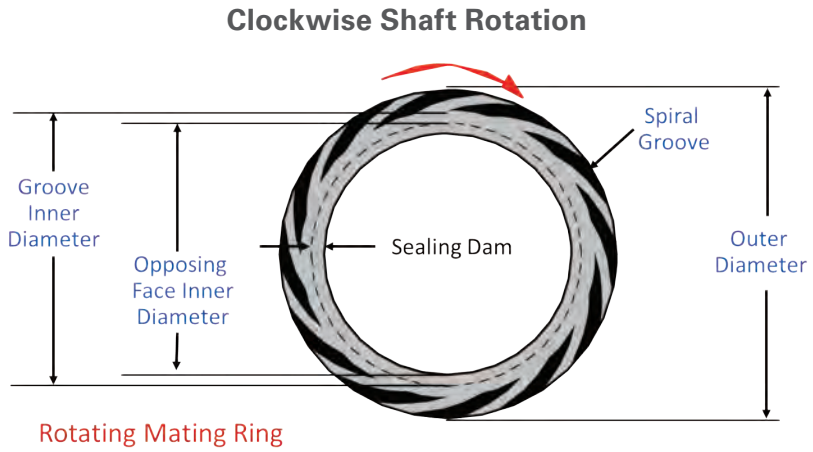


**Figure 5-21.** Cross-sectional view of rotating seal face.

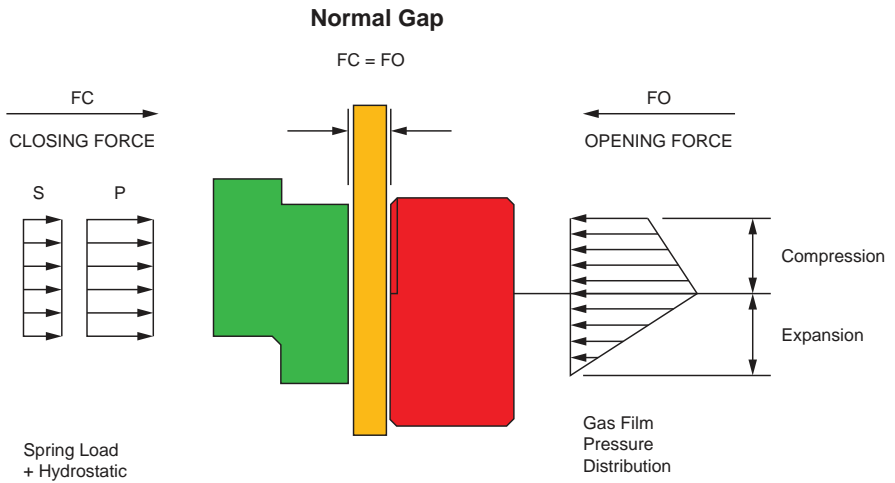


**Figure 5-22.** Balance of opening and closing forces on a dry gas seal (DGS).

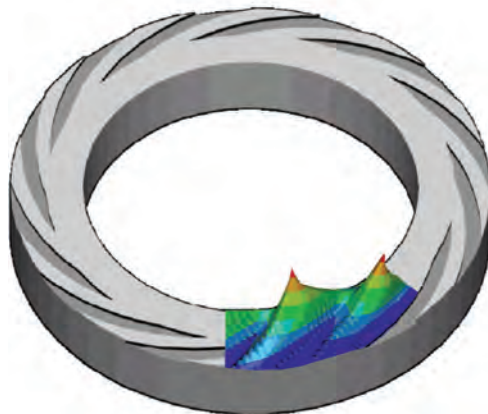


**Figure 5-23.** Pressure distribution on a DGS face.

Dry seals can also have an intermediate labyrinth seal located between the primary and secondary seals (*Figure 5-22*). The function of this intermediate labyrinth is to isolate the primary vent from the secondary vent. Secondary seal gas, which must be an inert gas such as nitrogen, may be injected between the secondary seal and the intermediate labyrinth. This gas also requires the same cleanliness as the primary seal gas. Some of the secondary seal gas passes through the labyrinth into the primary vent, rendering a non-combustible mixture in the primary vent. The remainder of the secondary seal gas passes through the secondary face seal into the secondary seal vent.

Several different rates of gas leakage, for gas leaking across the seal faces into the vent have to be defined (*Figure 5-23*):

**Maximum dynamic** primary seal leakage rates per seal at the compressor’s highest pressure and speed under dynamic operating conditions.

**Normal** leakage rates at operating conditions depend on suction pressure and speed, and are typically less.

The static leakage rate (when the compressor is not running) is lower than the dynamic leakage rate.

The leakage defined above should not be confused with the amount of seal gas that has to be supplied, since the vast majority of the seal gas, as explained later, will leak across a labyrinth back into the process gas.

Primary seal gas can be obtained from the compressor discharge or supplied by a separate source. Either way, the seal gas must meet specific standards of supply temperature, cleanliness, dryness, and pressure to assure the efficiency and long-term operation of dry face seals. Seal gas must be provided during start-up, normal operations, shutdown and pressurized hold, and at any time there’s process gas in the compressor casing.

When the dry seal assembly is provided with an intermediate labyrinth between the primary and the secondary seal faces, an inert gas (nitrogen) may be injected into the area between the labyrinth and the secondary seal. The injected gas is referred to as secondary seal gas. Its use is not mandatory, even if the dry seal has an intermediate labyrinth.

A separation seal assembly (*Figure 5-24*), which is separate from the dry gas seal assembly, is installed between the dry gas seals and the compressor lube oil drain cavity (bearings). Separation seals are the most outboard component of the complete seal system (*Figure 5-25*). Separation seals, also called buffer seals, barrier seals or circumferential seals by the industry, prevent bearing

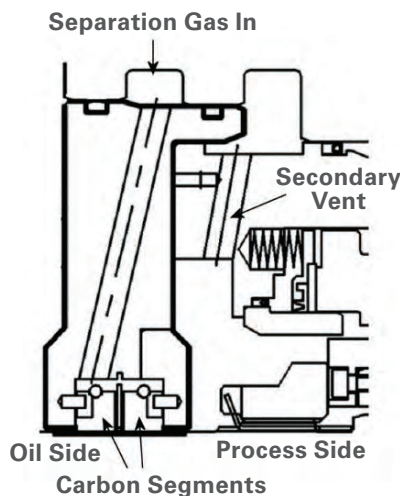


**Figure 5-24.** Typical separation seal assembly.

lube oil from migrating along the shaft to the dry gas seals (Figure 5-26). In addition, they prevent seal gas from entering the lube oil system.

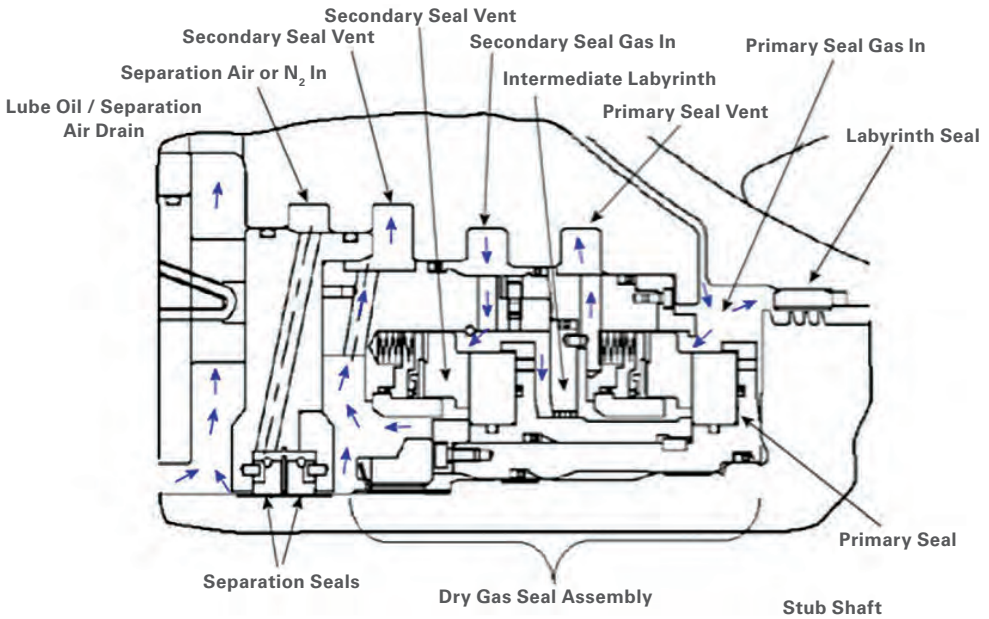


Figure 5-25. Tandem seal assembly with intermediate-labyrinth seal.

### Spiral Groove Comparison



Uni-directional Spiral Groove

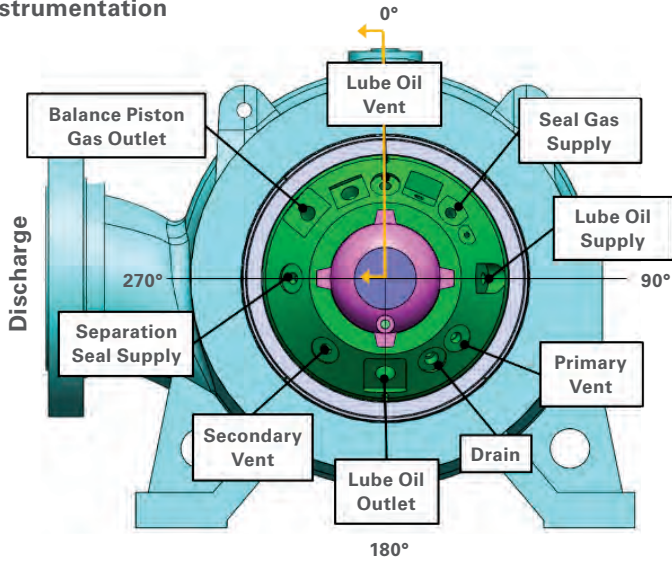


Bi-directional Spiral Groove

Figure 5-26. Uni-directional and bi-directional groove patterns.

The capability to operate a centrifugal compressor at elevated discharge temperatures allows high pressure ratios, while avoiding the cost of additional intercoolers. Concerns are focused on the impact on dry gas seals, as well as on hub and shroud shaft seals and the balance piston seals. Figure 5-27 shows the results of a highly instrumented compressor test at high discharge temperatures measured at various locations on the endcap, as well as at the location of the dry gas seal. The tests, which also took different lube oil supply temperatures into account, showed the successful operation at high compressor discharge temperatures with no apparent degradation of aerodynamic compressor and seal performance.

### Endcap Instrumentation



TC	Location Description	Circumferential Positions ( ° )
1	DGS Back Wall	0
2	DGS OD	0, 90, 180, 270
3	End Cap Secondary Vent ID	0, 90, 180, 270
4	Embedded DGS	0, 180
5	Embedded Balance Piston	0, 180
6	End Cap Surface	0, 90, 180, 270

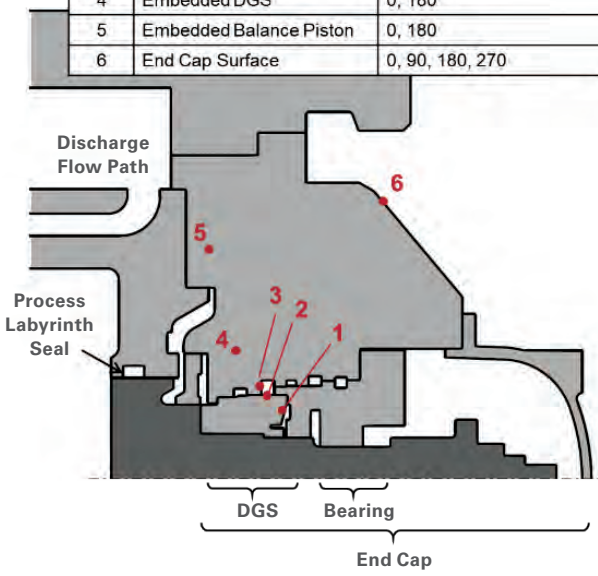


**Figure 5-27.** Measuring local temperatures for compressor operation at high discharge temperatures.

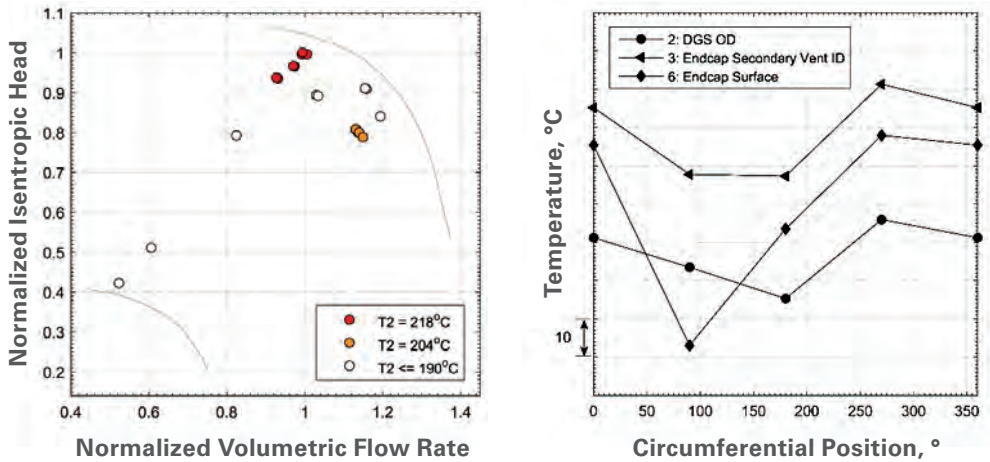


**Figure 5-28.** Tests at high discharge temperatures for validation of local temperature distribution, dry gas seal operating temperatures and balance piston seal durability.

Circumferential temperature variation around the end cap: Generally, the warm side of the compressor corresponded with the discharge flange side (*Figure 5-28*). The end cap surface temperature exhibited additional variation compared to the DGS and secondary vent, due to its proximity to the balance piston outlet port and the lube oil supply port. Linear trends with respect to compressor discharge temperature were shown as an adequate fit to predict the amount of variation at TC3 and TC6 locations (the end cap secondary vent and end cap surface), but the linear trends at the TC2 DGS location were not as strong.

Temperatures near the DGS cartridge are significantly lower than compressor discharge temperatures, and operating conditions at higher discharge temperatures may be achievable with existing DGS materials (*Figure 5-29*).

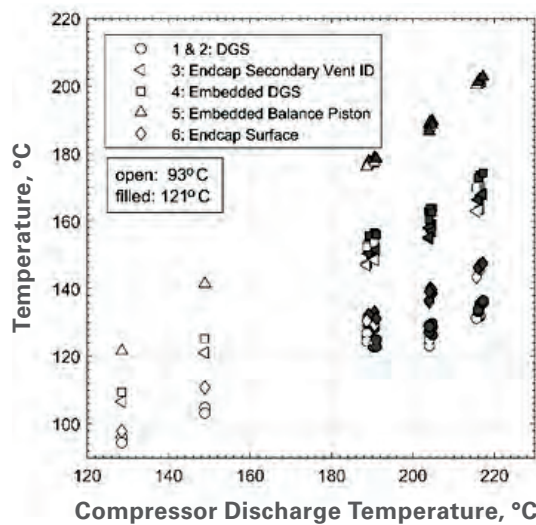
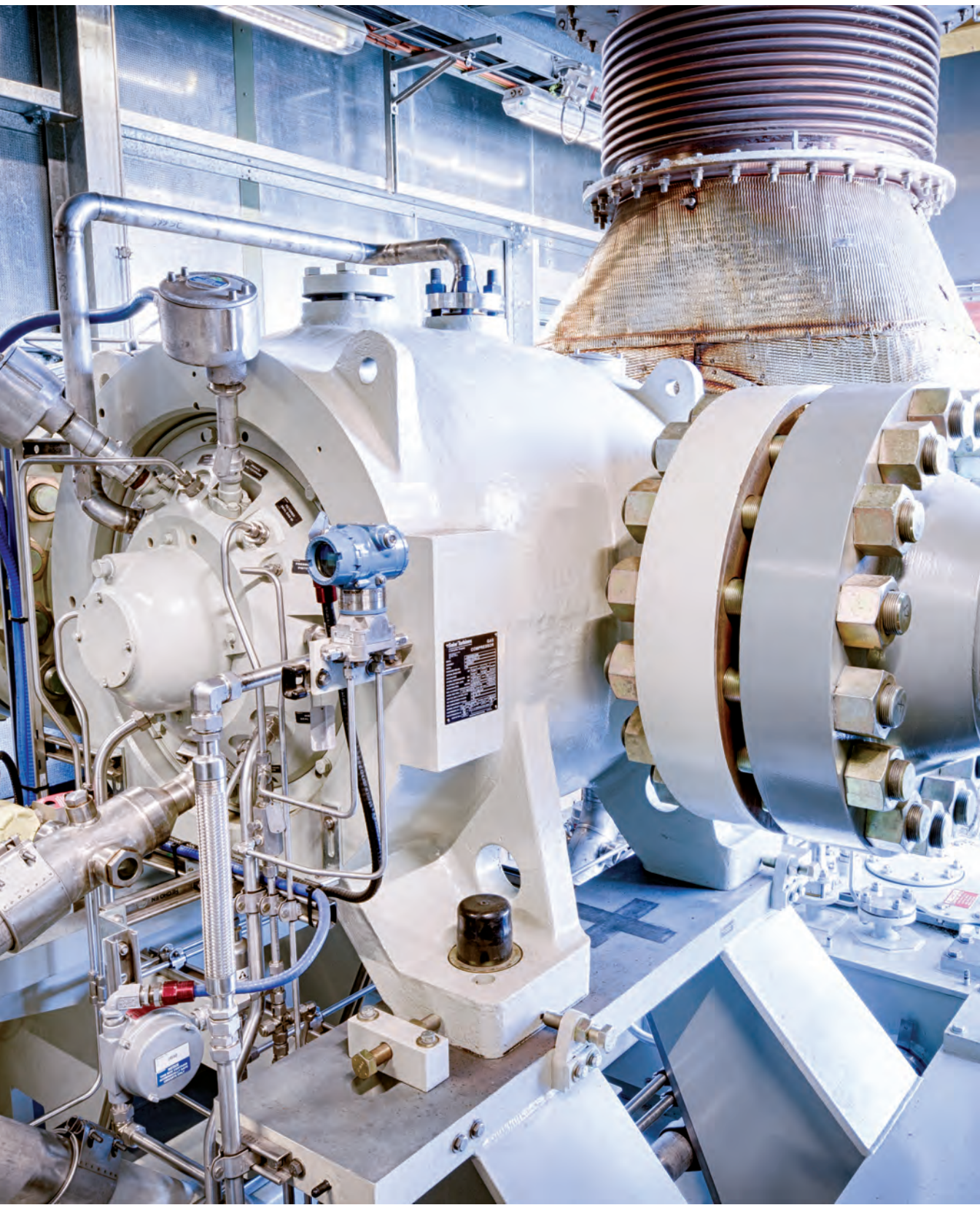


**Figure 5-29.** The endcap temperature distributions compared to discharge temperatures ranged from the warmest at the balance piston (about 95%) to the coolest at the DGS (about 65%).





## CHAPTER 6

# CONTROL OF CENTRIFUGAL COMPRESSORS

Compressor control requires two primary objectives: meeting the external process requirements and keeping the compressor within its operational boundaries. Typical control scenarios that have to be considered are process control, starting and stopping units, and fast or emergency shutdowns [1], [2], [3]. Controlling a centrifugal compressor involves understanding the interaction of a compressor (with a given operating characteristic) and with the process (having a distinct behavior).

Regarding the compressor, discussing the different control devices, such as variable speeds, guide vanes, throttles or recycle valves, is necessary. Different compressor operating conditions such as surge, stall, and choke must be considered. Knowing whether a steady-state compressor map is still valid in the case of fast transients is also important.

The control system must be addressed as related to instrumentation and device requirements, as well as the control methods of the drivers. Additionally, the goal of the control system must be defined. The requirements to protect the process as well as the equipment have, of course, priority. But other goals need to be defined, too, particularly if the station involves multiple compression units, either in series or in parallel. Possible goals can be to minimize fuel consumption, to minimize maintenance costs or to maximize throughput.

For the process, one must understand the relationship between the flow through the system and the pressures imposed on the compressor. These relationships are different depending on their rate of change. In other words, one must expect different system responses for fast and slow changes, as well as steady-state conditions.

Different upstream and midstream applications lead to different compression system characteristics and control requirements, which in turn, are the result of compressor requirements, such as high pressure ratio or wide operating range, and the process requirements. Multiple unit installations—with multiple compressors per train, and installations where the train has to serve multiple gas streams—require specific process control considerations that match the compressors with the process system behavior and the objectives of the station or system operator.

The behavior of compressors during emergency shutdowns will be discussed at the end of this section. The control system's function is simply to initiate the shutdown and to open the recycle valve as fast as possible. However, the interaction of the compressor and this system, in a highly transient situation, is of interest. The behavior during emergency shutdowns has been covered in great detail in a number of papers, for example by Botros et al. [4,5], Kurz et al. [6], Morini et al. [7] and Blieske et al. [8].

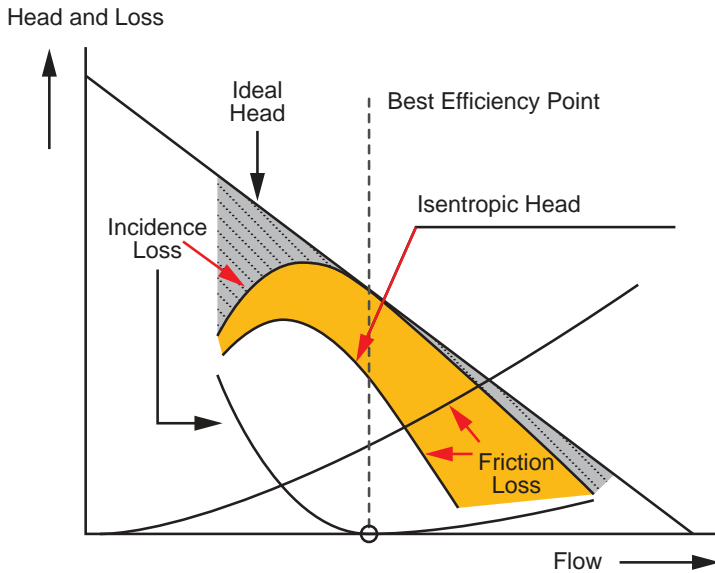


**Figure 6-1.** Head-flow characteristic of a compressor at constant speed. Operational flow at higher or lower than the design flow causes incidence losses.

## THE CENTRIFUGAL COMPRESSOR

Centrifugal compressor behavior can be described by its head-flow-efficiency relationships. These relationships were explained in detail in the previous chapter on aerodynamics. The basic relationship, for a compressor at constant speed is shown again in *Figure 6-1*. The compressor shows a distinct relationship between head and flow. In the case of machines with backwards bent impellers (the type in general used in upstream and midstream compression applications), the head of the compressor increases with reduced flow. Due to the increase in losses when the compressor is operated away from its design point, the curve eventually become horizontal, and subsequently starts to drop again. The curve section with positive slope is usually not available for stable operation. When the flow is increased beyond the design flow, the losses also increase, and increase the slope of the curve, sometimes to a vertical line. This is discussed in more detail in the section on compressor aerodynamics.

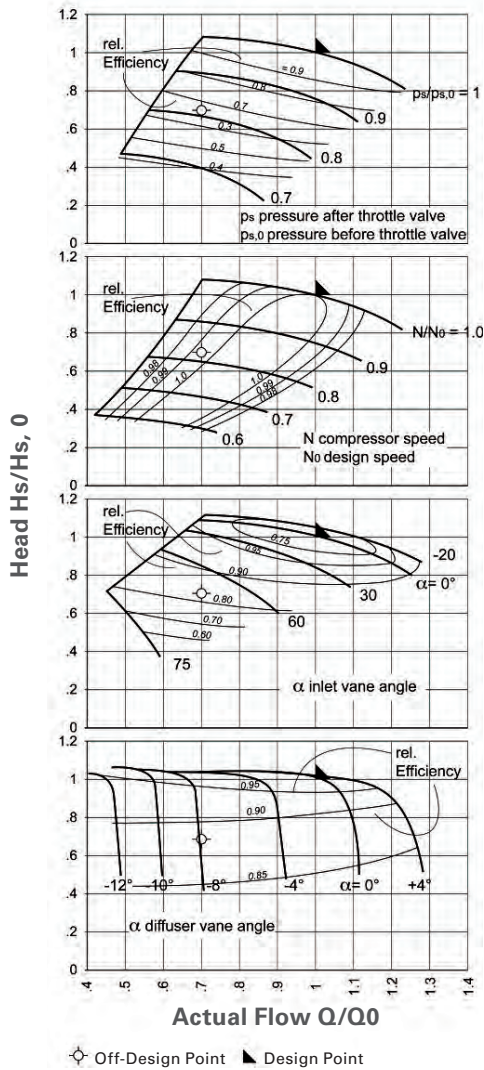


**Figure 6-2** Control methods for centrifugal compressors: Throttling, variable speed, and adjustable guide vanes (Rasmussen et al. [9]).

Applying different control mechanisms—such as speed variations, adjustable inlet vanes, or adjustable diffuser vanes—enables the compressor to operate on a family of curves, as can be seen in *Figure 6-2*.

*Figure 6-3* indicates the effectiveness and efficiency of different control methods. A compressor that can be operated at varying speeds is of particular importance in upstream and midstream applications, since this is the most effective and efficient control method. (*Figures 6-2 and 6-3*). Using a throttle, recycling (*Figure 6-4*) or adjustable inlet vanes are very effective ways to reduce the volumetric flow, but they're not very efficient, because the power consumption is not reduced at the same rate as a speed-controlled machine. This control scheme works for one or more compressors, and can be set up for machines operating in series, as well as in parallel.

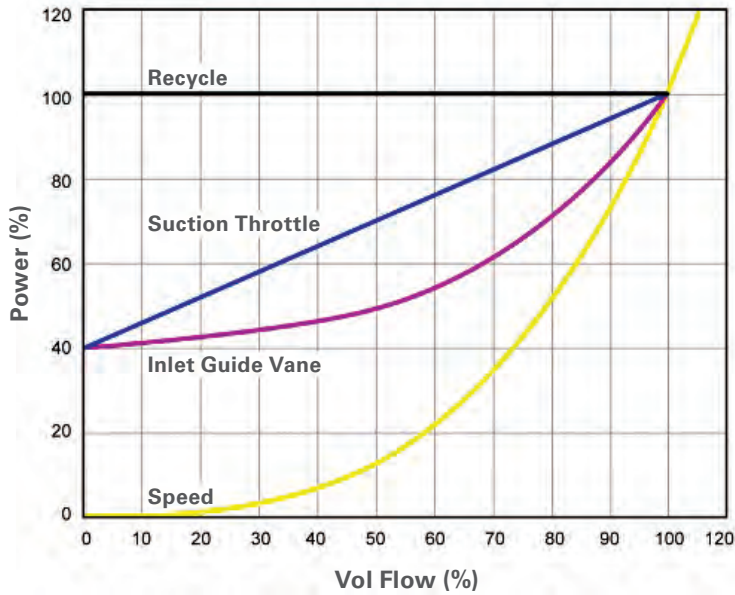


**Figure 6-3.** Power consumption for different control methods.

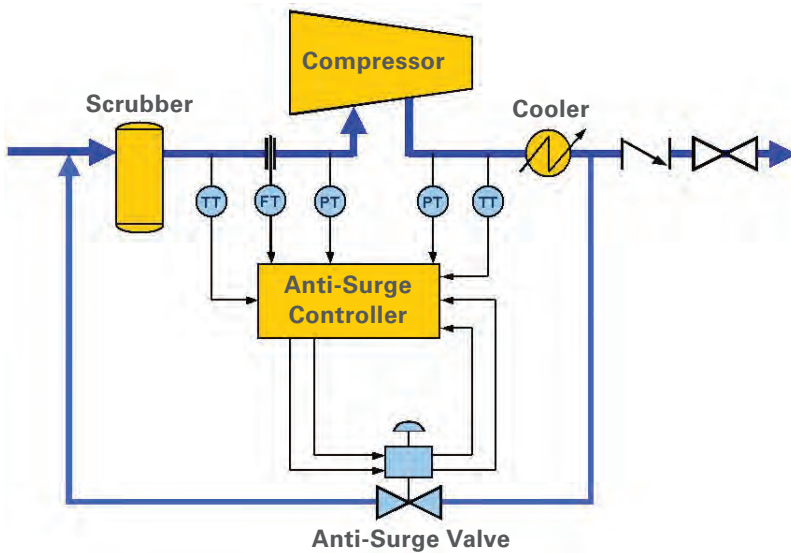


**Figure 6-4.** Recycle System

If speed control is not available, the compressor can be equipped with a suction throttle or with variable guide vanes. If available, the latter configuration in front of each impeller is rather effective, but the mechanical complexity usually proves to be prohibitive in pipeline applications. The former is a mechanically simple means of control, but it has a detrimental effect on overall efficiency.

## COMPRESSOR PROTECTION

Within the control system, subsystems protect the compressor, as well as its driver. In general, process control will be enabled as long as the compressor and its driver stay within acceptable, predefined boundaries. For the compressor, these boundaries may include:

- Maximum and minimum operating speed
- Stability limit (aka surge line)
- Choke or overload limit (on some machines)
- Pressure, temperature, torque limits

## STATION LEVEL

Further, at the station level, if multiple units are used, control can be exercised by selecting the number of units in operation. Compressor configurations within a station can include:

- Single compressors
- Single compressors supplied from or delivering into multiple headers
- Multiple compressors operated in parallel
- Multiple compressors operated in series
- Multiple compressors, or compressors with multiple sections operated in a train

Variations may include:

- Multiple compressors in a train with control of intermediate pressures
- Multiple compressor trains in parallel

### Series and Parallel Layouts

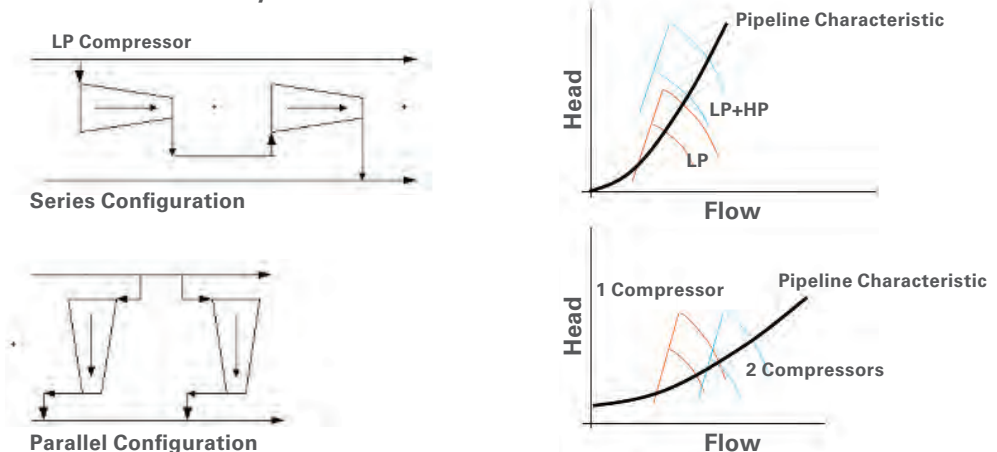


**Figure 6-5.** Compressors in series and parallel configurations.

If compressors operate in parallel, each will see about the same suction in discharge pressure, but the flow will be split between the machines. If compressors operate in series, the discharge pressure of the first machine becomes the suction pressure of the next machine and so on. All machines process the same flow (unless there is recycling or side streams), but the overall pressure ratio is divided between the machines. In some instances, the gas is cooled with intercoolers (*Figure 6-5*).

With multiple units on a station, the question becomes how to control them to achieve certain objectives. These objectives may be minimizing the running hours of units, optimizing the capability to absorb load swings, minimizing fuel consumption or emissions. The first objective requires running as few units as possible, while the second may require running all or most units at partial load for most of the time. Minimizing fuel consumption, which also equates to minimizing CO<sub>2</sub> production, will usually involve strategies to cover the load with as few units running as possible (i.e. running units as close to full load as possible or not running them at all). The question then becomes is it better to run the operating units with one at full load and the remaining unit at part load; or, to run all units at partial load. It is important to note that in all scenarios, the load (i.e., the power made available to the compressor) is the control variable. The compressor speed is a result.

If the driver is a two-shaft gas turbine, a few basic guidelines follow from the fact that a gas turbine achieves its best efficiency running at or near full load:

- For two identical units running, the answer is usually to run both of them at equal partial load. This is accommodated by operating the compressors at equal turndown or at equal gas turbine load (i.e., equal gas producer speed).
- For more than two identical units running, the difference in fuel usage between N units running at the same load, and some units running at full load, and the remaining units at partial load, is usually very small. The optimum is then more often determined by the resulting operating points of the compressors.
- For units that are not identical, it is usually better to load the more efficient unit and capture the load swings with the less efficient unit. In some instances, these schemes are also dictated by the starting reliability of individual units, i.e., a low starting reliability may dictate operational schemes that are otherwise less fuel efficient.

Many control schemes for multiple independent compressors employ turndown equalization. These schemes seek to operate all compressors at the same turndown. Turndown equalization for compressors operating in series works backwards from turndown equalization for compressors operating in parallel. In series operation, one has to increase the speed (and thus power) of the unit where turndown has to be reduced. For units in parallel, increasing the speed (and power) of the unit will increase its turndown. This is due to the different boundary conditions. In parallel operation, all units see the same suction and discharge pressure, but the flow depends on the power that is fed into the compressor. In series operation, the flow has to be the same through all machines (unless recycle is employed). Increasing the power for one of the machines will increase the amount of head that said machine will produce relative to the other machine, thus reducing its turndown.

## CONTROL OF COMPLEX CONFIGURATIONS

In this example, control of a three-body compressor train with two side streams is discussed. The train is driven by a two-shaft gas turbine, allowed to operate over a wide speed range (*Figure 6-6*). The speed of the train is the result of the equilibrium between power output from the gas turbine and power consumption of the compressor train. In other words, if the gas turbine power is increased, the train will increase its speed. Each compressor symbol (Compressor 1, Compressor 2, Compressor 3) comprises the compressor and its aftercooler. Each compressor has its own recycle valve, and there are check valves between the compressor sections. Therefore, four means of controlling the train are available: train speed and three recycle valves. Essentially, two control systems are available: one, the process control system (depending on the case, will control one of the flows or pressures), and two, the anti-surge system for each of the compressors.

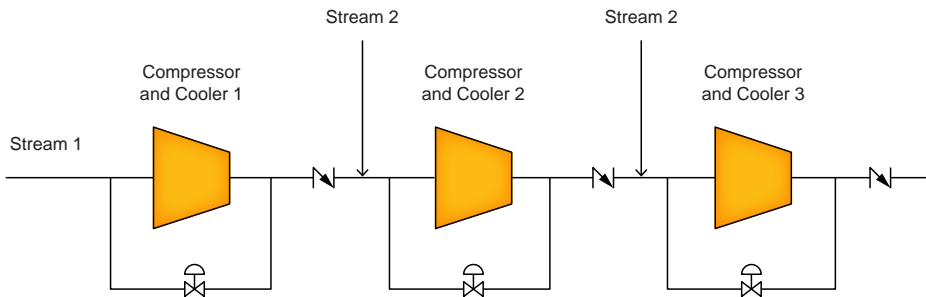


**Figure 6-6.** Section compressor train with two side streams.

## SERIES-PARALLEL CONSIDERATIONS

In some applications, gas storage for example, it's advantageous to be able to switch two compressors from series to parallel operation and vice versa. In doing so, the operating range can be significantly increased. In series operation, the units can provide high head, while in parallel, the flow range is increased.

It is desirable to be able to switch from series to parallel operation, and vice versa, while the compressors are running at or near full load. This is possible with an appropriate arrangement of valves. The most elegant solution involves a control valve and two check valves (*Figure 6-7*). With the control valve open, the machines operate in series, while with a closed valve, they operate in parallel. The check valves will automatically open and close based on the pressure differential over these valves, and therefore don't have to be controlled. In this arrangement, the opening and closing speed of the control valve is not particularly important.

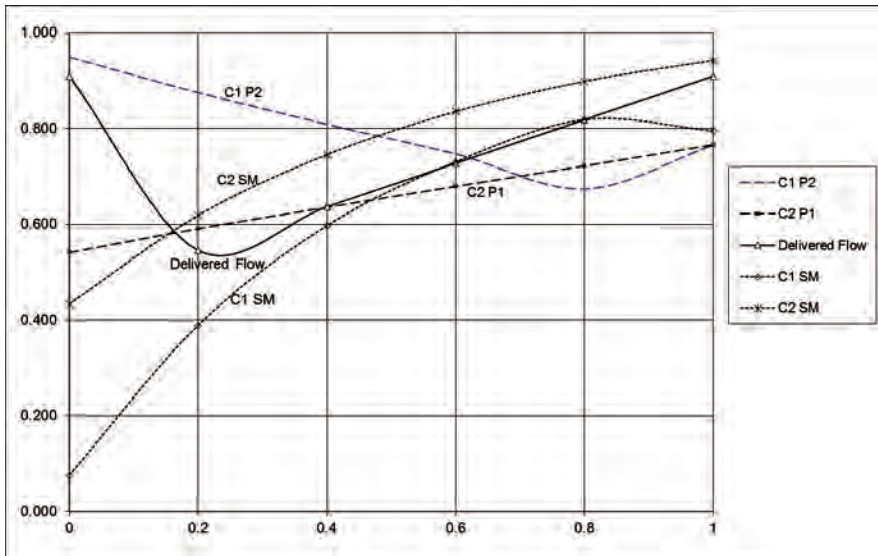
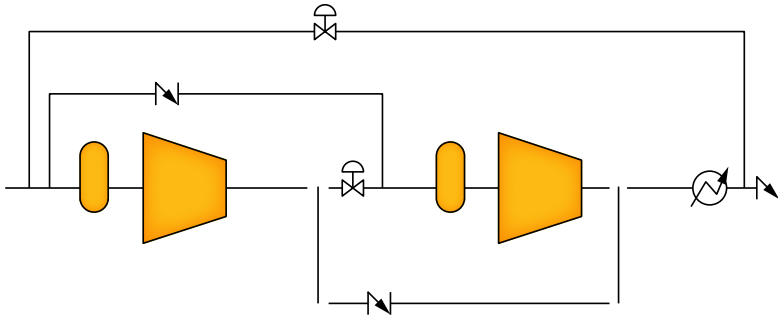


**Figure 6-7.** Compressors for series and parallel operation. Transfer from parallel to series arrangement (C1 is the LP compressor, C2 is the HP compressor, P1 and P2 are the suction and discharge pressures, respectively, SM is the surge margin for the compressors). The transfer is controlled by the control valve, with the check valves opening and closing automatically. The control valve is open for series operation, and closed for parallel operation. The delivered flow is the same at the beginning and the end of the transfer.

The transfer from parallel to series configuration is simulated in *Figure 6-7*. It is shown that neither machine will enter into surge. The LP compressor will be designed with higher flow staging than the HP compressor.

## PROCESS CONTROL WITH CENTRIFUGAL COMPRESSORS DRIVEN BY TWO-SHAFT GAS TURBINES

Centrifugal compressors, when driven by two-shaft gas turbines, are usually adapted to varying process conditions by changing compressor speed. This is the most natural way of controlling a system, because both the centrifugal compressor and the power turbine of a two-shaft gas turbine can operate over a wide range of speeds without any adverse

effects. A typical configuration can operate down to 50% of its maximum continuous speed, and in many cases even lower. Reaction times are very fast, thus allowing a continuous load using modern, PLC based controllers.

Gas-turbine-driven centrifugal compressors are typically controlled by varying the power input from the gas turbine. The compressor speed is then the result of the equilibrium between power input from the gas turbine and absorbed power from the compressor (Figure 6-8). Electric motor drives typically control the speed of the compressor, and the power consumption is the result.

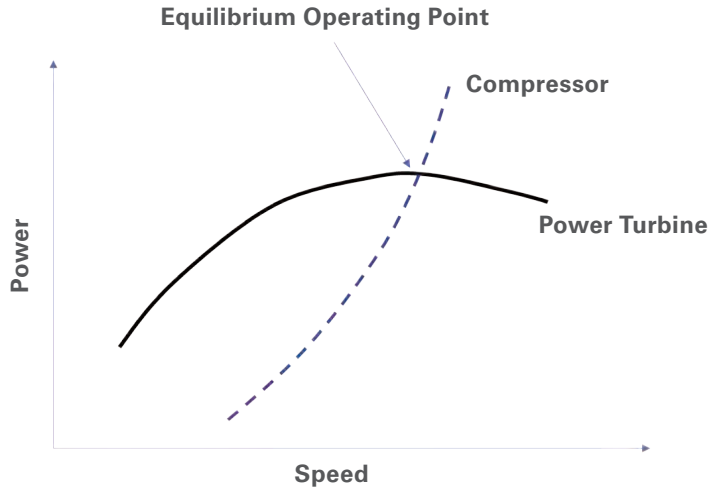


**Figure 6-8.** Speed-power relationship for a centrifugal compressor and the power turbine. The power turbine curve assumes a constant gas generator operating condition.

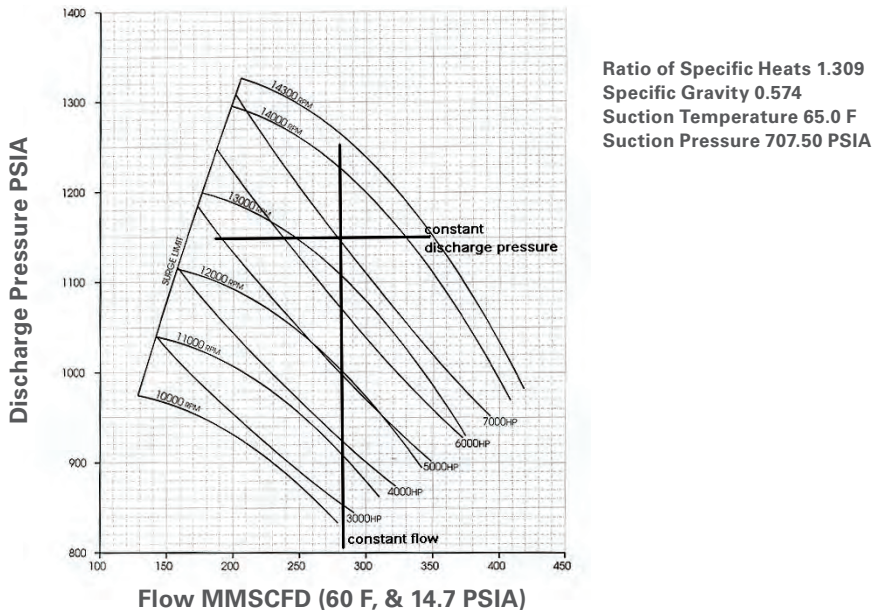


**Figure 6-9.** Centrifugal Compressor Performance Map: Operating at flow control or discharge pressure control.

A simple case is flow control. The flow into the machine is sensed by a flow metering element (such as a flow orifice, a venturi nozzle or an ultrasonic device). A flow setpoint is selected by the operator. If the discharge pressure increases due to process changes, the controller will increase the fuel flow into the gas turbine. As a result, the power turbine will produce more power, causing the power turbine together with the driven compressor, to accelerate. Thus, the compressor flow is kept constant (mode: constant flow in *Figure 6-9*). From *Figure 6-9*, it can be seen that both the power turbine speed and the power increase in that situation.

If the discharge pressure is reduced or the suction pressure is increased due to process changes, the controller will reduce the fuel flow into the gas turbine. As a result, the power turbine will produce less power and cause the power turbine, together with the driven compressor, to decelerate. Thus, the compressor flow is kept constant (Mode: constant flow in *Figure 6-9*).

Another possible control mode is to run the unit at maximum available driver power (or any other, constant driver output). In this case, the operating points are on a line of constant power in *Figure 6-9*.

*Figure 6-10* shows how compressors automatically adapt to changing operating conditions. Two control scenarios are considered: Running the compressor with a constant power setting, or running the compressor to maintain constant flow. In either case, the process is assumed to maintain the same pressures, for example, because the gas is delivered into a larger pipeline. If the gas gets heavier (specific gravity increases), the compressor will run slower because the same process conditions require less head. It must be noted that the control system will not prescribe the speed. Also, the specific gravity does not have to be known. The control system simply maintains either the power input, or it measures the flow and adjusts the power input to maintain the flow. If the gas gets lighter, the compressor will run faster. Since the flow at constant power is reduced, the compressor may reach the point where the surge protection is activated, and the compressor will start to recycle gas. Lowering the gas temperature will cause the compressor to run slower, and increasing the suction pressure will also lead to a speed reduction. If the compressor is controlled by constant power, the flow will increase significantly at that point.

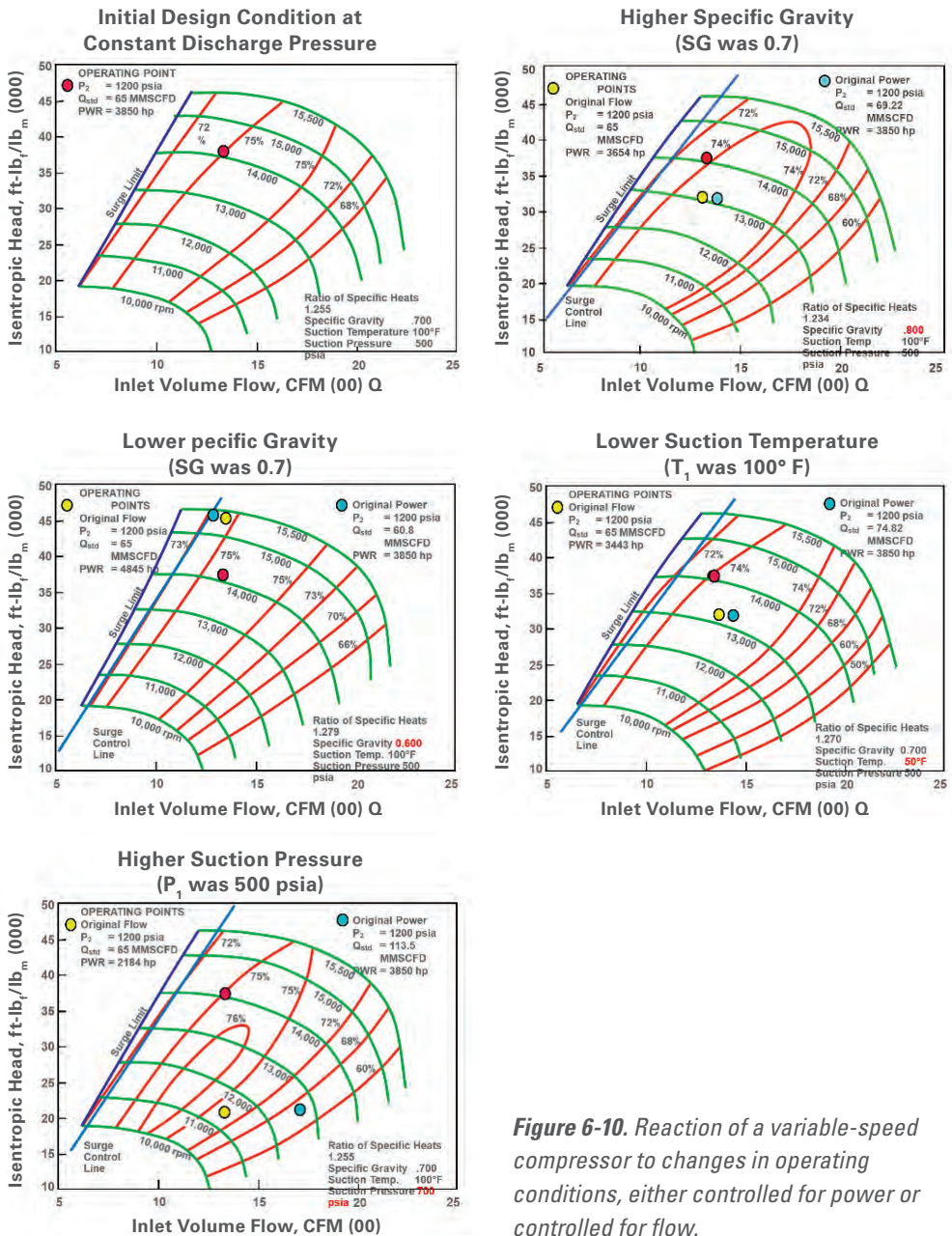


*Figure 6-10. Reaction of a variable-speed compressor to changes in operating conditions, either controlled for power or controlled for flow.*

## INTERACTION OF THE COMPRESSOR & COMPRESSION SYSTEM

The operating point of a compressor is determined by the interaction between the system it operates in and the compressor operating characteristics. For example, if a compressor operates at a steady state in a pipeline, then an increase in flow through that pipeline will require an increase of the pressure ratio (thus the head) of the compressor station, due to the increased friction losses in the pipeline.

The maximum flow is limited by either the maximum allowable speed of the compressor train, or the maximum available driver power. If more than one compressor operates at

a station, they can either operate in parallel or in series. Control strategies can be set to attempt running all compressors at that station using the same surge margin. Additionally, with multiple units available at a station, it is often advantageous to shut one or more units down, rather than operating all of them in deep partial load.

## **BASIC PROCESS CONTROL WITH A GAS TURBINE DRIVER**

The control system for a gas turbine driver process control is set up to run the engine to maximum gas generator speed (i.e., full load), unless it runs into another limit first. Limits can be established based on compressor suction pressure, compressor discharge pressure or compressor flow. If, for example, suction pressure is controlled, the engine will run at full load unless the suction pressure drops below its set point. In that case, the gas producer speed is reduced. In the case of discharge pressure control or flow control, the engine will run at full load unless the discharge pressure or the compressor flow exceeds its set point.

## **BASIC PROCESS CONTROL WITH ELECTRIC MOTOR DRIVES**

For constant speed electric motor drives, process control has to be accomplished using one of the other, previously mentioned control methods (Figure 6-2). The complication lies in the fact that control methods such as recycle control and suction throttling have only limited capability to reduce the compressor's absorbed power (Figure 6-3). Thus, a certain level of oversizing the driver is required to make sure that there is enough power available to operate the compressor at some point on its constant speed line.

For electric motor drives allowing variable compressor speeds (i.e. Variable-Speed Gearboxes or Variable-Frequency Drives), the usual control variable is speed. Unlike the gas turbine drives described above, the speed of the drive is adjusted to meet the process control objective, until the required power exceeds the driver's capability.

## **SURGE AVOIDANCE**

Surge avoidance, while the compressor is on line, is one of the process controls for the left boundary of the compressor map. The intervention of surge control should be virtually unnoticeable. It should be as though the compressor has infinite turndown.

Understanding the principles of surge avoidance initially will make understanding the remaining process controls easier. Some remarks about control dynamics and measurements will make the concept of surge avoidance and its importance easier to understand.

Successful surge avoidance involves five essentials. (White et al [3]):

- 1. A Precise Surge Limit Model:** It must predict the surge limit over the applicable range of gas conditions and characteristics.

- 2. An Appropriate Control Algorithm:** It must ensure surge avoidance without unnecessarily upsetting the process.
- 3. The Right Instrumentation:** Instruments must be selected to meet the requirements for speed, range, and accuracy.
- 4. Recycle Valve Correctly Selected for the Compressor:** Valves must fit the compressor map. They must be capable of large and rapid, as well as small and slow, capacity changes.
- 5. Recycle Valve Correctly Selected for the System Volumes:** The valve must be fast enough and large enough to ensure the surge limit is not reached during a shutdown. The piping system is the dominant factor in the overall system response. It must be analyzed and understood. Large volumes will preclude the implementation of a single valve surge avoidance system [3], [4], [5], [6].

This section does not cover the behavior of surge control systems during emergency shutdowns. All that needs to be mentioned at this point is that the volume of the pipes and vessels between the compressor discharge nozzle, the check valve and the recycle valve should be kept as small as possible. If concerns about surge during emergency shutdown arise, a separate hot recycle valve can be installed.

## SYSTEM BEHAVIOR

The system within which the compressor operates—that is, the piping, valves, and vessels—exhibits some relationship between the flow through the system and the pressure drop imposed by the system.

In the context of compressor applications, it is important to understand this relationship, since it has a profound impact on the selection of the correct compressor. Further, these relationships tend to be different in steady-state operation versus transient operation.

The pipe system within which the compressor operates will impose its characteristic on the compressor. Three fundamental steady-state system characteristics must be considered (*Figure 6-11*):

- 1.** Strong head-flow relationship (A)
- 2.** Weak head-flow relationship (B)
- 3.** Integrative relationship (C)

The case of strong head-flow relationship is, for example, seen in gas pipelines. Under steady-state conditions, the pressure loss in the pipeline which imposes the suction and discharge pressure on the compressor station increases significantly when the flow through the pipeline has to be increased. The pressure levels are thus dictated by friction losses, which depend on the gas velocity in the pipe.

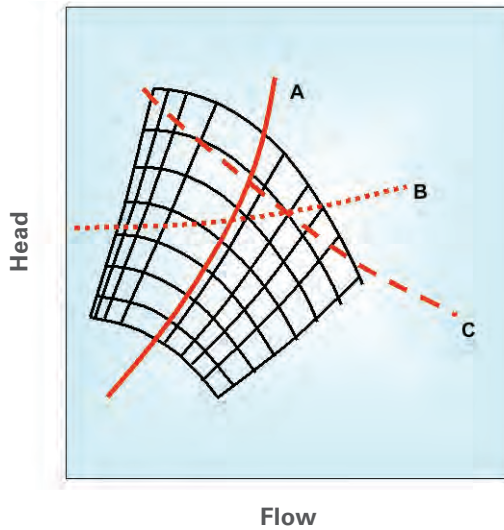


**Figure 6-11.** System characteristics and compressor map.

In a weak head flow relationship, the head requirement for the compressor head stays more or less constant with changes in flow. This behavior is found in refrigeration compressors, but also for situations where the process dictates a constant suction pressure (e.g., separator pressure), while the discharge gas is fed via a short pipe into a larger flowing pipeline. The compressor discharge pressure is more or less dictated by the pressure in the large pipeline. Friction losses, therefore, have a very small effect, resulting in very small changes in pressure losses with flow.

In an integrative relationship for example, as exists in storage applications (Kurz and Brun [11]), the compressor fills a large cavity. That means the compressor discharge pressure is increased as a function of the cumulative flow into the cavity, as a result of filling it with gas. Similar conditions can be found in gas-gathering applications where (on a much slower scale) the field pressure (and with it the compressor suction pressure) decline as a function of the cumulative flow out of the gas field. These fields also have a strong head-flow relationship, i.e., increasing the flow at any given time would lower the compressor suction pressure.

The interaction between compressor characteristic and system characteristic then becomes a basic ingredient for the control approach. *Figure 6-12* shows how the power input provided by the driver can be used to control the compressor operating point within the constraints of the system's behavior.

For given load setting (e.g. NGP), compressor will operate at a point determined by available power and pipeline characteristic.

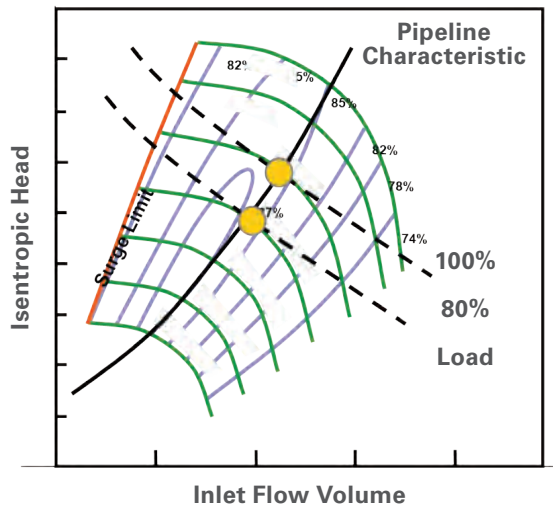
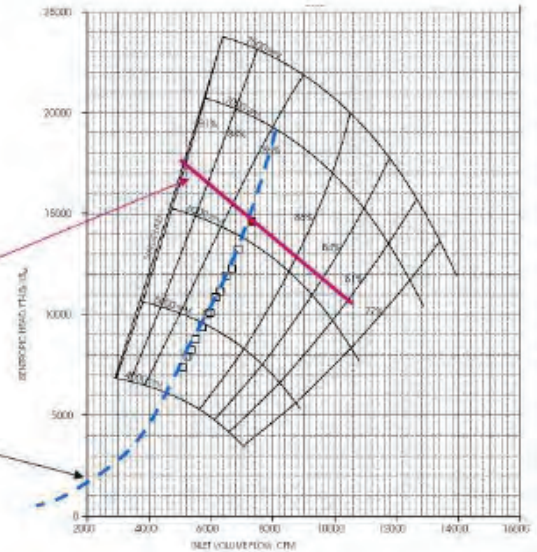


Figure 6-12. Available power, compressor map and pipeline characteristic.

Compressor power  $P$  is a function of mass flow  $W$  and actual head  $H$ , and thus related to the coordinates in the compressor map (Figure 6-12) of inlet density  $\rho$ , inlet flow  $Q$ , isentropic head  $H_s$  and efficiency  $\eta$ :

$$P = W \cdot H = \rho Q \cdot \frac{H_s}{\eta}$$

This defines the line of constant power in Figure 6-12.

Further, the transient system behavior must be considered (Figure 6-13). For example, a pipeline can be operated in a transient condition by feeding more gas into the pipeline than what is taken off on the other end. This is usually referred to as "line packing." In general, pipelines are operated under slowly changing operating conditions. While a pipeline under steady state conditions requires a unique station pressure ratio for a given

flow (Figures 6-11 and 6-12), this is no longer true under transient conditions. If the pipeline operates under transient conditions, for example, during line pack after a fast increase in driver power, or, if one of the compressors has to be shut down, the steady state relationships are no longer valid.

Dynamic studies of pipeline behavior reveal a distinctly different reaction of a pipeline to changes in station operating conditions than a steady-state calculation. In steady state (or, for slow changes), pipeline hydraulics dictate an increase in station pressure ratio with increased flow, due to the fact that the pipeline pressure losses increase with increased flow through the pipeline.

However, if a centrifugal compressor receives more driver power, and increases its speed and throughput rapidly, the station pressure ratio will react very slowly to this change. This is due to the fact that initially the additional flow has to pack the pipeline (with its considerable volume) until changes in pressure become apparent. Thus, the dynamic change in operating conditions would lead (in the limit case of a very fast change in compressor power) to a change in flow without a change in head. If the power setting is maintained, the compressor operating point would then start to approach the steady state line again, albeit at a higher speed, pressure ratio, flow, and power.



**Figure 6-13.** Typical operating points, if transient conditions are considered, in this case due to a fast engine acceleration from 50% to 100% load (Kurz et al [13]).

Experimental data presented and analyzed by Blieske et al. [8] indicates that the steady state compressor map is still usable even in transient situations.

## INTERACTION BETWEEN THE SYSTEM AND THE COMPRESSOR

For any situation, the process determines the suction and discharge pressure the compressor 'sees.' Based on some control setting (available power, speed, guide vane setting) the compressor will react to the situation by providing a certain amount of flow to

the system. Thus, the flow into the system is a result of the compressor characteristic (its map) and some external control setting.

Different controls elicit different scenarios in these control situations. If the compressor is controlled by the level of power that's supplied, then the speed at which the compressor runs is a result of the interaction between compressor and process. If the speed of the compressor is controlled, the required power is an outcome. The same is true for a constant speed machine (which in that sense is just a special case of a compressor that's forced to operate at a set speed).

Recycle control and throttle control are essentially supplemental ways to control the compressor in certain situations. Recycling gas still maintains the system suction and discharge pressure as long as the compressor stays on line, but it allows the compressor to provide more flow than desirable or available from the system. Throttle control allows the system to reduce suction pressure or the system discharge pressure the compressor experiences.

Obviously, there are impossible outcomes. The compressor will not be able to operate at conditions where the speed is too high or too low, where the power demand is too high, or where the operation would cause an instability, such as surge. If the compressor is not capable of operating at the system imposed suction and discharge pressure due to constraints of power, speed, or flow range, it will go into full recycle, i.e., the compressor will operate within the constraints of a new system, that is a throttle-valve-controlled recycle loop.

It should be noted that the above principles also apply to transient situations, such as line pack in pipelines (Kurz, et al. [12], and even highly transient situations, such as during an emergency shutdown (Kurz and White, [6]; Moore et al.,[13]). Again, the system (which is essentially the recycle loop as soon as check valves separate the recycle loop from the main system) imposes a certain suction and discharge pressure on the compressor; the available power comes from the inertia of the drive train, and the compressor speed is a result of the interactions.

## **CONTROL OBJECTIVES**

In a discussion of control, one has to define the goal of a control system. The requirements to protect the process as well as the equipment, are priorities, of course. But other goals need to be defined, too, particularly if the station involves multiple compression units, either in series or in parallel arrangements. Possible goals can be to minimize fuel consumption, minimize emissions, minimize maintenance costs or maximize throughput.

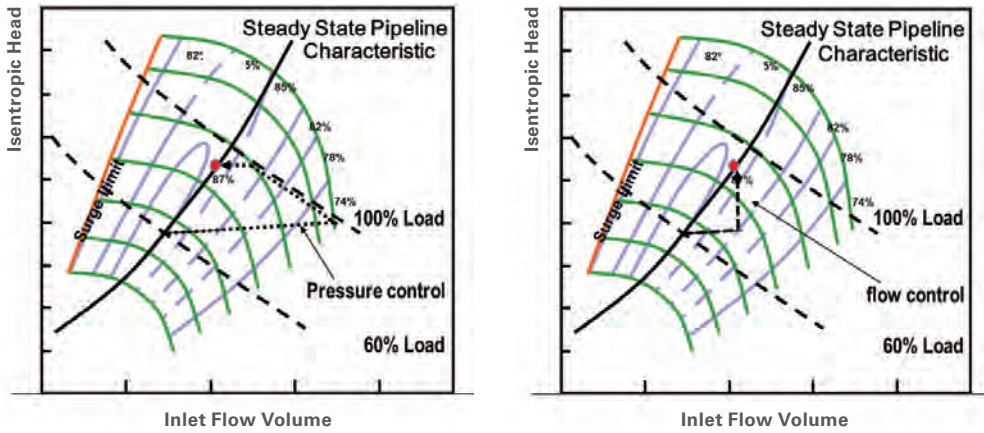


**Figure 6-14.** Load increase. Pressure control (left), flow control (right).

Each of these goals has to be translated into operational requirements for the compressors. For example, in a compressor station with three identical units, minimizing fuel consumption may be accomplished by running only the minimum number of units necessary for the duty. Generally, this will also minimize maintenance cost (since the cumulative running hours are minimized), unless the gas turbine incurs additional maintenance based on the number of starts.

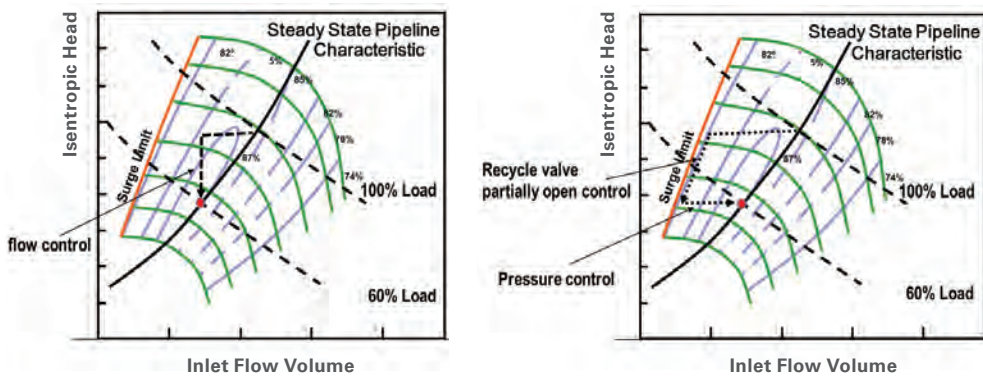


**Figure 6-15.** Load reduction. Flow control (left), pressure control (right).

From a process standpoint, pressure, power, speed and flow can be controlled. For compression applications, controlling a process variable such as flow, suction or discharge pressure is the goal. Speed and power are irrelevant from a process standpoint, except for machinery protection or to maximize production (i.e. operation at full load or full speed). Among the process variables in a compressor station, pressures tend to change relatively slowly, while flow changes quickly.

For compression applications, pressure (except as a limiting factor) is also often not very relevant. However, it's often used for control purposes in pipelines, possibly because it's easier to monitor, especially if reciprocating compressors are involved. That leaves flow

control as the most advantageous way of controlling a compressor application. *Figure 6-14* shows how the compressor tends to react under different control scenarios. It follows (Kurz et al., [12]) that the fastest way to get to a new operating point is to accelerate the engine to full power.

Both flow and pressure control will essentially make the engine operate at full load until the control objective is achieved (*Figure 6-14*). Pressure control will lead to a large flow increase into the pipeline, thus causing a faster pressure rise inside the pipeline. In other words, pressure control will usually bring the compressor to the new set point faster than flow control in systems with a strong head-flow relationship (*Figure 6-11, Curve A*).

The case where the unit is supposed to run at reduced flow is slightly more complicated, because it also requires consideration of the anti-surge system (*Figure 6-15*). Upon setting the control set point to a lower flow (or pressure), the gas turbine will reduce power (by reducing gas producer speed). This will lead the compressor operating point to approach the surge control line. Upon crossing the control line, the recycle valve will open to keep the compressor from surging. The combination of an opened recycle valve and reduced power will bring the compressor to the new set point. Notably, there is no concern about interactions between power control and surge control.

## **SURGE AND SURGE AVOIDANCE**

The phenomenon of surge was mentioned earlier in this chapter, as well as in Chapter 1 on Compressor Aerodynamics. All modern compressors have anti-surge systems as part of their control systems. These systems detect when the compressor gets too close to the surge line and, as a response, gradually open a recycle valve. If this system does not work, control systems have, as a backup, a system that detects surge. If it does, the compressor shuts down. The behavior of a compressor during emergency shutdown or during other fast process changes, must also be discussed.

But first, the nature of surge must be considered. This is important, because surge is a system issue and can only occur as a result of the interaction between a compressor and the system components (pipes, valves, coolers) around it. Stall, for example, may be a precursor to surge, but it is not surge. For the purpose of this discussion, surge is defined as a situation where the flow through the compressor is reversed. The cause is that the system imposes a discharge pressure on the compressor that the compressor is no longer able to overcome. System dynamics usually dictate the transient nature of surge, i.e., flow reversal through the compressor lowers the discharge pressure, so the compressor will come out of surge, only to go back into surge if the system geometry is not changed.

Precursors of surge are often increased compressor vibrations or small flow pulsations. These are often described as mild surge. Their nature is, however, more related to the onset of stall in one of the compressor components, which can lead to a flattening or even a dip in the head-flow curve.

## OPERATION DURING REVERSE FLOW

While the control system is supposed to keep the compressor from operating in surge, a brief mention of the compressor situation when the system fails to prevent surge is warranted. Test data exists describing the behavior of a compressor when it is subject to reverse flow conditions. Kurz et. Al. [6] described the behavior of a compressor during emergency shutdown against a closed recycle valve, and recently, Belardini et. Al. [15] presented a detailed study focused on compressor behavior in reverse flow. Aust [16] published detailed measurements of a centrifugal compressor during surge cycles (Figure 6-16). Besides the normal, stable operation, the area of stable, reverse flow can be identified, as well as an unstable transition area. Currently, the determination of the forces and damage during surge cycles are the subject of research. In general, control systems are designed to prevent the compressor from surging, but anecdotal evidence suggests that most industrial compressors survive surge events without measurable damage.

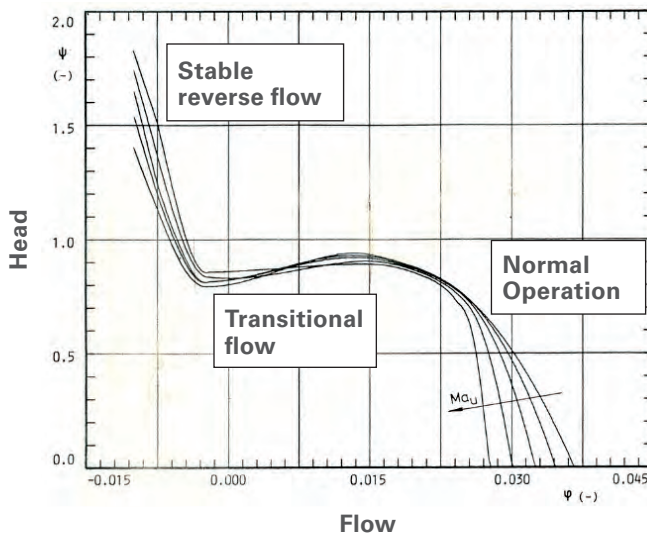


**Figure 6-16.** Behavior of a single-stage centrifugal compressor at positive and negative flow, showing isentropic head coefficient versus flow for machine Mach numbers from 0.57 to 0.85 (Aust [16]).

## STABILITY

Because surge is a system issue, the surge line—the limit where the compressor would move to a reverse flow situation—is determined by the interaction between the system and the compressor. From a control perspective, the surge line is simply a line on the compressor map that the control system is set up to prevent crossing. Therefore, the surge line could be determined by the onset of surge, but also the onset of rotating stall or the onset of high vibrations. The latter two clearly are not 'surge'. Figure 6-17 illustrates such a situation. The compressor has a dip in the head-flow map, likely due to component rotating stall. The manufacturer, therefore, sets the control line such that the compressor is kept out of rotating stall. On a test stand, the compressor may surge at a much lower flow (broken line).

For this discussion, it is better to focus on the stability line, which is the limit line at which the system is stable. What does 'stable' mean? If a compressor operates at a certain operating point, and a small disturbance (say, a slightly higher discharge pressure) occurs, then in a stable system, the compressor will return to its original operating point after the disturbance disappears. In an unstable system, it will continuously move away from the operating point.

A compressor curve with a continuous rise in head and reduced flow is thus generally stable (Figures 6-18 and 6-19), because an increase in discharge pressure will automatically cause a reduction in flow, which will cause the system to move to a lower discharge pressure again. As related to the transitional flow in Figure 6-16, a slight increase in pressure would force an increase in flow, causing instability. Figures 6-18 and 6-19 also indicate that the stability limit is not defined by the compressor, but rather by the compressor-system interaction.

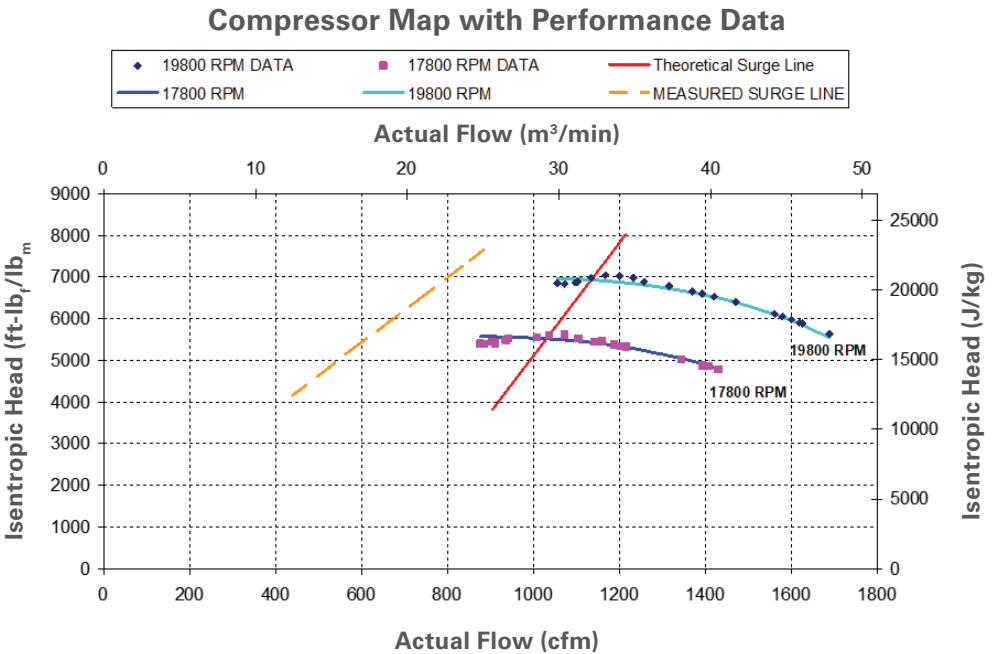
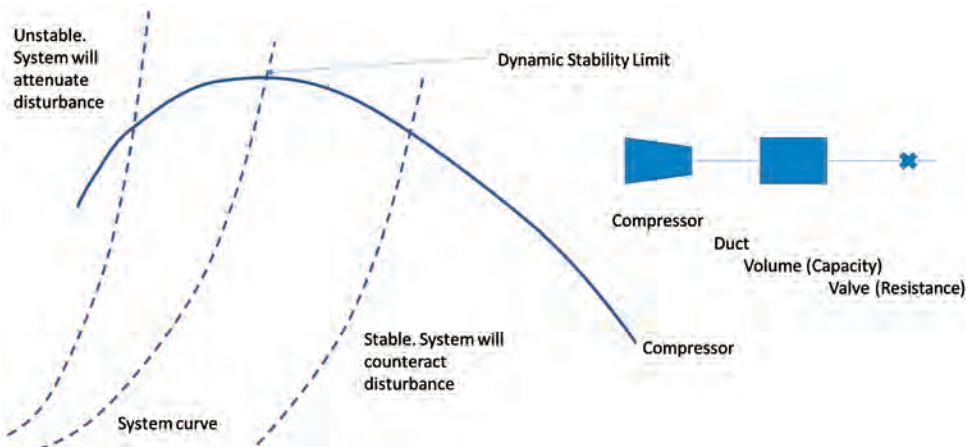
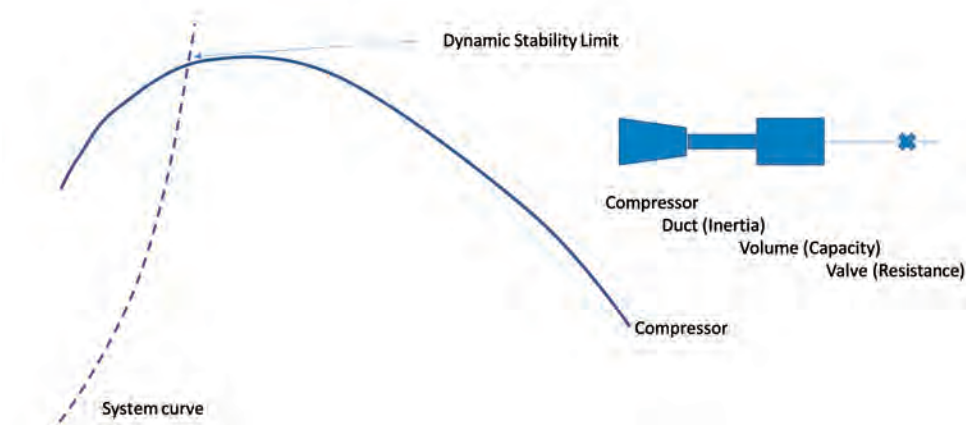


Figure 6-17. Where is the surge line?

### System Stability (without downstream piping inertia)



### System Stability (with downstream piping inertia)



Figures 6-18 and 6-19. System stability without and with downstream piping inertia.

## THE SURGE CONTROL SYSTEM

The surge avoidance system prevents surge by modulating a surge-control (bypass) valve around the compressor (Figure 6-20). A typical system consists of pressure and temperature transmitters on the compressor suction and discharge lines, a flow differential pressure transmitter across the compressor flow meter, an algorithm in the control system, and a surge control valve with corresponding accessories.

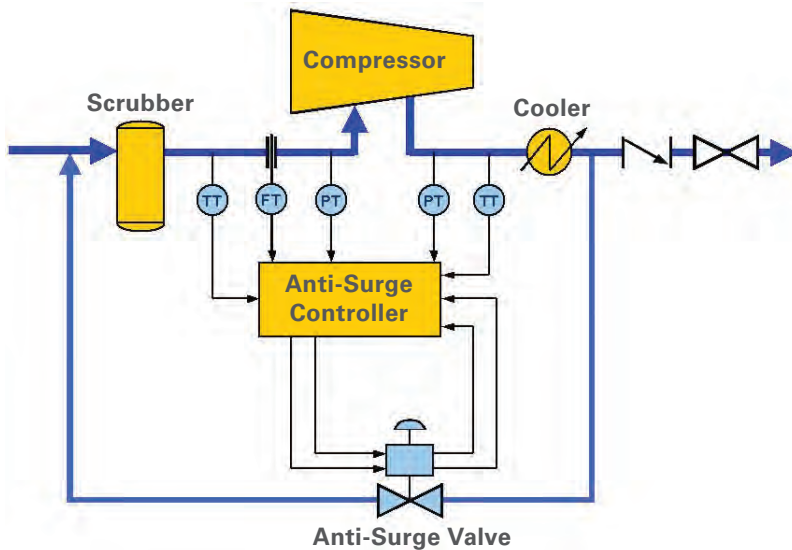


**Figure 6-20.** Surge avoidance system schematic.

A surge avoidance system determines the compressor operating point, using the pressure, temperature and flow data provided by the instrumentation. The system compares the compressor operating point to the compressor's surge limit. The difference between the operating point and the surge limit is the control error. A control algorithm (P+I+D) acts upon this difference, or "error," to develop a control signal to the recycle valve. When opened, a portion of the gas from the discharge side of the compressor is routed back to the suction side, and head across the compressor is prevented from increasing further. When the operating point reflects more flow than the required protection margin flow, the surge-control valve moves toward the closed position and the compressor resumes normal operation.

Successful surge avoidance involves five essentials:

- 1. A Precise Surge Limit Model** – It must predict the surge limit over the applicable range of gas conditions and characteristics.
- 2. An Appropriate Control Algorithm** – It must ensure surge avoidance without unnecessarily upsetting the process.
- 3. The Right Instrumentation** – Instruments must be selected to meet the requirements for speed, range, and accuracy.
- 4. Recycle Valve Correctly Selected for the Compressor** – Valves must fit the compressor. They must be capable of large and rapid, as well a small and slow, changes in capacity.
- 5. Recycle Valve Correctly Selected for the System Volumes** – The valve must be fast enough and large enough to ensure the surge limit is not reached during a shutdown. The piping system is the dominant factor in the overall system response. It must be analyzed and understood. Large volumes will preclude the implementation of a single-valve, surge-avoidance system.

## THE SURGE LIMIT MODEL

In order to avoid surge, it must be known where the compressor will surge. The more accurately this is predicted, the greater the amount of the compressor's operating range will be available to the user. A compressor's operation is defined by three parameters: Head, Flow and Speed. The relationship between the compressor's operating point and surge can be defined by any two of the three (*Figure 21*).

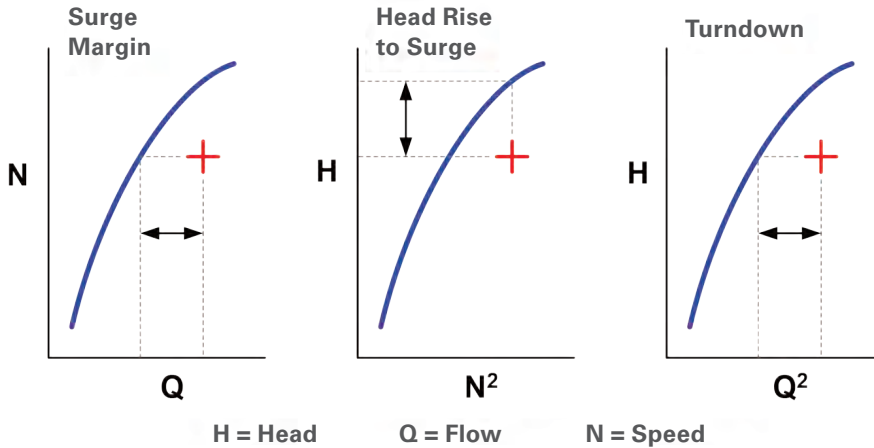


**Figure 6-21.** Surge limit in different systems of reference.

The first two models on the left of *Figure 6-21* involve speed. The speed of the compressor at an operating condition is strongly influenced by changes in gas composition, because the machine mach number will change. The head versus flow relationship on the right provides a means for modeling the surge limit without being affected by gas conditions or characteristics. The parameters of the surge limit model on the right can be measured in terms of head across the compressor and head across the flowmeter (*Figure 6-21*) [8].

$$H_p = K \cdot \frac{\left(\frac{P_D}{P_S}\right)^\sigma - 1}{\sigma} \cdot T \cdot SG \cdot Z \quad (1)$$

This is the basic equation for head. It applies both to the head of the compressor (with  $p_d$  and  $p_s$  discharge and suction pressure) or the head across the flow meter monitoring the flow through the compressor, so there are common terms. These common terms (units, gas temperature, specific gravity and compressibility) are equal in both equations and can be cancelled. This results in a simplified model that is referred to as "reduced head" versus "reduced flow."

$$H_{REDUCED} = \frac{\left(\frac{P_D}{P_S}\right)^\sigma - 1}{\sigma} \quad (2)$$

## THE CONTROL ALGORITHM

A surge avoidance control needs to be able to react appropriately to changes in power or the process. There are two very different situations to which the system must respond.

If the operating point slowly crosses the protection line—that is, at the same rate it has been moving left for the past several hours—movements opening the recycle valve should be small and slow. The interdiction of the surge avoidance control should be unnoticeable. It should be as though the compressor had infinite turndown.

Conversely, if the operating point races across the compressor map, the recycle valve should begin opening before the operating point crosses the protection line. Reaction of the control should be aggressive to protect the compressor. In this case, the concern is less about the process, as it has already been impacted.

A sudden change in the system produces a control response. This is a standard control test. Ping it and see how it rings. *Figure 6-22* reflects reactions of variously tuned controls. Low gains produce a slow response. A critically damped control produces an aggressive response but settles down quickly. If the gains are too high, the system will oscillate.

What does a surge avoidance system do most of the time? Hopefully nothing! Then, with very little margin, it must act aggressively, probably requiring gains higher than could be maintained stable to protect the compressor. To avoid instability, the gains are reduced to close the valve. Once surge has been avoided, the control system should bring the process back on line slowly and smoothly to avoid further upsets.

The need for extremely high gains is driven by the following: Surge avoidance systems normally utilize commonly available plant-process-control components. As such, these components are designed for ruggedness, reliability, and low maintenance. In general, they are not focused on speed of data acquisition. Information about changing process conditions is often 1/10 of a second old. As will be seen in later sections, significant advances in surge-control-valve action have been made recently. However, the response of the valve is typically the dominant lag in the system.

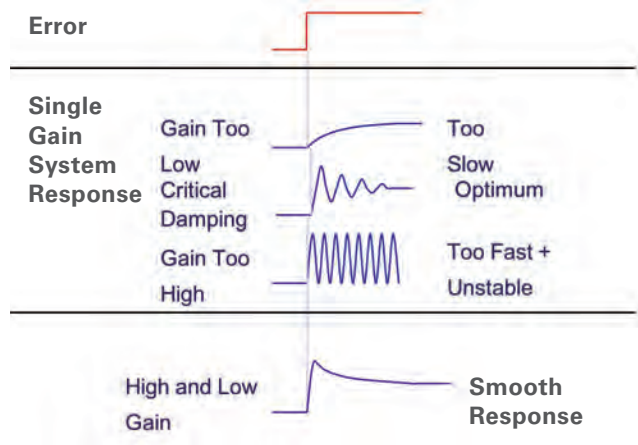


**Figure 6-22.** Reaction of a control system to an error signal.

## INSTRUMENTATION

To avoid surge, the control needs to know where the compressor is operating in relation to surge in real time. Again, how close the protection margin can be placed to surge depends

on how accurately and how quickly the change in flow is reported to the control. Correctly selected, instrumentation is essential. The system must have accurate measurements of the suction and discharge pressures and temperatures, and the rate of flow. Flow is the most important parameter as it will move the fastest and farthest, when approaching the surge limit. Ideally, the flow transmitter should be an order of magnitude faster than the process. Unfortunately, compared to pressure and temperature transmitters, flow transmitters tend to be slow. Even the best surge-avoidance control will allow a compressor to surge, if it is connected to a slow transmitter.

## FLOW-MEASURING DEVICES

Most commercially available flow-measuring devices (*Figure 6-23*) are accurate enough for surge avoidance, however, it is the transmitter that slows things down. A differential pressure transmitter's response time is inversely proportional to its range; thus, the stronger the signal, the faster the response.

Devices that develop high DP signals are desirable. Those with low signal levels tend to have low signal-to-noise ratios. Transmitters for low DP signal ranges typically have slow response times. Devices that create an abrupt restriction or expansion to the gas, such as orifices, cause turbulence and, subsequently, create noise.

It is preferable to place the flow-measuring device on the suction side of the compressor. Typically, variations in pressures, temperatures and turbulence of the gas are lower upstream of the compressor. Also, the device must be inside the innermost recycle loop (*see Figure 6-20*).

At a minimum, failure of the device will cause the compressor set to be shut down until the device can be replaced. If the failure results in pieces being ingested by the compressor, it can cause an expensive overhaul. For this reason, devices that are cantilevered into the gas stream are not recommended. Low-cost, flow-measuring devices do not necessarily result in cost savings over the long run.

Low Permanent Pressure Loss (PPL) devices are often recommended, however, their benefits may be marginal. The lost-power, cost-impact of operating a device can be calculated. For example, a flow meter developing a 100-inch H<sub>2</sub>O signal and a 50% PPL flowing 100 MMSCFD (50 lb/sec) is equivalent to about 20 hp.

As noted, strong-signal devices are highly preferred. Pitot types (Annubars & Verabars) have a relatively low-signal level, around 25 inches H<sub>2</sub>O. In the middle are orifices and venturis with a moderate signal of around 100 inches H<sub>2</sub>O. Compressor suction-to-eye provides a strong signal, (around 700 inches" H<sub>2</sub>O) with the added benefit of not causing any additional pressure loss.

Suction-to-eye uses the inlet shroud or inlet volute of the compressor as a flow-measuring device. This feature is now available on many compressors. The design requirements for the inlet volute and the flow measuring device have several things in common. Performance of the first stage impeller and the device is dependent on the uniform direction and velocity of the flow presented to it.

Placement of the eye port is critical to the operation of suction-to-eye flow measurement. As the impeller approaches surge, an area of recirculation begins to develop at the outer perimeter of the inlet to the impeller. If the eye port is placed too close to the impeller's outer perimeter, the relationship of the DP to flow will be affected. Fortunately, the meter factor ( $C'$ ) typically remains nearly the same for the same surge margin. Hence, selecting the meter factor at the desired surge-protection margin will contribute to effective surge avoidance.

In a typical pipeline application (600 psi suction pressure), suction-to-eye will develop 25 psid (692 inches  $H_2O$ ). This is nearly seven times the differential of an orifice plate. Typically, the signal-to-noise ratio is high, and there is no additional permanent pressure loss. For surge avoidance, the suction-to-eye method is strongly recommended.

### COMPRESSOR INSTRUMENTATION

Optimal performance of any control system is dependent on the speed, accuracy, and resolution of the instrumented process conditions. To achieve optimal performance, the instruments should have performance specifications an order of magnitude better than the requirements for the system. Typical gas-compression systems have a first-time constant of about one second; hence, no instrument should have a first-time constant of greater than 100 ms. The surge-control system is expected to discriminate between single-digit percentages of surge margin; hence, measurement of the process parameters should be accurate to 0.1%. The final control elements (recycle valves) probably can resolve 1% changes in their command signals; hence, the process variables should be resolved to at least 0.1% (10 bits) of their normal operating range. Over-ranging transmitters degrade resolution.

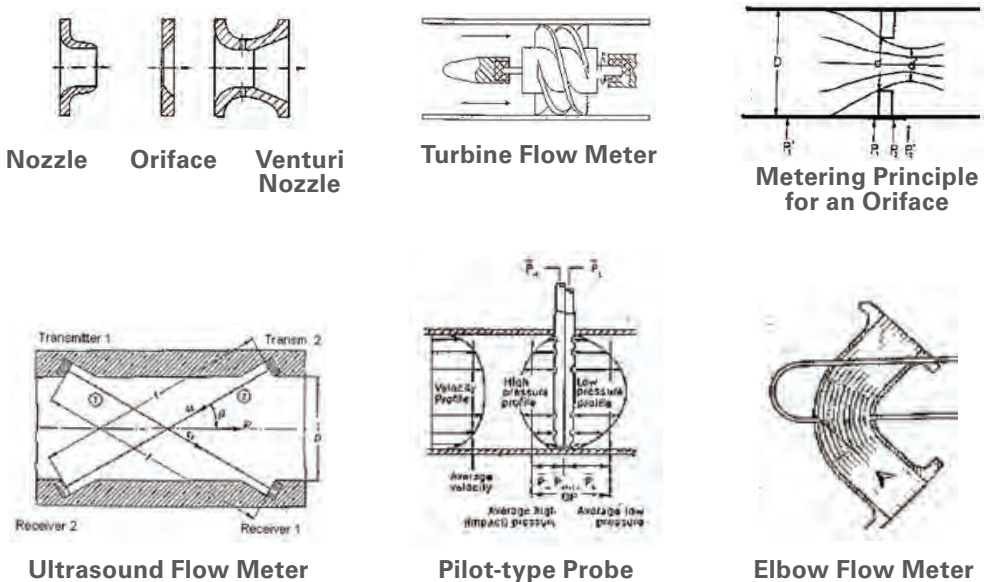


**Figure 6-23.** Flow-measuring devices.

## THE SURGE CONTROL VALVE

Earlier, how the control should react differently to gradual and rapid approaches to surge was discussed. Likewise, the valve must address these two very different requirements. For the gradual approach, it should behave like a small valve and produce smooth throttling. For the rapid approach, it should act like a large, fast valve to handle sudden major changes.

There are three general valve characteristics (*Figure 6-24*): quick opening, where most of the valve's capacity is reached early in its travel; linear, where capacity is equal to travel; and equal percentage, where most of the capacity is made available towards the end of the valve's travel. All three types of valves have been used in various configurations as recycle valves.

Equal-percentage valves, and in particular noise-attenuating ball valves, are recommended for surge avoidance systems with a single surge-control valve. They perform like smaller valves when nearly closed and bigger valves when close to fully open. *Figure 6-25* is a comparison of two types of equal-percentage valves. For a given valve size, the noise-attenuating ball valve is often twice the cost of the globe valve, but it provides approximately three times the Flow Coefficient (Cv) or capacity. Also, it is more reliable as it is less susceptible to fouling and improper maintenance.

Employing a valve with an equal percentage characteristic may provide the capacity needed to avoid surge during a shutdown, while maintaining enough resolution at less than 50% capacity to provide good control at partial recycle. With an equal percentage characteristic, the valve typically has greater resolution than a single linear valve selected to fit the compressor.

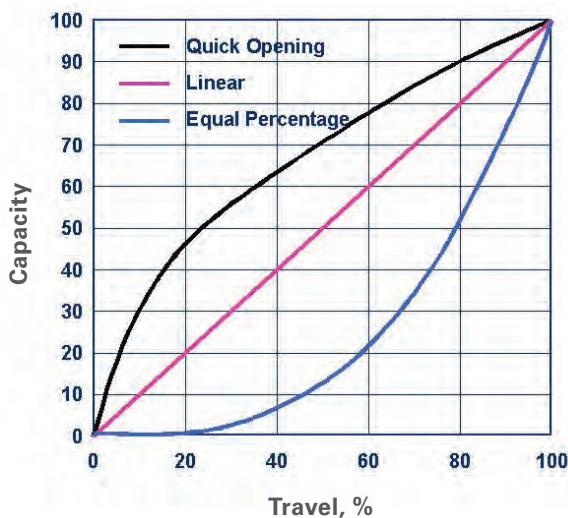


**Figure 6-24.** Valve Types

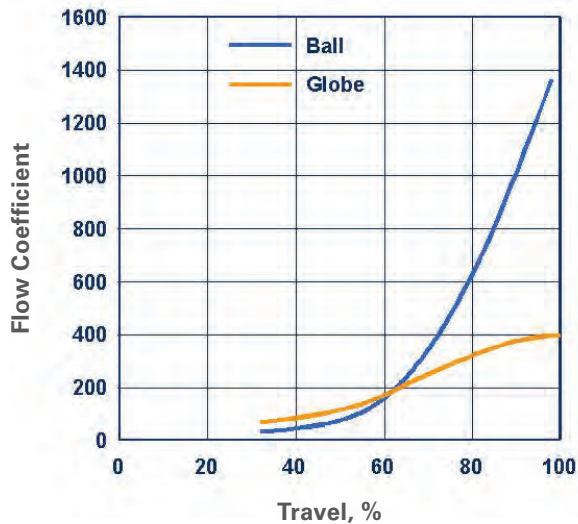


**Figure 6-25.** Comparison of ball and globe valves.

## MULTIPLE VALVES

If the volumes on either side of the compressor are large, use of multiple valves may be needed. If an integrated approach is used, the total valve capacity will be reduced.

Probably the most common is the hot-and-cold, recycle configuration (Figure 6-26). Usually the cooled (outer) valve is modulating, and the hot (inner) valve is a quick opening on-off type.

Generally, the two valves are sized independently. If the cooled valve has a solenoid, its capacity can be considered with that of the shutdown valve; subsequently, the shutdown valve can be smaller.

An alternate to this configuration is having a second cooled valve in parallel with the first. This arrangement provides some measure of redundancy. During control, the two valves are operated in cascade. That is, they have different

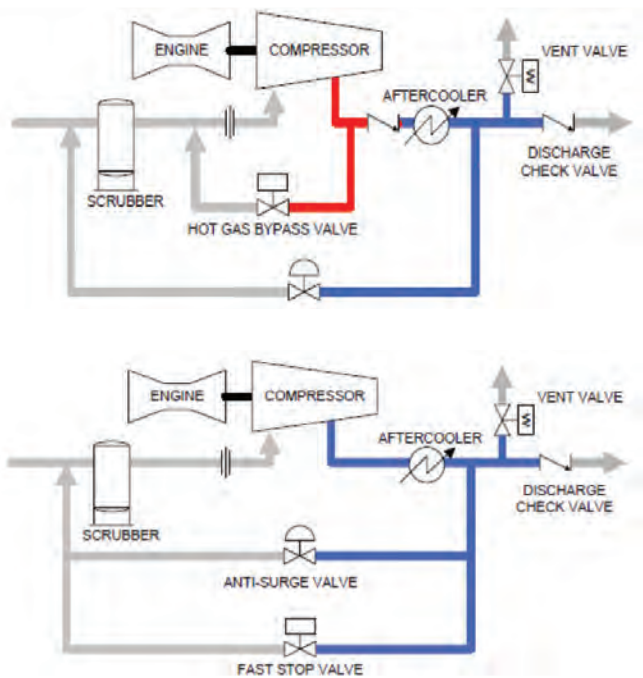


**Figure 6-26** Arrangements with fast-stop (hot-gas bypass) valve (top) and separate recycle (anti-surge) valve (bottom).

set points, say 9% and 10% surge margin. Under normal movements of the operating conditions, only the 10% surge-margin valve (primary valve) will open. If movement is fast enough to push the operating point down to 9%, the secondary valve will open. If the primary valve becomes fouled and no longer positions properly, the control can place it in the secondary position, and the secondary valve becomes the primary valve. This change can be made without taking the compressor offline.

The advantages of the two parallel valves do not come without a price. In normal operation, 2% to 5% of the pressure rise across the compressor will be lost across the cooler. In the shutdown scenario, the required flow through the cooler to avoid surge may be 2 or 3 times the normal flow. This will result in 4 to 9 times the pressure drop across the cooler. This additional pressure drop may significantly increase the needed recycle valve-capacity.

Recycle valves need to be fast, and capable to be positioned accurately. They also need to be properly sized for both the compressor and the piping system. A valve well suited for modulating recycle around the compressor may not be suitable for a shutdown. (See the Review of Piping Volumes section below.)

For some two-valve applications, single-purpose valves may be suitable, one for controlled recycling, and one for shutdown. A valve having linear characteristics is appropriate for controlled recycling, and a valve having quick-opening characteristics such as a globe or ball valve is appropriate for shutdown.

For applications where the compressor speed lines are fairly flat (little increase in head for a decrease in flow) from the design conditions to surge, extra-fast depressurization may be required. To achieve this, two quick-opening valves may be employed. In this case, a single 6-inch linear-characteristic valve is replaced by two 4-inch quick-opening valves. The two 4-inch valves should have slightly less flow capacity (Cv), but they will open nearly 45 milliseconds faster. For linear valves, 50% travel equals 50% capacity. For quick-opening valves, capacity approximately equals the square root of travel. As such, the two 4-inch valves will have 70.7% of their fully open capacity at 50% open. Comparing the two arrangements, 250 ms after the shutdown is initiated, the two 4-inch, quick-opening valves will have 56% more flow capacity than the single 6-inch linear valve.

For throttling, the valves are operated in cascade or split range. For most controlled recycling, only one valve is opened. Although the valves have a quick-opening characteristic, the valves are smaller, thus the capacity based on percent travel is less. The two quick-opening valves operated in cascade or split-ranged will have the same Cv as the 6-inch linear valve at 25% travel.

## VALVE ACTUATION

As previously discussed, there are two operational scenarios for the surge avoidance system; modulating (minimum flow control) and rapid depressurization for shutdown. By inserting a three-way solenoid valve into the positioner's output, the valve can be made to open with either a proportional (4-20 mA) signal for modulating control, or a discrete (24 VDC) signal for total fast opening.

The primary difference between a surge-control valve and a standard-control valve is in its actuation system. The preferred actuator for surge avoidance is spring return, fail open. This design is simple, reliable, and ensures the compressor is protected in the event of a power failure. Both spring-and-diaphragm and spring-and-piston actuators are used. The spring-and-diaphragm actuator is most commonly used on globe valves. The spring-and-piston actuator is more often used on ball valves. The more powerful spring-and-piston actuators are required on rotary valves due to the greater forces required to accelerate the mass of the ball. Some ball valves are not suitable for surge control applications because their shafts and attachments to the ball are not strong enough to transmit the torque required to open these valves at the required speeds.

Surge-control valves must be able to open very quickly. As such, their actuators will have strong springs, very large air passages, and shock absorbers at their ends of travel. This must be considered when sourcing recycle valves for surge avoidance.

The accessory unique to a surge-control valve assembly is the single-sided booster or exhaust booster. Essentially, this is a differential-pressure relief device. Opening the booster vents the actuator pressure to the atmosphere. The threshold for opening is about 0.5 psid. There is a small restriction (needle valve) between the control pressure from the positioner via the three-way solenoid valve and the top of the booster. Small, slow reductions in pressure (opening the valve) do not cause the booster to open. Large, fast reductions in pressure developing more than 0.5 psid across the restriction, cause the booster to open. If the solenoid valve is deenergized, the top of the booster is vented to the atmosphere, and the booster fully opens.

Standard industry quick-exhausts are not recommended for this application. They have a high threshold for opening (typically 2-to-4 psid) and an equally high threshold for reclosing. Although they may work well for fully opening the valve, they will not work well with the positioner.

Positioners should be selected for high capacity and quick response to changes in their control signals. Most of the major valve manufacturers have released second and third generation smart positioners that are suitably fast for this application. *Figures 6-27 and 6-28* show globe and ball valves with the preferred instrumentation configurations.

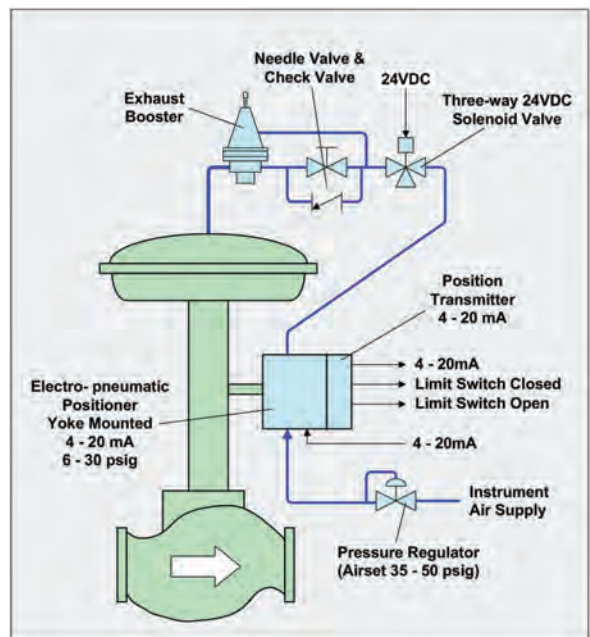


**Figure 6-27.** Globe valve assembly.

## RECYCLE VALVE SIZING TOOL

The recycle valve needs to be sized based on the expected operating conditions of the compressor. A valve-sizing program can facilitate matching a recycle valve to a compressor. The compressor data is entered into the tool in its normal form (pressures, temperatures, heads, speeds and flows). Various operating conditions for a specific application are then entered, such as the minimum and maximum operating speeds, pipe operating pressures, temperatures, relief valve settings and cooler data, if applicable. The tool calculates the equivalent valve capacities or Cv information from that data.

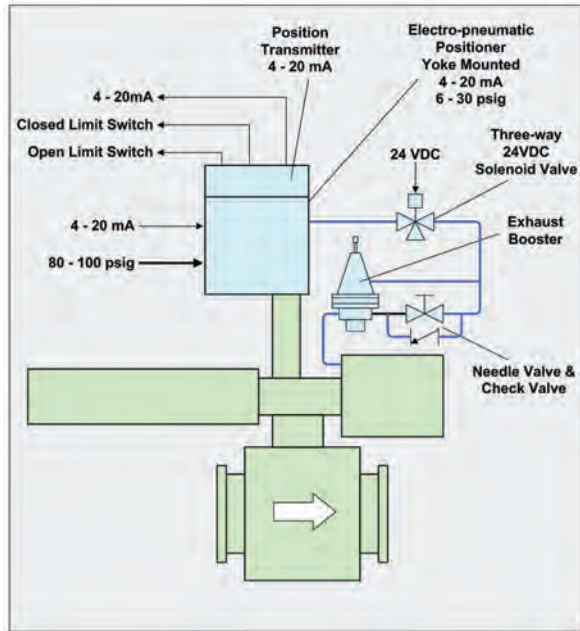


Figure 6-28. Ball valve assembly.

Typically, the surge limit of a compressor equates to a single valve capacity or Cv (Figure 6-29). The valve can be selected based on valve Cg, Cv and Xt tables from surge-control valve suppliers. As previously described, a single surge control valve application will have an equal-percentage-characteristic. Once a valve is selected, several performance lines of a specific opening can be developed and overlaid on the compressor map. The equal percentage characteristic valve should be set at approximately two-thirds travel at the surge conditions. The valve evaluation in Figure 6-30 shows such a valve superimposed on the compressor map, with its flow characteristic at 60%, 70% and 100% open.

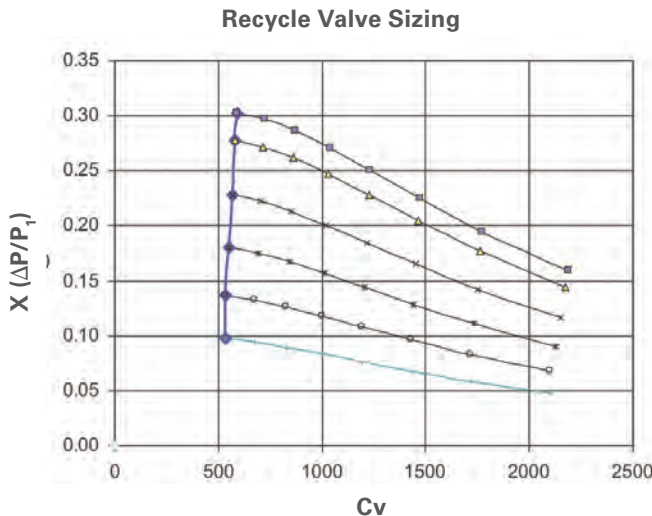
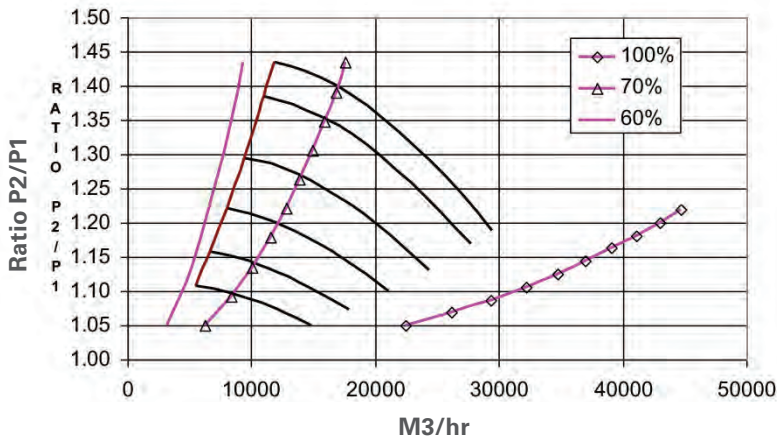


Figure 6-29. Almost constant Cv at the surge limit.

### ISA Recycle Valve Evaluation Equal Percentage Characteristic



**Figure 6-30.** Valve matched to compressor.

### REVIEW OF SYSTEM VOLUMES

The design of the piping and valves, together with the selection and the placement of instruments, will significantly affect the performance of an anti-surge control system. This should be addressed during the project planning stage, because the correction of design flaws can be very costly once the equipment is installed and in operation.

As described above, the control system monitors the compressor operating parameters, compares them to the surge limit, and opens the recycle valve as necessary to maintain the flow through the compressor at the desired margin from surge. In the event of an emergency shutdown or ESD, where the fuel to the gas turbine is shut off instantly, the surge valve opens immediately, essentially at the same time the fuel valve is closing.

The worst-case scenario for a surge control system is an Emergency Shutdown (ESD), particularly if the compressor is already operating close to surge when the engine shutdown occurs. If an ESD is initiated, the fuel supply is shut off immediately and the compressor will decelerate rapidly under the influence of the fluid forces counteracted by the inertia of the rotor system. Based on test data and theoretical considerations, a 20% to 30% drop on compressor speed within the first second after shutdown is common. A 30% loss in speed equates to approximately a loss in head of about 50%. Therefore, the valve must reduce the head across the compressor by about half at the same time as the compressor loses 30% of its speed.

The larger the volumes are in the system, the longer it will take to equalize the pressures. Obviously, the larger the valve, the better its potential to avoid surge. However, the larger the valve, the poorer its controllability at partial recycle. The faster the valve can be opened, the greater the flow that can pass through it. There are, however, limits to the valve opening speed, dictated by the need to control intermediate positions of the valve, as well as by practical limits to the power of the actuator. The situation may be improved by using a valve that's only boosted to open, thus combining high opening speed for surge avoidance with the capability to avoid oscillations by slow closing.

If the discharge volume is too large and the recycle valve cannot be designed to avoid surge, a short recycle loop (hot recycle valve) may be considered (Figure 6-26), where the recycle loop does not include the aftercooler.

While the behavior of the piping system can be predicted quite accurately, the question about the rate of deceleration for the compressor remains. It is possible to calculate the power consumption for a number of potential steady-state operating points. They are imposed by the pressure of the discharge volume, which dictates the head of the compressor. For a given speed, this determines the flow that the compressor feeds into the discharge.

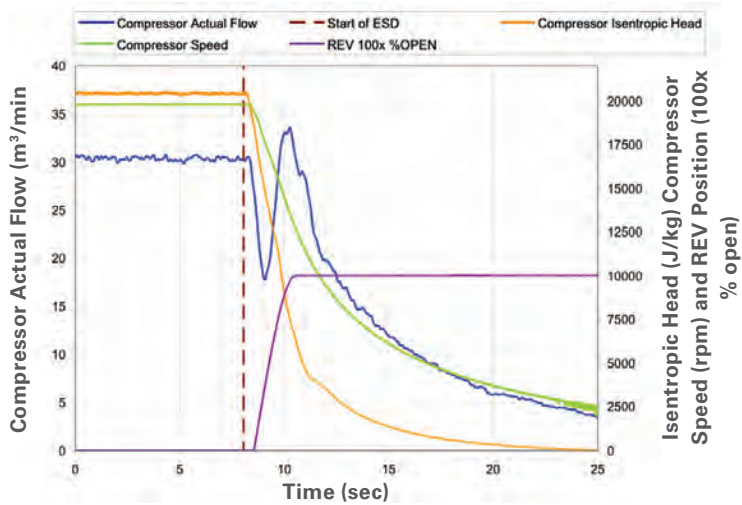
## EMERGENCY SHUTDOWN

Earlier, it was mentioned that a compressor is protected from surge by a controlled recycle system. However, situations exist where the operating conditions change so fast that the control function is overridden, and the control system opens a recycle or anti-surge valve as fast as possible.

In these situations, safety considerations require the units to be shut down as fast as possible (Kurz et al., [1]). This is usually referred to as emergency shutdown (ESD). Should this happen, the fuel supply (for a gas turbine driver) or the electricity (for an electric motor) is turned off instantly. Due to the inertia of the train, the train speed will decay at a certain rate after the power is shut off. In such an ESD, the anti-surge valve opens (*Figure 6-20*)—regardless of the compressor's operating point—at maximum opening speed to the fully open position.

In that situation, the process system dictates, as described above, the suction and discharge pressure for the compressor. However, the compressor speed decays, and so does the capability of the compressor to produce head. Therefore, the discharge pressure has to be reduced, which is done by recycling gas from the discharge side of the compressor to the suction side, while at the same time, isolating from the downstream process with a check valve (*Figure 6-20*). It is obvious that the slower the speed decays, the more time the system has to lower the pressure ratio. Therefore, a slower-speed decay is helpful to avoid surge.

*Figure 6-31* shows the behavior of the compressor in such a situation. While the speed drops rapidly, the process determines the compressor head that the compressor must overcome. The fast opening of the recycle valve reduces the system head. The flow initially is significantly reduced, and only starts to increase again due to the opening of the valve. The essential events in this shutdown occur within a second or so of the shutdown initiation. The valve is fully open after about two seconds. Due to the fast decay in speed, keeping the compressor from surging during the first few seconds is critical, while surge events at lower speeds usually lack the energy to cause any damage [6], [7].



### Compressor Map with Transient Events from 19800 RPM

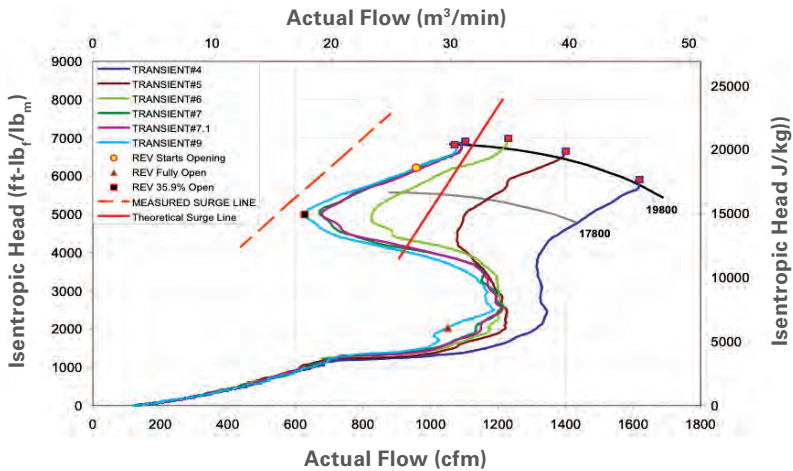


**Figure 6-31.** Compressor during ESD: (top) Compressor actual flow, head and speed, recycle valve position vs. time. (bottom) Traces of Compressor operating points during ESD from various operating conditions. (Moore et. al. [13]).

The behavior of the compressor during an ESD is highly dependent on the system dynamics, in particular the gas volume between compressor discharge, discharge check valve and recycle valve, as well as the size and opening speed of the anti-surge valve. This is due to the fact that the difference between suction pressure and discharge pressure has to be reduced fast. The more gas can flow through the anti-surge valve, and the smaller the volume on the pressure side (as well as the volume on the suction side), the faster this is accomplished (Figures 6-20, 6-32). For control purposes, the anti-surge valve should be relatively small, to allow for precise flow control. To keep the compressor from surging during ESD, one would like a larger valve than optimal for the control purpose. Also, while a small gas volume is desirable between compressor discharge, discharge check valve and recycle valve, the potential need for a cooler often increases this volume to the point, where a single valve cannot be sized for control and ESD. Figure 6-32 shows two surge

system options among multiple arrangements, where two valves are employed to overcome this difficulty.

Both arrangements assume the use of an aftercooler in the recycle loop to allow for infinite recycle. *Figure 6-32a* shows the use of a hot bypass valve that is only active for an ESD. This valve is not a control valve; it simply has to open as fast as possible during an ESD. Since the hot bypass loop is not cooled, the inlet temperature in the compressor can increase significantly during an ESD. The second option (*Figure 6-32b*) shows two valves in parallel. The fast stop valve also does not need to be a controlled valve. During an ESD, both valves open.

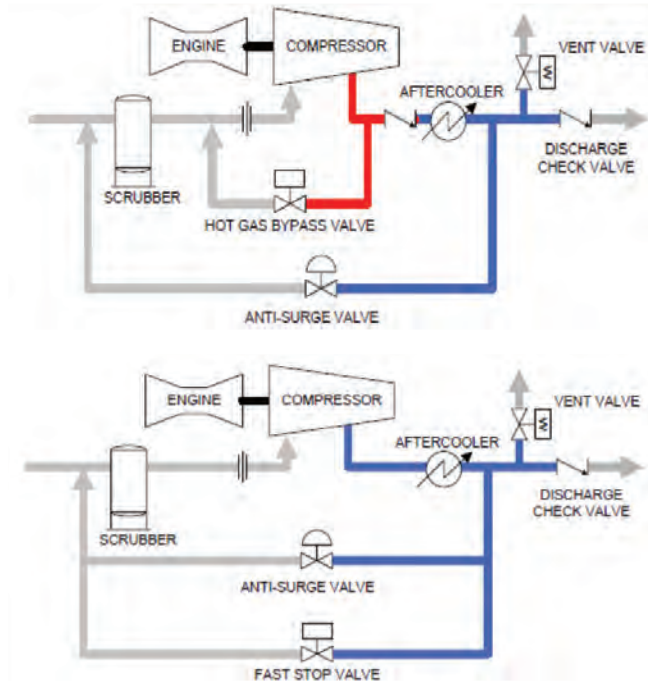


**Figure 6-32.** Arrangements with fast stop (hot gas bypass) valve (top) and separate recycle (anti-surge) valve (bottom).

Another key factor to consider is the shutdown behavior of the driver. During a safety-critical emergency shutdown, the driver is deenergized instantly, i.e. the fuel supply to the

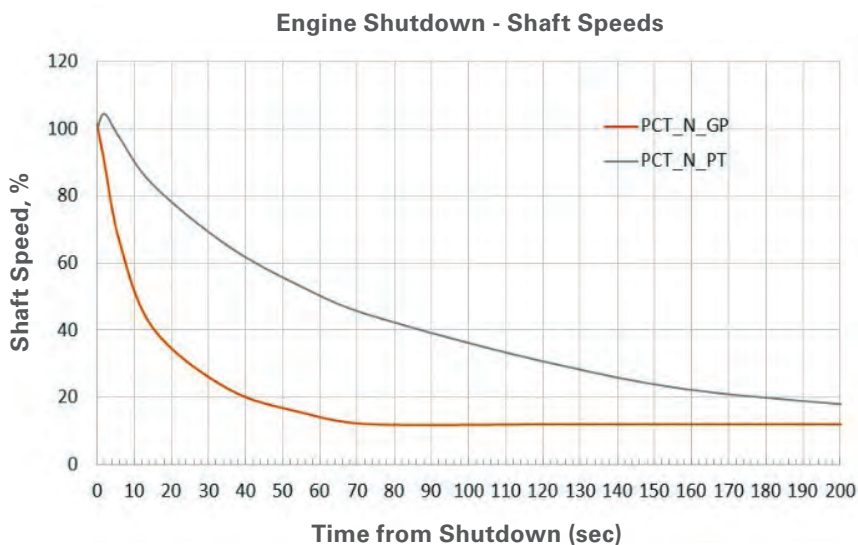


**Figure 6-33.** Engine shutdown simulation (shaft speeds), 23MW industrial gas turbine. PCT\_N\_GP is the gas producer speed; PCT\_N\_PT is the power turbine speed [17].

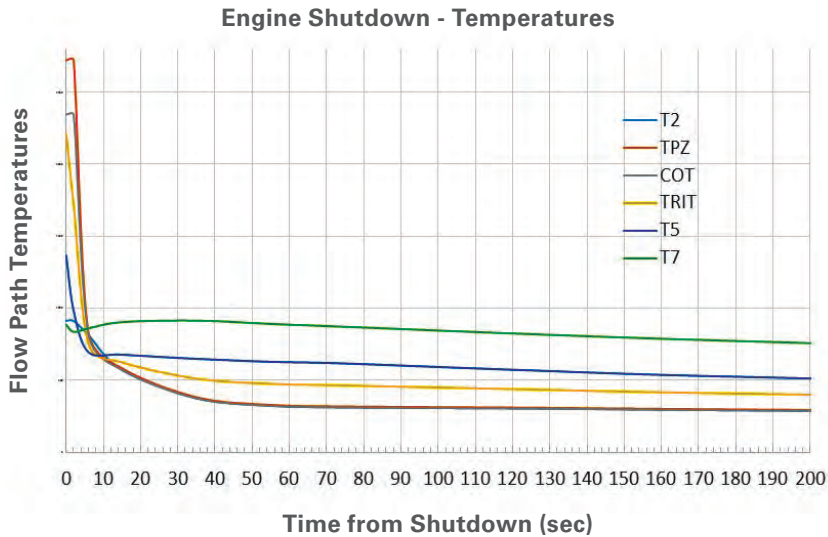


**Figure 6-34.** Engine shutdown simulation (temperatures), 23MW industrial gas turbine (T2, T5, T7 are the respective temperatures at the compressor exit, the power turbine inlet and the exhaust temperature. TRIT is the firing temperature, and TPZ is the primary zone temperature [17]).

gas turbine, or the electricity supply to a motor is instantly stopped. Despite the fuel cutoff, the gas turbine continues producing power for a brief, but critical moment.

The gas turbine is stopped by closing the fuel valves. As can be seen in *Figures 6-33 and 6-34* (Kurz et al. [17]), the gas turbine still produces power even after shutting off the fuel supply due to the gas producer thermal and mechanical inertia. The output decays fast. For midsize two-shaft gas turbines, the residual power typically becomes negligible at about 300 ms after the fuel valve is shut down.

The fast decay in power output is primarily due to the fast drop in the temperature of the exhaust gas supplied to the power turbine. In *Figure 6-34*, this is the temperature T5 of the gas entering the power turbine, which declines even faster than the ‘firing temperature’, that is the temperature of the gas leaving the combustor, or entering the gas producer turbine rotor (TRIT).

The general system behavior can be described by applying conservation laws for energy, inertia, heat transfer, compressor and valve characteristics. For relatively short pipes, with a limited volume (such as the systems desired for recycle lines), the pressure at the valve and the

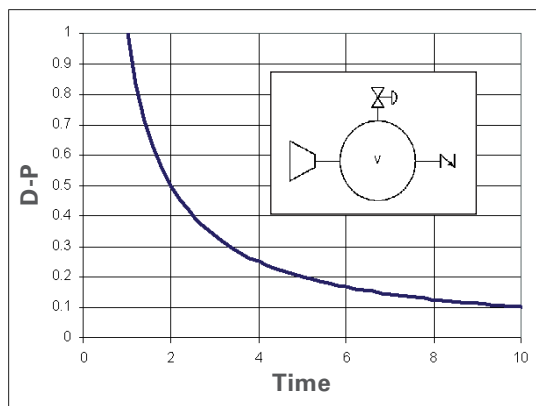


**Figure 6-35.** Simplified system and transient characteristic.

pressure at the compressor discharge will not be considerably different. For situations like this, the heat transfer can also be neglected. In such a simple system, the boundaries for the gas volume on the discharge side are established by the discharge check valve, compressor, and recycle valve (*Figure 6-20*). The volume on the suction side is usually orders of magnitude larger than the discharge volume and, therefore, can be considered infinite. Thus, to simplify the analysis of a system, the suction pressure can be considered constant. This is not a general rule, but is used to simplify the following considerations.

This yields the simplified system, consisting of a volume filled by a compressor and emptied through a valve (*Figure 6-35*). Basically, the dynamic behavior of the system is that of a fixed volume where the flow through the valve is a function of the pressure differential over the valve. In a surge avoidance system, a certain amount of the valve's flow capacity will be consumed to recycle the flow through the compressor. Only the remaining capacity is available for depressurizing the discharge volume. In such a system, mass and momentum balance have to be maintained (Sentz [18], Kurz and White [19]). From this complete model, some simplifications can be derived. They're based on the type of questions that need to be answered.

For relatively short pipes, with limited volume (such as the systems desired for recycle lines), the pressure at the valve and the pressure at the compressor discharge will be very similar. Also, due to the short duration of any event, the heat transfer can be neglected. Therefore, mass and momentum conservation are reduced to:

$$\frac{dp_2}{dt} = \frac{k \cdot p_2}{V} [Q - Q_v]$$

The volume ( $V$ ) is filled by the compressor with a flow ( $Q$ ) coming from the compressor, and emptied by the flow ( $Q_v$ ) through the valve. The valve flow is determined by the pressure ratio ( $p_2/p_1$ ). The compressor operating point also changes based on the pressure ratio ( $p_2/p_1$ ). For any time, the equation above enables you to calculate the change in compressor discharge pressure ( $p_2$ ).

This also means that the discharge pressure change depends on the capability of the valve to release flow at a higher rate than the flow coming from the compressor. It also shows that the pressure reduction for a given valve will be slower for higher pipe volumes ( $V$ ).

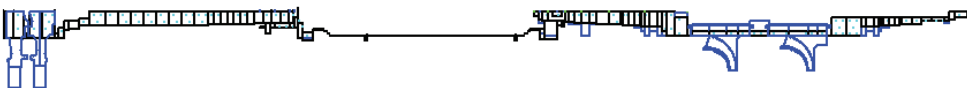


**Figure 6-36.** Power turbine rotor, coupling and compressor rotor contribute to the system inertia.

In a shutdown situation, the compressor speed decelerates, because its inertia (*Figure 6-36*) is counteracted by the absorption of power while still pumping gas. The behavior of the compressor during ESD is thus governed by two effects. The inertia of the system consisting of the compressor, coupling and power turbine (and gearbox where

applicable) is counteracted by the torque (T) transferred into the fluid by the compressor (mechanical losses are neglected). The balance of forces thus yields:

$$T = -2\pi \cdot J \cdot \frac{dN}{dt}$$

Knowing the inertia (J) of the system (Figure 6-36) and measuring the speed variation with time during rundown yields the torque and, thus, the power transferred to the gas.

$$P = T \cdot N \cdot 2\pi = -(2\pi)^2 \cdot J \cdot N \cdot \frac{dN}{dt}$$

If the rundown would follow through similar operating points, then  $P \sim N_3$ , which would lead to a rundown behavior of:

$$\frac{dN}{dt} = \frac{k}{J(2\pi)^2} N^2 \rightarrow \int N^{-2} dN = \frac{k}{J(2\pi)^2} \int dt + c \rightarrow N(t) = -\frac{1}{\frac{k}{J(2\pi)^2} t - \frac{1}{N_{t=0}}} \quad (10)$$

Figure 6-37 shows the behavior of a compressor during rundown with a non-functional recycle valve. It shows the rapid deceleration of the compressor once the gas turbine fuel supply is turned off. It also shows periods where the compressor actually surged (determined by compressor vibrations).

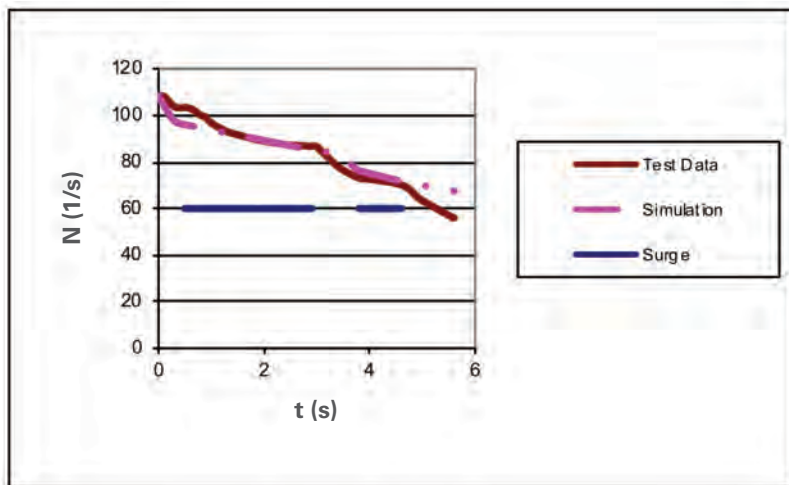


Figure 6-37. Speed of a compressor during emergency shutdown.

## START-UP CONSIDERATIONS

The design of the anti-surge and recycle system also impacts the start-up of the station. Particular attention must be given to the capability of starting up the station without having to abort the start due to conditions where allowable operating conditions are exceeded. Problems may arise from the fact that the compressor may spend a certain amount of time

recycling gas, until sufficient discharge pressure is produced to open the discharge check valve (*Figure 6-20*) and gas is flowing into the pipeline.

Virtually all of the mechanical energy absorbed by the compressor is converted into heat in the discharged gas. In an uncooled recycle system, this heat is recycled into the compressor suction, and then more energy is added to it. A cubic foot of natural gas at 600 psi weighs about 2 lb (depending on composition). The specific heat of natural gas is about 0.5 Btu/lb (again depending on composition). One Btu/sec equals 1.416 hp. If the recycle system contains 1000 cubic feet, there is a ton of gas in it. 1416 hp will raise the temperature of the gas about 1 degree per second. This approximates what happens with 100% recycle. Eventually, at 100% recycle, this will lead to overheating at the compressor discharge. The problem usually occurs when there is a long period between the initial rotation of the compressor and overcoming the pressure downstream of the check valve.

Low-pressure-ratio compressors often do not require aftercoolers. Four strategies can be employed to avoid overheating the uncooled compressor during start-up:

1. Accelerate quickly
2. Delay hot gas reentering the compressor
3. Dilute hot gas reentering the compressor
4. Throttled recycle

Compressors without cooling capability must be accelerated and placed on line quickly to avoid overheating. Uncooled compressor sets cannot be started and accelerated to idle. They must be accelerated quickly through the point where the discharge check valve opens and the recycle valve closes. If acceleration slows when the discharge pressure is met, and recycle valve closes slowly, a shutdown may still occur. Often, standard start sequences are very conservative and can be shortened to reduce the time it takes to bring a compressor on line.

Extending the length of the recycle line downstream of the recycle valve increases the total volume of gas in the recycle system. This reduces the heat buildup rate by delaying when the hot gas from the compressor discharge reaches the suction. Some heat will be radiated through the pipe walls. If the outlet is far upstream into a flowing suction header, dilution will occur.

*Figures 6-38a and 6-38b* outline a solution to a rather difficult starting problem for a compressor

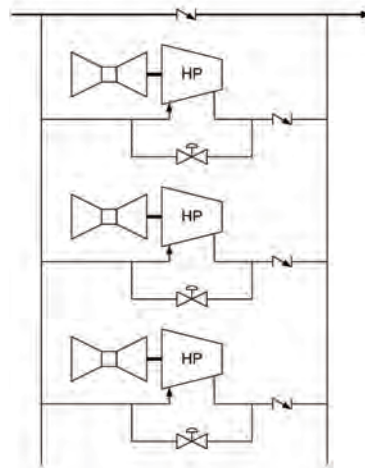


**Figure 6-38a.** Original station layout.

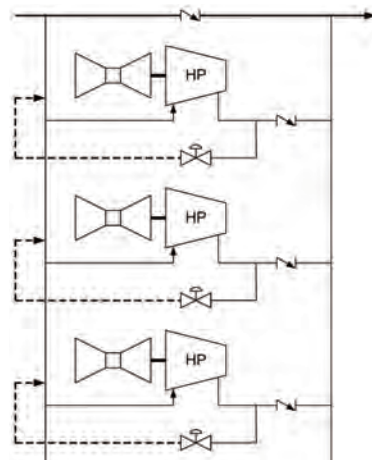


**Figure 6-38b.** Improved station layout.

station without aftercooling capability. In *Figure 6-38a*, to start the first unit is relatively easy, because there is virtually no pressure differential across the main line check valve, and therefore the unit check valve will open almost immediately, allowing the flow of compressed gas into the pipeline. However, if one additional unit is to be started, the station already operates at a considerable pressure ratio, and therefore the unit check valve will not open until the pressure ratio of the starting unit exceeds the station pressure ratio.

Ordinarily, the unit would invariably shut down on high temperature before this can be achieved. By routing the recycle line into the common station header (*Figure 6-38b*), the heat from the unit coming on line is mixed with the station suction flow. This equalizes the inlet temperature of all compressors; higher for the compressors already on line, lower for the compressor coming on line. With this arrangement, overheating of a compressor coming on line is nearly always avoided.

*Figure 6-39* shows the problem of a conventional system that includes 3000 ft of 24 in. pipe without aftercooling. The temperature in the recycle line starts to rise and, assuming a shutdown setpoint of 350° F, the compressor would shut down after about 20 minutes.

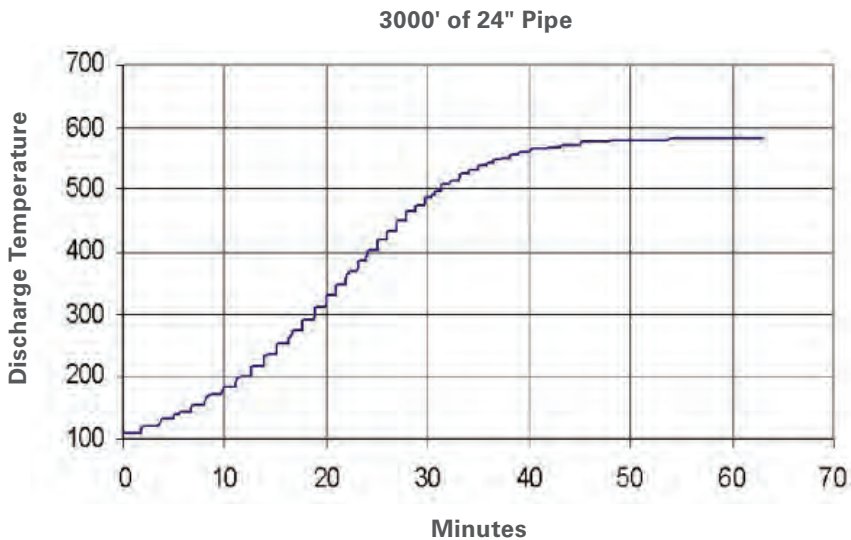


**Figure 6-39.** Temperature buildup.

The three-part *Figure 6-40* outlines the startup event with the revised system. The power turbine and the compressor start to rotate once the gas producer provides sufficient power. Subsequently, the gas temperature rises, but because the discharge pressure required to open the check valve is reached fast enough, overheating can be avoided. The temperature rise in the recycle loop during startup is shown as a function of (*Figure 6-40a*) power turbine and compressor speed, (*Figure 6-40b*) gas producer speed and (*Figure 6-40c*) time (in minutes).

The power turbine starts to turn at about 75% gas producer speed, at which point the temperature starts to rise. After the discharge check valve opens (at 0.2 minutes after the compressor starts to rotate), 95% gas producer speed and 70% power turbine speed, the

temperature drops rapidly. Further analysis of the start-up problem indicates the advantage of throttling the recycle valve, rather than starting the unit with the recycle valve fully open.

With the valve-sizing tool described previously, the exact valve opening that will be required to maintain a specific surge margin at steady-state operation can be determined. As the compressor is accelerating, flow is increasing. The pressure in the discharge is lower and the pressure in the suction is higher than they would be, if the compressor operated at this steady-state speed. This is due to the effect of the suction and discharge volumes. This also causes the flow to be higher, and subsequently, the surge margin will be higher. As such, if the valve is set at a fixed position to obtain a fixed small surge margin, the actual surge margin will be higher during acceleration.

To use this strategy safely, the control must be able to sense a loss of acceleration (flame out), and if detected, open all recycle valves immediately. As the compressor's volumes, up and downstream, cause the surge margin to be higher during acceleration, they make surge avoidance more challenging with the loss of speed.

*Figure 6-30* illustrates this. At 70% open setting, the startup of the compressor is significantly closer to the surge line than at 100% open setting. For any given speed, the power requirement of the compressor is lower when it is closer to surge than when it is farther in choke. Therefore, for a given amount of available power, the start is quicker if the compressor operates closer to surge. If the rate of acceleration is quicker, the heat input into the system is lower. Actively modulating the surge during start-up is virtually impossible as the parameters defining the surge limit of the compressor are too low to be practically measured. Returning to *Figure 6-30*, the surge limit of a compressor matches well with a fixed travel (constant Cv) line for a recycle valve. As such, a compressor can be started with a fixed recycle valve position.

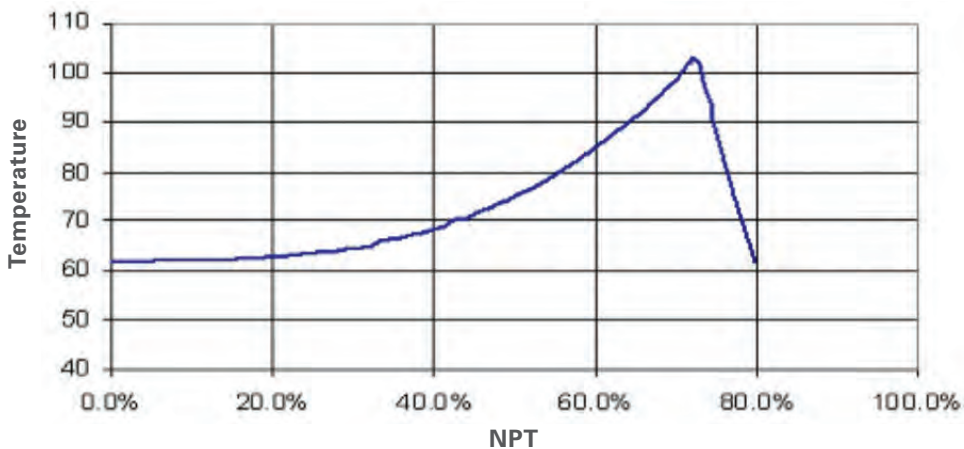


**Figure 6-40a.** Temperature (°F) vs. NPT (%).

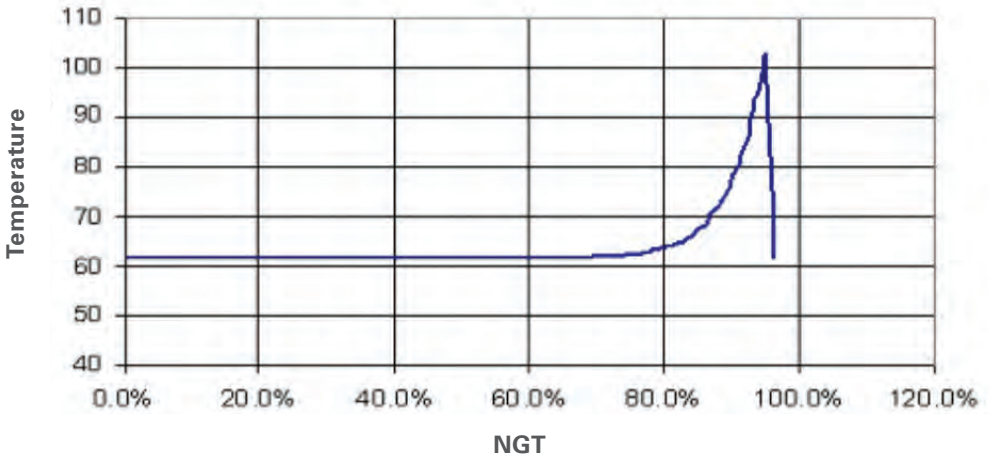


**Figure 6-40b.** Temperature (°F) vs. NGP (%).

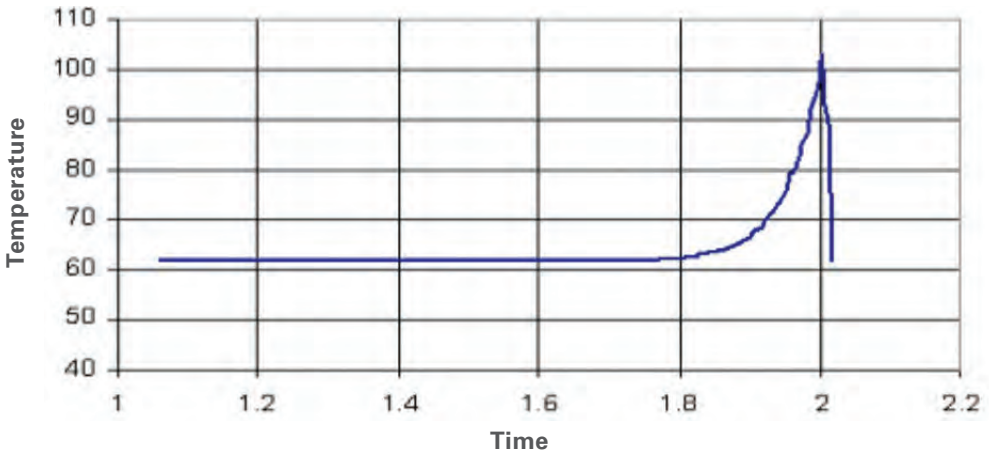


**Figure 6-40c.** Temperature (°F) vs. Time (min.).

## REPLACING RECIPROCATING COMPRESSORS

In many instances, centrifugal compressors are used to replace reciprocating compressors. Because the operating characteristics of reciprocating compressors, described by:

- A near vertical head-flow characteristic at constant speed.
- Control devices that lead to discontinuous changes in characteristics (unloading, deactivation, clearance control).
- Operating map is not continuous (pulsation, rod reversal, etc.).

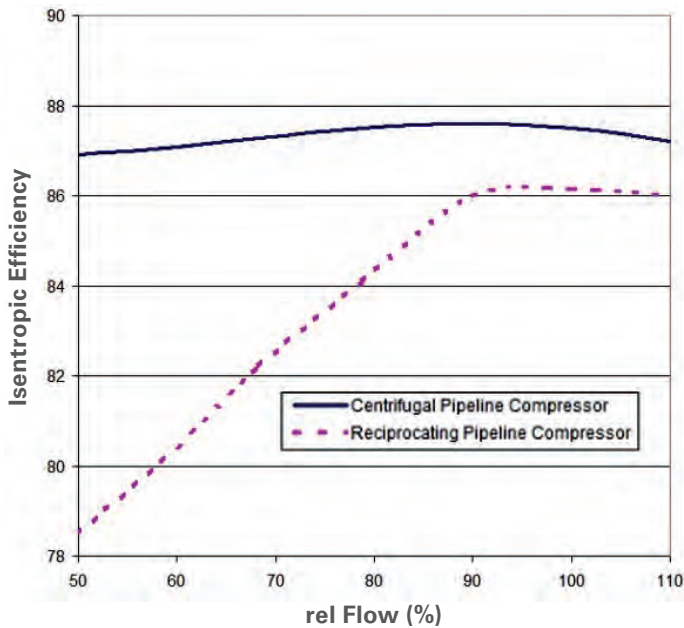


**Figure 6-41.** Compressor efficiency at different flow rates based on operation along a steady-state pipeline characteristic (pressure ratio at 100% flow = 1.4).

The different operating characteristics of the driver and the compressor, applied to the prevailing system characteristics, lead to different operating points compared to a centrifugal compressor applied to the same system characteristics. Therefore, suboptimal results will often occur if the centrifugal compressor that replaces one (or often several reciprocating compressors) is sized to simply replicate the operating points that were observed during the operation of the reciprocating compressor. Rather, the system characteristics should be studied to find the best centrifugal compressor solution.

For example, the impact of different compressor characteristics on the efficiency achieved under operating conditions imposed by the system is highlighted in *Figure 6-41*. A variable-speed centrifugal compressor is compared with a reciprocating compressor. Unlike a centrifugal compressor, a reciprocating compressor will deliver a lower efficiency when the pressure ratio drops (Noall and Couch [20]).

The typical steady state pipeline operation (*Figure 6-11*) will yield an efficiency behavior as outlined in *Figure 6-41*. This is the result of evaluating the compressor efficiency along a pipeline steady-state operating characteristic. Both compressors would be sized to achieve their best efficiency at 100% flow, while allowing for 10% flow above the design flow. Different mechanical efficiencies have not been considered for this comparison.

The reciprocating compressor efficiency is derived from valve efficiency measurements in Noall and Couch [20], with compression efficiency and losses due to pulsation attenuation devices added. The efficiencies are achievable with low-speed compressors. High-speed reciprocating compressors may be lower in efficiency. The graph shows the impact of the increased valve losses at lower pressure ratios for reciprocating machines, while the efficiency of the centrifugal compressor stays more or less constant (Kurz et. al. [21]).

## CHAPTER 6 REFERENCES

- [1] Kurz, R., Brun, K., 2017 "Process Control for Compression Systems", Proceedings of ASME Turbo Expo 2017, GT2017-63005.
- [2] Kurz, R., White, R.C., Brun, K., 2015, 'Surge Control and Dynamic Behavior for Centrifugal Gas Compressors', 3rd Middle East Turbomachinery Symposium, Doha, Qatar.
- [3] White, R.C., Kurz, R., 2006, 'Surge Avoidance for Compressor Systems', Proc. 35<sup>th</sup> Turbomachinery Symposium, Houston, Tx.
- [4] Botros, K.K., Ganesan, S.T, 2008," Dynamic Instabilities in Industrial Compression Systems with Centrifugal Compressors, Proc. 37<sup>th</sup> Turbomachinery Symposium, Houston, Tx.
- [5] Botros, K.K., 2011, "Single vs. Dual Recycle System Requirements in the Design of High Pressure Ratio, Low Inertia Centrifugal Compressor Stations", ASME GT2011-45002.
- [6] Kurz, R., White, R.C., 2004,"Surge Avoidance in Gas Compression Systems", Trans ASME JTurbo,Vol.126,pp.501-506.
- [7] Morini, M., Pinelli, M, Venturini, M., 2007,"Development of a One-Dimensional Modular Dynamic Model for the Simulation of Surge in Compression Systems", ASME JTurbo, Vol. 129, pp437-447.
- [8] Blieske, M., Kurz, R., Garcia-Hernandez, A., Brun, K., 2011,"Centrifugal Compressors During Fast Transients", Trans ASME JEGTP ,Vol.133, pp072401.
- [9] Rasmussen. P.C., Kurz, R., 2009, "Centrifugal Compressor Applications", 38<sup>th</sup> Turbomachinery Symposium., Houston, TX.
- [11] Kurz, R., Brun, K., 2009, Assessment of Compressors in Gas Storage Applications, ASME GT2009-59258.
- [12] Kurz, R., White, R.C., Brun, K., 2014, 'Transient Operation in Pipeline Compressor Stations', ASME Paper GT2014-25016.
- [13] Moore, J.J., Garcia-Hernandez, A., Blieske, M., Kurz, R., Brun, K., 2009, 'Transient Surge Measurements of a Centrifugal Compressor Station During Emergency Shutdowns', Proc. 38<sup>th</sup> Turbomachinery Symposium, Houston, Tx.
- [15] Belardini, E., Rubino, D.T., Tapinassi, L., Pelella, M., 2016, Four Quadrant Centrifugal Compressor Performance, Proc. 1<sup>st</sup> Asia Turbomachinery and Pump Symposium, Singapore.
- [16] Aust, N., 1988, Ein Verfahren zur digitalen Simulation instationaerer Vorgaenge in Verdichteranlagen, Diss. UBwHH, Hamburg, Germany.
- [17] Kurz, R., Mendoza, R., Burnes, D., Saxena, P., Alexander, S., 2018, On Gas Turbine Safety in Offshore Operations, ASME GT2018-75003.
- [18] Sentz, R.H., "The Analysis of Surge," Texas A&M Turbomachinery Symposium, 1980.

[19] Kurz, R., White, R.C., 2004, "Surge Avoidance in Gas Compression Systems", Trans ASME JTurbo Vol.126, pp.501-506.

[20] Noall, M., Couch, W., "Performance and Endurance Tests of Six Mainline Compressor Valves in Natural Gas Compression Service," Gas Machinery Conference, Salt Lake City, Utah, 2003.

[21] Kurz, R., Winkelmann, B., Mokhatab, S., 2010, "Efficiency and Operating Characteristics of Centrifugal and Reciprocating Compressors", Pipeline and Gas Journal, 2010.





## CHAPTER 7

# COMPRESSOR DRIVERS

Gas compressors can be powered by different types of drivers, including gas turbines, steam turbines, expanders, or electric motors. Some attempts have been made to drive centrifugal compressors with reciprocating gas engines, but the speed mismatch and the operating characteristics of a gas engine complicate this combination. [1,2]

Gas turbines for compressor drives are usually two-shaft designs, with a free power turbine. This design facilitates a large speed range. Some applications utilize single-shaft gas turbines, but only provide very limited speed variations.

Steam turbines and expanders provide a wide range of speeds, similar to twin-shaft gas turbines. However, steam turbines are rarely used in upstream and midstream applications, because unlike downstream applications, usually no process steam or pressurized process gas is available. Expanders are also used in refrigeration cycles.

The basic electric motor drive is a constant-speed motor, usually driving the compressor via a gearbox. So-called Variable Speed Hydrodynamic Drives (VSHD) are capable of varying their output speeds, while using a constant-speed motor. Lastly, a Variable Frequency Drive (VFD) can be utilized. Since an electric motor's speed is determined by the frequency of the electric current and voltage supplied to the motor, modifying the power supply frequency by using a variable-frequency drive is a convenient way to vary the motor's speed. Variable frequency drives either use a gearbox between the motor and the compressor, or accommodate directly driven applications without a gearbox. Gas turbines (adapted from [2]) use thermodynamic principles of the Brayton cycle, which essentially defines the requirements for the gas turbine components.

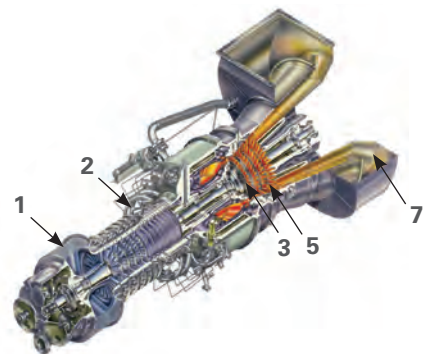
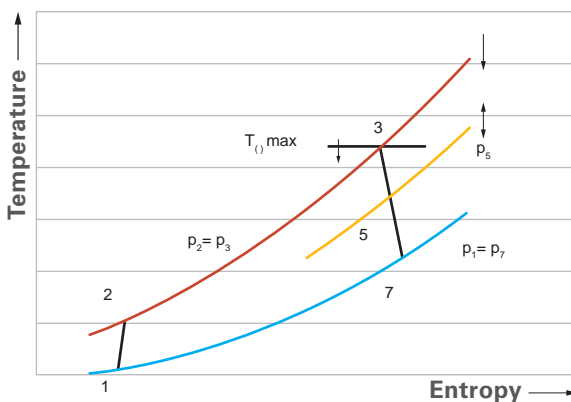


**Figure 7-1. Brayton Cycle**

The Brayton or gas turbine cycle (*Figure 7-1*) involves compression of air or another working gas, and the subsequent heating of this gas (either by injecting and burning a fuel or by indirectly heating the gas) without a change in pressure, followed by the expansion of the hot, pressurized gas. The compression process consumes power, while the expansion

process extracts power from the gas. Some of the power from the expansion process can be used to drive the compression process. If the compression and expansion process is performed efficiently enough, the process will produce useable power output.

The process is thus substantially different from a steam turbine (Rankine) cycle that does not require the compression process, but derives the pressure increase from external heating. The process is similar to processes used in diesel or Otto reciprocating engines that also involve compression, combustion, and expansion. However, in a reciprocating engine, compression, combustion and expansion occur at the same place (the cylinder), but sequentially, in a gas turbine, they occur in dedicated components, but all at the same time. The major components of a gas turbine include the compressor, the combustor and the turbine.

The compressor (usually an axial-flow compressor, but some smaller gas turbines also use centrifugal compressors) compresses the air to several times atmospheric pressure. In the combustor, fuel is injected into the pressurized air from the compressor and burned, thus increasing the temperature. In the turbine section, energy is extracted from the hot pressurized gas, thus reducing pressure and temperature. A significant part of the turbine's energy (50 to 60%) is used to power the compressor, and the remaining power can be used to drive generators or mechanical equipment (gas compressors and pumps). Industrial gas turbines typically utilize one of three primary arrangements for the major components:

Single-shaft gas turbines have all compressor and turbine stages running on the same shaft.

Two-shaft gas turbines consist of two sections: the gas producer (or gas generator) with the gas turbine compressor, the combustor, and the high pressure portion of the turbine on one shaft and a power turbine on a second shaft (*Figure 7-1*). In this configuration, the high-pressure or gas-producer turbine only drives the compressor, while the low-pressure or power turbine, working on a separate shaft at speeds independent of the gas producer, can drive mechanical equipment.

Multiple-spool engines: industrial gas turbines derived from aircraft engines sometimes have two compressor sections (the HP and the LP compressors), each driven by a separate turbine section (the LP compressor is driven by an LP turbine using a shaft that rotates concentrically within the shaft that is used for the HP turbine to drive the HP compressor), and running at different speeds. The energy left in the gas after this process is used to drive a power turbine (on a third, separate shaft), or the LP shaft is used as the output shaft.

The compressed air from the compressor enters the gas turbine combustor. Here, the fuel (natural gas, natural gas mixtures, hydrogen mixtures, diesel, kerosene and many others) is injected into the pressurized air and burns in a continuous flame. The flame temperature is usually so high that any direct contact between the combustor material and the flame has to be avoided, and the combustor has to be cooled, using air from the engine compressor. Supplemental air from the engine compressor is mixed into the combustion process for additional cooling.

The combustion process and emissions control are other important topics. Unlike reciprocating engines, gas turbine combustion is continuous. This is advantageous because the combustion process can be made very efficient, with very low levels of products having incomplete combustion such as carbon monoxide (CO) or unburned hydrocarbons (UHC). The other major emissions component, oxides of nitrogen ( $\text{NO}_x$ ), are not related to combustion efficiency, but are strictly related to the temperature levels in the flame (and the amount of nitrogen in the fuel). The solution to  $\text{NO}_x$  emissions, therefore, lies in reducing the flame temperature. Initially, this was accomplished by injecting massive amounts of steam or water into the flame zone, thus 'cooling' the flame. This approach has significant drawbacks, not the least of which is the requirement to provide large amounts of extremely clean water (the fuel-to-water ratio is approximately 1:1).

Since the 1990s, combustion technology has focused on systems often referred to as dry low  $\text{NO}_x$  combustion, or lean-premix combustion (*Figure 7-2*). The idea behind these systems is to make sure that the mixture in the flame zone has a surplus of air, rather than allowing the flame to burn under stoichiometric conditions. This lean mixture, assuming the mixing has been done thoroughly, will burn at a lower flame temperature, and thus produce less  $\text{NO}_x$ . One of the key requirements is the thorough mixing of fuel and air before the mixture enters the flame zone. Incomplete mixing will create zones where the mixture is stoichiometric (or at least less lean than intended), thus locally creating more  $\text{NO}_x$ . The flame temperature has to be carefully managed in a window that minimizes both  $\text{NO}_x$  and CO. Lean-premix combustion systems keep the  $\text{NO}_x$ , as well as CO and UHC emissions, within prescribed limits for a wide range of loads, usually between full load and about 40% or 50% load. In order to accomplish this, the air flow into the combustion zone has to be manipulated over the load range.

The gas turbine power output is a function of the speed, the firing temperature, and the position of certain secondary control elements, like adjustable compressor vanes, bleed valves, and in rare cases, adjustable power turbine vanes. The output is primarily controlled by the amount of fuel injected into the combustor. Most single-shaft gas turbines run at constant speed when they drive generators. In this case, the control system modifies fuel flow (and secondary controls) to keep the speed constant, independent of generator load. In general, higher loads will lead to higher firing temperatures.

Two-shaft machines are preferably used to drive mechanical equipment, because being able to vary the power turbine speed provides a very sophisticated way to adjust the driven equipment to process conditions. Again, the power output is controlled by fuel flow (and secondary controls), and higher loads will lead to higher gas producer speeds and higher firing temperatures.

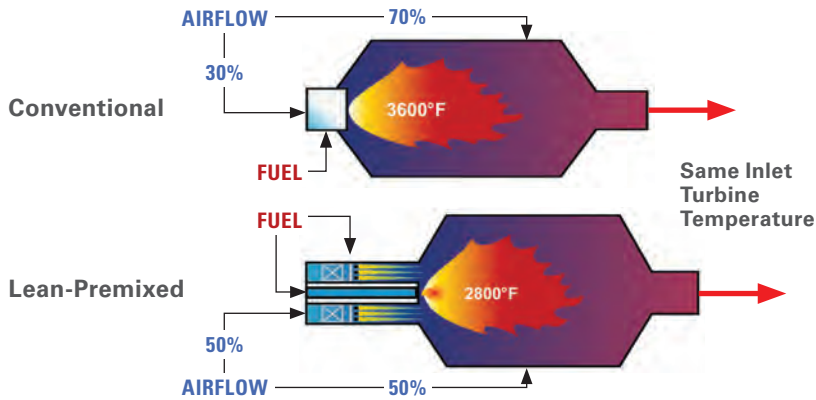


**Figure 7-2.** Conventional and lean-premix combustion systems.

Figure 7-3 shows the influence of ambient pressure and ambient temperature on gas turbine power and heat rates. The influence of ambient temperature on gas turbine performance is very distinct. Any industrial gas turbine currently in production will produce more power when the inlet temperature is lower, and less power when the ambient temperature increases. The rate of change cannot be generalized and is different for different gas turbine models. Full-load gas turbine power output is typically limited by the constraints of maximum firing temperature and maximum gas producer speed (or, in twin-spool engines, by one of the gas producer speeds). Gas turbine efficiency is less impacted by the ambient temperature than the power.

The humidity in the air impacts power output, but to a small degree, (generally, not more than 1 to 3%, even on hot, humid days). The impact of humidity tends to increase at higher ambient conditions. Lower ambient pressure, for example, due to a higher site elevation leads to lower power output, but has practically no impact on efficiency. It must be noted, however, that the impact of the inlet pressure drop on power and efficiency will be more severe, Figure 7-3.

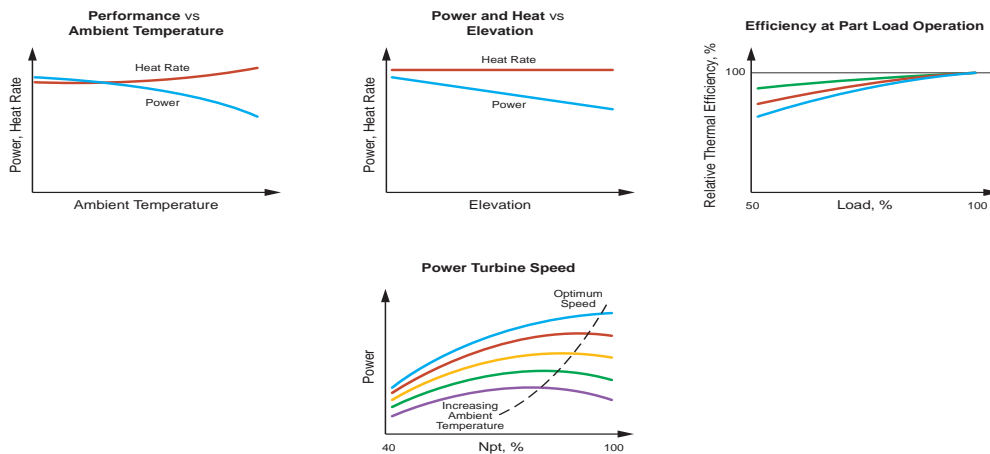


**Figure 7-3.** Performance Characteristics

Gas turbines operated at partial load will generally lose some efficiency. Again, the efficiency reduction operating at partial load is very model specific. Most gas turbines show a very small efficiency drop for at least the first 10% of load reduction. In two-shaft engines, the power turbine speed impacts available power and efficiency. For any load and ambient temperature, there is an optimum power turbine speed. Usually, reducing the load (or increasing the ambient temperature) will reduce the optimum power turbine speed. Small deviations from the optimum ( $\pm 10\%$  for example) have very little impact on power and efficiency (Figure 7-4).

Electric motor drive configurations include variable frequency drive (VFD) speed controlled motors that drive the compressor either directly or via a gearbox (Figure 7-5), and constant speed motors driving the compressor via a variable speed gearbox (VSHD, Figure 7-6).

Since the electric motor speed (for induction type motors, synchronous motors and permanent magnet motors alike) is determined by the frequency of the electric current and voltage supplied to the motor, a convenient way to vary the motor speed is to modify the power supply frequency by using a variable-frequency drive [1-3].

Another way to create a variable speed drive is by using a constant speed motor, and a variable-output-speed gearbox [1, 2], often referred to as Variable Speed Hydrodynamic Drive (VSHD). The basic VSHD components are a hydrodynamic torque converter coupled with a planetary gear. The planetary gear is designed as a superimposing gear, with the torque converter driving one of the planetary gear components. The torque converter acts as the control unit for the output speed. The VSHD uses a constant-speed electric motor. Both the VSHD and the VFD are controlled by setting their speeds, until the available power becomes a limit. For the purpose of this discussion, an adjustable-speed drive (ASD) is used to describe

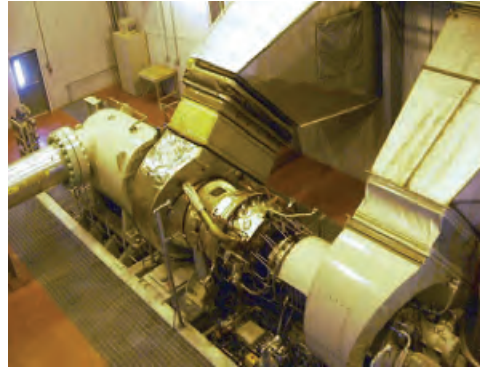


**Figure 7-4.** Compressor driven by a two-shaft gas turbine



**Figure 7-5.** Electric-motor drive package: constant-speed motor driving the compressor via a variable-speed gearbox.



**Figure 7-6.** Electric-motor drive package: VFD controlled motor driving the compressor via a speed-increasing gearbox.

various methods for adjusting the speed of a variable-speed compressor, such as variable-frequency drives (VFD) and variable-speed hydrodynamic drives (VSHD).

In many applications, the performance characteristics of the driver—for example, the power as a function of ambient conditions or the power output at various output speeds—are important considerations. In general, a VFD controlled motor is a constant torque machine, thus exhibiting a linear drop in power with speed (*Figure 7-7*), implemented by maintaining

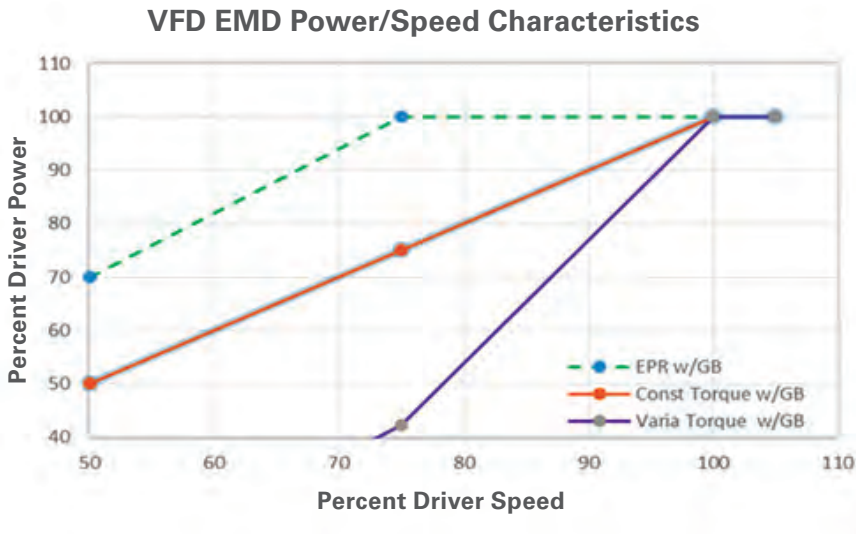


**Figure 7-7.** Speed-power characteristics for variable-frequency drives [1].

a constant Volts/Hz ratio, until, above a certain corner frequency, the motor becomes power limited. There are exceptions to this behavior, where the motor is oversized to provide constant power over a wider range (Expanded Power Range, EPR), or where the torque is reduced with speed, often for thermal reasons. The speed-power relationship has a significant impact on control concepts for variable-speed drives. In particular, the linear reductions of power seen in most VFD controlled electric motors imposes a limit on flexibility, compared to VSHD and two-shaft gas turbine drives.

A VSHD shows a speed-power relationship similar to a two-shaft gas turbine, but with a smaller usable speed range (*Figure 7-8*).

The fact that the electric motor output is not subject to changes in ambient temperature (within limits) is another important feature. This means the convenience of providing more power at lower ambient temperatures is lacking, but the same power is available on hot and cold days is an advantage. This can be important in applications where the load demand is dependent on ambient conditions.

Further, the starting characteristics, including the amount of torque at low speeds, or, for constant speed electric motors, the amount of additional current that's required during start-up must be considered (*Figure 7-9*).

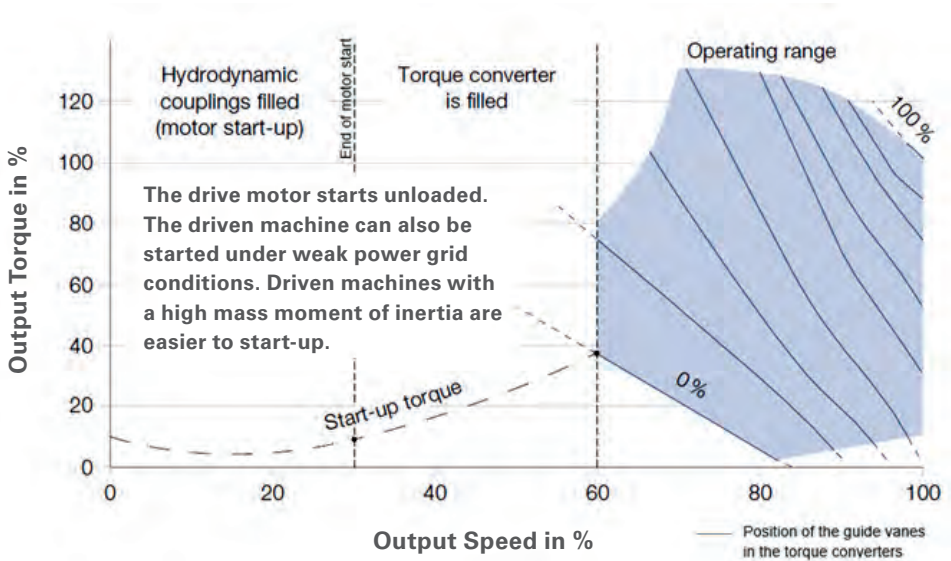


Figure 7-8. Operating map of a VSHD [1].

Whether the units are installed on shore, offshore or subsea determines access to maintenance intervention, as well as the environmental conditions (for example salt in the air) the equipment has to be designed for. For electric drivers, the question is also whether the electricity can be brought to site via transmission lines, or whether it has to be generated on site, usually with gas turbine driven generators.

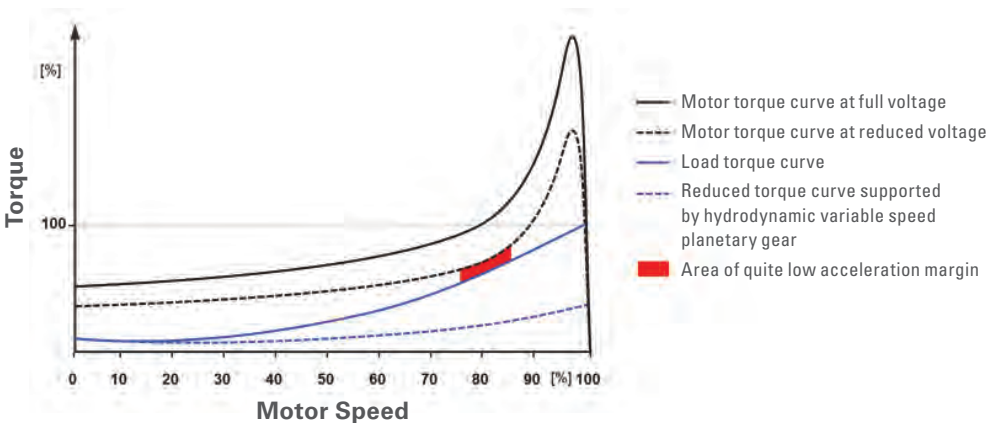


Figure 7-9. Squirrel-cage induction motor capability curve at different voltage levels and load torque curves [1].

## CHAPTER 7 REFERENCES

- [1] Kurz,R., Mistry,J., Davis,P., Cole,G., 2021, *Application and Control of Variable-Speed Centrifugal Compressors in the Oil and Gas Industry*, IEEE/PCIC Paper PCIC2020-AT-19.
- [2] Kurz,R., Winkelmann,B., Brun,K., 2019, *Performance of Industrial Gas Turbines*, Proc. 48<sup>th</sup> Turbomachinery Symposium, Houston, Tx.
- [3] Glasbrenner,M., Venkataraman,B., Kurz,R., Cole,G.J., 2017, *Electric-Motor Driven Gas Compressor Packages: Starting Methods for Large Electrical Motors and torsional Integrity*, Proc. 46<sup>th</sup> Turbosymposium, Houston, Tx.





## CHAPTER 8

# CENTRIFUGAL COMPRESSORS IN OIL & GAS APPLICATIONS

Found in reservoirs all over the world, oil and natural gas are contained in the pore spaces of the reservoir rock. Usually, reservoirs contain mixtures of lighter and heavier hydrocarbons, as well as  $\text{CO}_2$ , water, and sometimes  $\text{H}_2\text{S}$ . Some types of reservoirs allow the oil and gas to move freely, making it easier to extract. Other reservoirs restrict the flow of oil and gas and require special techniques to move the oil or gas from the pores to a producing well [1-3].



**Figure 8-1.** Natural gas movement from the well to the user.

Even today, with advanced technologies, more than two-thirds of the oil present may not be recoverable from some reservoirs. Once an oil or gas reservoir is discovered and assessed, the task is to bring a saleable product to a user, as well as to maximize the amount of oil or gas that can ultimately be recovered. In the past, natural gas was often seen as a byproduct of oil production, and may have been flared, especially if no infrastructure existed to deliver the gas to potential users. However, even in these situations, the gas can be used to enhance oil recovery. On the other hand, countries such as the United States have built extensive pipeline networks to transport gas from the well to users [1].

Figure 8-1 shows the path of natural gas from wells to users. In general, activities close to the oil and gas field are considered upstream, while activities involving the transport and storage of gas are considered midstream applications.

Many oil and gas wells are located on the ocean floor, and production requires an offshore platform (Figure 8-2) or subsea installations. The reservoirs are typically at elevated pressure. A series of valves and equipment ("Christmas Tree") is installed on top of the well, to regulate the flow of hydrocarbons from the well. Early in its production life, the underground pressure will often push the hydrocarbons all the way up the well bore to the surface. Depending on reservoir conditions, this "natural flow" may continue for many years.



**Figure 8-2.** Offshore drilling platform.

When the pressure differential is insufficient for the oil to flow naturally, mechanical pumps must be installed to bring the oil to the surface. This process is referred to as artificial lift [1].

Most wells follow a predictable pattern where production will increase for a short period, then peak and follow a long, slow decline (*Figure 8-3*). Reservoir conditions determine the shape of this decline curve, how high the production peaks, and the length of the decline. The decline curve can be positively influenced by:

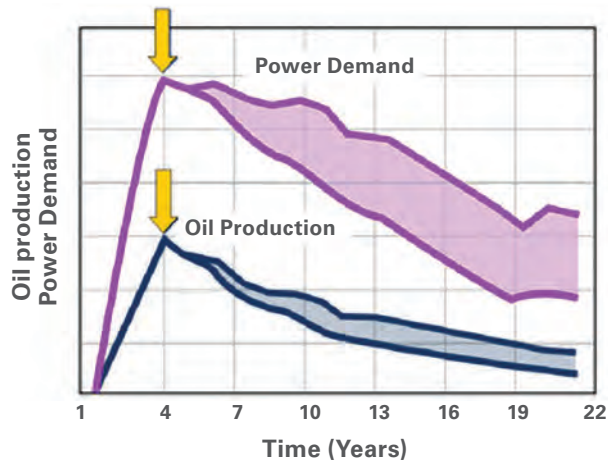


**Figure 8-3.** Typical change in oil production from an offshore well.

1. Cleaning out the well bore to help oil and/or gas move more easily to the surface.
2. Fracturing or treating the reservoir rock with acid around the bottom of the well bore to create better pathways for the oil and gas to move through the subsurface to the producing well.
3. Drilling additional wells.
4. Employing enhanced oil recovery (EOR) techniques.

Depending on reservoir conditions, the techniques collectively referred to as enhanced oil recovery (EOR) employ one of two methods designed to increase production:

1. Water injection ('water flooding').
2. Injection of various other substances (hydrocarbons, steam, nitrogen, carbon dioxide) into the reservoir to remove more oil from the pore spaces.

When geologists began studying time-lapse seismic monitoring results ('4-D'), they were surprised to discover that one of the most basic notions about the movement of oil in a reservoir—that it naturally settles between lighter natural gas above and heavier groundwater below—oversimplifies the behavior of real oil fields. Actually, most wells produce complex, fractal drainage patterns that cause the oil to mix with gas and water. It also became clear that traditional techniques may leave 60% or more of the oil behind. This led to the strategy of pumping natural gas, steam, carbon monoxide or nitrogen into the reservoirs. This injection spreads through the pores in the rock and pushes oil that otherwise would have been abandoned toward the existing wells. Applications where gas is injected into the oil reservoir for pressure maintenance and to enhance oil recovery by miscible flooding with lean, methane-rich gas are usually referred to as gas re-injection [3].

Most oil wells produce oil, gas and water. This mixture is separated at the surface. Initially, the oil well may produce mostly oil with a small amount of water. Over time, the

percentage of water increases. This produced water varies in quality from very briny to relatively fresh. Where this water cannot be used for other purposes, it may be reinjected into the reservoir—either as part of the waterflooding technique described above or for disposal (returning it to the subsurface).

The oil is then sent to a treatment plant for processing in a gas-oil separation system, where its pressure is reduced in several stages. In each decompression stage, the associated gas (also called flash gas) is released in a separator until the pressure is ultimately reduced to slightly above atmospheric pressure. The crude oil is then sent to a stabilizer column where it is heated and cascaded through a series of bubble trays spaced throughout the column. Hydrogen sulfide (if present) and any remaining light hydrocarbon boil-off from this process is collected at the top of the column, while the sweetened heavy crude is drawn off from the bottom. The stabilized oil is then cooled and stored. The streams collected from the top of the stabilizer unit are treated in accordance with environmental regulations.

Natural gas wells do not produce oil, but usually do produce some number of liquid hydrocarbons, which are called condensate. Natural gas liquids (ethane, propane, butane) are removed at a gas processing plant, along with other impurities, such as hydrogen sulfide and carbon dioxide. Natural gas liquids often have significant value as petrochemical feedstock. Also, natural gas wells often produce water, but the volumes are much lower than typically found in oil wells.

### Map of U.S. Interstate and Intrastate Natural Gas Pipelines

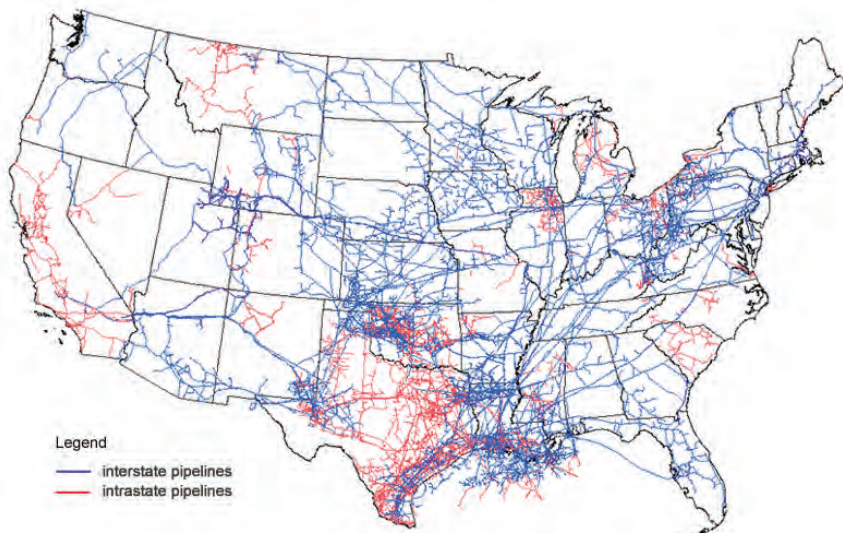


**Figure 8-4.** U.S. Transmission Pipeline Network.

Natural gas is usually transported through pipelines (Figure 8-4), except in cases where a pipeline cannot be economically built. In that case, the gas can be liquefied (LNG: Liquefied Natural Gas) and transported on a ship. As part of the transportation process in pipelines, gas can be placed in storage facilities, which often use former gas fields or salt

- A - Salt Caverns
- B - Mines
- C - Aquifers
- D - Depleted reservoirs
- E - Hard-rock caverns

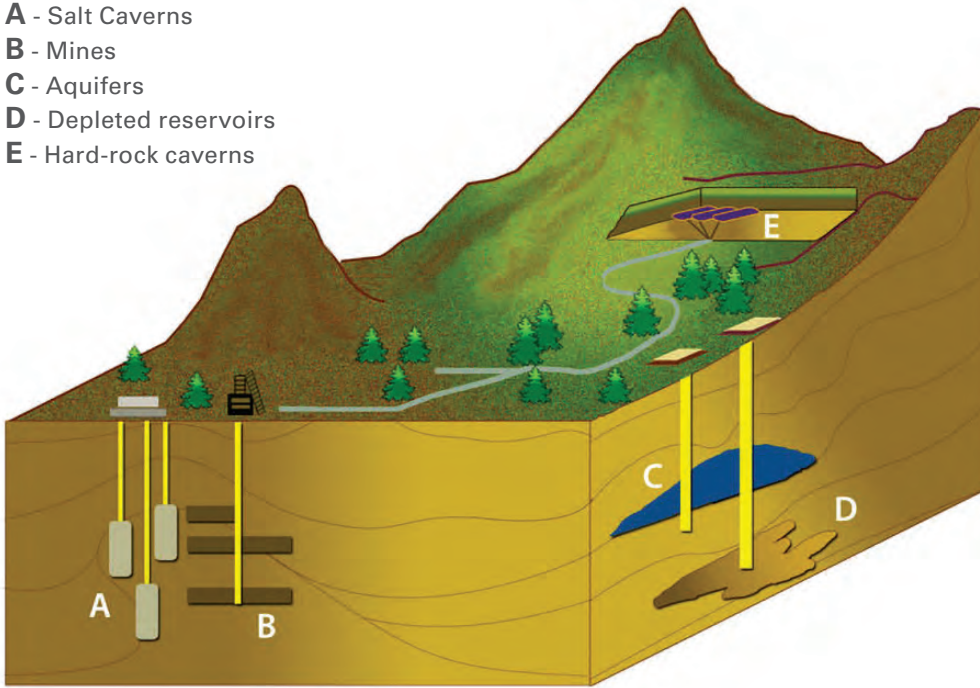


**Figure 8-5. Gas Storage**

caverns. This helps balance differences in supply and demand on a seasonal or daily basis (Figure 8-5).

Usually, all applications upstream, including a gas plant, are considered ‘upstream’ applications, while the applications related to bringing gas to the ultimate users are referred to as ‘midstream.’ Applications in refineries, chemical and processing plants are considered ‘downstream’ applications [1].

## TYPICAL GASES

Gas which has to be compressed usually consists of mixtures of light hydrocarbons (alkanes), nitrogen and carbon dioxide. In many applications, especially midstream pipeline and storage applications and in many upstream applications, the dominant component is methane. Often, especially in upstream applications near the well, the gas is saturated with water. Hydrogen sulfide may be present, and the gas may also have significant CO<sub>2</sub> levels. In refrigeration applications, heavier hydrocarbons may have to be compressed. The conversion of process variables (temperature, pressure, flow, gas composition) into variables relevant for the compressor (enthalpy, entropy, density) is performed using equations of state (EOS). Frequently applied EOS include Redlich-Kwong, Redlich-Kwong-Soave, Peng-Robinson, Lee-Kesler-Plocker, the Starling version of the Benedict-Webb-Rubin model, and the AGA 8 adaptation in ISO20765-1 [1,2,3].

Natural gas containing significant amounts of H<sub>2</sub>S and CO<sub>2</sub> is usually referred to as sour

gas (as opposed to sweet gas). A number of gas fields produce sour gas and, in many instances, the removal of  $H_2S$  and  $CO_2$  is part of the gas plant operation (see above). In some instances, sour gas is compressed untreated, in particular when it is used in gas re-injection applications [1]. In particular, higher levels of  $H_2S$  can lead to sulfide stress cracking of materials in an aqueous environment. Carbon dioxide alone is inert and not corrosive. It has, however, a high affinity for water, and when combined, forms carbonic acid, which corrodes carbon steel. In the presence of liquid water,  $H_2S$  and  $CO_2$  form corrosive acids, and one of the issues when compressing sour gas into the dense phase region is that water can drop out if the temperature is lowered. NACE MR0175 provides information on requirements and recommendations for the selection and qualification of carbon and low-alloy steels, corrosion-resistant alloys, and other alloys for service equipment used in oil and natural gas production and treatment plants. In environments containing  $H_2S$ , failures could pose a risk to plant personnel, the health and safety of the public, as well as the environment. NACE MR0175 also defines limits for  $H_2S$  partial pressure in the gas, depending on the pH value of the environment, beyond which special material considerations apply. The high toxicity of  $H_2S$  also requires specific attention to avoid and detect leakages [1].

## APPLICATIONS<sup>1</sup>

### *Upstream Reservoirs*

All oil and gas reservoirs produce hydrocarbon mixtures, albeit at different mole weights. Many oil reservoirs also produce gas (associated gas), and many gas reservoirs also produce heavier hydrocarbons, called condensates. Oil reservoirs can be classified in one of five ways. The distinction is primarily made by the mechanism that drives the oil from the reservoir to the well.

1. Undersaturated reservoirs tend to exhibit a rapidly declining reservoir pressure, and they produce very little, or no gas.
2. Undersaturated, solution-drive reservoirs also have a fast pressure decline, but produce gas. The produced gas-to-oil ratio is initially low, rises to a maximum, and then declines again.
3. Gas-cap drive reservoirs have pressure that tends to fall relatively slowly with a continuously rising produced gas-to-oil ratio.
4. Water drive reservoirs tend to maintain a high reservoir pressure and produce little gas.
5. Combinations of the above mechanisms.

All oil reservoirs only produce a fraction of the oil contained in the formation, even with enhanced recovery method such as water flooding) and steam or gas injection. Gas injection uses produced natural gas or a miscible gas such as  $CO_2$  [1].

<sup>1</sup>An effort has been made to use the most common industry definitions. However, some of the definitions are used interchangeably, and some applications might be combined in a single compressor or compressor train.

Gas reservoirs generally contain no oil, but produce gas or gas with varying amounts of condensates and/or water. Typically, primary recovery methods are sufficient for porous rock formations. Very tight formations (such as shale) require fracking to essentially increase the porosity. Dry gas reservoirs produce mostly methane and ethane, with minor amounts of heavier gases. The gas pressure in the reservoir pushes the gas to the surface. Typically, a choke is employed to control the flow rate. The gas pressure is reduced when the reservoir is producing. If the gas pressure required at the surface is at 500 psi (for example, to be fed into a pipeline), the reservoir flows gas until the reservoir pressure can no longer overcome this pressure. At that point, compression is necessary to further produce gas. Typically, production is continuous until the pressure at the well head drops below 70 to 100 psi (5 to 7 bar).

Condensate reservoirs contain larger amounts of heavier hydrocarbons, such as propane, butane and pentanes. They can exist as either a gas or a liquid, depending on pressure and temperature.

## OIL PRODUCTION OR WHAT TO DO WITH THE GAS?

Natural gas is often a by-product of oil production. Since the primary goal is producing oil, the question becomes: what to do with the gas? The first step is always to separate the oil (and water) from the gas (*Figure 8-6*). This separation is often done at about 40 to 80 bar (600 to 1100 psi). The problem is that the separation process still leaves gas dissolved in the oil and water vapor in the gas. To deal with the former, the pressure of the oil is reduced in one or more steps. At each step, the pressure reduction leads gas to flash from the liquid. The lower the pressure becomes, the heavier this flash gas becomes. It must be recompressed, usually to about the same pressure as the gas leaving the production separator. The gas can now be used in different ways (*Figures 8-7, 8-8 and 8-9*):

- Gas Lift
- Gas Reinjection
- Gas Export

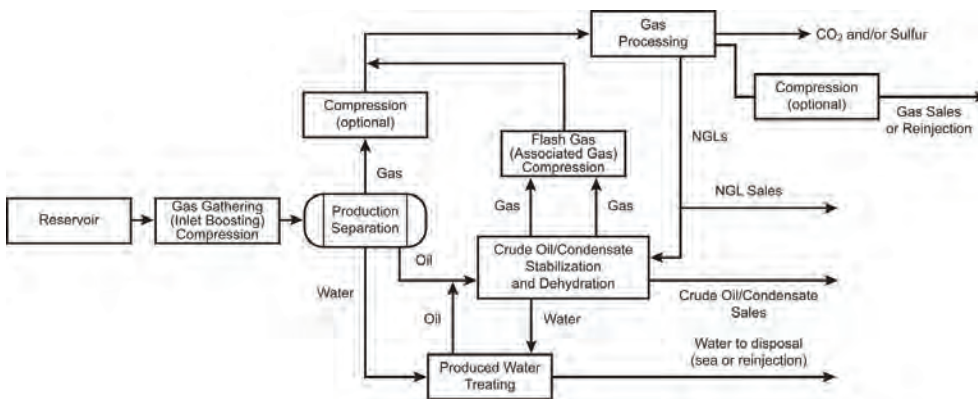


**Figure 8-6.** Oil and gas field production steps. Associated gas is found and produced along with oil. Non-associated gas is natural gas that is not in contact with or dissolved in oil.

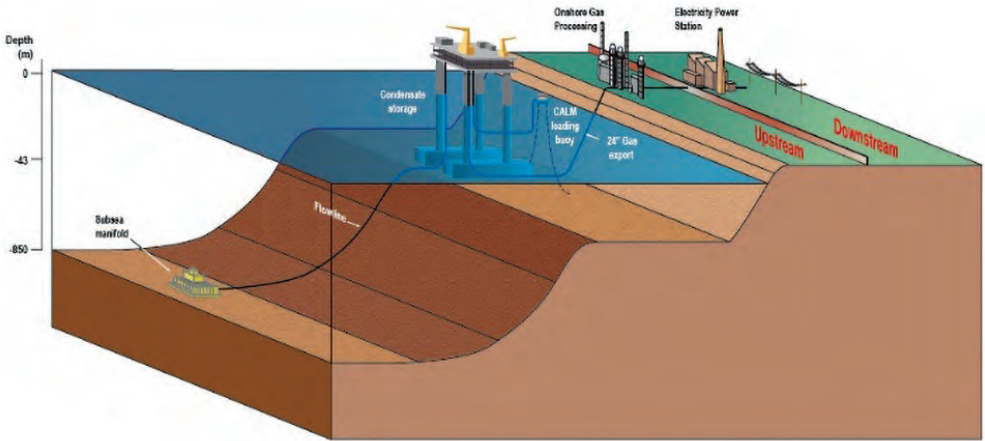


**Figure 8-7.** Offshore platform with depletion compression (gas-reinjection), condensate stabilization (flash gas compression), export compression to onshore gas plant via subsea export pipeline.

Gas lift (Figure 8-10) is a method of increasing oil flow by injecting gas into the well that aerates the crude, thereby enhancing the flow of crude to the surface. Some operators use the same compressor train to both feed a gas lift service and export compression to feed gas into a pipeline. Gas lift is a process in which produced gas is compressed to a higher pressure and recycled down the well casing through gas lift valves into the tubing at a predetermined depth to lighten the column of liquid in the tubing. This reduces the difference between the downhole pressure and the pressure at the well head. Compressor discharge pressures are typically 100 to 120 bar (1400-1700 psi), but sometimes up to 200 bar (2900 psi) may be required for such applications, necessitating compressors with relatively high throughput and a high compression ratio.

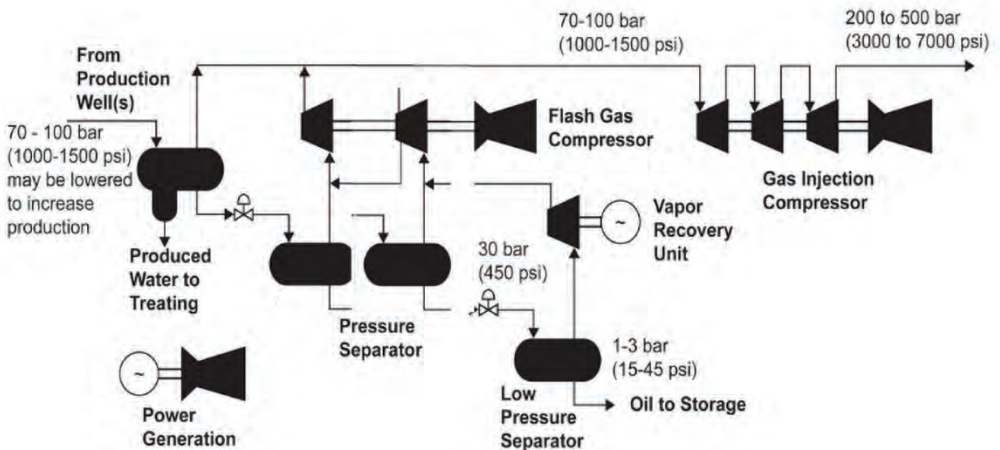


**Figure 8-8.** Combination of flash gas compression and gas reinjection.

Reinjection (*Figures 8-9 and 8-10*) is a method of enhancing oil recovery by compensating for the natural decline of an oil field's production by increasing the pressure in the reservoir. The desired production is restored by stimulating the recovery of additional crude oil. Using this technique, the field exploitation can be increased by up to 20%. The gas that is reinjected is usually the associated gas separated from the crude oil during the flash and stabilization phases. Other gases, such as nitrogen or carbon dioxide, may also be used. The gas is reinjected into the reservoir in dedicated wells, and the oil is forced to migrate toward the well bores of the producing wells. Gas-injection projects may also involve the injection of CO<sub>2</sub> or nitrogen into the reservoir. Especially for deep reservoirs, very high compressor discharge pressures 140 to 820 bar (2000 to 12,000 psi) are required. Due to the high aerodynamic forces the gas can exert on the rotors, these compressors are challenging from a rotordynamic standpoint. Recent advances in material technology enable associated sour gases containing high percentages of H<sub>2</sub>S and/or CO<sub>2</sub> to be re-injected without the need for sweetening. Depending on the depth and physical characteristics of the field, very high injection pressures may be required. High-pressure barrel compressors are normally used in this application [1].



**Figure 8-9.** Flash gas compression and reinjection.

## Gas Lift System

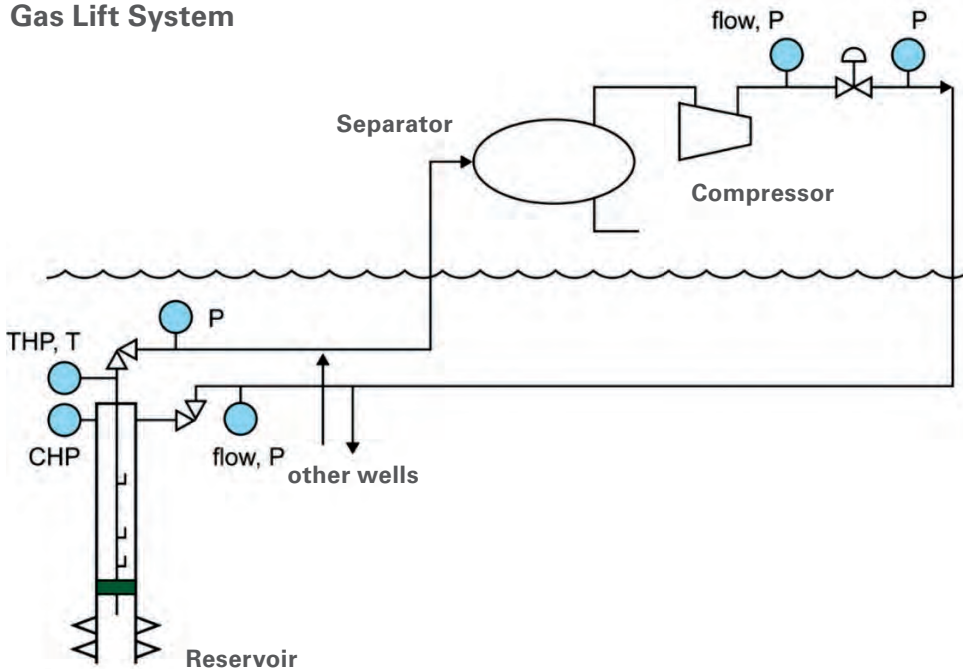


**Figure 8-10.** Schematic illustrates the typical gas-lift system.

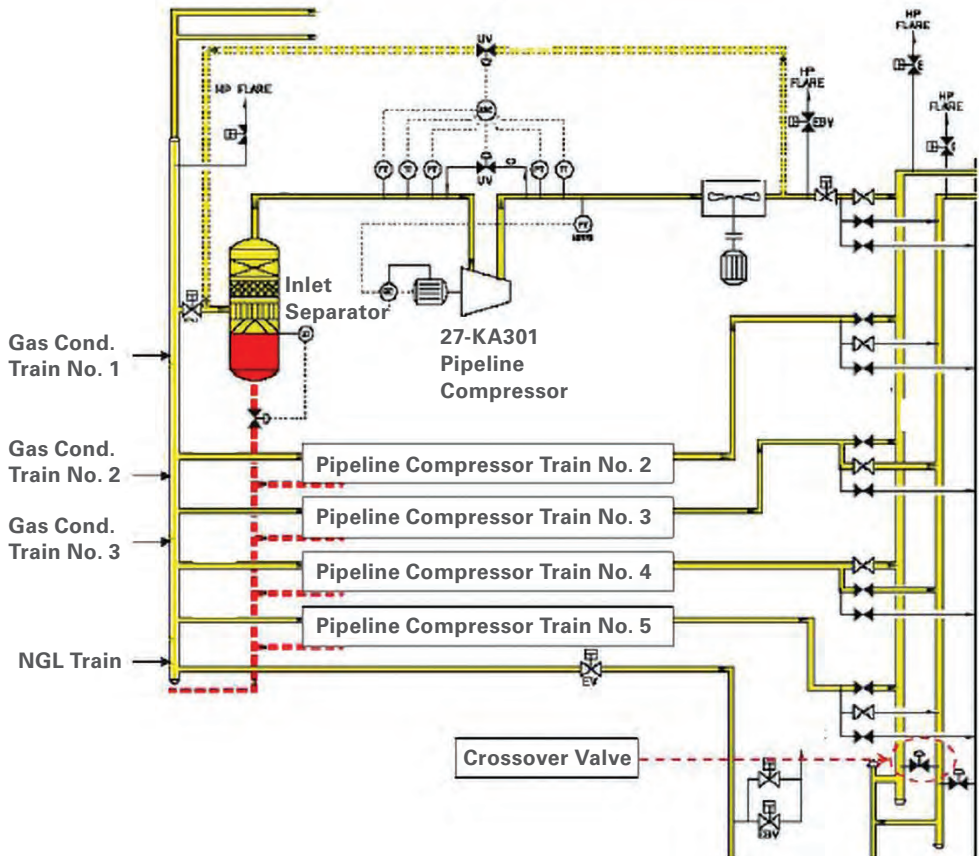


**Figure 8-11.** Illustration of sales gas export compression from an offshore platform.

If the platform or the oil field is located reasonably close to a potential consumer of the gas, it may be exported via a pipeline. Export gas is compressed to feed a subsea pipeline (an offshore platform) that transports the gas to shore. Discharge pressures are often high, typically 70 to 140 bar (1000 to 2000 psi), but sometimes as high as 200 to 240 bar (3000 to 3500 psi) to reduce pipe diameter, and also because the gas usually cannot be recompressed between the platform and the shore (Figure 8-11). Depending on whether this compressor receives gas at well pressure, or whether there is a gas gathering train upstream, configurations can vary from machines with only a few stages to triple-body trains [1]. Export compressors are also used in gas fields for the same purpose.

Tradeoffs are often the required compression power on the platform versus the cost of the pipeline, especially if pressure is not dictated by already existing systems. In many applications, the gas contains significant amounts of heavier hydrocarbons, and a concern is the formation of liquid slugs in the flow line, where dropping gas temperatures may then lead to harmful condensation.

In all the aforementioned applications, the water that stayed in the gas as a vapor can cause problems, since at high pressures and low temperatures, the water either can drop out as a liquid, thus creating corrosion problems, or form hydrates, which may clog flow lines. The task therefore becomes removal of water vapor in a dehydration unit (Figure 8-12) or avoiding hydrate formation and/or corrosion.

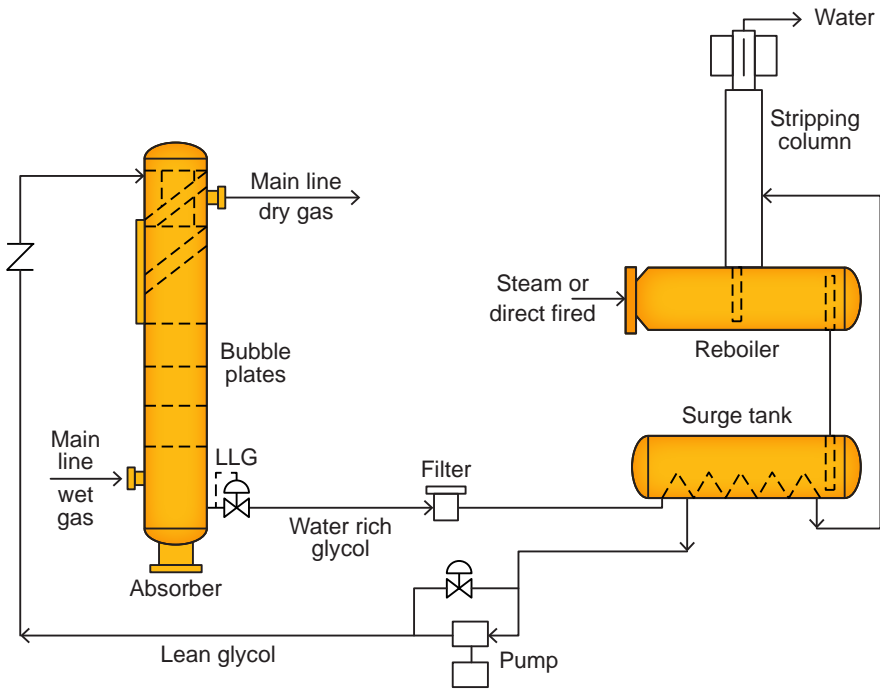


**Figure 8-12.** Water must be removed to avoid hydrate formation and/or corrosion.

Dehydration units are designed to absorb water vapor by using liquids like Triethylenglycol (TEG). The liquid can then be separated, and the absorbed water can be removed from the TEG by heating.

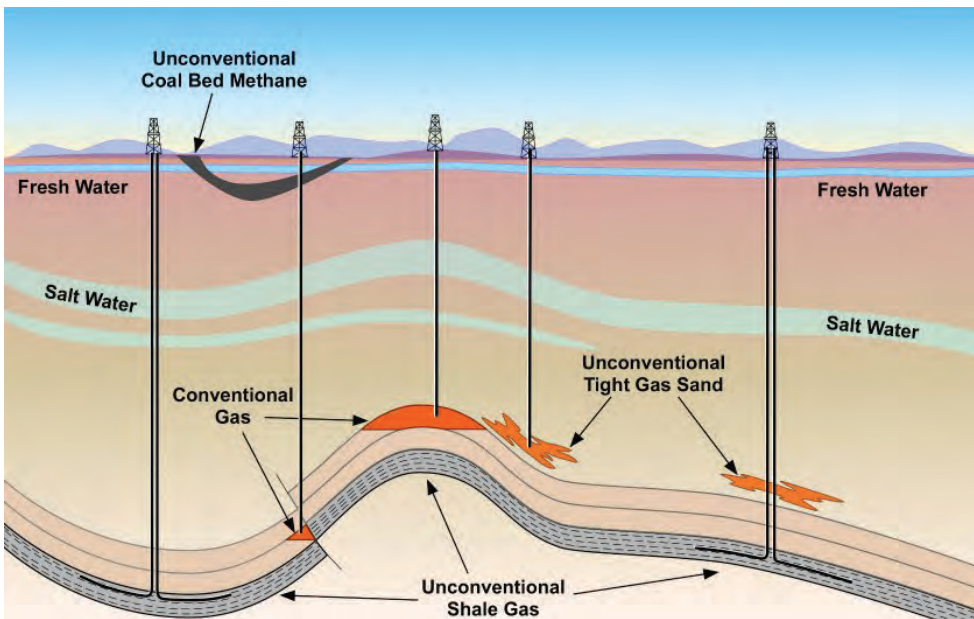


**Figure 8-13.** Different gas reservoirs may be present at several locations having differing compositions and multiple depths.

## Pressure Plot

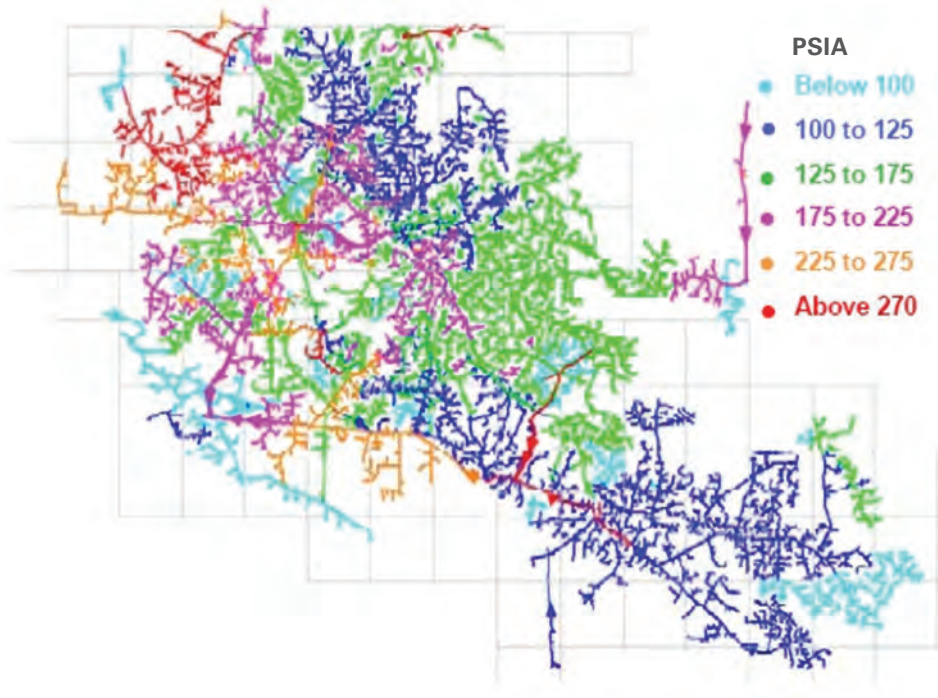


**Figure 8-14.** Gas field with a sprawling network of low-pressure pipes.

### GAS FIELD

Gas fields (*Figures 8-13 & 8-14*) produce gas of various compositions:

**Dry (Lean) Gas** - Water dry (no condensable water) gas with little or no heavier hydrocarbons that could be recovered as condensates.

**Condensate** - Heavier hydrocarbons in a gas field that form liquids by precipitation (mostly pentane and heavier hydrocarbons).

**Wet Gas** - Contains condensable hydrocarbons.

As described earlier, for many gas formations, the well head pressure drops (*Field pressure in Figure 8-15*) relatively fast, and, in order to produce a large fraction of the gas in the field, additional wells have to be drilled, and gas gathering compression has to be applied [1]. This compression duty sees low suction pressure (3 to 15 bar), and has to bring the gas pressure to about 80 to 100 bar. The compressors must be able to handle the fact that both the gas flow and the suction pressure will decline over time, while the discharge pressure stays relatively constant. Pressure ratios are high, so intercooling between compressor bodies is important (*Figure 8-16*). Depending on the rate of field decline, compressors are either sized for the final pressure conditions, or compressors are restaged. The approach with two or three individual compressor bodies has the advantage that the train can be optimized for the lower pressure ratio and higher flow during the early life of the field,

## Example Shale Gas Field Production vs Pressure Curve

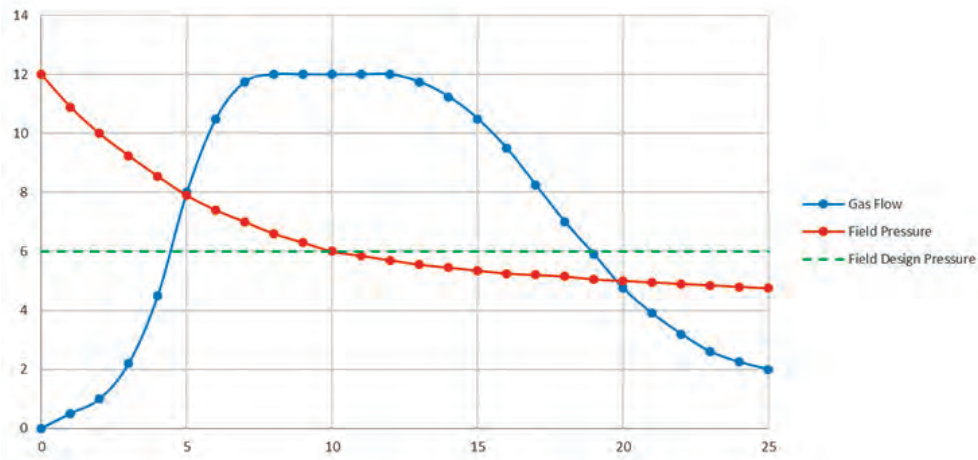


**Figure 8-15.** Well production profile.

using a single compressor body. An additional body can be added to optimize for the high pressure ratio and low flow in later years (Figure 8-17).

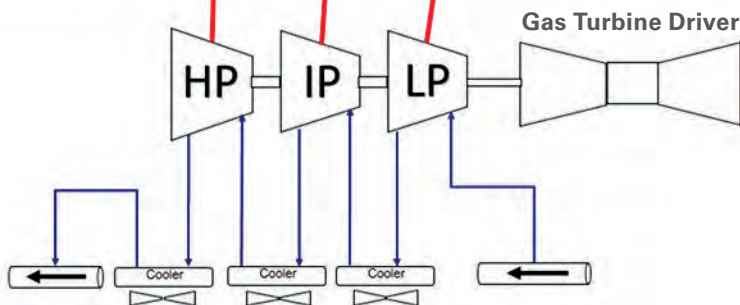
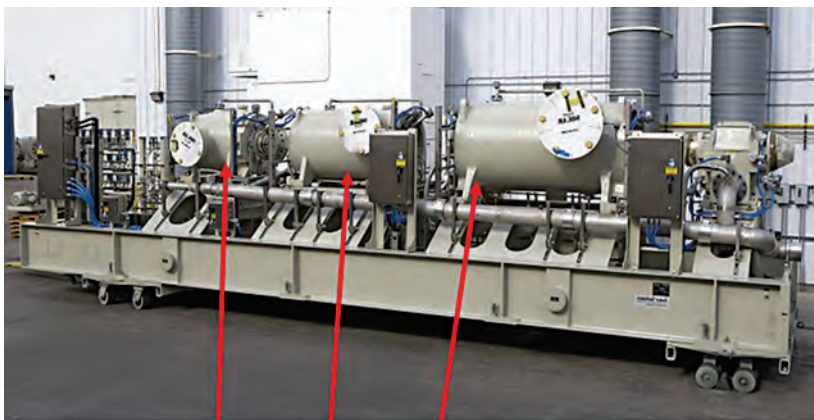


**Figure 8-16.** Gas gathering compressor train.

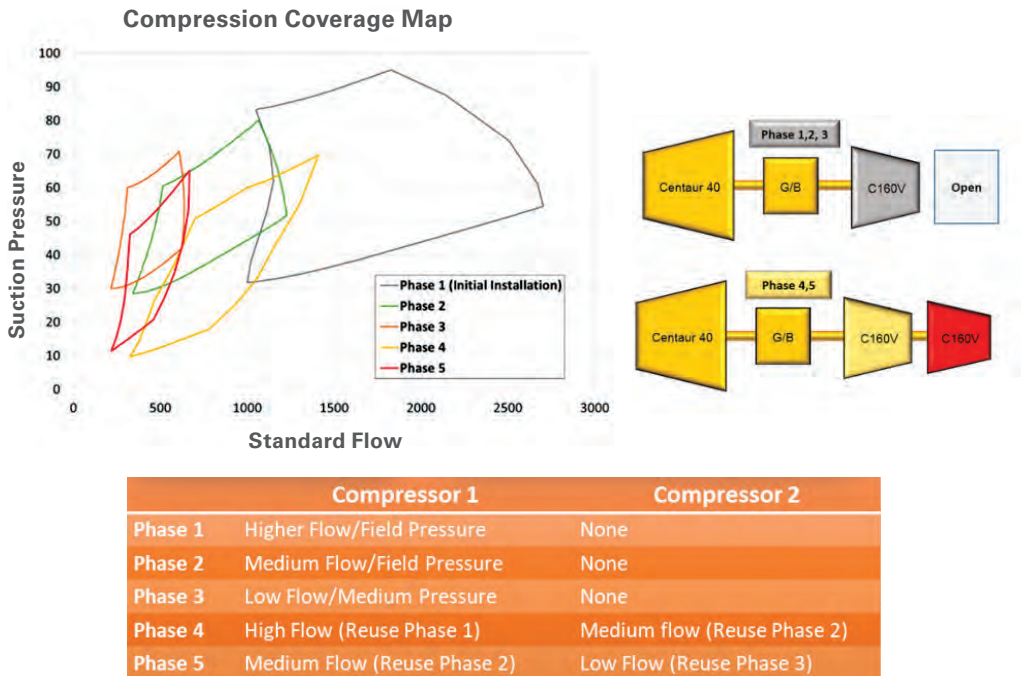


**Figure 8-17.** Illustration of declining gas field production over the course of several years and five phases.

The discussion on wet gas compression (i.e. compressing gas that carries liquids) has drawn significant attention. Predicting compressor performance becomes difficult, because a two-phase mixture at the inlet, and possibly at the compressor discharge requires consideration of evaporation effects and the resulting changes in flow and temperature in the compressor (Figure 8-18). The possibility of liquid slugs also creates risks for the machine, due to transient thrust loads or erosion from large droplets.

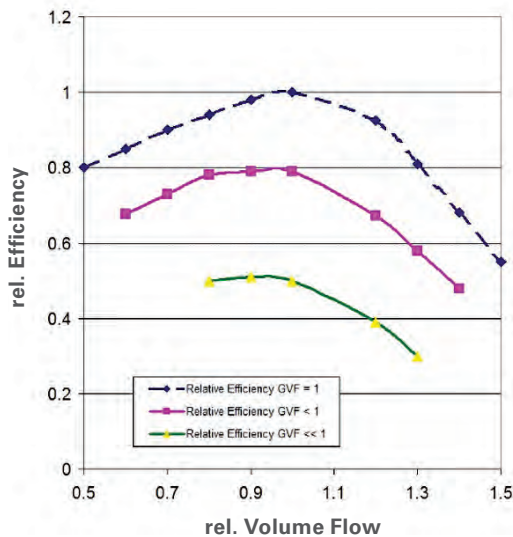


**Figure 8-18.** Compressor efficiency for different gas volume fractions (GVF) [1].

## GAS PLANT COMPRESSION

Gas plants (Figure 8-19) are designed to produce dry export gas (i.e. gas with very little water, a low hydrocarbon dewpoint, limited amounts of CO<sub>2</sub> and other contaminants) and LPG products (Ethane, Propane and Butane). For the range of gas compositions at the inlet, the plants have specified recovery targets for the heavier hydrocarbons. The process steps inside the plant include:

1. Primary separation
2. Frontend compression (boost compression, inlet compression)
3. CO<sub>2</sub> removal
4. Mercury/chloride removal
5. Gas dehydration
6. Gas expansion (turboexpander)
7. LPG/condensate fractionation
8. Dry (sales) gas compression
9. Storage and utility distribution.

In a gas plant, three compression functions must be facilitated:

1. Boost compression (inlet compression) to bring the gas from delivery pressure (from the gas gathering system) to plant pressure.

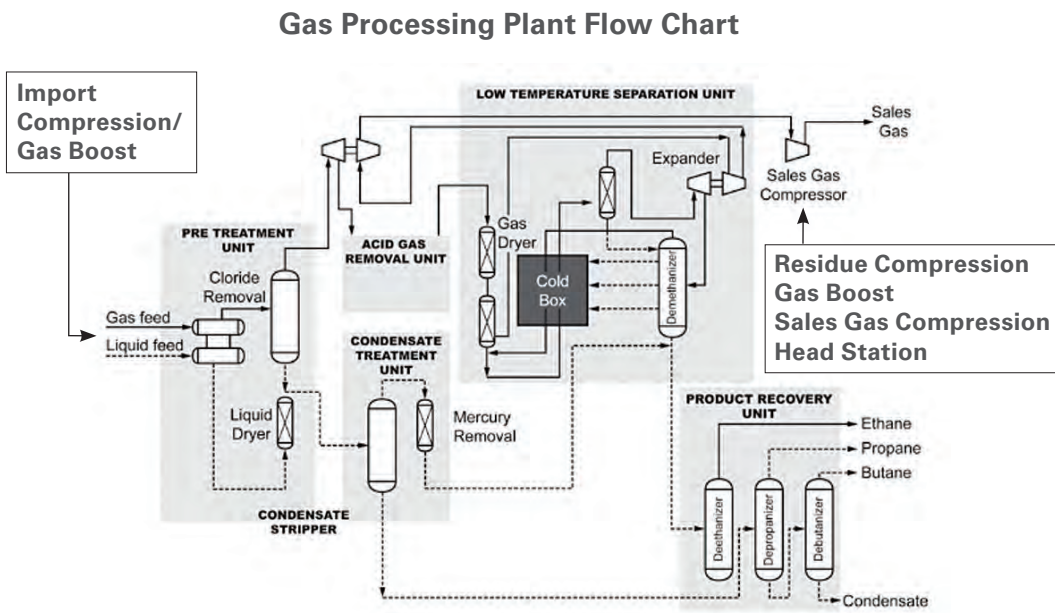
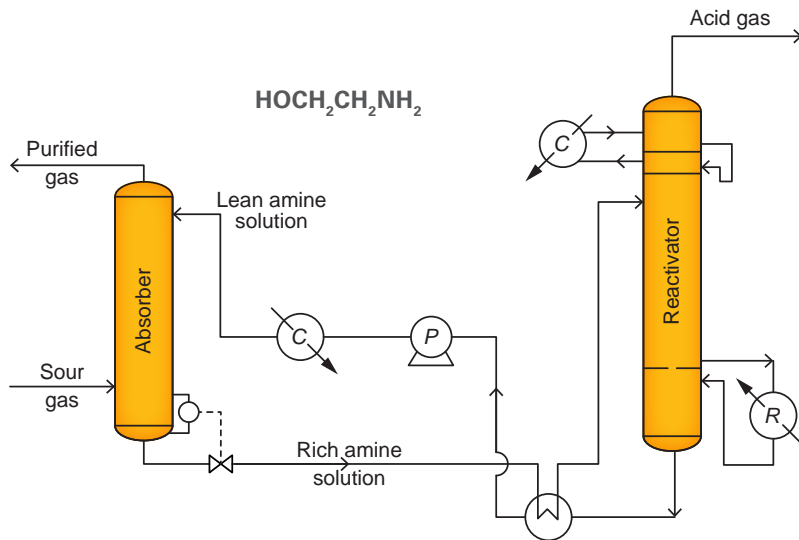


Figure 8-19. Typical gas plant schematic.



**Figure 8-20.** Amine process for  $\text{CO}_2$  and  $\text{H}_2\text{S}$  removal (using mono-ethanolamine  $\text{HOCH}_2\text{CH}_2\text{NH}_2$ ).

2. Recompression (sales gas compressor) to bring the natural gas from plant pressure to pipeline pressure, with a suction pressure of 15 to 30 bar (200 to 400 psi), and a discharge pressure of about 70 to 100 bar (1000 to 1500 psi) (depending on the pipeline). This function may also be referred to as pipeline head station (essentially depending on whether the compressor is operated by the gas plant or the pipeline operator).
3. Turbo expander/compressor for the low-temperature cryogenic cycle.

For the removal of  $\text{CO}_2$  in a gas plant typically either amine processes or membranes are used (Figure 8-20).

The necessary removal of  $\text{CO}_2$  is performed in an absorber, where a liquid amine solution is sprayed in the gas column, and absorbs the  $\text{CO}_2$ . The rich amine solution can then be heated, thus separating the amine from the  $\text{CO}_2$ . In many instances, the exhaust heat from a gas turbine can be used as a heat source for this process. After the heating in the reactivator, the amine can be reused.

## 2.2 MIDSTREAM

Compared to rail or trucks, pipelines provide a very cost-efficient method for transporting energy over long distances. However, gas flowing through a pipeline is subject to pressure losses that increase with flow velocity and the length of the pipe. Every 50 to 100 miles, a compressor station (Figure 8-21) is necessary to recompress the gas and compensate for the pressure losses. In general, operation as close as possible to the maximum operating pressure of the pipeline reduces power requirements for the compressors, and thus fuel consumption (Figure 8-22). Therefore, the distance from station to station is subject to careful optimization [1,2,4]: The closer the stations are spaced, the lower the pressure

ratio per station, as well as the overall pipeline power consumption. On the other hand, the capital expenditures to build the pipeline increase.

Optimal pipeline pressures—depending on the length of the pipe, as well as the cost of steel—are in the range of 40 to 160 bar (600 psi to 2200 psi) balancing the amount of power required to pump the gas with the investment in pipe. Today, most interstate and intercontinental pipeline systems operate at pressures

between 60 to 100 bar (1000 and 1500 psi), although operating pressures for older systems might be lower. The pipeline compressors are placed at regular intervals along the pipeline, usually spaced for pressure ratios between 1.2 and 1.8. Besides geographic necessities, the distance between compressor stations is usually determined by an optimization for CAPEX and OPEX, which establish the best pipeline diameter, number of stations and the station pressure ratios (*Figure 8-23*).

Pressure ratios higher than normal are found if pipelines operate in remote areas, or at subsea levels. Some pipelines transport gas over long distances, without significant gas takeoffs along the way and relatively constant operating conditions. Other pipelines form part of an intricate network with a variety of feeders and takeoffs along the line. In these networks, you'll often find compressor stations with a variety of sizes, capacities and compressor types.

Large daily and even hourly fluctuations can have a significant impact on pipeline system operating conditions. For any type of pipeline, the driver power and its dependency on ambient conditions play major roles in planning station layouts and system operation.

The gas usually has to be compressed to pipeline pressure at a head station (usually coming from a gas plant). This head station often sees pressure ratios of 3 or more.

Subsea pipelines often have only a head station (commonly referred to as export compression), but no stations along the line. They are either used to transport gas to shore from an offshore platform (see export compression), or to transport gas through large bodies of water. In either case, relatively high pressures (100 to 250 bar, 1500 to 3700 psi) are common [4].

A few onshore pipelines worldwide make use of the added compressibility of the gas at pressures above 140 bar (2000 psi, depending on gas composition) and operate as 'dense-phase' pipelines at pressures between 125 and 180 bar (1800 and 2500 psi). Not only natural gas is transported in pipelines, but also CO<sub>2</sub>. CO<sub>2</sub> is non-corrosive, as long as it is dehydrated. Most applications transport CO<sub>2</sub> in its dense phase, at pressures above 140 bar (2000 psi), in particular to avoid two-phase flows when ambient temperatures drop.



**Figure 8-21.** Pipeline compressor station with three compressor trains in parallel.

The gas pressure in a pipeline is reduced due to friction losses. They depend on the flow velocity of the gas in the pipe. The compressors at each compressor station take the gas from arrival pressure, and recompress (or boost) it back to the pipeline operating pressure. For a given pipeline, this means that the more gas goes through the pipeline, the higher the pressure ratio at the compressor station becomes. Many pipelines operate under constantly changing operating conditions, so that a steady operation is rare. Therefore, the true operating conditions at a compressor station require compressors having a wide operating range (*Figures 8-24 and 8-25*) [2].

If pipeline throughput has to be increased, three possible concepts can be utilized:

1. Building a parallel pipe (looping)
2. Adding power to the compressor station (i.e. adding one or more compressors to the station)
3. Or a combination of both.

If power is added to the station, the discharge pressure can be increased (assuming this is not already limited by the pipeline maximum operating pressure). The station will therefore operate at a higher pressure ratio. The added compressors can either be installed in parallel, or in series with the existing machines. If the pipeline is looped, the pressure ratio for the station typically is reduced, and the amount of gas that can be pumped with a given amount of power is increased. In either scenario, the existing machines may have to be restaged (for a higher pressure ratio and less flow per unit in the case of added power, or more flow and lower pressure ratio in the other case).

### Pressure/Flow Profile

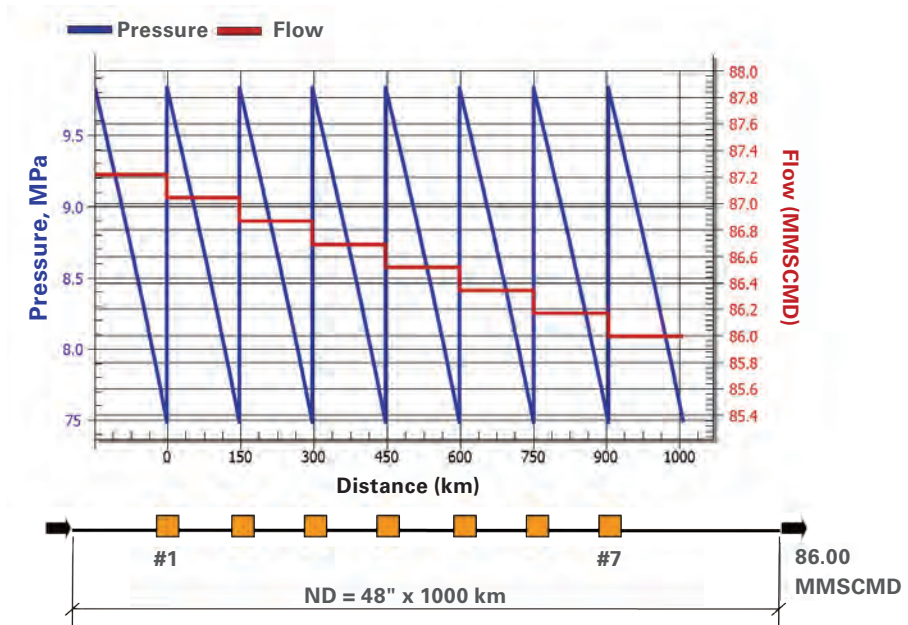


**Figure 8-22.** Graphic representation of pipeline pressure and flow.

**Present Value**  
1500 PSIA MAOP - 500 MMSCFD

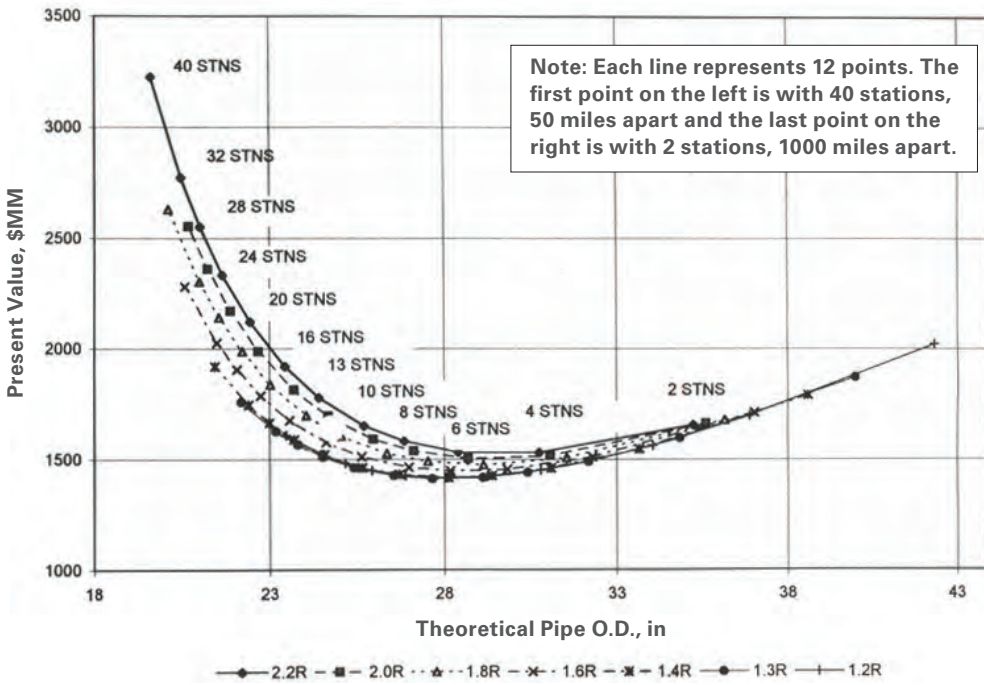


Figure 8-23. Pipeline design considerations are influenced by distance between stations [4].

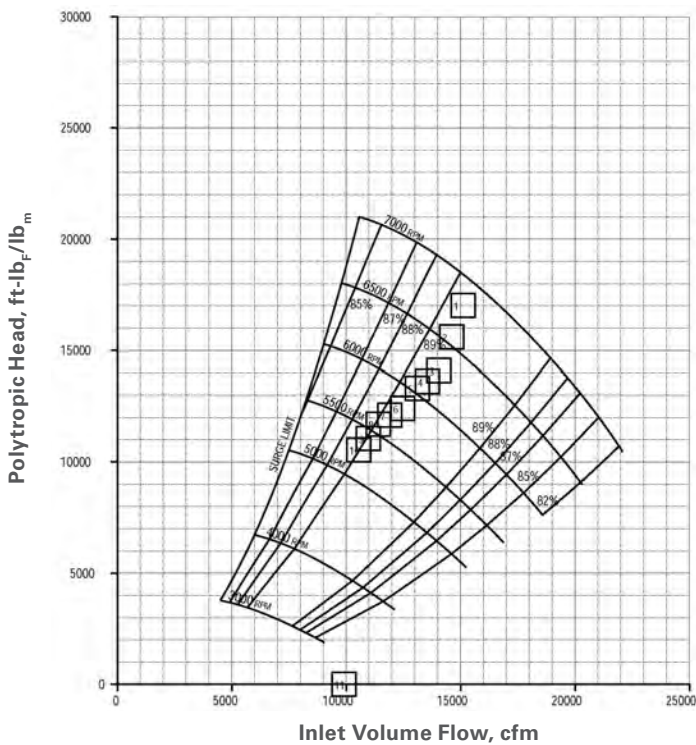


Figure 8-24. Steady-state pipeline operating conditions

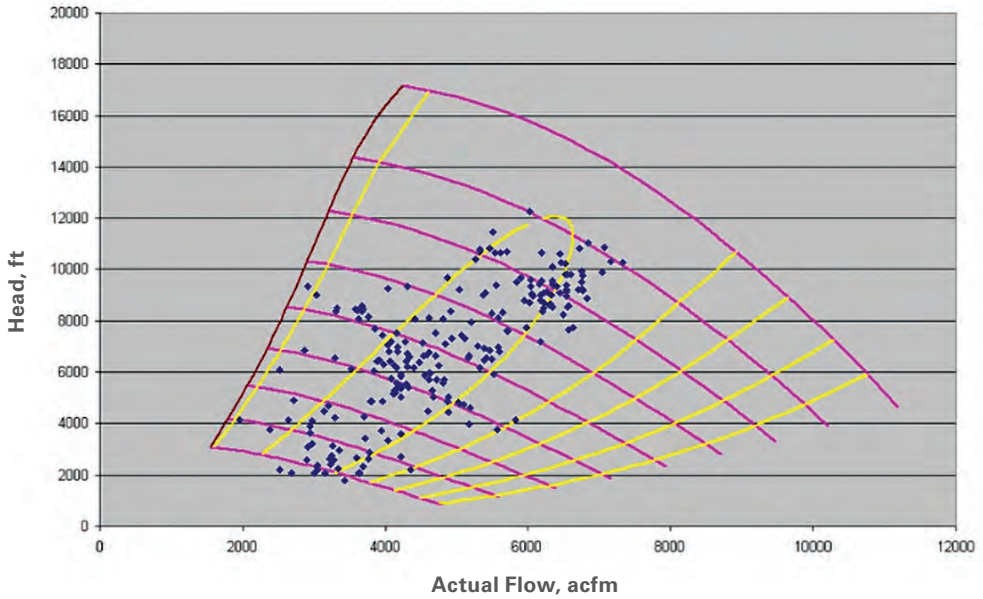
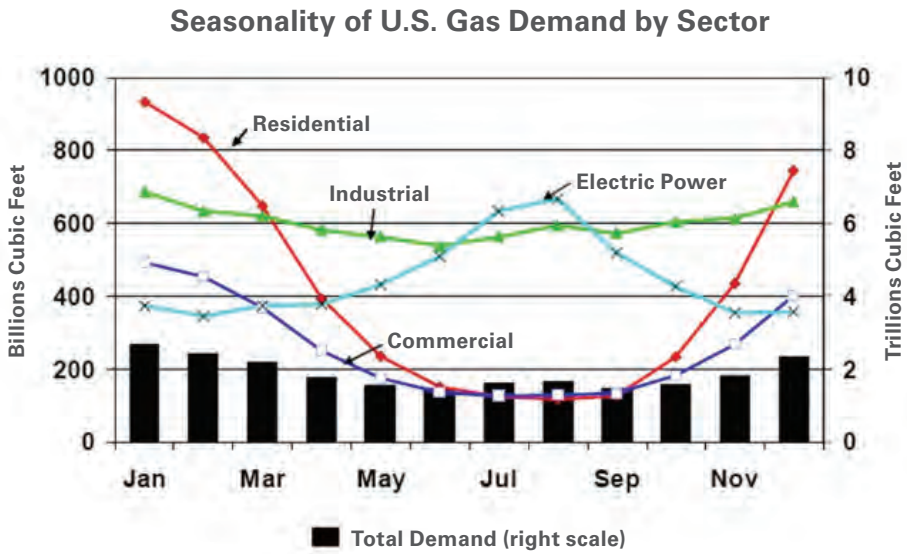


Figure 8-25. Upstream and midstream: the myth of the design point.



Based on latest 3-year averages; "Other" demand included in Total  
 Source: EIA Annual Energy Review 2005

Figure 8-26. Seasonal changes in U.S. gas demand and the corresponding need for gas storage.

## GAS STORAGE

The need for natural gas storage facilities dates back to the early 20<sup>th</sup> century in the US and Canada. These local-regional storage facilities assure natural gas supply during the winter heating season. This became necessary because the high winter demand frequently exceeded the capacity of the local pipeline and production infrastructure (*Figures 8-5 & 8-26*). The introduction of a gas spot market in the mid-80s also contributed to an increased demand for gas storage facilities. Currently, more than 400 storage facilities in North America and over 130 in Europe are in operation. The vast majority of these gas storage facilities use depleted hydrocarbon reservoirs, aquifers or salt caverns for storage. The former two options involve storage in porous rock layers, while the latter is created by washing a cavity out of a salt dome. These types of storage facilities are very safe, reliably preventing leaks or other safety hazards. In either case, the gas company injects natural gas into the storage field when demand is low and withdraws it from the storage field during times of high demand [1].

Historically, storage was used to respond to the peak demands on the coldest winter days. Natural gas demand used to be at its highest during winter, primarily due to home heating requirements (Figure 8-26). In recent years, however, mostly due to increased demand from natural gas fired power plants, demand has become less seasonal. Because of this shift, well-placed natural gas storage has become even more important to natural gas operations.

Today, North American natural gas storage plays a key role in balancing supply and demand, particularly consumption during peak-demand periods. Storage can reduce the need for both swing natural gas production deliverability and pipeline capacity by allowing production and pipeline throughput to remain relatively constant. Customers may use storage to reduce pipeline demand charges, to hedge against natural gas price increases or to arbitrage gas price differences. Pipelines and local distributors use storage for operational reliability and flexibility, providing an outlet for unconsumed gas supplies or a source of gas to meet unexpected demand.

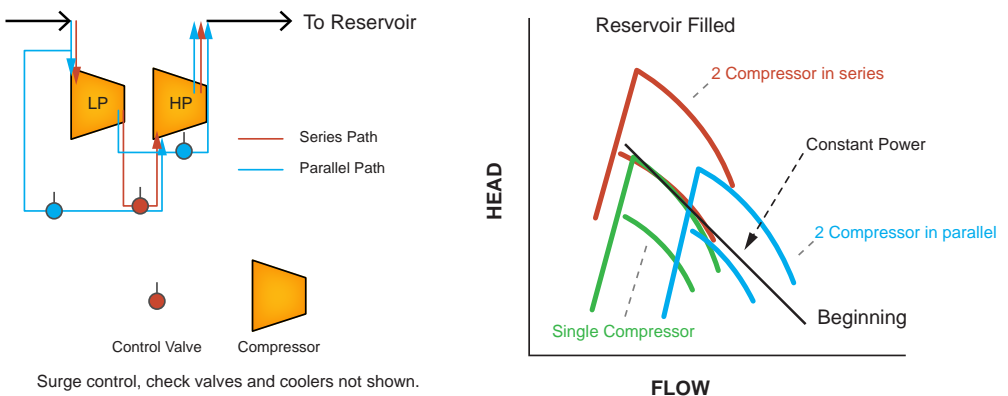
Storage at market trading hubs often provides balancing, parking and loan services. In the future, additional conventional storage will be needed to meet growing seasonal demands, and high deliverability storage will be required to serve fluctuating daily and hourly power plant loads. Gas supply and demand in many pipeline systems shows significant seasonal changes, which is further aggravated by the periodic influx of liquefied natural gas. Gas storage facilities, where gas is stored during times of low demand or high supply, and removed during times of high demand or reduced supply are an important means of managing the gas supply.

Gas compressors are required to inject gas from a pipeline into the underground for storage, and to extract gas from storage and feed it into the pipeline. Typical pipeline pressures range from 40 to 100 bar (600 to 1500 psi), and from this pressure, the gas has to be compressed to final storage pressure, typically between 100 and 200 bar (1500 and 3000 psi). The compressor duty is cyclical in nature. Traditionally, the cycles were seasonal,

with fluctuating pipeline and storage pressures gradually changing during the course of each season. However, based on spot-market fluctuations, daily demand cycles, market conditions, and/or short-term weather patterns, a facility may be required to change its operating patterns several times a day.

Gas compression is required to fill the storage facility, as well as recompress gas when the facility is emptied. The compression task is therefore described as filling a large, constant volume with gas. The limiting factor is the available driver power (*Figure 8-27*). The resulting operating conditions for the compressor are: initially, the low pressure ratio enables high flow conditions. The pressure ratio has to increase with an increasing amount of gas in the facility, therefore reducing the possible flow for a power-limited compression system (*Figure 8-27*). This can be efficiently accomplished with multiple compressors, capable of operating either in a series or a parallel configuration. The multiple compressors can either be driven by multiple drivers, or in a tandem configuration, by a common driver (*Figure 8-27*).

### Storage



### Reservoir Storage - Withdrawal Cycle

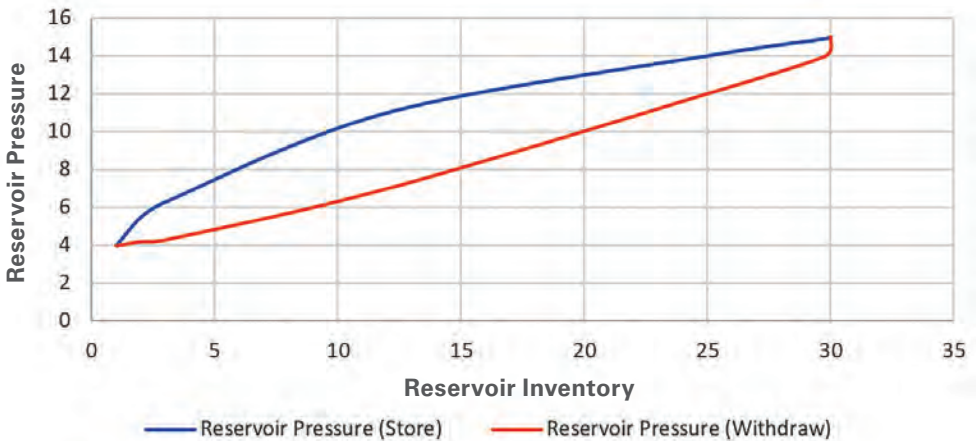
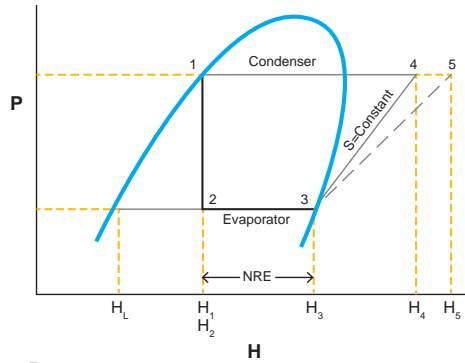


**Figure 8-27.** The gas compression functions required to operate a storage facility.

### 2.3 LNG

LNG is essentially large-scale refrigeration (Figure 8-28) to  $-160^{\circ}\text{C}$  ( $-260^{\circ}\text{F}$ ), which is the temperature required to liquefy natural gas. Although pipeline quality gas is used,  $\text{CO}_2$ , water and  $\text{H}_2\text{S}$  are removed for liquefaction. LNG product is methane + some heavies (1000-1100 Btu/scf).

The volume reduction from gas to liquid = 600:1. The LNG process evolved from small-scale refrigeration compressors powered by steam turbines (1969 was first commercial LNG export by Conoco Phillips from Alaska). Modern plants are built in large-scale capacities of 4.4 to 8.8 MMTPY capacity with GT or EM driven centrifugal compressors. (5.0 MMTPY ~ 65 MW compression hp). As shown in Figures 8-29 and 8-30 [1,2], the entire LNG process must be viewed from wellhead to consumer, not just the simple LNG production plant.



**Processes:**

- 1 to 2 = Expansion
- 2 to 3 = Evaporation
- 3 to 4 = Ideal (Isentropic) Compression
- 3 to 5 = Actual Compression
- 5 to 1 = Condensing

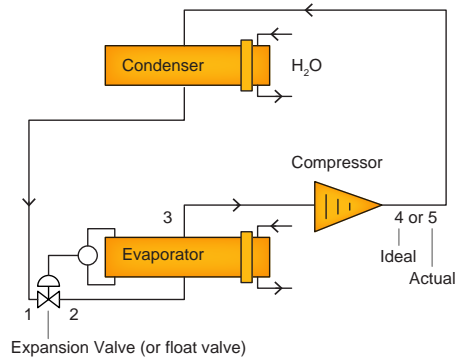
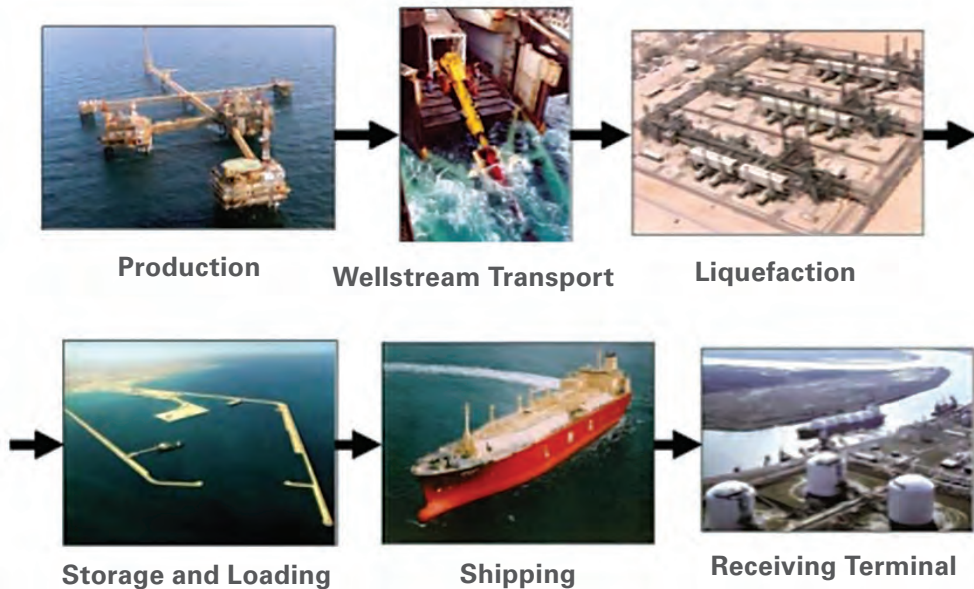
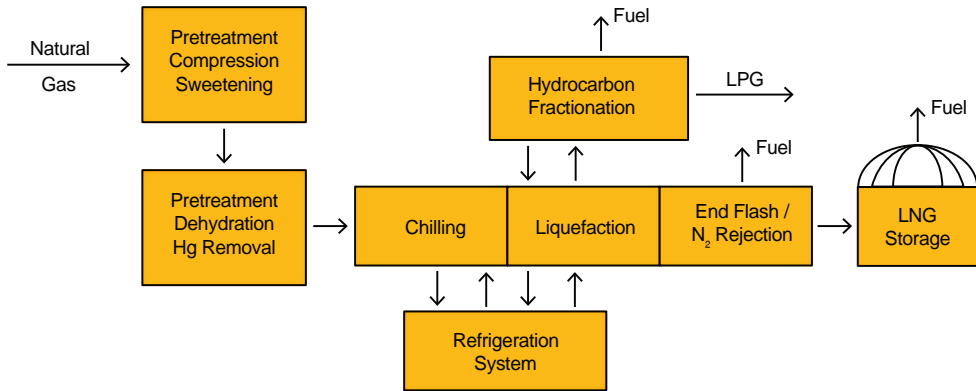


Figure 8-28. Basic refrigeration cycle.



(Courtesy ExxonMobil Corporation)

Figure 8-29. The complete LNG process from upstream to downstream.



**Several separate gas streams:**

- Natural Gas (to be liquefied)
- Refrigeration Gas(es)
- Fuel Gas

**Figure 8-30. LNG processing**

Specialized turbomachinery designs are required for large scale refrigeration cycles in LNG applications, pushing the envelope of the centrifugal compressor design flows, the cryogenic heat exchanger size and the horsepower rating of the refrigeration drives. Over the past 50 years, the refrigeration cycles and drivers have continuously evolved to meet the needs of ever larger LNG plants.

As the train size has leveled off and material costs continue to rise, many operators have “standardized” on two types of refrigeration cycles. These cycles effectively dictate compressor selection and horsepower requirements:

The APCI Split MR cycle (Split C3MR) requires two large industrial-frame turbines or synchronous electric motors in the 72-80 MW range.

The ConocoPhillips Optimized Cascade (CoP OC) cycle requires six, 30 MW-range gas turbines or electric motors.

Other refrigeration cycles may be closely or equally competitive in terms of efficiency, but difficult to justify given the risk of new technology qualification.

Figure 8-31 shows the mixed fluid cascade LNG cycle, and Figure 8-32 shows LNG cycle selections over the last 30 years.

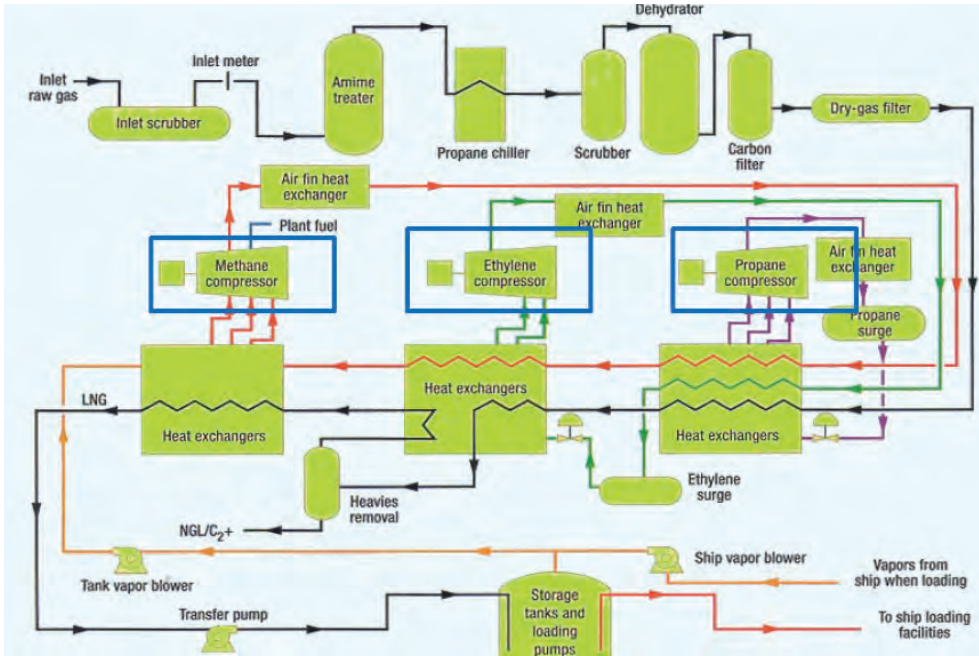


Figure 8-31. Mixed fluid cascade LNG process.

### LNG Refrigeration Cycle Selection

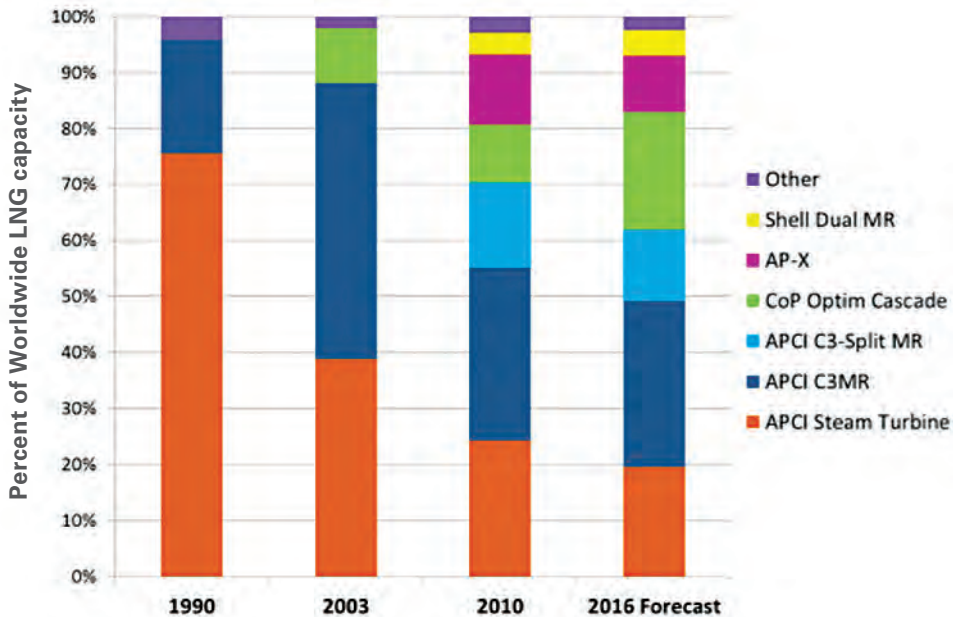


Figure 8-32. LNG refrigeration cycle selections.

True standardization will never be fully possible for LNG plants since each LNG facility must confront unique site development issues, electrical power options (or lack of), construction execution plans and the associated modularization strategy, and its own project economics.

## LNG TURBOMACHINERY

The evolution of LNG plants and the related turbomachinery can be divided into distinct time periods:

- 1. Steam Turbine Drive Era (1970-1989).** Early LNG improvements were mainly defined in terms of train capacity increases, gaining savings through economies of scale.
- 2. Gas Turbine Drive Development (1990-2009).** Efficiency gains and cycle improvements were characterized by new gas turbine validation and cycle innovations that pushed efficiency gains, as train capacities began to level off.
- 3. Recent (2010-current).** Higher capital costs and reliability concerns have dictated driver and cycle selection, resulting in more uniformity. Electric motor drive precedent has now been set, but still needs further development. A case for smaller train capacities has also driven users to install mid-size aero-derivative turbines instead of frame units. The modern era for LNG plants has just begun and will be determined by the next 20-year cycle.

The typical LNG process turbomachinery can be divided into three steps:

**Pre-cooling** - Propane compressor, typically largest flow rates and largest horsepower required. 60-70 MW for 4.5-5.5 Mmtpy. Pushes the limits of electric motor and variable-speed drives.

**Primary Liquefaction** - Ethylene or Mixed Refrigerant compressor may involve 2-4 stages of compression, 45-55 MW for 4.5-5.5 Mmtpy. Side streams typically used with interstage cooling. Use of more stages can help plant flexibility.

**Sub-cooling and Plant Fuel Compression** - Smallest and simplest design/drive.

Some important considerations for LNG turbomachinery include:

- LNG compressors typically run over a very tight range (+/- 10%). GT emissions and efficiency can be well controlled within this range.
- Size of drive equipment may limit EMD selection to maximum of 65-70 MW for VFD technology to date.
- Emissions / environmental sensitivity of area may restrict GT option although electric power on site for EM can be a challenge.
- Variable speed EMD often considered for ease in starting motor and capacity / speed changes.
- Significant process interdependencies.
- Propane is a heavier MW gas compared to pipeline NG with higher SOS. This changes centrifugal compressor design somewhat.

- Operational range more consistent than upstream or pipeline applications, so efficiency of drivers can be exploited to an extent.
- Large flow rates and equipment size, related maintenance strategies for large trains.
- Sidestream and intercooling designs: Differing strategies on mixing sidestream with large axial passage versus injection nozzles with greater mixing and also higher DP. Design predictions must be accurate to match process throughput.
- High flow coefficients and high Mach numbers produce narrow flow maps with limited choke and surge margin.
- Higher sensitivity to choke conditions and increased dynamic forces on blades.
- Importance of robust surge control system design.

Besides large scale LNG development, there is also a market for smaller scale LNG, in the range from 0.1 to 0.5MMTPA. They support efforts to use stranded gas reserves, or to provide an attractive fuel for vehicles, E&P efforts, locomotives, or ships. These smaller installations usually use less capital-intensive refrigeration cycles, like the Single Mixed Refrigerant (SMR) cycle, or a reverse Brayton cycle, using Nitrogen or Nitrogen mixtures as refrigerant. The single mixed refrigerant is usually a mixture of methane, ethylene and other hydrocarbons (*Figure 8-33*).

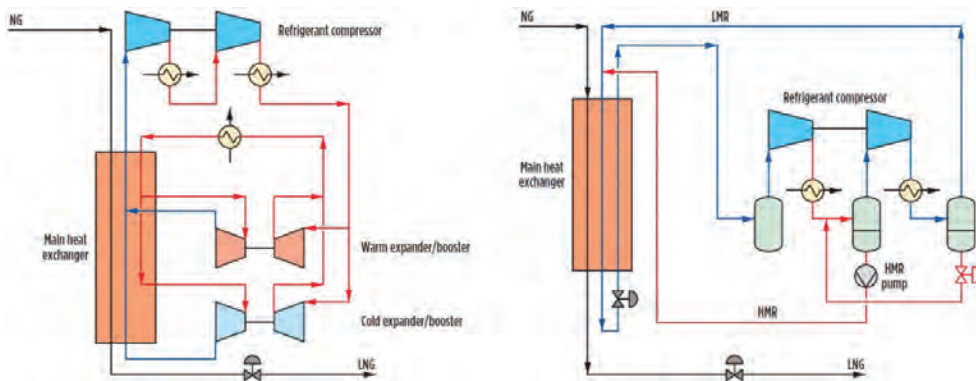


**Figure 8-33.** Nitrogen (left) and single mixed refrigerant (right), LNG refrigeration cycles. [1,2]

## CHAPTER 8 REFERENCES

- [1] Kurz,R., Gunn,B., Brun,K., 2020, Oil and Gas Applications for Centrifugal Compressors, Proc. Asia Turbomachinery and Pump Symposium 2020.
- [2] Brun,K., Kurz,R.,2019, Compression Machinery for Oil and Gas, Elsevier Gulf Professional Publishing.
- [3] Kurz,R., Brun,K., 2012, Upstream and Midstream Applications, ASME GT2012-68005.
- [4] Kurz,R., Ohanian,S., Brun,K., 2010, Compressors in High-Pressure Pipeline Applications, ASME GT2010-22018.





## CHAPTER 9

# OPTIMIZING COMPRESSOR STATIONS

*Rainer Kurz, Avneet Singh, Roman Zamotorin, Matt Lubomirsky*

The economic success of installations depends on factors such as availability, initial cost and equipment operating costs. The latter includes fuel, maintenance and possibly the creation of CO<sub>2</sub> and other greenhouse gases. In many instances, compressor installations consist of multiple compressors. These could be multiple compressors at the same station, operating in series or parallel configurations. These could also be compressors operating in various compressor stations along a pipeline. In either case, the compressors may not be identical in terms of size, performance and/or power consumption.

The challenge is to plan, size and control the units such that certain operating parameters—for example fuel consumption—are optimized. Other considerations may involve the minimization of operating hours per unit. The control system must rely on measurable parameters. The system has to be reliable even if parameters that are not directly measured change during operation. The optimization must consider the operational behaviors of the compressor and the driver, as well as the control methods, all of which have been previously discussed. Detailed discussion can also be found in references [1-6].

Optimization may also include discussions relating to space and weight requirements, especially in off-shore applications. Kurz and Sheya [7] provide a discussion on the relative merits of electric drivers vs. gas turbine drives in offshore applications.

Optimization issues were discussed in the past by Pinelli et. al., [8] for an offshore gas gathering application with gas turbine drivers, and Nøstebø et. al., [9] for an offshore gas export applications using electric motors as drivers, and Kurz et al., 2003 [10] or Zamotorin et. al., 2018 [11]. The former study investigates the arrangement of multiple compressor trains, either in parallel or series/parallel configuration for a declining gas field, that is a gas field where the gas suction pressure declines. Conditions are assumed to be steady state. The second study assesses a gas export station with five basically identical electric-motor-driven compressors in a parallel arrangement. Depending on the required gas flow, different strategies are discussed. The load-sharing strategy assumes that the operating compressors are controlled for equal turndown. The study by Kurz et. al., 2003 [6] evaluates the impact of the number of compressor units per station on fuel consumption, for changing pipeline operating conditions, and Zamotorin et. al., evaluate the impact of different control concepts.

The present study attempts to provide a more generalized view that involves consideration of the equipment in a station, but also can include the behavior of the entire compression system, using a pipeline with multiple compressor stations as an example. Different compressor control modes are considered and very simple, as well as the introduction of more complicated concepts. Unlike the referenced study by Nøstebø et al., [5], this discussion assumes gas turbine drivers, and considers in particular the impact of the changes in gas turbine efficiency with load and speed.

Compressor drivers exhibit performance characteristics that are dependent on their running speed and their load. *Figures 9-1 and 9-2*, for example, show the impact of load on efficiency and the impact of power turbine speed for a two-shaft industrial gas turbine.

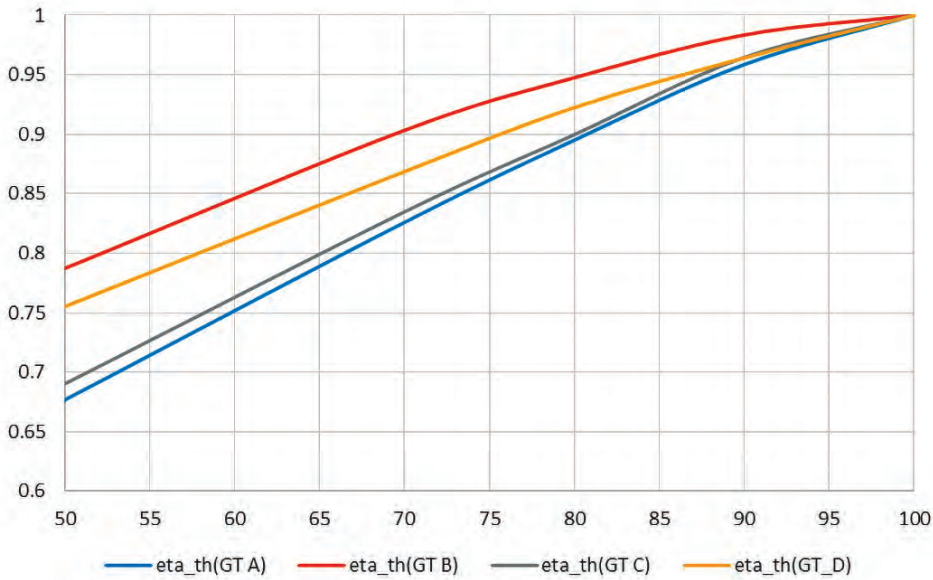


**Figure 9-1.** Thermal efficiency ( $\eta_{th}$ ) as a function of load for four different two-shaft gas turbines.

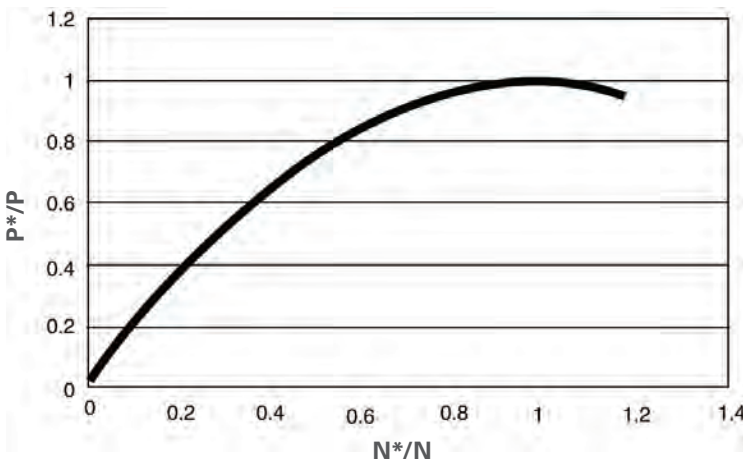


**Figure 9-2.** Power Turbine: Power versus Speed.

As described above, the working principles of an industrial gas turbine determine two important operating characteristics: power output increases with lower ambient temperatures and fuel efficiency is lower at partial-load operating conditions. Furthermore, the impact of different power turbine speeds on power and efficiency is relatively small, at least for the range of speeds not too far away from the power turbine's optimum speed. Industrial gas turbines typically develop their best efficiencies at full load, with the power turbine running at its optimum speed. Other drivers, such as electric motors, may show a more pronounced dependency on available power, depending on speed and a different relationship between load and efficiency.

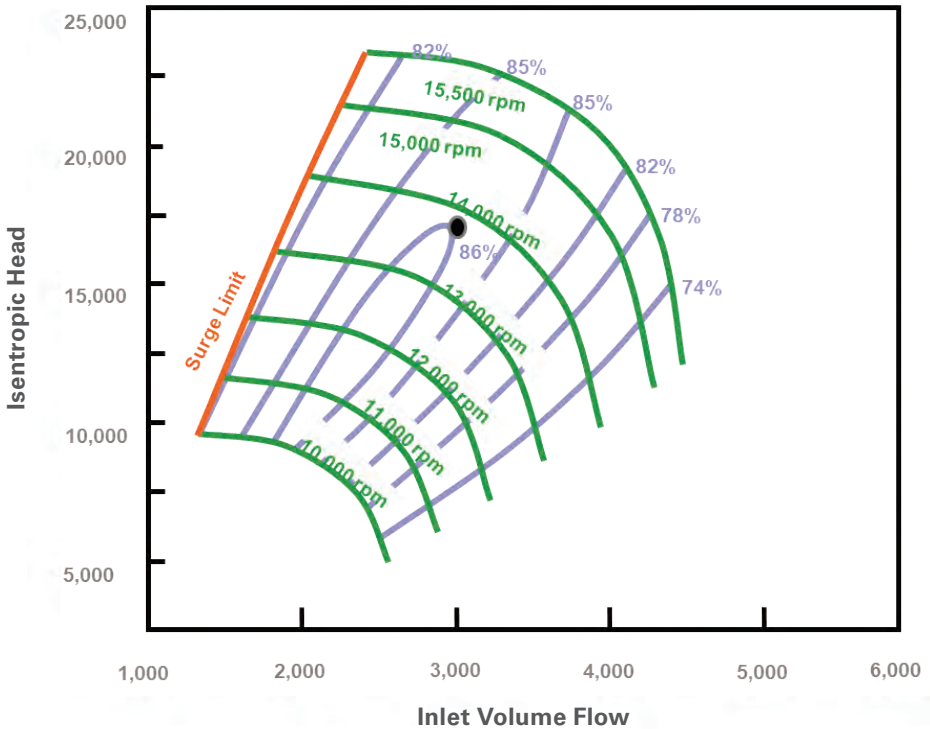


**Figure 9-3.** Performance map for a variable-speed centrifugal compressor.

The driven compressor for the applications in question is a centrifugal compressor, that is coupled with the power turbine, either directly or via a fixed-ratio gearbox. Therefore, the most effective and efficient way of controlling the compressor operation is by varying its speed (*Figure 9-3*). A centrifugal compressor can work at its best efficiency over a wide range of speeds. It should be noted that ‘control by varying the speed’ does not mean ‘controlling the speed.’ The control mode typically applies to a process parameter, for example: suction pressure, discharge pressure or flow. Any deviation from the controlled parameter will lead to an adjustment of the engines power output, which will result in a change in compressor speed as discussed in the chapter about controls.

If multiple units operate in a station, different ways of load sharing are possible. Two frequently used methods involve, either keeping all engines at the same relative load or keeping all driven compressors at the same distance from their surge line, thus at the same turndown. Turndown is defined as the distance of the compressor operating point from the surge line for constant head.

The operating point of the driven compressor is determined by the system in which it’s working. The system (for example a pipeline upstream and downstream from a compressor station) imposes the suction and discharge pressure on the compressor. The compressor reacts to it, based on the power available, with a certain flow. The flow, in turn, may alter the suction and discharge pressure the system imposes on the compressor.

The pipe system within which the compressor operates will impose its characteristic on the compressor. Three fundamental steady-state system characteristics need to be considered (Figure 9-4):

**A - strong head-flow relationship**

**B - weak head-flow relationship**

**C - integrative relationship**

For example, the case of a strong head-flow relationship (A) is seen in gas pipelines. Under steady-state conditions, the pressure loss in the pipeline, which imposes the suction and discharge pressure on the compressor station, increases significantly when the flow through the pipeline must be increased. The pressure levels are thus dictated by friction losses, which depend on the gas velocity in the pipe. In a weak head flow relationship (B), the head requirement for the compressor head stays more or less constant with changes in flow. This behavior is found in refrigeration compressors, but also for situations where the process dictates a constant suction pressure (e.g., separator pressure), while the discharge gas is fed via a short pipe into a larger flowing pipeline, so the compressor discharge pressure is more or less dictated by the pressure in the large pipeline. Friction losses, therefore, have a very small effect, resulting in very small changes in the pressure losses with flow.

In an integrative relationship (C), which exists for example in storage applications (Kurz and Brun [6]), where the compressor fills a large cavity. That means the compressor discharge pressure is increased as a function of the cumulative flow into the cavity, as a result of filling the cavity with gas. Line (C) is essentially showing a series of operating conditions at constant power. Similar conditions can be found in gas-gathering applications where (on a much slower scale) the field pressure (and the compressor suction pressure along with it) declines as a function of the cumulative flow out of the gas field. Additionally, these fields also have a strong head-flow relationship, i.e., increasing the flow at any given time would lower the compressor suction pressure.

Unfortunately, minimizing fuel consumption is not the only optimization goal used. Other characteristics that play a role include maximizing availability, possibly also for short term events, leading to partly loaded units in anticipation of a rapid increase in load (in the world of power generation, this would be called a spinning reserve). Minimizing the number of starts or minimizing running hours could be other requirements.

## OPTIMIZATION IN THE PLANNING STAGE

When a compressor station or a number of related compressor stations in a pipeline are planned, certain considerations must be made (Kurz et. al., 2003 [5]). These include:

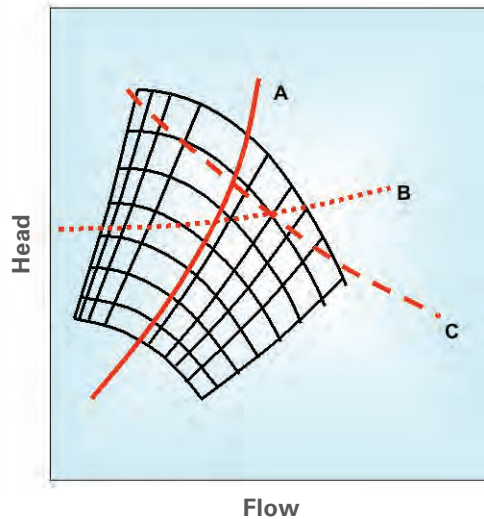


**Figure 9-4.** System characteristics and compressor map.

- Steady-state and transient capabilities and requirements of the system.
- Growth requirements and capability.
- Total cost of ownership and delivered cost to shippers and customers.

The first consideration involves the capability to cope with changes in flow capacity on all time scales (i.e., hourly, daily, seasonally). The pipeline hydraulics relate pressure losses to the flow through the pipeline, determining the compressor operating conditions in terms of head and actual flow, and subsequently determining the required power from the driver. Contractual requirements and obligations, such as pressures and volumes at transfer points, also must be considered.

The second consideration deals with the fact that the nominal capacity of a pipeline may grow when additional customers demand an increased supply of natural gas. In fact, many new pipelines start out with 50% or less capacity and grow to full capacity over several years, or are sized for easy expansion. Often, predicting the growth rate involves a significant degree of uncertainty. The growth scenarios, if foreseeable, drive a station's layout to possibly allow additional power to be installed at the station level later or additional stations to be installed along the pipeline. The alternative scenario, where the pipeline usage declines over the years (e.g., because the gas supply from the field declines), is also a possibility.

You must distinguish between growth scenarios that increase pipeline capacity by adding power along the pipeline and scenarios that add power and loop the pipeline<sup>1</sup>. The former scenario will always require an increase in pressure ratio at the station. Often, replacing single-stage compressors with two-stage compressors, or installing compressors in series to meet the higher pressure ratio is necessary. The latter scenario will usually increase the flow through the station and will be covered by installing additional units parallel to the existing ones.

Total cost of ownership reflects the cost to install, operate and decommission the station. While the first two considerations reflect the capability to generate revenue, the latter focuses on the necessary costs. These costs ( $c_i$ ) may appear at any point in time during installation, operation and decommissioning of the station. An easy way to compare cost of ownership is to use a net present value (NPV) calculation, assuming a fixed discount rate "r" for "n" time periods:

$$NPV = \sum_{i=1}^n \frac{c_i}{(1+r)^i}$$

## LOST REVENUE

Revenue reduction resulting from equipment downtime is an important element in calculating the total cost of ownership. To determine the lost revenue, total annual downtime is multiplied by the estimated lost revenue per hour (Hsu and Hasselfeld [12]).

<sup>1</sup>Looping a pipeline means installing an additional pipeline parallel to the existing one.

Another problem lies in the modeling of risk through the useful life of the project, as well as the economic value associated with this risk. The risk can range from hardware selection to maintenance practice and control system set points. The net effect of these risks translates into downtime or added fuel costs and, hence, added cost or reduced production output<sup>2</sup>. In many cases, lost production for a day creates a loss on the same order of magnitude as the fuel cost for one driver for a whole year. A few days of otherwise lost production can "pay" for the cost of a spare gas turbine. The requirement derived from this is to plan the stations such that they are tolerant to planned and unplanned outages. This could mean installing a spare unit or to optimize the installation such that the failure or downtime of one unit has the smallest possible impact on the capacity of the overall pipeline. It also means that the downtime in case of failure or planned outage must be minimized. Possible concepts include engine exchange programs, available spare engines, and preventive maintenance to name a few.

Studies at the start of the planning process typically assess station size. For pipelines, the starting point is the distance the pipeline has to cover and the amount of gas that needs to be transported. Optimization studies then assess the impact of pipe diameter, operating pressure, and number of compressor stations. Tradeoffs include the cost for the pipe, the cost for the compression equipment, and the operating cost for the different choices. Larger pipes reduce the amount of compression power to be installed, but increase the cost for the pipe. Having stations closer together reduces the amount of power to be installed and reduces the fuel cost, but increases maintenance requirements. *Figure 9-5* shows the result of such an evaluation, with the recommendation for a 28-inch pipe, and a compressor station pressure ratio of about 1:4.

## CHANGING OPERATING CONDITIONS

While some compressor stations are more or less operated at constant load, many installations see widely fluctuating operating conditions. These fluctuations are, in concept, foreseeable during the planning stage. Given the load dependency of the driver efficiency, a station that runs under a wide range of loads will often operate in part load, thus incurring higher fuel consumption, unless one has multiple units, with the option to shut down units, rather than operating in part load. First, consider the desirable number of compressors in station as related to the range of load fluctuations. Finally, consider the impact of changing ambient temperature. Since the engine output changes with the inlet temperature, even at constant station flow demand (that is, with the compressors consuming constant power), the engine load (relative to the maximum available power) can fluctuate with changing ambient temperatures.

*Figure 9-6* outlines a typical operating scenario for pipeline stations, showing a wide variety of operating points (Case A) and another scenario for a typical interstate pipeline (Case B). Here, data for four stations along the pipeline during summer and winter conditions were averaged. For the purpose of this evaluation, the load (i.e., the power requirement relative

<sup>2</sup>Lost revenue can be considerable. Assuming gas prices of \$3 U.S. per MMBtu and an LHV of 900 Btu/SCF, a pipeline pumping 500 MMSCFD achieves a revenue of 500 MMSCFD X 900 MMBtu/MMSCF X \$3/MMBtu = \$1,350,000 U.S. per day. For comparison, the fuel cost for a typical 7,000-hp driver would be approximately \$1,500,000 U.S. per year.

## Present Value 1500 PSIA MAOP - 500 MMSCFD

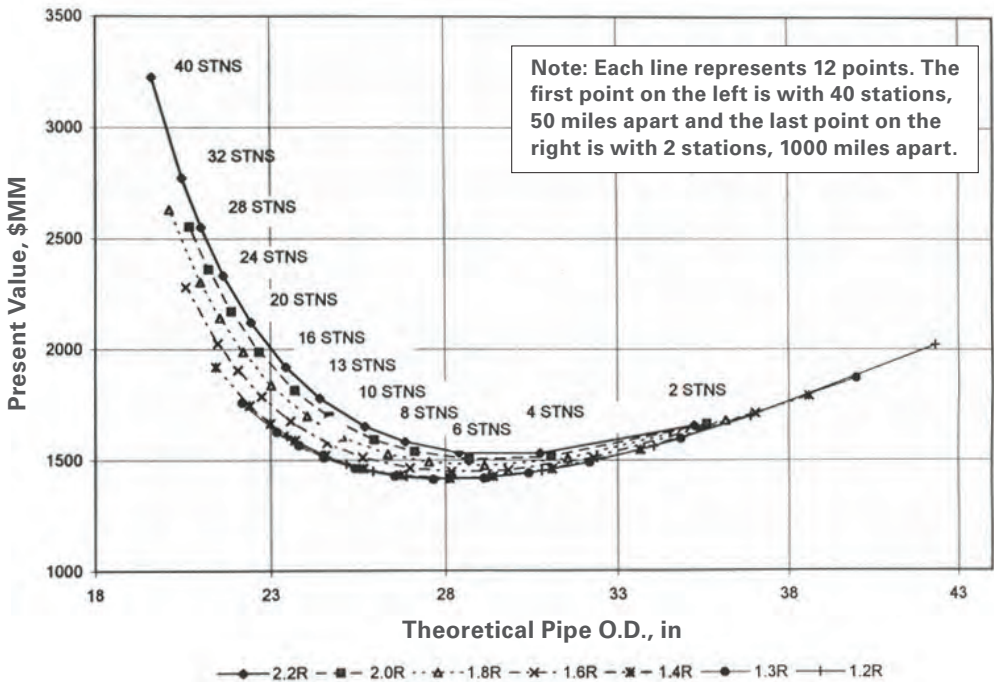


**Figure 9-5.** Pipeline optimization.

to the available power at each station and respective ambient conditions) for each of the two scenarios were mapped into different load classes.

The data in load classes lend themselves to a study that assesses the effect of different station designs, in particular the number of units used. Fuel usage can be calculated, as well as the emissions for Case A and Case B, (Figure 9-6) assuming the following scenarios<sup>3</sup>:

1. One 100% unit with  $\eta_{th} = 35\%$  at full load and a compressor with  $\eta_s = 87\%$
2. Two 50% units with  $\eta_{th} = 34\%$  at full load and a compressor with  $\eta_s = 86\%$
3. Two 50% units with  $\eta_{th} = 35\%$  at full load and a compressor with  $\eta_s = 87\%$
4. Three 33% units with  $\eta_{th} = 32\%$  at full load and a compressor with  $\eta_s = 85\%$
5. Three 33% units with  $\eta_{th} = 35\%$  at full load and a compressor with  $\eta_s = 87\%$

The figure then shows the relative fuel usage (and thus also CO<sub>2</sub> emissions) for the different scenarios, based on a part-load efficiency penalty as outlined in Figure 9-1.

<sup>3</sup>Obviously, this calculation can be performed for a real scenario by taking into account a large number of different operating points, with the actual engine and compressor performance for each of these points.

Because different gas turbines exhibit different behaviors regarding their respective part-load efficiencies, each series of calculations is performed using a curve that reflects the steepest drop in part-load efficiency and one that reflects the least-step drop in part-load efficiency in *Figure 9-1*. There is a minimum in fuel usage for the curve that reflects the steepest drop in part-load efficiency and one that reflects the least steep drop in part-load efficiencies in three units (which incidentally is the station layout). The more stations used, the less important the slope for part-load efficiency becomes. The minimum in fuel usage also implies a minimum in CO<sub>2</sub> production.

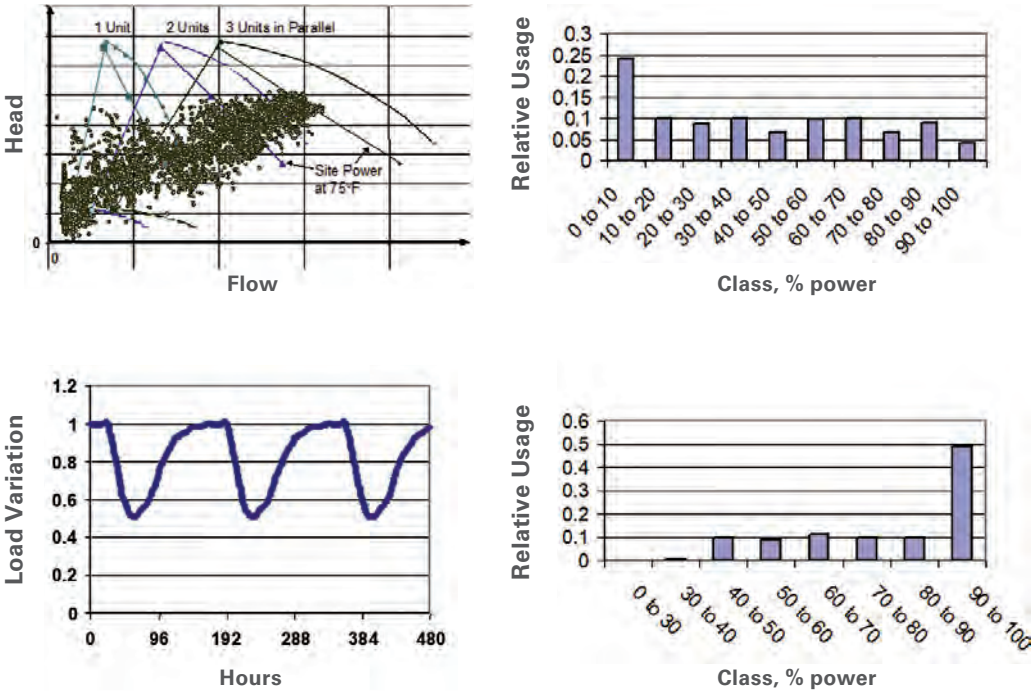


**Figure 9-6.** Case A for a pipeline with large load fluctuations (top), Case B for pipeline with smaller fluctuations (bottom).

Case A (*Figure 9-7*) exhibits a clear advantage of multi-unit stations. Because the smaller units are operated closer to full load for most of the time, the resulting fuel usage is lower than for single-unit stations. This holds true for both slopes in part-load efficiency and even if the smaller units achieve a lower base efficiency than the larger units. For virtually all cases, a station with three or four units minimizes the fuel usage. Additional units yield no additional benefits.

Case B (*Figure 9-8*) gives a somewhat different picture. Comparing *Figures 9-8 (left) and 9-8 (right)* shows that the conclusion regarding the optimum number of stations depends highly on the baseline efficiency of the packages involved. If the smaller units have the same design efficiency as the larger units, then a three-unit station is advantageous. If we assume lower efficiencies for the smaller units than for the larger units, a one or two unit station uses less fuel.

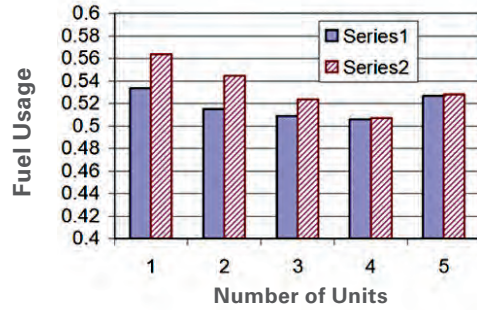
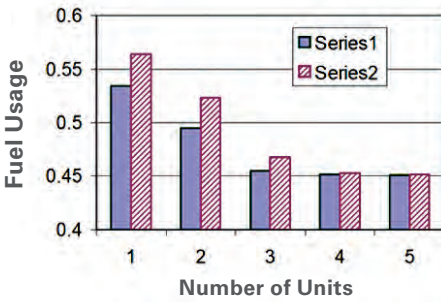


**Figure 9-7.** Case A, Scenarios 1, 3, 5 (left) and Scenarios 1, 2, 4 (right)

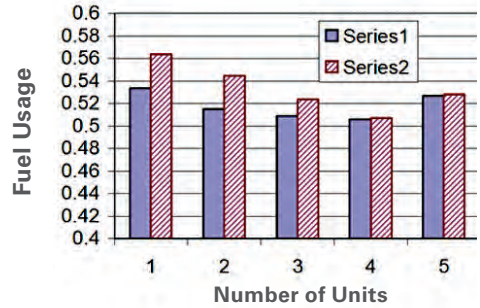
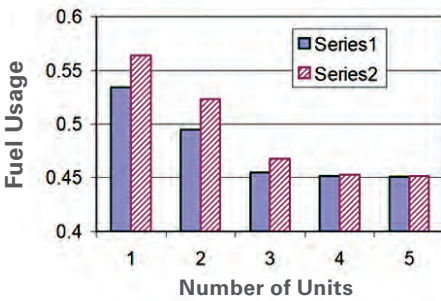


**Figure 9-8.** Case B, Scenarios 1, 3, 5 (left) and Scenarios 1, 2, 4 (right)

Having said that, it again needs to be emphasized that a station outage may result in significantly higher costs due to lost revenue than the fuel cost for an entire year. Obviously, a standby unit reduces the exposure significantly. Also, if the station uses multiple units, then the unavailability of one of these units has a smaller impact on the amount of gas that can be produced (admittedly, the chances that one out of four units fails are higher than the chances that one out of two units fails).

Besides fluctuations in the required compressor power, as described above, you may also encounter situations where the ambient temperatures show large swings, especially between summer and winter conditions. Depending on the number of units in a station, the situation during low ambient temperatures may enable shutting down a unit entirely. Of course, if the station flow is to be maintained, the compressors in operation will

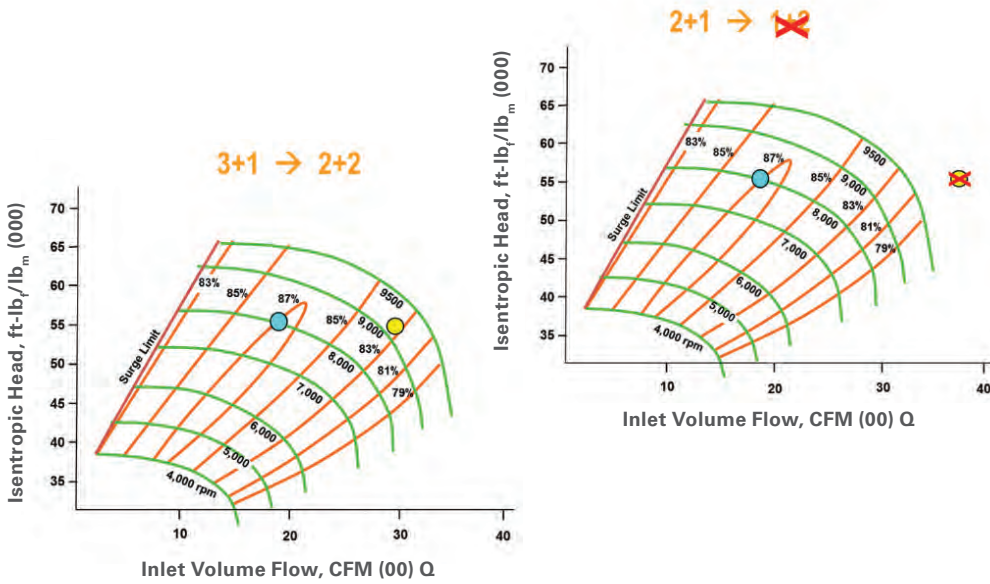


Figure 9-9. Two units vs three units: Capability to shut a unit down.

see a larger flow (Figure 9-9). In the figure above, the advantage of smaller units (three units in a station) over larger units (two units in a station) is illustrated. The station with three units can accommodate the shutdown of a unit, while for a station with two units, the compressor that remains in operation will not be able to handle the increased flow. Shutdown of units, instead of running units in part load has a positive impact on fuel consumption (Figure 9-10) and maintenance cost (a unit that is shutdown does not accrue fired hours; a unit operating in part load does).

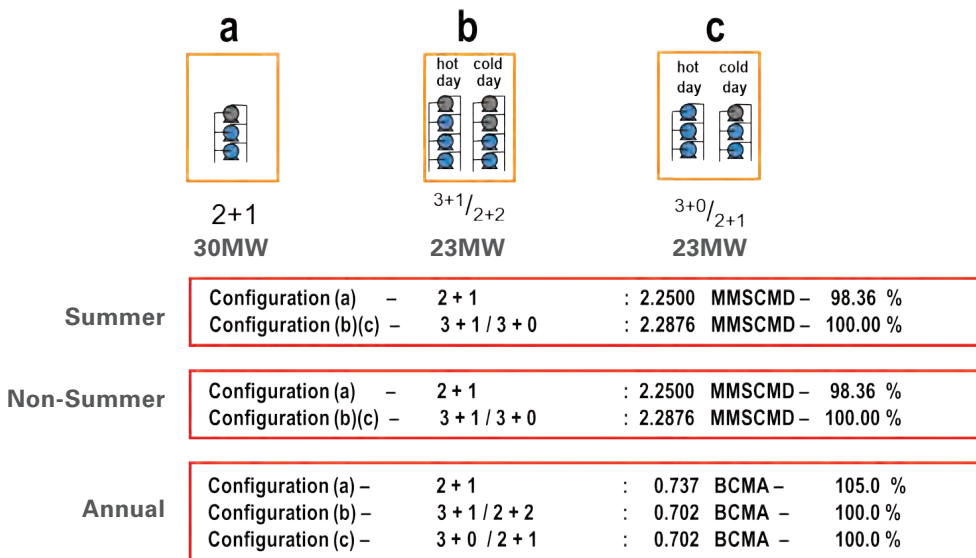
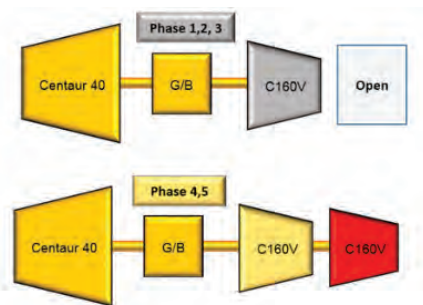
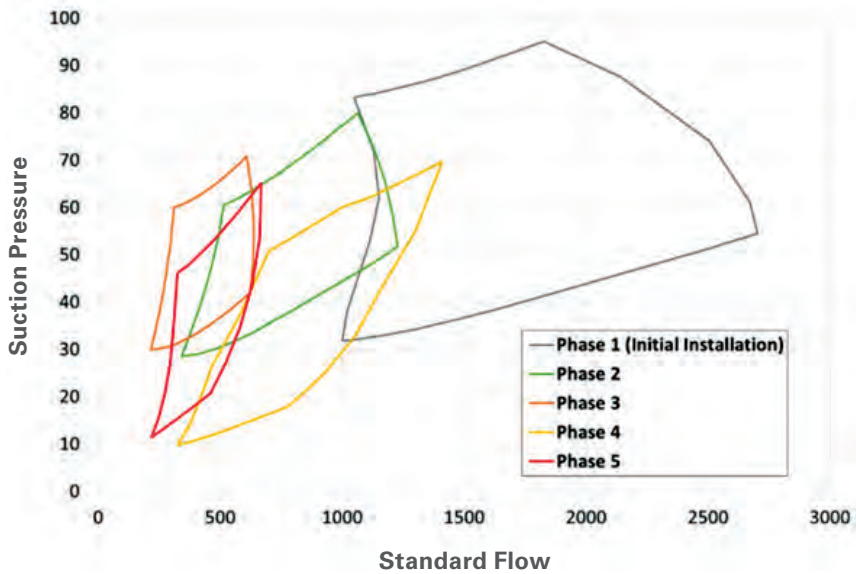


Figure 9-10. Fuel Consumption

## Compression Coverage Map



	Compressor 1	Compressor 2
Phase 1	Higher Flow/Field Pressure	None
Phase 2	Medium Flow/Field Pressure	None
Phase 3	Low Flow/Medium Pressure	None
Phase 4	High Flow (Reuse Phase 1)	Medium flow (Reuse Phase 2)
Phase 5	Medium Flow (Reuse Phase 2)	Low Flow (Reuse Phase 3)

**Figure 9-11.** Declining gas field.

In cases where the operating conditions change significantly over time, which is a situation frequently encountered in installations near oil or gas fields, concepts that take advantage of package flexibility may be considered. The example below shows a situation at a declining gas field, where, over time, gas flow and suction pressure dropped. The addition of another compressor to the train to accommodate the declining suction pressure, and the resulting increase in pressure ratio had been planned, so the skid was prepared to accept an additional compressor body. Together with targeted restages, that enabled reuse of existing aerodynamic hardware, the wide range of operating conditions was covered (Figure 9-11).

## BASIC OPERATIONS OPTIMIZATION

On the station level, simple, but very effective methods include the concept of loading all involved units evenly, and running the least number of units necessary. The downside of this approach is that if done consistently, the number of starts and stops for the units increases. Loading units evenly can either be accomplished by running all compressors at the same distance from their respective surge line, or by running all gas turbines at the same load setting, for example by equalizing their gas producer speed relative to the speed at full load (Zamotorin et al., 2018 [11]).

Additional considerations are required if the units involved are different in size and operating characteristics. Many compressor stations combine units of different size and vintage. The newer units may be less expensive to operate, may have a higher fuel efficiency, and may be bigger (in terms of power output) compared to the older units. One of the key tasks may be to restage the compressors of the older units in order to be able to contribute at a reasonable cost to the station operation. For the purpose of this study, it's assumed that this has happened.

More involved methods would include simulations of entire systems (for example, of a pipeline with multiple compressor stations, and multiple compressor units per station) using numerical simulations.

## SIMPLE SCHEME

A simple, but very effective scheme is outlined as follows: Assume a compressor station with one large unit (KC), and three smaller units (TC), all operating in parallel. For simplicity, each of the smaller units produces half the power of the larger unit [11]:

$$P_{KC} = 2 P_{TC}$$

and the compressors are aerodynamic scales, thus maintaining aerodynamic similarity. The parallel operation forces all units to operate at the same suction and discharge pressure. Based on the above, the total available station power  $P = 5 P_{TC}$ .

Different load steps can now be defined:

**Step 1:**  $P = P_{TC}$

**Step 2:**  $P = P_{KC}$  or  $P = 2 P_{TC}$

**Step 3:**  $P = P_{KC} + P_{TC}$  or  $P = 3 P_{TC}$

**Step 4:**  $P = P_{KC} + 2P_{TC}$

**Step 5:**  $P = P_{KC} + 3P_{TC}$

For all power demands that are higher than step n, but lower than step n+1, the running units are equally loaded.

Further considerations have to be made to decide which options should be pursued for steps 2 and 3. One consideration could be maintenance cost. It could well be that the larger unit accrues lower maintenance cost per fired hour than two of the smaller units. Similarly, if the larger unit is more efficient than the small units, one would opt for starting the larger unit in steps 2 and 3.

Another option would be to analyze the typical load cycle for the station. If the load typically rises beyond step 3 relatively fast, it might be advantageous to start the large unit in step 2. If, however, the load often just stays between steps 1, 2 and 3 (as is the case for stations that have seasonally lower loads), then these steps may be better covered by the smaller units.

Lubomirsky et. al. [12] pointed out in a study on pipeline availability and fuel optimization that in situations that show, in particular, significant variation in ambient conditions, this simple control schematic is rather powerful, both in terms of minimizing fuel consumption, but also in minimizing the running hours, and thus the maintenance cost of the units.

As mentioned earlier, units at the station level can be controlled by load equalization or by turndown equalization [11]. All simulations in this section assume compressor operating points at constant head. *Figure 9-12* shows the simulation results for different control methods at a compressor station with two compressor sets of different size (Unit 1 with 1.5 times the power of Unit 2). Compared are the cases where the units are equally loaded (with either the small or the large unit leading) or where they are controlled for equal turndown.

Equal load is usually accomplished by controlling the gas producer speed of the gas turbine. As can be seen, the fuel consumption for a certain station flow demand is about the same

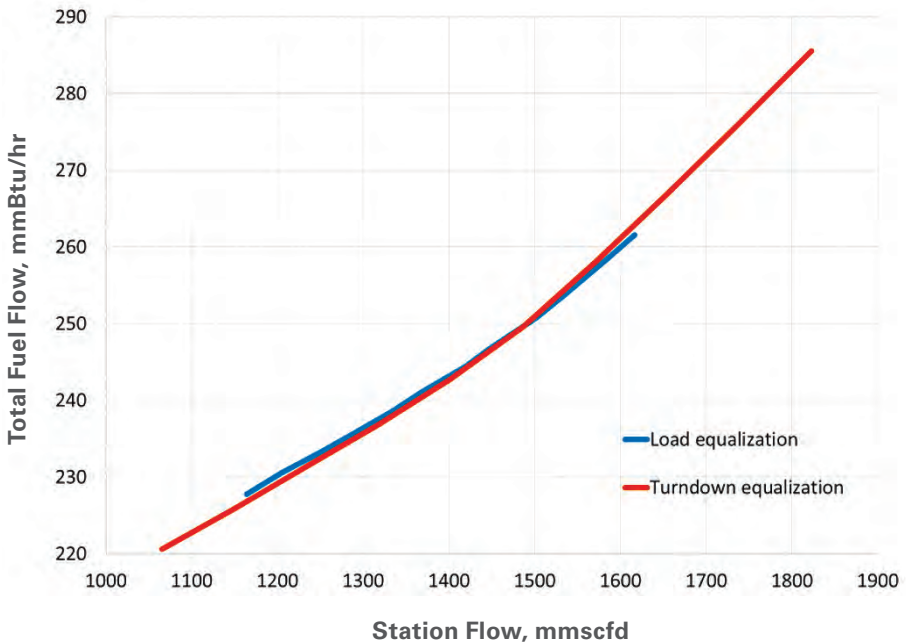


**Figure 9-12.** Load equalization. Equal load, with either the 15MW (20,000 hp) or the 22.5MW (30,000 hp) engine leading versus equal turndown for the compressor.

for either control method. There is a significant advantage for the equal turndown method at low and high flows, where the equal load method is limited either by surge line on one unit or by maximum speed on the other. Turndown equalization has a wider allowable flow range, since it is more tied to compressor maps and initially the compressor selection had been done based on turndown evaluation, not engine load. It is probable to find compressor selections, which will provide the same operating range, if at station design and if there is a particular request to find an optimized solution based on sharing the load equally. However, using turndown equalization just might be easier.

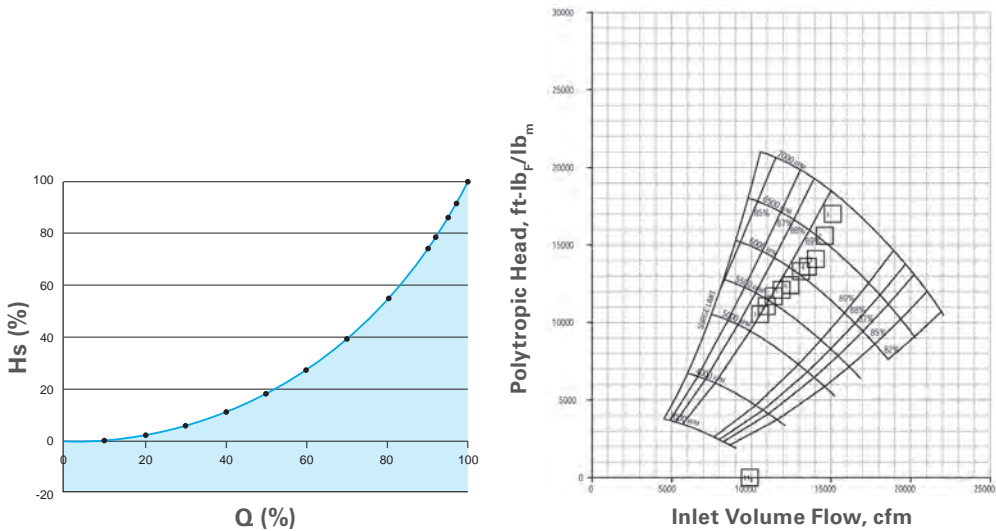


**Figure 9-13.** Steady-state pipeline compressor head flow relationship, and relationship plotted into a centrifugal compressor map.

### BEYOND THE STATION

Optimizations that involve multiple, but connected compressor stations require modeling of the connecting pipes. In other words, pipeline hydraulics have to be considered [11]. This leads to a number of constraints for the individual compressor station that are not obvious on the station level. A key feature is that for a pipeline, pipeline flow and station pressures are not independent. In other words, if the flow through the pipeline is increased, the pressure ratio for the compressor station has to increase too (Figure 9-13).

Generally, variable-speed centrifugal compressors are uniquely suited for this type of operating characteristic, because all steady-state points can be placed near the compressor’s best efficiency point, while the wide range allows for suitable deviations imposed by non-steady-state operation [5]. Even with massive load changes (bringing the driver from 50% to 100% load within less than a minute for example), the compressor will not operate at constant head and varying flow for more than a few seconds [6].

Figure 9-14 shows the layout of such a pipeline of a given length ( $L_{tot}$ ), five compressor stations (1 through 5) at roughly equal distance, and a side stream entering the main pipe just upstream of station 3. The simulation considers the fuel consumption of each of the

stations, as well as the line pack (i.e. the gas stored in the pipeline system itself). The pipeline geometry (diameter, roughness), maximum allowable operating pressure (MAOP), site elevations, and local ambient temperatures are known.

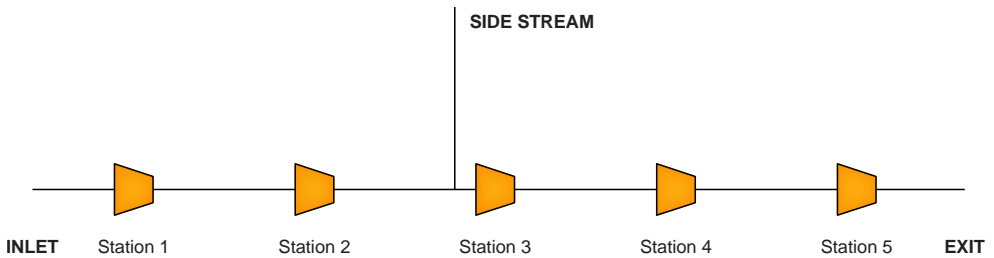


**Figure 9-14. Pipeline Schematic**

The compressor stations use a variety of different centrifugal compressors, all of them driven by two-shaft gas turbines. Recycle as well as shut down of individual units are possible, and have to be considered as part of the simulation. Also, an entire station can be bypassed. A summary of the installed units is shown in *Table 9-1* [11].

In the study, the actual operating conditions for all units were used as a starting point. In this situation, all but two units in station 5 were running, and all of them at relatively low load (*Table 9-2*). The optimized scenario consumed 74% of the fuel compared to the original situation. The two major contributing factors are the smaller number of units running at higher load, and the generally lower gas velocity in the pipe (*Figure 9-15*), which significantly reduced the pressure losses. This was accomplished by running station two with more units at a higher load. The higher load on Station 2 was achieved by running at higher head despite being in recycling mode.

Station	Number of Units	Power Class of Units (MW)	Total Installed Power (MW)
1	0	0	0
2	2	14.5	29
3	2	15.3	30.6
4	2	15.3	30.6
5	5	3 ea 6 1 ea 7.8 1 ea 11.2	37

**Table 9-1. Installed Power**

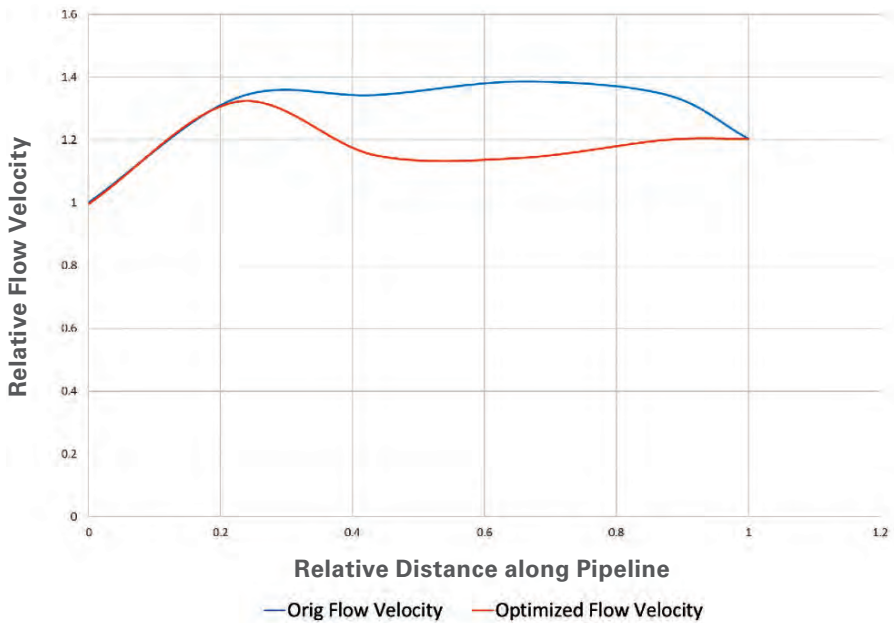


**Figure 9-15.** Optimizing fuel consumption involves shifting the load between stations, thereby reducing both the flow velocities and ultimately the pressure drop in the pipeline. The flow velocities in the pipeline at various stations are shown. Optimization allows for lower flow velocities in parts of the pipeline, thus reducing power consumption at the compressor stations. It can also be seen that, apart from the optimization of the pipeline hydraulics, the recipe given in the previous section seems to be approximately replicated by the numerical optimization.

Station	Number of Units Running	Average Load of Running Units	Number of Units Running (optimized)	Average Load of Running Units (optimized)
1	0	N/A	0	N/a
2	2	56%	2	70%
3	2	57%	1	94%
4	2	63%	1	83%
5	3	96.6%	1	97%

**Table 9-2.** Station Load

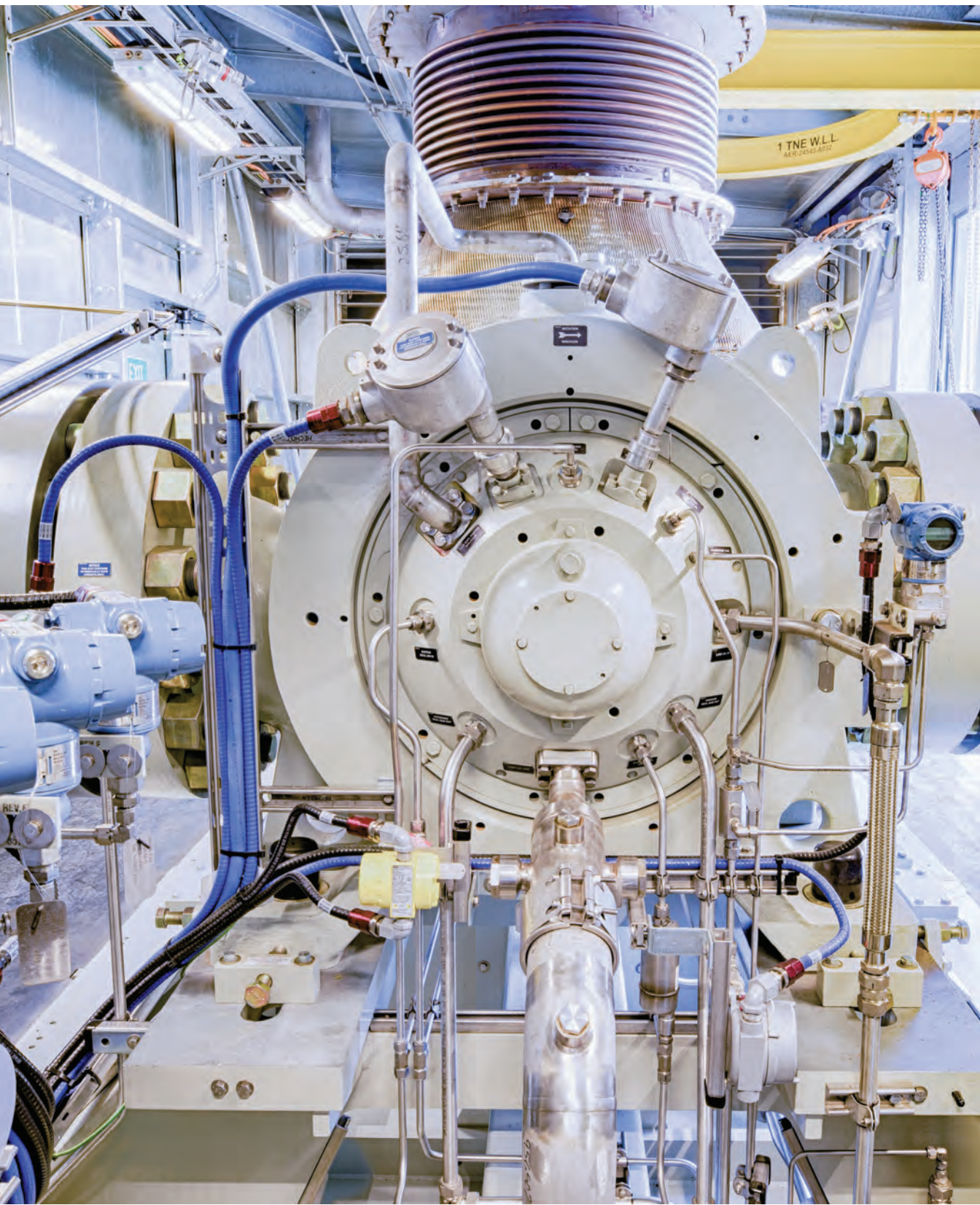
Understanding the behavior of turbomachinery equipment and the overall system allows appropriate methods for fuel and operational optimization on the station level and for entire pipelines. Optimization can and should happen both during system planning, as well as during system operation.

In the planning phase, key influence factors include the number of stations and the number of units, based on assessments of the variability of the operating conditions. Variability will occur on various time scales.

During operation, relatively simple rules can be derived based on the conceptual understanding, or from evaluation of more complex studies. The concepts described herein work even if units are not identical and can be entirely based on measurable parameters. The challenge is to control the units, such that certain operational parameters—fuel consumption for example—are optimized. The control system must rely on measurable parameters, even if parameters that are not directly measured (such as the gas composition for the compressor) change during operation. The methods to control all compressors for the same turndown provides good results regarding both efficiency and operating range, compared to controlling all gas turbines for the same load. Modelling the entire pipeline facilitates further optimization that cannot be achieved if the optimization is only performed at the station level.

## CHAPTER 9 REFERENCES

- [1] Kurz,R., Gunn,B., Brun,K., 2020, Oil and Gas Applications for Centrifugal Compressors, Proc. Asia Turbomachinery and Pump Symposium 2020.
- [2] Brun,K., Kurz,R.,2019, Compression Machinery for Oil and Gas, Elsevier Gulf Professional Publishing.
- [3] Kurz,R., Brun,K., 2012, Upstream and Midstream Applications, ASME GT2012-68005.
- [4] Kurz,R., Ohanian,S., Brun,K., 2010, Compressors in High Pressure Pipeline Applications, ASME GT2010-22018.
- [5] Kurz,R., Ohanian,S., Lubomirsky,M., 2003, On Compressor Station Layout, ASME GT2003-38019.
- [6] Kurz,R., Brun,K., 2018, Process Control for Compression Systems, ASME JEngGTP, Vol.140 No.2.
- [7] Kurz,R., Sheya,C.,2005, Gas Turbines or Electric Drives in Offshore Applications, ASME GT2005-68003.
- [8] Pinelli,M.,Mazzi,A., Russo,G., 2005, Arrangement and Optimization in an Off-shore Natural Gas Extraction Station, ASME GT2005-68031.
- [9] Nostebo,V.S.,Bakken,L.E.,Dahl,H.J., 2007, ASME GT2007-27367.
- [10] Kurz,R., 2006, Turbomachines and Pipeline Simulations,PSIG Seminar, Aachen, Germany.
- [11] Zamotorin,R., Kurz,R., Lubomirsky,M., Zhang,D., Brun, K.,2018, Control Optimization for Multiple Gas Turbine Driven Compressors, ASME GT2018-75002.
- [12] Lubomirsky,M., Kurz,R., Klimov,P., Mokhatab,S., 2009, Station Configuration Impacts Availability, Fuel Consumption and Pipeline Capacity, Pipeline and Gas Journal, Feb.2010.



## CHAPTER 10

# IMPORTANCE OF TESTING

The importance of testing that develops information useful for decision making cannot be overstated. Testing of gas compressors requires conditions that facilitate the gathering of conclusive compressor performance data utilizing well-defined conditions. While using concepts developed in earlier chapters, this section discusses different test methods, the task of defining representative test conditions, and the reduction of test data to yield meaningful information about compressor performance.

Industry-wide accepted test codes such as ASME PTC-10 [1], ISO 5389-1992 [2] typically define factory tests, and must be adapted if used for site performance testing. The Gas Machinery Research Council (GMRC) [3] provides guidance for site performance tests. This text will not address specific requirements of these codes, but attempts to outline general concepts. The requirements for obtaining valid test data and the concepts of uncertainty analysis are highlighted. Particular attention is given to at-site tests, which require gathering data based on a particular compressor installation, and therefore, usually won't comply completely with the requirements of test codes.

Also, parameters such as power consumption, efficiency and/or operating range need to be defined as part of test results. *Figure 10-1* shows a factory test facility, while *Figure 10-2* shows the situation during a site performance test.



**Figure 10-1.** Titan 130 driven C41D closed-loop validation testing, San Diego.

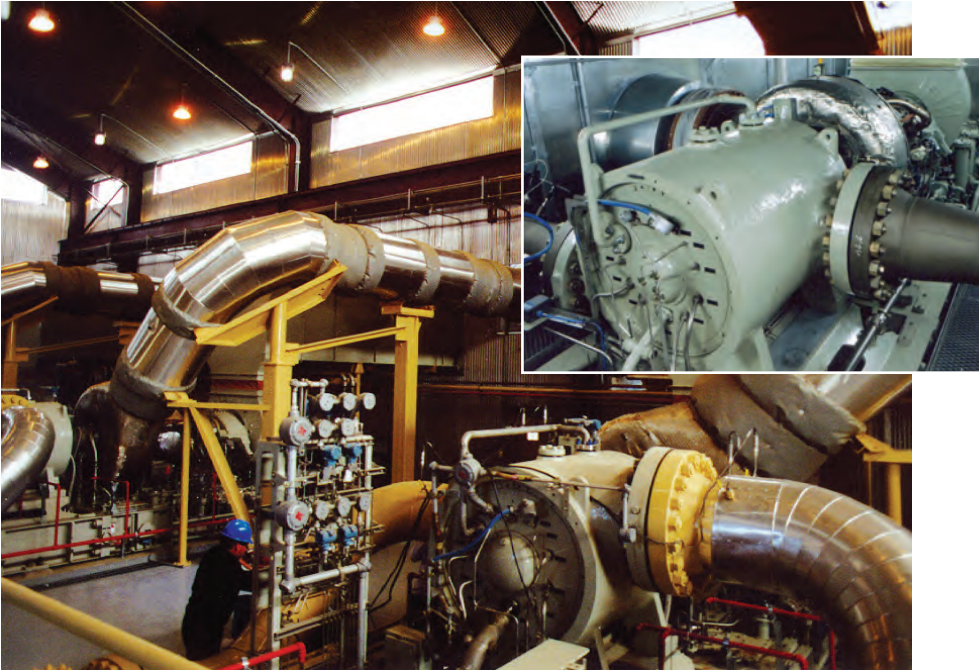


**Figure 10-2.** Typical setup for a site test.

For development purposes, tests on scaled components are an integral part of the compressor development process and can be used to research systematic-design parameter variations (e.g. blade count, impeller back-sweep angles and/or exit width).

Test rigs enable use of more detailed instrumentation, especially for locations that are difficult to access in the actual compressor (*Figure 10-3*). This also enables the use of validation and calibration CFD tools (*Figure 10-4*).

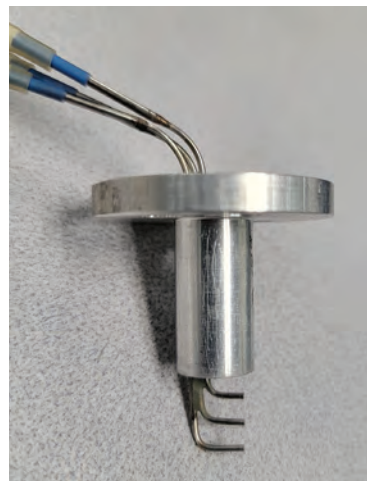
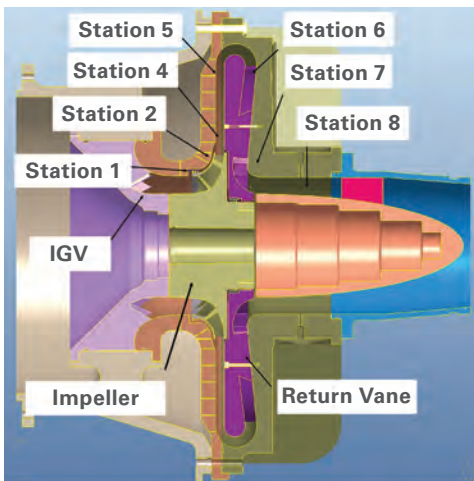


**Figure 10-3.** Compressor rig traverse locations and custom rake for rig insertion.

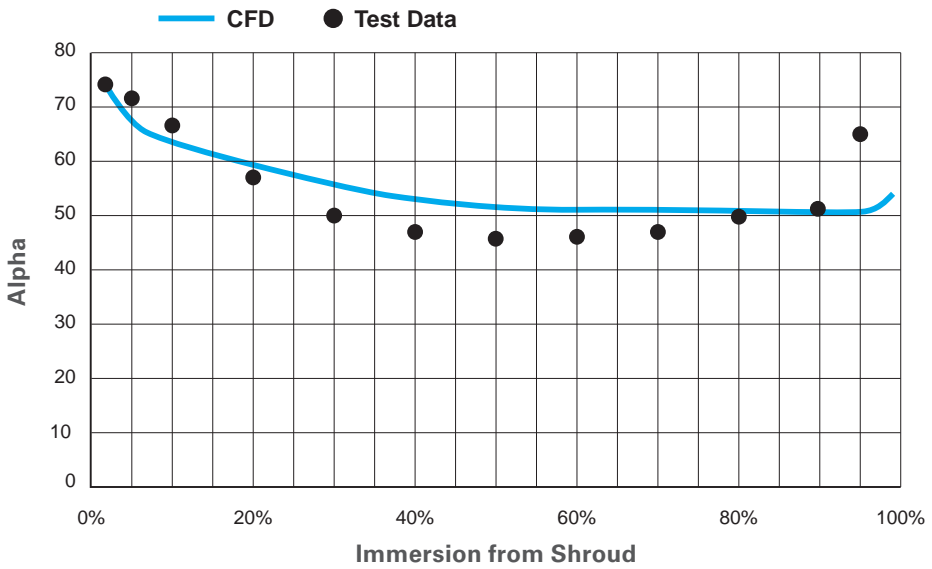


**Figure 10-4.** Flow angle Alpha 4 along the diffusor; comparison of ATF test data to CFD calculations.

Examples for the evaluation of design variations are given in *Figures 10-5 and 10-6*.

### Aero Test Rig: C2 Impeller: Volute, $Z = 13, Z = 15$

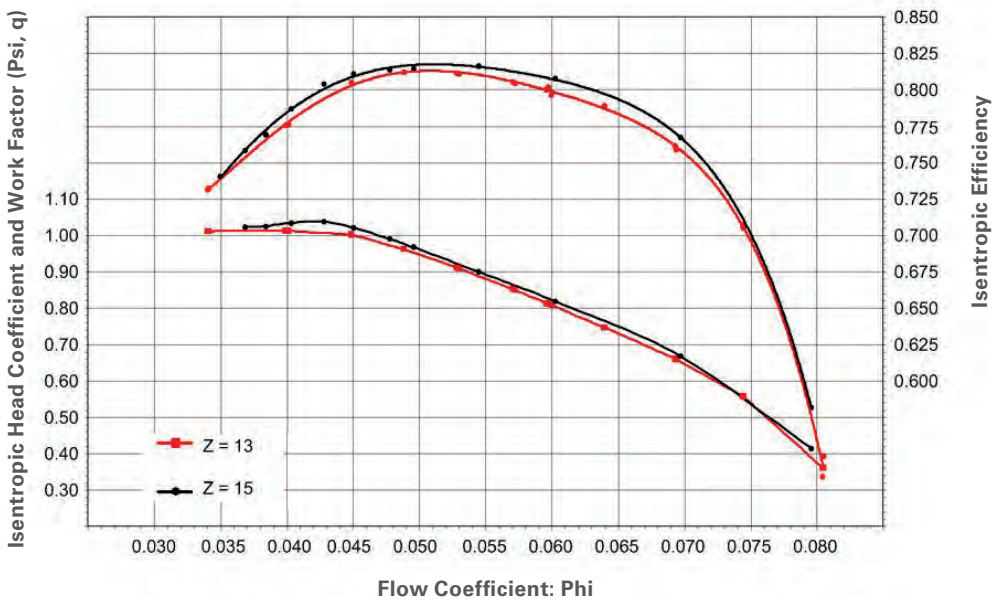


**Figure 10-5.** Stage performance effects with changes in impeller blade count.

## Aero Test Rig: C2\_50A and C2\_50B Impellers

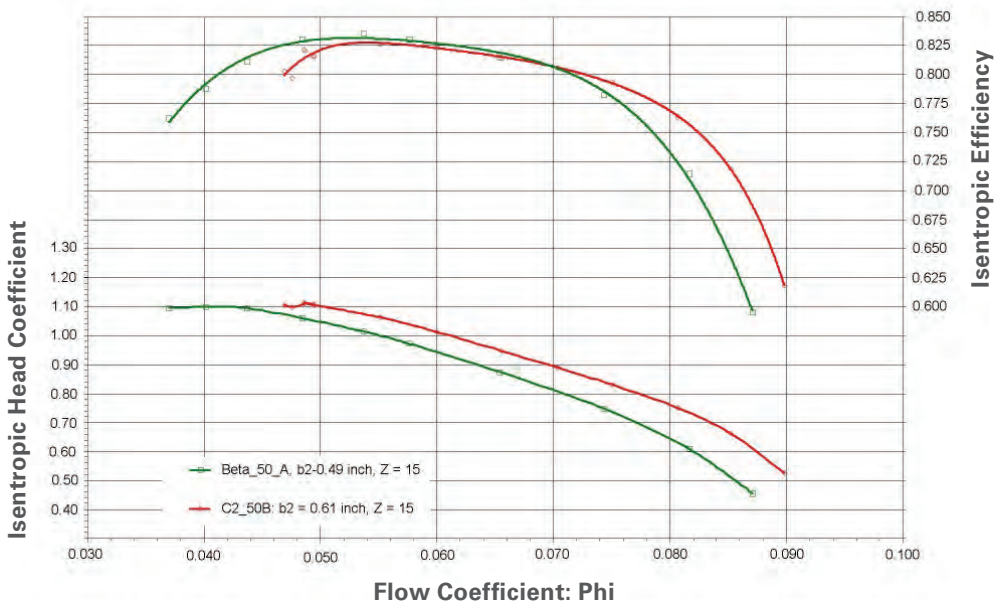


**Figure 10-6.** Stage performance effects with changes in blade exit width.

### TEST METHODS

If a compressor or one of its sections is designed to work under specified conditions in terms of ( $p_1$ ,  $p_2$ ,  $T_1$ , Flow, gas), the best test is obviously a test that exactly reflects these conditions. In general, this is not possible, because even when the compressor is installed at site, the conditions are usually different from the conditions originally specified [4, 5].

Methods that enable correcting data from tests with different gases or different inlet pressures and temperatures to the datum conditions are available, as long as certain parameters relate to aerodynamic similarity are met. In other words, if these parameters are met, the flow through the compressor preserves the velocity polygons, as well as the Mach number and the Reynolds number. Such a test will verify the aerodynamic performance of the compressor (i.e. its efficiency or operating range). Other tests—for example, testing at design speed, design power or design discharge pressure—verify the compressor’s mechanical performance and integrity. The latter type of test is not addressed here.

For most compressors in oil and gas industry applications, only tests in pressurized, closed loops or at site, can provide operating conditions to verify compressor efficiency. However, even tests using ambient air, provided the Mach number is preserved, provide meaningful information about the operating range of the machine.

Usually, the operating points for the test are determined by the facility, and the test may not be conducted at the desired condition. Also, when test data are taken over time for condition-monitoring purposes, the data are taken for different operating conditions. Therefore, comparison of data taken or predicted at different conditions is needed. Note that the gas compressor test may serve several purposes, for example:

1. To determine compressor performance.
2. To load the gas turbine to full load, thereby determining the gas turbine output and full-load heat rate.
3. To verify the performance of the entire train.

For tests, it's always advantageous to compare the test data with other, redundant measurements. For example, the gas turbine driver full-load performance, or the electric motor drive-power output may be known from other tests. If the compressor can be operated with the engine running at full load, the compressor shaft power equals the engine full load output. This engine performance can then be corrected to factory test conditions [4], and should be reasonably close to the factory test results. If the gas turbine fuel flow can be measured, a similar comparison can be made for the heat rate. If the results from the site test and the factory test are reasonably close, confidence in the site test results is improved. Otherwise, reasons for the discrepancy should be determined.

The goal of a test should be to create conditions that are as close as possible to the original design conditions, whether for a site test or a factory test.

To compare test data for a centrifugal compressor, using non-dimensional parameters for head and flow is very useful. Efficiency is already a non-dimensional value.

Using the Flow Coefficient:

$$\phi = \frac{Q_s}{\frac{\pi}{4} D_{1,tip}^2 u} = \frac{Q_s}{\frac{\pi^2}{4} D_{1,tip}^3 N}$$

and the volume flow ratio, in other words, the ratios between the flow into the compressor and out of the compressor are preserved:

$$(Q_s / Q_d)_t = (Q_s / Q_d)_a$$

while meeting the Head Coefficient (isentropic or polytropic):

$$\psi^* = \frac{H^*}{\frac{u^2}{2}} = \frac{2H^*}{(\pi D_{1,tip} N)^2} \quad \psi^p = \frac{H^p}{\frac{u^2}{2}} = \frac{2H^p}{(\pi D_{1,tip} N)^2}$$

the velocity polygons are preserved.

It should be noted that  $\Psi$  and  $\phi$  at the beginning of the test are unknown, because the exact speed of the compressor required to meet head and flow are also determined during the test.

Using the non-dimensional values eliminates the requirement to test the compressor precisely at the same speed as predicted, or precisely the same gas composition as specified. *Figure 10-7* shows a typical, non-dimensional compressor map.

**C75 SE-DEL, s/n G7530102, C753 (705) F1F-E6M-D4R  
Closed-Loop Performance, 7000 RPM**

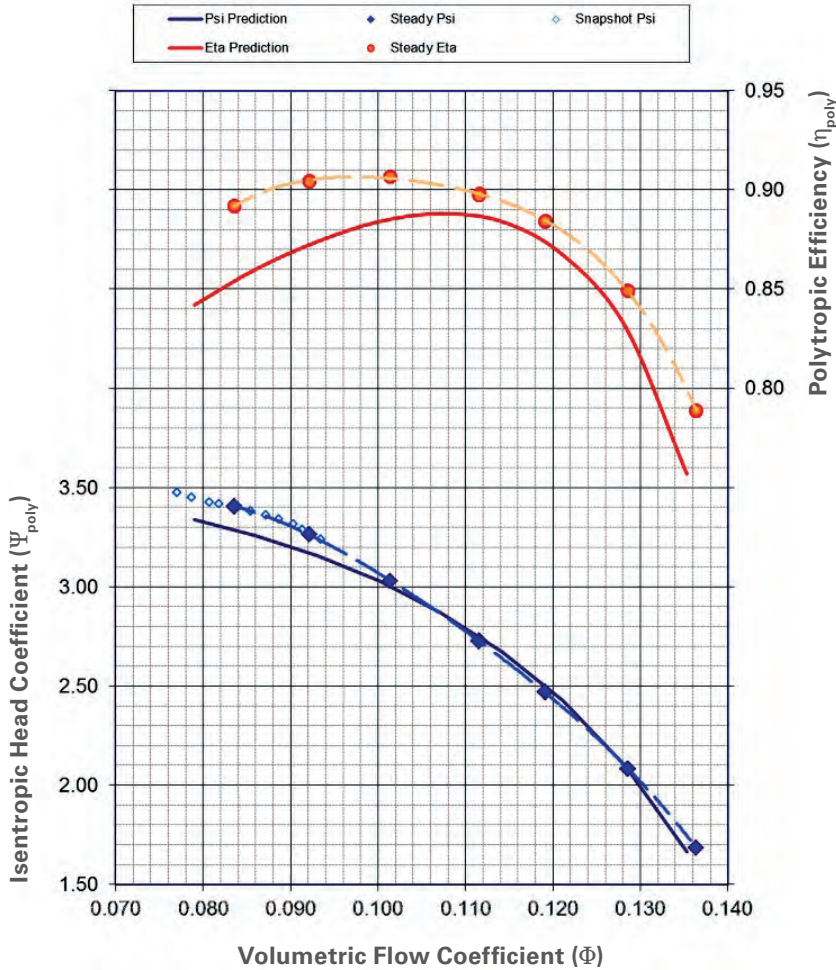


**Figure 10-7.** Non-dimensional compressor map and test results from a ASME PTC 10 type 2 test compared with initial predictions. Test data like this can be used to improve the prediction models for future projects.

The other parameters that need to be maintained to accomplish similarity (although with some possible deviations) are:

Machine Mach Number:

$$Ma_u = \frac{u}{\sqrt{k_s Z_s RT_s}} = \frac{\pi D_{ip} N}{\sqrt{k_s Z_s RT_s}}$$

Machine Reynolds Number:

$$Re_u = \frac{\pi D_{tip} N b_{tip}}{v_s}$$

Typically, only some of the similarity parameters can be brought exactly into accordance with the desired acceptance criteria, especially when the gas composition during the test is different from the design gas. The most important parameters are head and flow coefficients, the volume ratio and the machine Mach number.

When keeping the flow coefficient the same as the design case, the velocity triangles at the inlet into the first stage remain the same. Together with the head coefficient, this defines a singular operating point of the compressor, as long as the fan law remains applicable. If the volume flow ratios between inlet and outlet are kept the same as the design case, the velocity triangle at the outlet of the compressor also will be the same. Generally, this requirement involves keeping the same machine Mach number over the machine (at least approximately).

For most applications, the Reynolds number similarity is of lesser importance because the Reynolds numbers are relatively high and clearly in the turbulent flow regime. Additionally, the loss generation in centrifugal compressors is only partially due to skin friction effects; i.e., due to effects that are primarily governed by Reynolds numbers.

Certain deviations between design and test case for these parameters are acceptable and unavoidable. In general, as long as the deviations between test and design stay within limits as described in ASME PTC-10 [1], or in ISO5389 [2] a simple correction based on the fan law can be used. Namely, the test point must be at the same combination of  $\phi$  and  $\Psi$  (Eq. 14 and 15) as the design point. The limitations of the fan law are also discussed by Brown (1991). Pipeline compressors, with usually only one or two impellers per body, are typically less sensitive to deviations from the above parameters (Figure 10-8). Multistage machines show more sensitivity.

During site performance tests (*Figures 10-2 and 10-8*), the test conditions may be considerably different from the design conditions, and could be outside of the limits established in ASME PTC-10 [1]. In more general terms, the fan law is no longer applicable, and easy corrections for Mach numbers and volume/flow ratios are not available. In this case, the design programs of the compressor manufacturer can be used to recalculate the compressor performance for the changed design conditions, that is new curves for head coefficient versus flow coefficient and efficiency vs. flow coefficient are generated for the new conditions.

ASME PTC-10 assumes for a Type 1 test where the test gas is almost identical to the gas for the specified acceptance conditions. In a field test, the gas composition cannot be controlled by the equipment manufacturer, and the test gas might deviate from the specified gas. In case the actual test gas deviates significantly, the compressor performance can be recalculated for the actual test gas.

Deviations also occur if the gas was specified incompletely, for example, by only defining the specific gravity rather than a full gas composition.

## INSTALLATION OF TEST EQUIPMENT

Appropriate test instrumentation, together with the location of the test instruments are specified in the aforementioned power test codes. The properties to be measured are pressures, temperatures, flows (which may also require pressure and temperature measurements) and speed.

### Site Performance Test Instrumentation

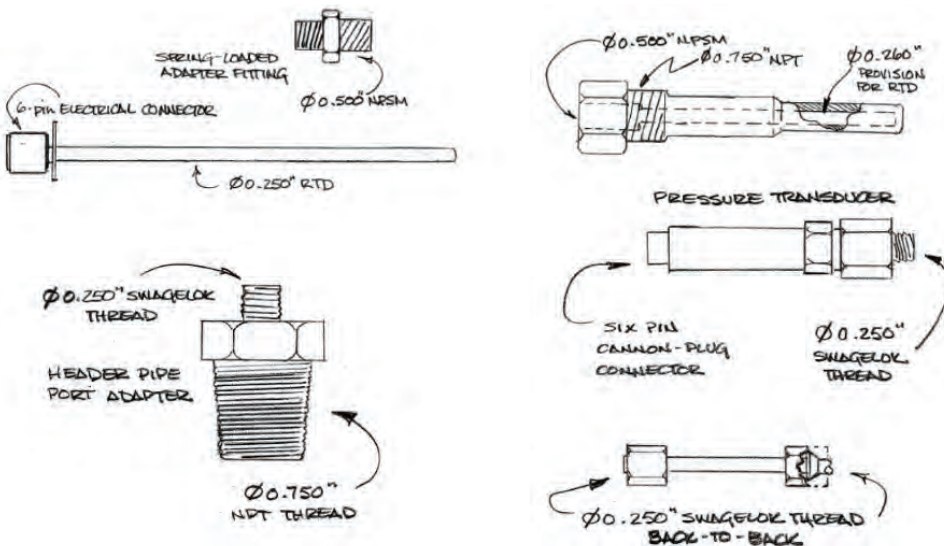
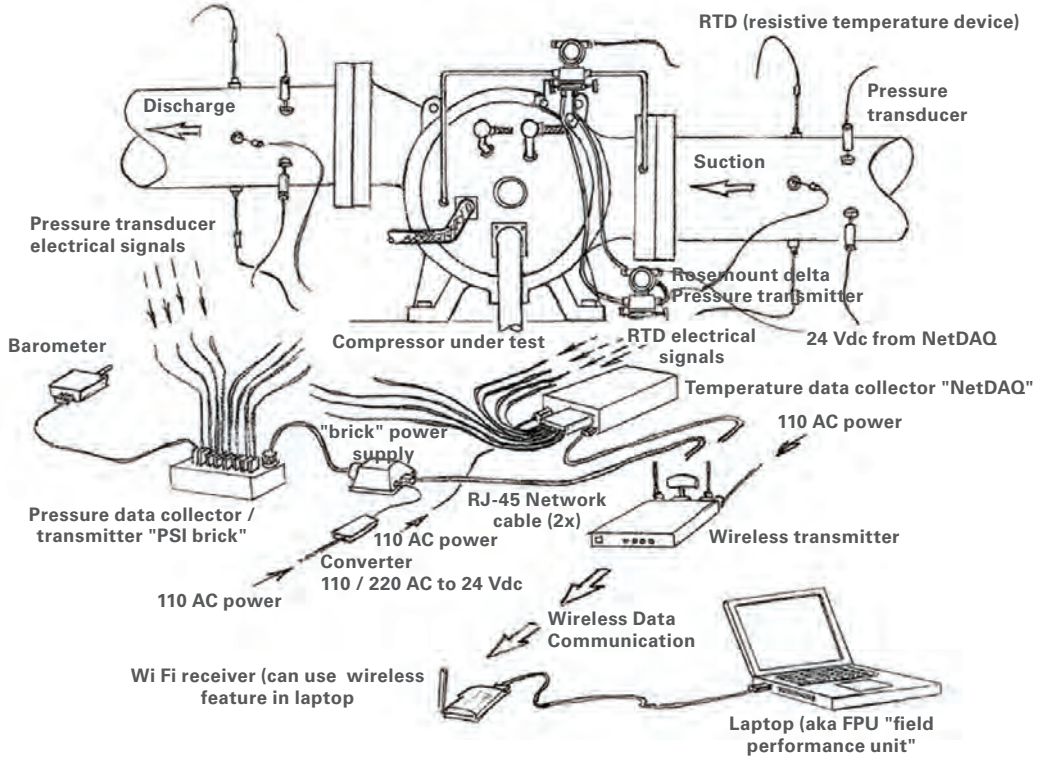
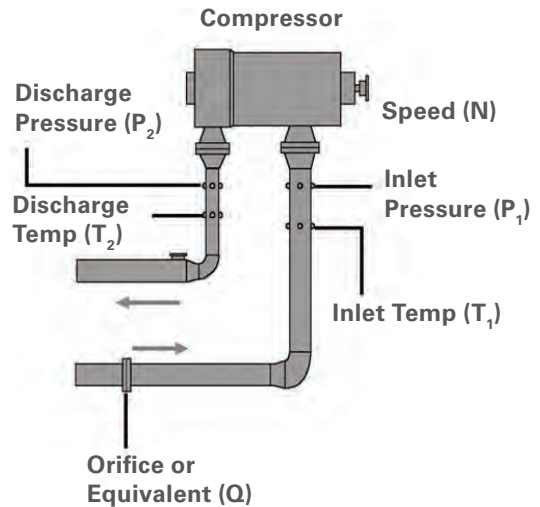


Figure 10-8. Field Test Installation

Provisions must be made during the construction phase of the gas compressor station to accommodate the installation of the necessary instrumentation, such as thermowells and pressure taps. If those instruments are not part of the permanent installation, block and bleed valves should be installed ahead of the pressure sensing device to facilitate change out during engine and/or compressor operation.

Sufficient lengths of straight pipe between measuring positions on the pipe and elements like elbows, valves, reducers and/or diffusers must be provided. The distance between gas compressor flanges and elbows (or a reducing transition upstream of the compressor) should be at least three pipe-inside diameters. If an expanding transition is located upstream of the gas compressor, there should be at least six diameters. The distance between the orifice plate and upstream elbows and valves should be at least ten inside pipe diameters of straight pipe. Downstream of the orifice should be at least five diameters. Inlet and discharge pressures and temperatures shall be measured at designated points. *Figure 10-9* shows a typical arrangement.

Instruments must be calibrated to a reference, and calibration certificates for all test instrumentation used for the performance test should be available.



**Figure 10-9.** Typical test instrumentation arrangement.

## FACTORY PERFORMANCE TEST DATA

If performance data from the factory test (or another, previously conducted site test) of the compressor is available, it is actually data from an independent test, using a different measurement chain. Deviations between this data and the data from the site test provides valuable insight into the test accuracy of both the factory test and the site performance test.

## SITE TEST CONDITIONS

It is recommended that three complete speed lines be tested in order to fully validate the compressor performance, however, process conditions do not always allow for the realization of three complete speed lines. If conditions do not permit testing of three speed lines, then the test should concentrate on the design point.

For each test point, data shall be taken during a 10-minute interval. At least three sets of data shall be taken. All data readings for one test point shall be scanned at the same instant.

For each individual acceptance point, a number of points, embracing the specified point, shall be taken and averaged.

Before readings are taken for any individual test point, steady-state operating conditions must be achieved. Steady-state is achieved if all of the following apply during the 10-minute interval:

- Operating speed constant within 5 rpm
- Fluctuations of the efficiency reading no larger than  $\pm 0.5$  points from average, while head and actual flow remain within  $\pm 0.5\%$  from average, respectively. This is significantly lower than the limits in other specifications [4, 5, 6], but it is achievable in practice.
- The driving gas turbine (where applicable) must be heat soaked for at least several hours (depending on the size and design of the gas turbine), if the compressor test point requires full load to avoid drift. In case of a drift, adjustments to maintain the allowable deviations can be made.

## MEASUREMENT PHILOSOPHY

Where several independent instruments are used to measure a pressure or a temperature value, the value of that pressure or temperature used for the evaluation will be the arithmetic average of the individual instrument's readings scanned at the same instant.

Where four independent instruments are used to measure a temperature or pressure value, and one recorded observation is inconsistent due to measurement error, its value will be discarded, and the value of the measurement determined from the average of the other three. Where fewer than four independent measurement devices are used, all values shall be used and averaged to determine the measurement value.

An attempt shall be made (depending on the actual conditions) to test at five or more operating points on the same speed line ranging from choke to as close to surge as conditions allow. The acceptance point shall be bracketed by two nearby test data points.

Site tests sometimes have to be performed without the steady-state operating conditions that are always achieved in factory tests. While steady-state conditions are desired, the following table gives an approximate increase of test uncertainties for absorbed power (ISO 5389-1992, [2]). Practical experience shows that deviations due to unsteady operation are underestimated by the data given in [2]. Any fluctuation in power higher than about 0.5% will add to the uncertainty of the results.

Fluctuation in absorbed power about the mean value (%)	Added Uncertainty (%)
2	0
3	0.5
4	1
5	2

**Table 10-1.** Impact of unsteady test conditions per ISO5389-1992.

**Data Reduction: How to get power, flow and efficiency from all these pressures and temperatures (Adapted from [5]).**

### SINGLE GAS COMPRESSOR

The flow through the compressor (as well as the gas turbine fuel flow) have been measured using one of several possible flow measuring devices. If the device is a flow orifice, the relationship between the flow and the measured temperatures and pressures is as follows:

$$W = C \cdot E \cdot \frac{\pi}{4} \cdot d^2 \sqrt{2 \cdot \Delta p \cdot \rho_1}$$

C and E are discharge coefficients and the velocity approach factor, respectively, and d is the orifice throat diameter. The coefficients can be determined either from the orifice manufacturer's data sheets or from such codes as ASME PTC-19.5 [6] or ISO 5167 [7].

Other devices (venturi, pitot-type probes, etc.) have formally similar relationships between the flow and the measured pressures and temperatures. Devices that do not use the pressure differentials (such as turbine flow meters, ultrasonic flow meters and Coriolis flow meters) will be supplied by their respective manufacturers with appropriate methods to calculate actual flow and standard flow or mass flow. It must be noted that, while the standard flow through the flow measuring device and the compressor are identical (as long as no leaks or flow divisions are present), the actual flow will be different because the pressure and temperature at the compressor nozzle will be different from the actual flow through the flow measuring device. For now, you can state that any flow measuring device will provide you with either the standard flow (SQ)<sup>1</sup> or the mass flow (W).

The knowledge of pressure and temperature at the compressor inlet nozzle enables calculation of the actual flow (Q<sub>s</sub>) with:

$$Q_s = \frac{W}{\rho_s} \quad \text{or} \quad Q_s = \frac{SQ \cdot \rho_{std}}{\rho_s}$$

<sup>1</sup>Standard conditions can be 60°F and 14.70 psia, 60°F and 14.73 psia, or 15°C (59°F) and 760 mm Hg (14.7 psia). Many countries use "normal" conditions, such as 0°C (273.15 K, 32°F) and 1013.25 mbar (1 atm, 14.7 psia).

The density in the above equations must be determined using an equation of state. The general relationship is:

$$\rho = \frac{P}{Z(p,T) \cdot R \cdot T}$$

The compressor head (H) can be determined from the measurement of suction and discharge pressure and temperature. The relationship between the pressure, temperature and the enthalpy (h) are defined by the equations of state described below.

By using the equations of state, the relevant enthalpies for the suction, the discharge and the isentropic discharge state can be computed. The isentropic head (H\*) is:

$$H^* = h(p_d, \Delta s = 0) - h(p_s, T_s)$$

The actual head H is<sup>2</sup>:

$$H = h(p_d, T_d) - h(p_s, T_s)$$

The isentropic and polytropic efficiencies then become:

$$\eta^* = \frac{H^*}{H} \quad \eta^p = \frac{H^p}{H}$$

It should be noted that the polytropic efficiency is defined similarly to the isentropic efficiency, using the polytropic process instead of the isentropic process for comparison. The actual head, which determines the absorbed power, is not affected by the selection of the polytropic or isentropic process. However, the isentropic head is unambiguously defined by the users process data (i.e., gas composition, suction pressure and temperature, discharge pressure), while the polytropic head for full definition additionally requires the compressor efficiency or the discharge temperature.

With the flow from above, the aerodynamic or gas power of the compressor, then, is determined to be:

$$P_g = \rho_i Q_i H = \frac{P_i}{Z_i R T_i} Q_i H$$

The absorbed power ('brake power') P is calculated by dividing the internal Power (Gas Power) by the mechanical efficiency  $\eta_m$ :

$$P = P_G / \eta_m = \frac{W}{\eta_m} [h(p_{t2}, T_{t2}) - h(p_{t1}, T_{t1})] = \frac{W}{\eta_m} \cdot \frac{H^*}{\eta^*}$$

<sup>2</sup>In US units, the enthalpy difference (BTU/lb) has to be multiplied by the 'mechanical equivalent of heat' (778.3 ft lb/BTU) to get the head (ft lb/lb).

After considering the mechanical efficiency ( $\eta_m$ ) (typically around 98 to 99%), which accounts for minor bearing, seal and windage losses, the absorbed (or "brake") power ( $P$ ) of the compressor becomes:

$$P = \frac{P_g}{\eta_m}$$

The determination of the surge point or the surge line is also related to measurements of head and flow. The main challenge lies in the fact that steady-state conditions are required for any of the measurements discussed herein. By definition, surge is a non-steady condition. Even close to surge, most readings start to fluctuate. The determination of flow at surge is, thus, much more inaccurate than measurements further away from surge.

The method to use increased vibration levels as an indication of surge, or incipient surge, is even more inaccurate because the increased vibration levels might be generated by the onset of rotating stall (which is by no means identical with the onset of surge) or other conditions.

## EQUATIONS OF STATE

The aero-thermodynamic performance of a gas compressor is defined by enthalpy and entropy differences, so an additional problem arises: enthalpies and entropies cannot be measured directly, but have to be calculated by the use of an Equation of State (EOS). The state of any fluid consisting of known components can be described by any given pair of its pressure, specific volume and temperature. EOS approximate these relationships. The equations can also be used to calculate enthalpy and entropy from the condition of a gas given by a pressure and a temperature (Baehr, [8]).

The simplest equation of state is the equation for a perfect gas:

$$p v = p/\rho = RT$$

$$H = h_2 - h_1 = c_p(T_2 - T_1)$$

$$H^* = c_p T_1 \left[ \left( \frac{p_2}{p_1} \right)^{\frac{k-1}{k}} - 1 \right]$$

Real gases and in particular gas mixtures, however, display complex relationships between pressure, volume and temperature (p-v-T). EOS use semi-empirical equations to describe these relationships, in particular the deviations from perfect gas behavior:

$$\frac{p}{\rho} = Z(p,t) \cdot R \cdot T$$

They also allow for the calculation of properties that are derived from the p-v-T relationships, such as enthalpy (h) and entropy (s). Because EOS are semi-empirical, they might be optimized for certain facets of gas behavior, such as liquid-vapor equilibriums and

not necessarily for the typical range of temperatures and pressures in various compression applications. Because different EOS will yield different values for density, enthalpies and entropies, the EOS has to be agreed upon before the test.

Usually, it is not possible to select a “most accurate” EOS to predict enthalpy differences, since there usually is no “calibration normal” to test against. All the frequently used EOS (RK, BWR, BWRS, LKP, RKS, PR) show reasonably correct enthalpies [9]. It is just not possible to decide which of them is more accurate for a given application (Kumar et al, 1999). Therefore, it is recommended to use the EOS for test data reduction that was also used for the performance prediction. This procedure is also recommended in VDI 2045 (1993) to avoid additional test uncertainties.

Figure 10-10 shows the effect of different EOS on the results for a given set of typical test data. The isentropic efficiency was calculated based on four equations of state, using the Redlich-Kwong equation as a reference. Depending on the pressure ratio, the four different EOS deliver four different results for the same measured conditions. For the calculations in the example, the following conditions were used. Suction condition was always at  $T_1 = 20^\circ\text{C}$  ( $68^\circ\text{F}$ ) and  $p_1 = 50$  bar (725 psia). The gas was compressed to varying end pressures ( $p_2$ ) with  $T_2$  chosen such that the reference EOS (RK) yields 80% efficiency. The results are shown in Figure 10-11. Differences as high as 2% exist among the EOS models. Clearly, it cannot be concluded that a certain EOS will always lead to higher efficiency than another EOS.

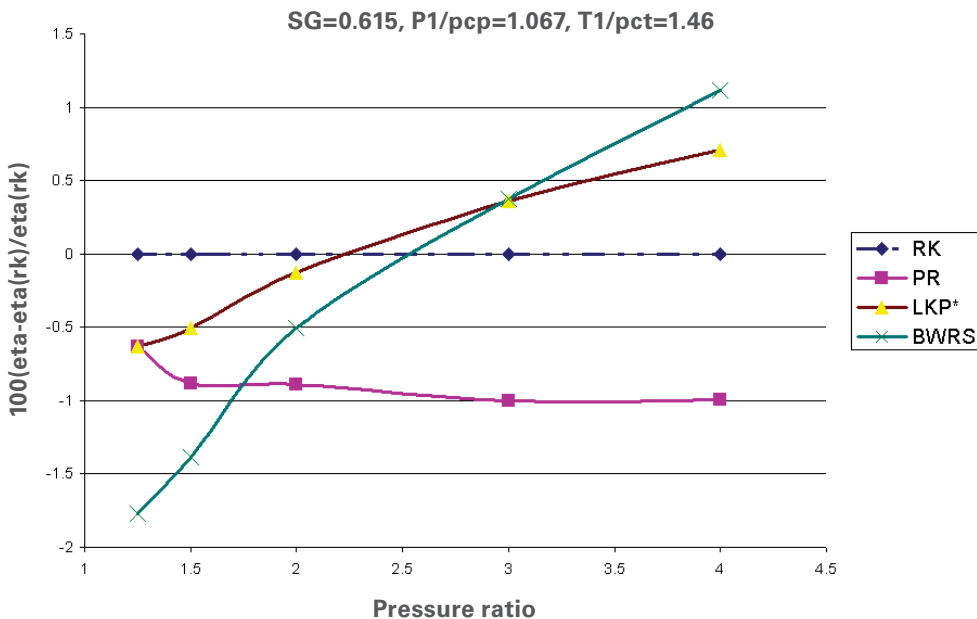


**Figure 10-10.** Isentropic efficiency differences among EOS for a natural gas mixture (when  $p_1 = 50$  bar (725 psia),  $T_1 = 20^\circ\text{C}$  (68oF) and varying  $p_2$ ,  $T_2$  chosen to give  $\eta = 80\%$  for RK EOS).

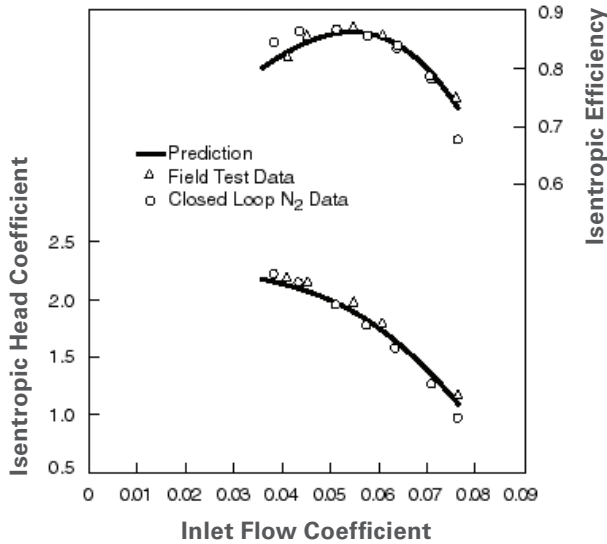


**Figure 10-11.** Comparison of results based on test with nitrogen and field test with natural gas.

An example shows the results of an actual compressor test (Figure 10-11). Identical configurations were tested with nitrogen and during a field performance test with a natural gas mixture containing about 95% methane (Kurz and Brun, 1998). The RK EOS was used to reduce the data. The close correlation between both sets of data is an indicator for the general validity and accuracy of the approach using EOS.

**Considerations for trains with multiple compressors**

In trains with multiple compressors, each compressor is treated individually, both as far as pressure, temperature, flow measurements and gas compositions are concerned, but also with regards to the design points. The latter requirement is due to the fact that site conditions rarely allow both (or all three) compressors to operate at their respective design points at the same time. Therefore, their power consumption has to be determined individually, and later added up. If all compressors are completely instrumented, the power requirement of the train (and thus the power generated by the driver) can be determined.

**Considerations for compressors with multiple sections**

The particular challenge for compressors with multiple sections is to correctly separate the absorbed power for the individual sections. The difficulty arises from the fact that there can be significant mass transfer (due to leakage across the division wall) and possibly heat transfer (again, across the division wall) from section to section. It should be noted that the measurement of the overall power consumption of the compressor is not affected by these internal transfers. However, they can lead to observed efficiencies that are too high for the first section, and too low for the second section, or vice versa. For compressors with n multiple sections, the absorbed power is:

$$P = \frac{1}{\eta_m} \cdot \sum_{i=1}^n P_{G,Section\_i}$$

This relationship is valid, as long as all flows in and out of the system are considered. Internal leakage does not affect it.

The main difficulty in the determination of the performance of individual sections lies in the fact that the interstage leakage has an impact on the observed section performance. The interstage leakage can be determined by either:

1. Measuring the flow into the first section inlet, the first section discharge and the second section inlet.
2. Measuring the flow into the first section inlet, measuring the flow into the second section inlet, and estimating the leakage flow based on theoretical considerations or factory test data.

Either method will yield the inlet flow used in the calculations above.

## **TEST CONDITIONS VERSUS REFERENCE CONDITIONS: COMPARING TEST DATA**

### ***Test Uncertainties***

Test uncertainties are an expression of the uncertainty of the measuring and testing process. For example, a machine tested with 84% efficiency may have an actual efficiency somewhere between 82% and 86%, assuming 2% test uncertainties.

The test uncertainty is basically a measurement of the quality of the test. An increased test uncertainty increases the risk of failing the test if the turbomachinery is actually performing better than the acceptance level, but it reduces the risk of failing if the turbomachinery performance is lower than the acceptance level. Because it is normal practice to use a lower performance than predicted as an acceptance criteria, it is in the interest of the manufacturer, as well as the user to test as accurately as possible (*Figure 10-12*).

Test uncertainties are caused by the following factors:

- Instrument accuracy and calibration
- Instrument location and installation
- Number of instruments
- Reading errors
- Unstable process

When considering instrumentation tolerances, the whole measuring chain needs to be considered. The instrument, such as the RTD, thermocouple or pressure transducer, has a certain accuracy and a certain quality of calibration. However, the overall error is also influenced by the location of the instrument (flow measurements with insufficient straight runs), the way the instrument is installed (thermocouples in thermowells without heat conductive paste or insufficient immersion depth), potential reading errors (especially if gauges are used), or the accuracy of the digital voltmeter, and the calibration quality.

Test uncertainties need to be clearly distinguished from building tolerances. They cover the inevitable manufacturing tolerances and the uncertainties of the performance predictions. The actual machine that is installed on the test stand will differ in its actual performance from the predicted performance by the building tolerances, which are entirely the manufacturer's responsibility.

Measurement uncertainty is a function of the specific measurement process used to obtain a measurement result, whether it is a simple or complex process. Measurement uncertainty analysis provides an estimate of the largest error that may reasonably be expected for the specific measurement process. If the measurement process is changed, then the uncertainty analysis must be reexamined and changed as appropriate. Errors larger than the stated uncertainty should rarely occur in actual laboratory or field measurements, if the uncertainty analysis has been performed correctly. [10]

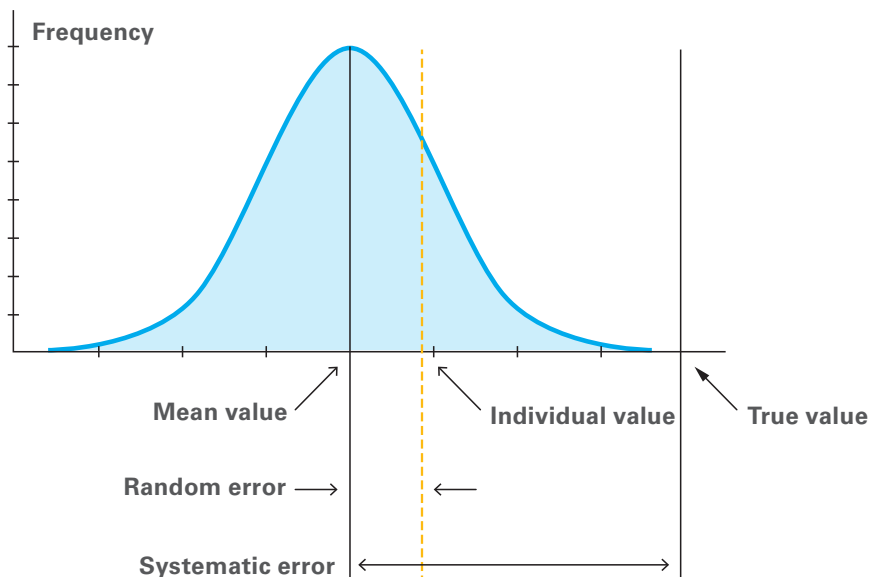


**Figure 10-12.** Simultaneously occurring systematic and random errors. [11]

Prior to any discussion about uncertainty, one should briefly clarify and differentiate the definitions of measurement accuracy, error, precision, linearity, bias, and hysteresis.

Error is defined as the difference between measured and true value and, thus, includes all sources that contribute to any variation between a measurement chain's input and output (Figure 10-12).

Accuracy is simply the lack of error, and it allows one to bound the range of output a measurement chain provides for a given input.

<sup>3</sup>We use measurement chain instead of instrument, since errors occur not just at the device, but due to the measurement location, data conversion etc.

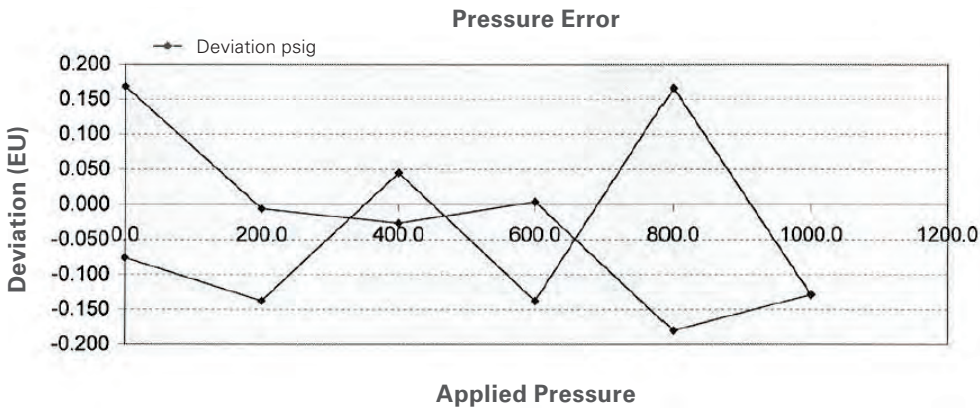


**Figure 10-13.** Hysteresis of a pressure transmitter.

Precision, linearity, hysteresis, and bias are somewhat less abstract in their definitions. Namely, precision defines the quality of reproducible measurements from an output reading. In other words, it is the number of significant digits a measurement chain provides with perfect accuracy. Linearity is a statistical term that compares the deviation of a system’s output to a straight-line assumption. Clearly, few physical systems behave linearly over a wide range and, thus, linearity must always be stated with an upper and lower limit. Linearity is usually determined from a statistical linear co-relation analysis with the result expressed as a “k-value”, where k=1.0 presents perfect linearity. Hysteresis (Figure 10-13) has nothing to do with an instrument’s accuracy degradation over time, but rather refers to the instrument’s (or system’s) output dependency on directionality of the input. In most cases, hysteresis is defined as the maximum difference in instrument reading for a given input value when the value is approached first with increasing, and then with decreasing input signals. Hysteresis is often caused by energy absorption in the elements of the measuring instrument or system.

Two fundamental types of errors must be distinguished (Figure 10-12):

**Random Error (Precision Error)** – Repeated measurements of a given performance parameter do not and are not expected to agree exactly. There are always numerous small effects which cause random scatter of the measured data. There is inaccuracy of the measurement of the control parameter (i.e. Trit) due to its random error. There is also the variation with time in either the performance parameter or the control parameter (also called the “set point”).

**Bias Error (Fixed Error)** – Occurs when there’s a systematic deviation of a measurement chain’s output from a fixed input. It results from several individual bias errors. The bias errors have to be estimated and included in the uncertainty analysis. Bias can be a complex functional form over the chain’s operational range, but in many cases, it’s just the consistent over or under reading of input data. A constant offset is the simplest example of bias. Unlike precision, bias can and should be eliminated during the instrument calibration process, but that is not always possible for the entire measurement chain. Since the bias has to be estimated, the estimate itself has an uncertainty. Thus, you can also treat the bias error as a normally distributed uncertainty. An example would be pressure measurements

in a pipe with non-uniform pressure distribution, where the non-uniformity is not known. Using an average value, with an estimated uncertainty is a possible approach.

Test uncertainty calculations distinguish between random and systematic errors. It is worthwhile to estimate the level of random errors present for typical site performance tests. For this purpose, a set of test data is evaluated. The calculated test uncertainty for systematic errors in isentropic head, actual flow and absorbed power was on average 2.3%, 2.5% and 2.6% respectively. The data was taken as follows: After steady state for a given operating point was established, one data point per second was taken for ten seconds. This was repeated five times. Then, the compressor was moved to a new operating point, and the process was repeated. The set of data contains 86 of the ten-second data sets. Within each of these 10-second data sets, the standard deviation for isentropic head, actual flow and absorbed power were calculated. While the standard deviation for isentropic head was always below 0.02%, the standard deviation for flow and power could be as high as 0.3%. In other words, in all cases, the impact was at least one order of magnitude smaller than the impact of the expected systematic test uncertainty.

This leads to the observation that for a well-conducted site performance test, random uncertainties are much smaller than systematic uncertainties. Based on observations on a large number of different site tests, this seems to be generally true.

All of the above are factors that contribute to, but are fundamentally different from the definition of measurement uncertainty. Uncertainty does not refer to a single instrument's accuracy, but evaluates the complete range of possible test results for a particular test condition. As previously stated, no test can be performed with all variables fixed, such that each input into the test system is a range rather than a point. Consequently, the measured output from the system must also be a range rather than a point, and must account for all possible input combinations of all input variables.

It is important to understand that if the input ranges to the system are defined as statistical bounds, such as 95% confidence intervals, then the output from the uncertainty analysis will also present the same 95% confidence interval statistical bounds. Similarly, if the inputs are absolute measurement errors, then the uncertainty analysis will also yield absolute errors. Therefore, whatever the type of uncertainty range is for the input variables, will also be the type of uncertainty range for the result. Consistent application and definitions of the input variable's uncertainty ranges is thus critically important in any uncertainty analysis.

Furthermore, prior to determining a test uncertainty, it is important to know whether the measured variables in the test are independent or dependent, as this determines the method of uncertainty calculation that must be employed.

The following are typical measurement uncertainties for the entire measurement chain:

- Pressure                    0.5 - 2.0%
- Temperature            0.5 - 4°F
- Flow                        0.5 - 2.0%
- Gas Composition        1.0 - 5.0%
- Torque                     1.0 - 1.5%
- Equation of State        0.2 - 2.5%

Further, if the process shows fluctuations, it will influence the accuracy of the test results. This assumes well calibrated instrumentation.

The use of package instrumentation leads to a considerably lower accuracy compared to tests conducted with dedicated test instrumentation, especially due to higher calibration standards for the test instrumentation. Package instrumentation is normally selected to allow for sufficient accuracy for trending. For trending purposes, the absolute accuracy of a measurement is not important, but rather the difference from certain baselines. Package displays usually do not take changes in gas composition into account. Furthermore, dedicated test instrumentation is calibrated on a regularly scheduled basis and maintained continuously.

Performing an uncertainty calculation to determine what possible conclusions can be drawn from the test data is a good practice.

For the uncertainty analysis [11,12,13,14], it is assumed that all measurement parameters can be considered to be independent, and that parameters have associated statistical bounds, such as a 95% confidence interval ( $\Delta u$ ), rather than absolute error limits. All parameters are also assumed to have Gaussian normal distributions around their respective mean values, such that the uncertainties can be properly combined using the root-square sum method. The total uncertainty ( $\Delta F$ ) for a given function,  $F = f(u_1, u_2, \dots, u_n)$  is, thus, determined from:

$$\Delta F = \sqrt{\left(\Delta u_1 \frac{\partial f}{\partial u_1}\right)^2 + \left(\Delta u_2 \frac{\partial f}{\partial u_2}\right)^2 + \dots + \left(\Delta u_n \frac{\partial f}{\partial u_n}\right)^2}$$

For this method, the overall uncertainty ( $\Delta F$ ) has the same statistical meaning as the individual uncertainties ( $\Delta u$ ). Namely, if  $\Delta u$  represents a 95% confidence, then the result for the total uncertainty ( $\Delta F$ ) is also a 95% confidence interval.

While many test procedures use the rigorous application of Eq. 20 to determine the uncertainty of test results, the method has its limitations: for complex relationships (e.g., when Equations of State have to be considered, or if, for a polytropic work and efficiency, a multistep iterative approach is used), the equation above is rather difficult to use because the partial derivatives of all variables are not easy to obtain.

An elegant way out is the following (Moffat, [12]). If a data reduction program exists (e.g., a program that calculates compressor shaft power from flow, pressure and temperature measurements), then the same program can be used to estimate the uncertainty of the result. This is accomplished by sequentially perturbing the input values by their respective uncertainties and recording their effects. Any term in Eq. 20 can be approximated (assuming that the error is relatively small) by:

$$\left(\Delta u_1 \frac{\partial f}{\partial u_1}\right) \cong f(u_1 + \Delta u_1) - f(u_1)$$

That means the contribution of the variable  $u_1$  to the uncertainty in  $f$  can be found by calculating  $f$  twice: once with the observed value of  $u_1$  and once for  $u_1 + \Delta u_1$ , and then subtracting the two values of  $f$ . When several variables are involved, the overall uncertainty

can be found by sequentially perturbing the individual variables ( $u_i$ ) and then finding the square root sum of the squares of the individual terms. This can be accomplished using a spreadsheet.

## TEST UNCERTAINTY SAMPLE CALCULATION

The test uncertainty calculation in this example follows the ASME PTC 19.1 Taylor Series Method (TSM) [13], for error propagation. Because the PTC 10 code uses an iterative method for the calculation of polytropic work and polytropic efficiency, the partial differentials in the Taylor series have to be replaced by finite differences.

It is assumed that the uncertainties for the temperature and pressure measurements are known, and the process gas is 100% methane, so the gas composition is not subject to uncertainties.

This example does not consider the uncertainty associated to the equation of state (EOS) that is used to predict the thermodynamic properties of the gas. As shown in the work of Sandberg, the ability to accurately determine the thermodynamic properties of the gas, and hence the performance of the compressor, can be influenced by the EOS that is selected for the evaluation. Special care is required during the test planning phase when selecting the appropriate EOS.

The relevant uncertainties that were used for pressures and temperatures include the systematic uncertainties of the entire measurement chain, and are determined according to ASME PTC-19.1 with a 95% confidence interval. It is further assumed for this example that the systematic errors in temperature and pressure are not correlated. ASME PTC-19.1 also provides guidance for correlated systematic errors.

The sample case uses the following conditions:

### **Sample Case**

<b>P1</b>	psia	1000
<b>P2</b>	psia	1891.1
<b>T1</b>	degF	100
<b>T2</b>	degF	209.4

### **Gas Composition** (Mol %)

**Methane** 100

The calculations for polytropic efficiency and polytropic work use REFPROP 9.1 [15, 16] for the thermodynamic calculations.

The systematic uncertainties of the measurement chains for temperatures and pressures with a 95% confidence interval used for the example are:

**T1:** 0.2°F

**T2:** 0.25°F

**P1:** 5 psi

**P2:** 9.45 psi

The sensitivity of the polytropic efficiency and polytropic work have been calculated using a perturbation analysis in which the expressions for these performance parameters are evaluated using the nominal values for the measured variables (inlet and discharge pressures and temperatures), and subsequently evaluated by implementing a perturbation (perturbation = nominal value + systematic uncertainty) in each one of the measured variables, while keeping the other variables at their nominal values (see *tables 10-2 and 10-3* below).

The total systematic uncertainty is calculated as:

$$Abs. Uncert = \sqrt{\sum (\Delta_i)^2}$$

Where  $\Delta_i$  corresponds to the difference between the value of the performance parameter (polytropic efficiency or polytropic work) evaluated under nominal conditions and the value for that parameter evaluated under the perturbed condition for variable  $i$ . Here, variable  $i$  represents P1, P2, T1 and T2.

*Tables 10-2 and 10-3* show the sample calculations for polytropic efficiency and polytropic work, respectively.

Parameter	Uncertainty	Nominal Value	P1	P2	T1	T2
P1 (psia)	5	1000	1005	1000	1000	1000
P2 (psia)	9.45	1891.1	1891.1	1900.55	1891.1	1891.1
T1 (deg F)	0.2	100	100	100	100.2	100
T2 (deg F)	0.25	209.4	209.4	209.4	209.4	209.65
Poly Effy	-	0.821	0.8123	0.8296	0.8231	0.8186
Delta squared ( $\Delta_i$ ) <sup>2</sup>	-	-	7.569E-05	7.4E-05	4.41E-06	5.76E-06
Abs. Uncert	-	0.012642	-	-	-	-

**Table 10-2.** Sample calculation of the systematic uncertainty for polytropic efficiency.

Parameter	Uncertainty	Nominal Value	P1	P2	T1	T2
P1 (psia)	5	1000	1005	1000	1000	1000
P2 (psia)	9.45	1891.1	1891.1	1900.55	1891.1	1891.1
T1 (deg F)	0.2	100	100	100	100.2	100
T2 (deg F)	0.25	209.4	209.4	209.4	209.4	209.65
Poly Head	-	34791.2	34512.5	35060.6	34782.8	34800.8
Delta squared ( $\Delta_x$ ) <sup>2</sup>	-	-	77673.69	72576.36	70.56	92.16
Abs. Uncert	-	387.8309	-	-	-	-
Rel. Uncert	-	0.011147	-	-	-	-

**Table 10-3.** Sample calculation of systematic uncertainty for polytropic work.

The results give a systematic uncertainty for polytropic efficiency  $b_x = 0.012642$  and for polytropic work  $b_x = 387.8309$  ft lb<sub>f</sub>/lb<sub>m</sub> (or 1.1147%).

ASME PTC-19.1 requires systematic and random uncertainties be treated separately. For the purpose of this example, assume a random uncertainty for head and efficiency, that would be found for a test with multiple data points for each test point, based on the analysis of the scatter of the test results, per ASME PTC-19.1 to be  $s_x = 0.003$  for polytropic efficiency and  $s_x = 40.1$  ft lb<sub>f</sub>/lb<sub>m</sub> for polytropic work.

The expanded uncertainty  $U_x$  then becomes (ASME PTC-19.1, Sect.5) for the polytropic efficiency:

$$U_x = \sqrt{0.012642^2 + (2 * 0.003)^2} = 0.013994$$

and for the polytropic work:

$$U_x = \sqrt{(387.8309 \frac{ft \ lb_f}{lb_m})^2 + (2 * 40.1 \frac{ft \ lb_f}{lb_m})^2} = 396.0364 \frac{ft \ lb_f}{lb_m}$$

with a confidence level of 95%.

The results would then be reported as follows:

Polytropic efficiency  $\eta_p = 0.821 \pm 0.014$

Polytropic work:  $W_p = 34791.2$  ft lb<sub>f</sub>/lb<sub>m</sub>  $\pm 396.0$  ft lb<sub>f</sub>/lb<sub>m</sub>

In the example above, it becomes immediately obvious that the major contribution to the uncertainty comes from the pressure data. In other words, in order to improve the accuracy of the results, the effort should be focused on improving the pressure measurements.

The example, very realistic, also shows the small impact of random uncertainty, which can well be neglected in its influence on the test results.

The beauty of this scheme lies in the fact that:

- It does not matter whether the uncertainty is given as an absolute or relative number.
- The procedure can be implemented using any of the commercial spreadsheet programs.
- Any value in the table can be the result of a complex, even iterative calculation.

More details about test uncertainty calculation can be found in [4,13,14,15]. It must be stressed that bias and random errors have to be treated separately. It also should be noted the method described is a valid adaption of ASME PTC-19.1 [13]. For performance curves, the influence of uncertainties on the values of both axis can be expressed by an uncertainty ellipse (*Figure 10-14*).

## INTERPRETATION OF TEST DATA

If the test data deviate from the predictions or from other test data by more than the level of test uncertainty, the reasons must be explored (*Figure 10-14*). Assuming the test data are reduced correctly, it must be determined whether the test conditions were close enough to the conditions for the prediction.

Using redundant data for comparison is usually desirable. Examples follow:

Determine the shape of the head-flow and flow efficiency curves, and compare them with predictions. If the curves are just shifted to the left or right, the flow measurement is suspect. Another necessary step is comparing the whole measured  $\phi$ - $\Psi$ - $\eta$  curve with the predicted curve. For compressors, it might be found that the head-versus-flow curves have just shifted horizontally, which points to an incorrect flow measurement. If some points of the curve match the predictions and others do not match, variations of the gas composition during the test could be the cause. Data from a site test for a compressor station close to several wells may serve as an example. The solid line represents the prediction for head and efficiency, the symbols indicate test data taken during two tests. Test 1 experienced significant fluctuations in gas composition, while test 2 was somewhat more stable.

Additional evidence may come from a comparison between compressor absorbed power and expected driver available power: Determine the absorbed power and compare it with the expected power from the driver. For a gas turbine, full load factory test data is usually available. The compressor should be operated at a point that requires the gas turbine to operate at full load. The absorbed compressor power should be close to the factory-tested gas turbine power (corrected to the site test conditions regarding ambient conditions and power turbine speed), assuming the gas turbine is in new and clean condition. For compressors driven by an electric motor, the motor, gearbox and VFD efficiencies can be used to compare the measured electric power consumption to the absorbed compressor power.

**Head and Efficiency Low:** A comparison to available other test data should be made. If the head was already low in a factory test, then the results from the site test may just confirm the factory test findings. A wrong flow measurement can make the compressor look like it's not producing the correct head and efficiency (see above). Other reasons include damaged impellers, or damaged seals. Both issues can be eliminated by visual inspection, if possible. Damaged balance piston seals can also be detected by monitoring the pressure (or flow) in the balance piston return line. Ingested inlet strainers that are caught in the inlet (or other obstructions) can cause significant pressure drop between the measurement location and the actual compressor inlet, thus generating the false impression that the compressor is low in head and efficiency.

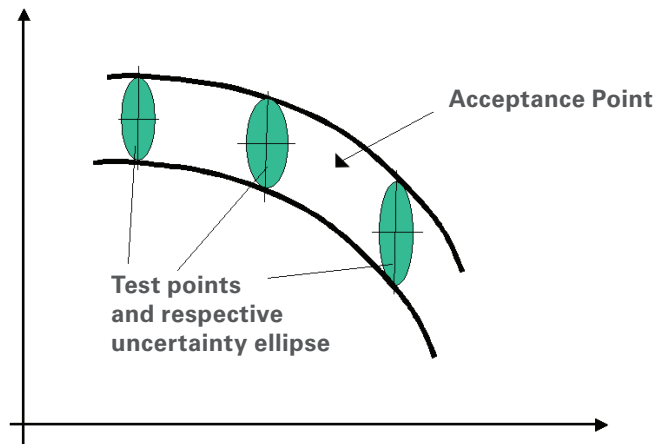


**Figure 10-14.** Uncertainty

Any data taken must be corrected to the same datum conditions. For gas compressors, the non-dimensional curves are a good tool. However, large deviations in Mach number especially in multistage machines, need to be avoided (Figure 10-15). The effects of

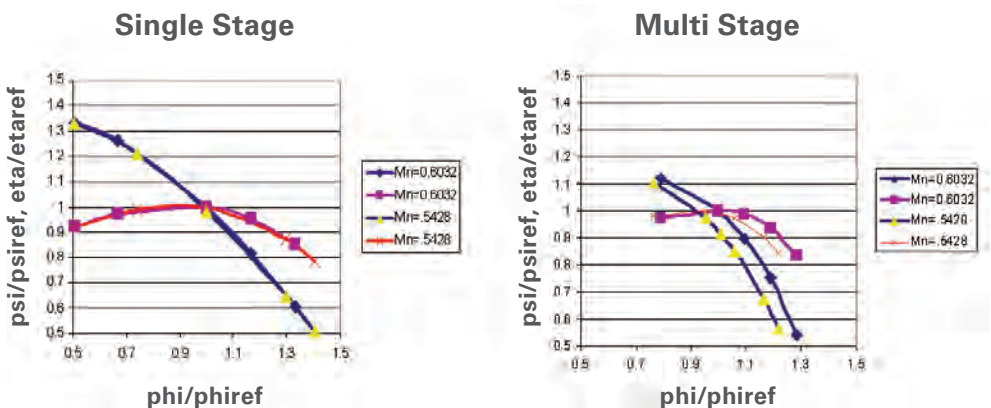


**Figure 10-15.** Impact of machine Mach number deviations for single-stage and multi-stage machines.

different Mach numbers or different volume/flow ratios ( $Q_s/Q_d$ ) may be responsible for the deviations. In such cases, it is always helpful to repeat the prediction procedure for the actual test conditions.

In many instances, redundant measurement can increase the confidence in the results. The compressor gas power can be checked by comparing the results with the gas turbine power and heat rate from the factory test, corrected to site test conditions (Kurz, 1999). In this case, it is also recommended to thoroughly clean the gas turbine air compressor prior to the test: 3% and more engine power has been recovered after cleaning the air compressor. Electric motors allow a convenient measurement of the electric power input. Corrected by the motor efficiency, the gearbox efficiency, the losses in the variable frequency drive (if applicable), and the motor shaft power can be calculated and compared to the measured compressor power.

## **INSTALLATION OF TEST EQUIPMENT**

During construction of a gas compressor station, provisions must be made to accommodate the installation of necessary instrumentation, such as thermowells and pressure taps, if not part of the permanent installation. Block and bleed valves should be installed ahead of the pressure-sensing device to facilitate change out during engine and/or compressor operation.

Sufficient runs of straight pipe between measuring positions and components such as elbows, valves, reducers and/or diffusers must be planned. The distance between gas compressor flanges and elbows (or a reducing transition upstream of the compressor) should be at least three times the pipe's inside diameter. If an expanding transition is located upstream of the gas compressor, there should be at least six inside pipe diameters. The distance between the orifice plate and upstream elbows and valves should be at least ten inside pipe diameters of straight pipe. Downstream of the orifice, pipe should be at least five diameters.

Inlet and discharge pressures and temperatures shall be measured at agreed-upon points. *Figure 10-9* shows a typical arrangement. Instruments must be calibrated to reference, and calibration certificates for all test instrumentation used during the performance test should be available.

## **FACTORY PERFORMANCE TEST DATA**

If compressor performance data from the factory test (or another, previously conducted site test) is available, it is actually data from an independent test, using a different measurement chain. Deviations between this data and the data from the site test provides valuable insights into the accuracy of both the factory test and the site performance test.

## **SITE TEST CONDITIONS**

Three complete speed line tests are recommended in order to fully validate compressor performance, however, process conditions don't always enable completion of three complete speed line tests. If that's the case, then testing should concentrate on the design point. For each test point, data should be taken during a 10-minute interval. At least three sets of data should be taken. All data readings for one test point shall be scanned at the same instant. For each individual acceptance point, a number of points, embracing the specified point, shall be taken and averaged.

### **OPERATING SPEED CONSTANT WITHIN 5 RPM**

Before readings are taken for any individual test point, steady-state operating conditions must be achieved. Steady state is achieved if all of the following apply during the 10-minute interval.

- Operating speed remains constant within 5 rpm
- Fluctuations of the efficiency reading no larger than +/- 0.5 points from average, while head and actual flow remain within +/- 0.5% from average, respectively. This is significantly lower than the limits in other specifications [14], [16], but is achievable in practice.
- The driving gas turbine (where applicable) must be heat soaked for at least several hours (depending on the size and design of the gas turbine), if the compressor test point requires full load to avoid drift. In case of a drift, adjustments to maintain the allowable deviations can be made.

## **MEASUREMENT PHILOSOPHY**

Where several independent instruments are used to measure a pressure or a temperature value, the value of that pressure or temperature used for the evaluation will be the arithmetic average of the individual instrument's readings scanned at the same instant.

It is good practice to perform a test uncertainty calculation as part of data gathering and evaluation process. Obviously, data with an uncertainty of 3% cannot yield conclusions that require an accuracy of 1%. If the test point does not match the prediction or other test results, a test uncertainty ellipse (can be drawn). The two axes of the ellipse represent the test uncertainties for the parameters on the x and y axis, respectively. If it still covers the prediction, the test results might be correct. The uncertainty ellipse in Figure 10-14 expresses the fact that not only is the measured power subject to test uncertainties, but also the ambient temperature. When comparing field test results with factory tests, the influence of test uncertainties in both tests must be considered. Whatever factory test results are available can be used for comparison and verification purposes. Whatever the deviation might be, it is best if it can be detected, discussed and possibly corrected during the test. A good relationship with a trusted manufacturer can help in finding causes for discrepancies.

Another reason for test data discrepancies can be found in the way the test is conducted. If the test data wasn't gathered while the equipment operated under steady-state conditions, they may not be useful. The requirements for steady-state operation are mentioned above.

The time requirement to achieve heat soaking should be provided by the gas turbine manufacturer. As a rule of thumb, one hour is required for smaller engines (below 8000 hp), while larger engines may require two or more hours. A well conducted test will yield repeatable and reliable results. In *Figure 10-16*, the results of several tests at two different stations, including data for four identical compressors, tested consecutively, can serve as proof for this statement.

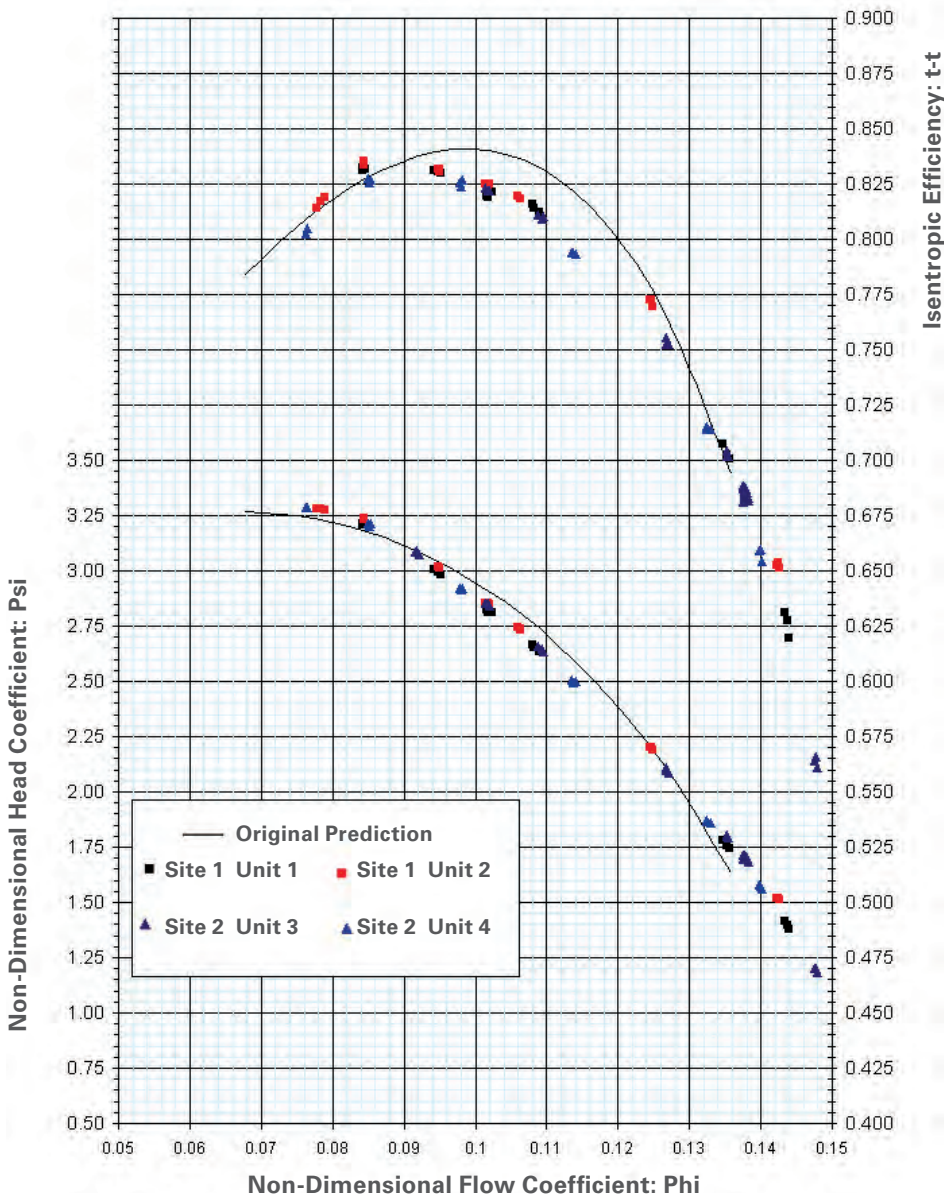


**Figure 10-16.** Repeatability of field tests.

## CHAPTER 10 REFERENCES

- [1] ASME Performance Test Code, PTC 10 -1997, Performance Test Code on Compressors and Exhausters', The American Society of Mechanical Engineers, New York 1997.
- [2] ISO 5389-1992, 1992, "Turbocompressors – Performance Test Code," International Standards Organization.
- [3] Brun, K., Nored, M., 2006, Guideline for Field Testing of Gas Turbine and Centrifugal Compressor Performance, Release 2.0, Gas Machinery Research Council.
- [4] Kurz, R., Brun, K., Legrand, D.D., 1999, "Field Performance Testing of Gas Turbine Driven Compressor Sets," 28<sup>th</sup> Turbomachinery Symposium, Houston, TX.
- [5] Kurz, R., Brun, K., 2005, Site Performance Test Evaluation for Gas Turbine and Electric Motor Driven Compressors, Proc. 34<sup>th</sup> Turbomachinery Symposium, Houston, TX.
- [6] ASME PTC 19.5, 2004, Flow Measurement.
- [7] ISO 5167, 1980, Measurement of fluid flow by means of pressure differential devices inserted in circular cross-section conduits running full.
- [8] Baehr, HD, 1981, Thermodynamik, Springer, Berlin.
- [9] Kumar, S.K., Kurz, R., and O'Connell, J.P., 1999, "Equations of State for Gas Compressor Design and Testing," ASME Paper 99-GT-12.
- [10] Wells, C., 1992, Measurement Uncertainties Analysis Techniques Applied to PV Performance Measurements, NREL TP 411-4125.
- [11] Haesselbarth, W., 2006, Guide to the Evaluation of Measurement Uncertainty for Quantitative Test Results, Eurolab Technical Report 1/2006.
- [12] Moffat, Robert J. "Identifying the True Value-The First Step in Uncertainty Analysis." Proceedings of the 34<sup>th</sup> International Instrumentation Symposium. Instrument Society of America, May 1988.
- [13] ANSI/ASME, Measurement Uncertainty. Supplement to ASME Performance Test Codes, PTC 19.1-1985. The American Society of Mechanical Engineers, New York 1985.
- [14] Brun, K., Kurz, R., 2001, Measurement Uncertainties Encountered during Gas Turbine Driven Compressor Field Testing, TransASME JEGTP, Vol. 123, pp.62-69.
- [15] American Gas Association (AGA) Report No. 8, 1994, "Compressibility Factors of Natural Gas and Other Related Hydrocarbon Gases."
- [16] Kunz, O., Wagner, W., 2012, "The GERG-2008 Wide Range Equation of State for Natural Gases and Other Mixtures: An Expansion of GERG-2004," J. Chem. Eng. Data, 2012, 57(11), pp 3032-3091.





## CHAPTER 11

# RESTAGE: CENTRIFUGAL GAS COMPRESSORS

*Avneet Singh, Rainer Kurz*

Compressor installations in the gas transmission and production industry are subject to changing operating conditions. Many pipelines typically experience seasonal variations in conditions, as well as different daytime and nighttime operations. Many industry production operations are faced with continuously changing well conditions or declining well production. A wide-range, well-designed compressor can provide operational flexibility to handle these changing conditions.

Even though centrifugal gas compressors driven by gas turbines provide tremendous operational flexibility, the economics of restaging make them a great option to optimize operations when facing new circumstances or conditions. While primarily driven by compressor efficiency gains, flow capabilities and/or improvements in fuel efficiency, important restaging considerations also include downtime costs and the ease of restaging.

Most turbomachinery OEMs use similar design tools such as CFD, FEA and CAD, manufacturing technologies and developmental testing in their design processes. Gas compressor products, however, are distinctly different due to different design philosophies. For example, some OEMs design compressors with high efficiencies within a narrow range by using low-solidity airfoil (LSA) vaned diffusers, while other OEMs design compressors that can be operated across a wide flow range with acceptable efficiencies.

While it's important to offer high-efficiency gas compressor solutions to meet the initial conditions: pressure, temperature, gas composition, flow, etc., changes in operating conditions such as gas field depletion and natural gas demand increases are the primary considerations in production- and pipeline-compressor applications. Of equal importance is the ability to easily restage gas compressors to reduce life-cycle costs and minimize downtime costs.

### **GAS COMPRESSOR DESIGN PHILOSOPHIES**

Aerodynamics, rotordynamics and mechanical design are the three primary technical focuses of gas-compressor design. Serviceability must also be part of the design criteria, as gas compressors can be in service for many years or even decades. The operating conditions are different for every compression project. Depending on the specific requirements, compressors have to handle different operating parameters such as flows, suction and discharge pressures, suction temperatures, gas compositions, power levels and train configurations, as well as specific customer requirements. To cover all different applications in the oil and gas industry, manufacturers either employ pre-engineered, standardized compressors, or some level of design customization.

The difference between these two approaches is not in the sophistication of the design, nor in the capability to show better performance under project-specific operating

conditions. The main difference is that customized designs are engineered to perform on a specific project, while most—if not all engineering for pre-engineered designs—are completed long before an order is placed. This also includes the testing required for design verification.

Standardized designs utilize pre-engineered components and pretested designs. For a specific application, aero components are selected from a family of impellers and stators, which have already been tested individually or inside a compressor. This approach to pre-engineered design provides a shorter response time, as well as proven performance and durability. Compressor aero performance characteristics are predicted and continuously refined through test data. Since a particular family of aero components can cover a large flow range as shown in *Figure 11-1*, different staging combinations can replace the existing staging to optimize the operation based on a new set of conditions. This is called compressor restage. The rotordynamic stability envelope also has to be verified by testing as shown in *Figure 11-2*. This standard design method reduces the risk to a minimal level, for both users and OEMs.

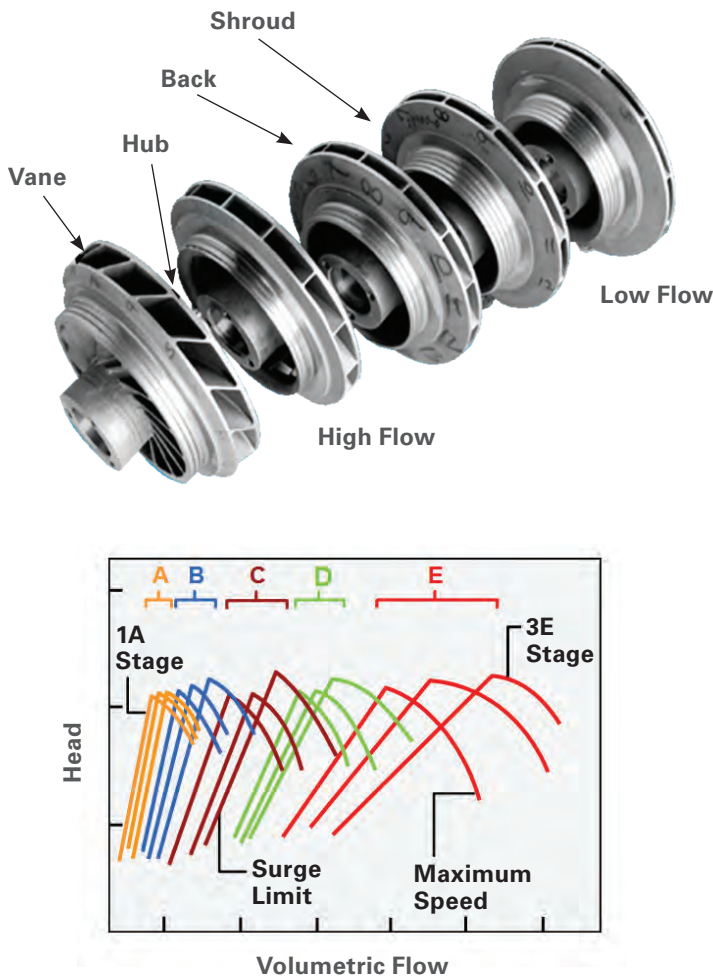


**Figure 11-1.** A typical impeller family and performance curves.

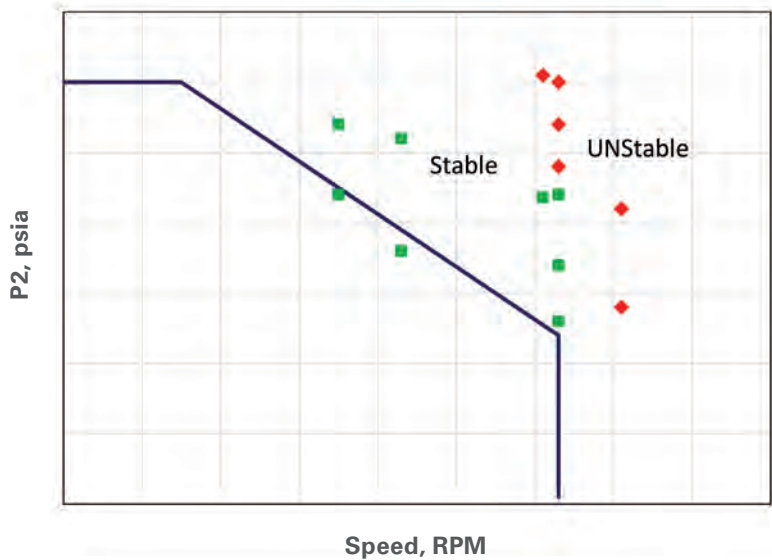


**Figure 11-2.** A typical stability envelope as related to compressor speed.

After new equipment is installed, the maintenance requirements for centrifugal compressors are minimal. Two major events must be considered during the machine’s operation:

- Damage due to foreign object debris (FOD)
- Large change in operating conditions to the extent that the economics favor a restage of the compressor (or, in extreme cases, the addition or removal of a compressor body).

Although rare, damage due to FOD creates the need for an immediate response to restore the capability to operate the station, especially if there is limited or non-existent stand-by capacity. If only stationary components (like inlet vanes) are damaged, the operation may continue. If impellers are damaged, they must be replaced. Often in situations like this, only the first stage is damaged. Designs that facilitate quick replacements provide a significant advantage in operational downtime. The latter event is usually planned. Frequently, operating conditions change gradually, and the point where a compressor restage makes economic sense is predictable.

In pipeline applications, the economics of restage are most likely dictated by the potential improvement in throughput capacity, or the opportunity to reduce fuel consumption and corresponding emissions. Avoiding recycle, as well as avoiding operation in choke, while neither damaging nor disruptive, can fall in either category. For oil production applications, the ability to lower suction pressure drives compressor restages. These questions supported by case studies will be addressed later in this chapter.

Economics also raise questions involving cost and downtime. While many OEMs recommend the replacement of the entire rotor and stator components if a restage is required, opportunities to make use of existing hardware exist, if the compressor design is conducive to component reuse.

## MODULAR DESIGN

The modular rotor design was recognized by API [1]. As shown in *Figure 11-3*, stub shafts, impellers, and spacers (if needed) are bolted together to form a modular shaft. The tie-bolt is stretched to a level that the torque can be transmitted through the interface between components.

In the standard design method, one of the key concepts is that all the aerodynamic components from one compressor family must be mechanically interchangeable. Modular design is a way to take full advantage of interchangeable aerodynamic components. With modular rotor design and interchangeability of aero components, the compressor can have thousands of combinations within a common mechanical design.

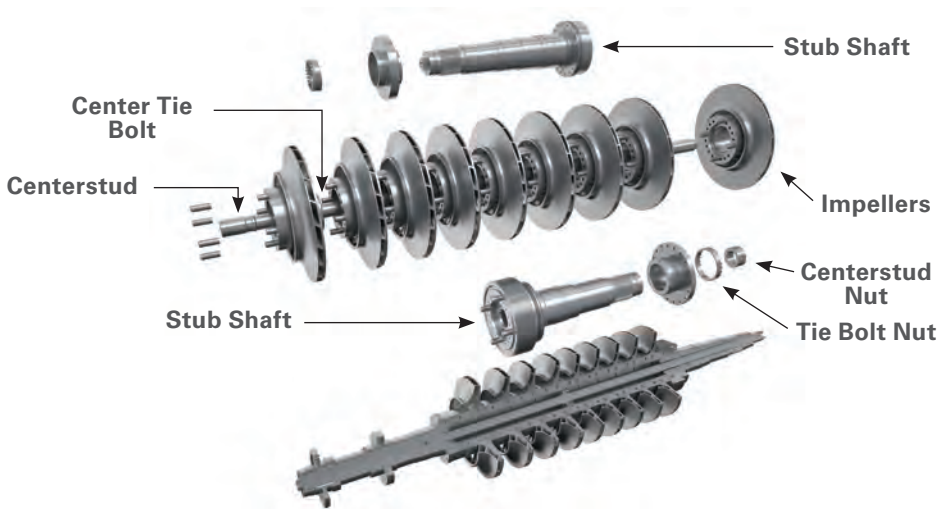


**Figure 11-3.** A typical modular rotor design.

Traditionally, the industry has used solid-shaft rotor construction methods. The impellers are shrink-fitted onto a solid shaft. The rotor is centered by two halves of stationary components, which is called a split-case design. When the compressors run as designed under clean gas and at design conditions, the difference between solid shaft and modular shaft designs is negligible (*Figures 11-4 and 11-5*). But when the compressor requires overhaul or restage, there is a significant difference in terms of cost, lead time, and sustainability between both designs. Modular rotor design is easier to disassemble since it doesn't require the expensive and difficult shrink-fit process. Thus, it is more restage and overhaul friendly. The impellers that can be reused are easily salvaged to reduce the cost and minimize downtime. The impellers that are displaced by the compressor restage can be stored for use in future restages.

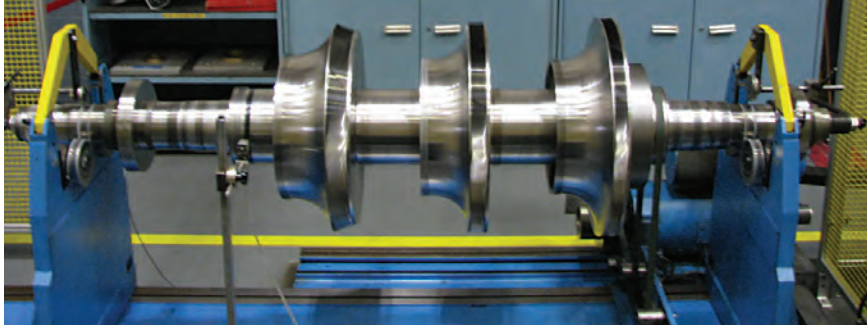


**Figure 11-4.** A typical modular rotor on the balance machine.

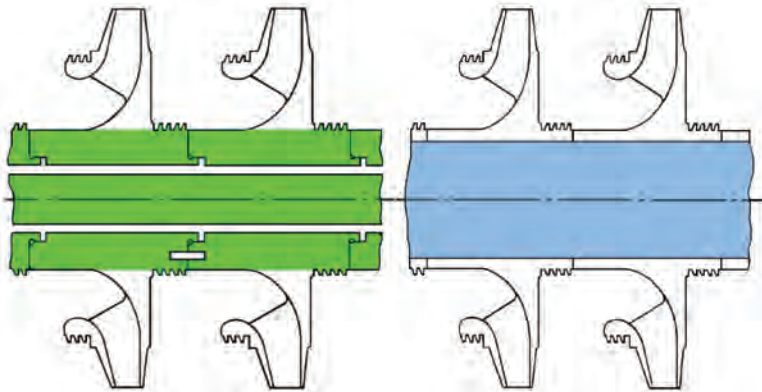


**Figure 11-5.** Comparison of modular rotor (left) to solid-shaft rotor (right).

The main concern with the modular rotor is rotor stiffness. In 2009, J. Moore and A. Lerche [2] evaluated an industrial tie-bolt rotor against an equivalent solid rotor and concluded that modular rotor design met the required API separation margin criteria. Not only that, the solid rotor has a higher amplification factor and unbalance response. The solid rotor has about 10% lower log decrement value and lower stability threshold than the modular rotor (Figure 11-5). Comparison of modular rotor (left) to solid-shaft rotor (right).

## ENGINE MATCHING

The centrifugal compressor and its driver have to be matched regarding speed and power consumption. When using electric drives, the match between compressor and driver is done via a gearbox, which also adds torsional damping to the system. When matched with a two-shaft gas turbine, good practice is matching the compressor speed at the design point or the rated point with the power turbine operating in the vicinity of its optimum speed. In general, the more powerful the gas turbine, the slower its power turbine wants to run. For example, while a gas turbine in the 6000 hp class has a maximum power turbine speed of 16500 rpm, a 20000 hp class gas turbine may have a maximum power turbine speed roughly half that number.

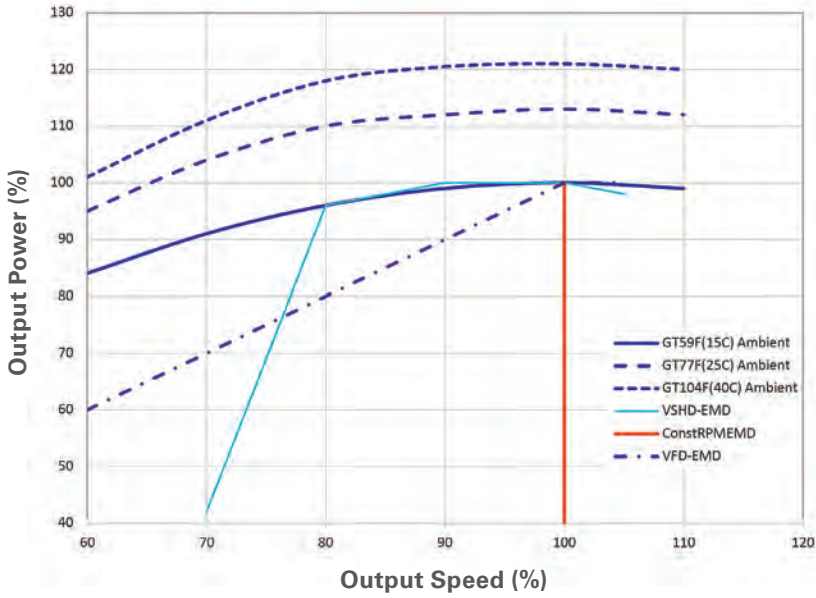


Figure 11-6. Speed-power characteristics of compressor drivers.

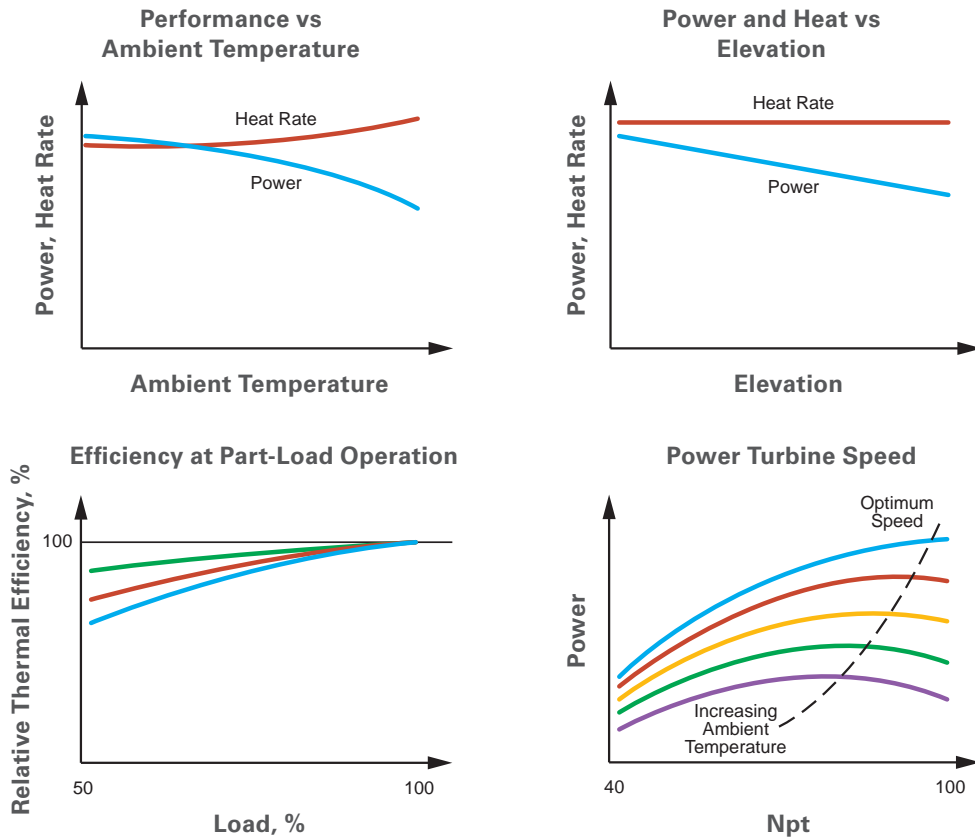


Figure 11-7. Four gas turbine performance characteristics.

Understanding the speed-power characteristics of different drivers is also important. While a power turbine actually produces more torque at low speeds than at high speeds, a VFD driven electric motor produces constant torque at best (*Figure 11-6*). If the driver is a gas turbine, other factors must be considered (*Figure 11-7*). Gas turbine uprates at engine overhauls may provide more power than originally installed. One manufacturer over the years brought an engine that was originally introduced at 10,000 hp in several steps to a power level of 16,000 hp today. The gas turbine provides far more power on cold days. Operating the gas turbine fully loaded is also advantageous.

## PRINCIPLES OF GAS COMPRESSOR RESTAGE

### Gas Compressor Performance

In reality, gas conditions always change in either pipeline or production compressors. If conditions oscillate around the design point for a typical wide-range compressor, no restaging is needed. However, when conditions change in one direction away from the design point, compressor restaging should be considered.

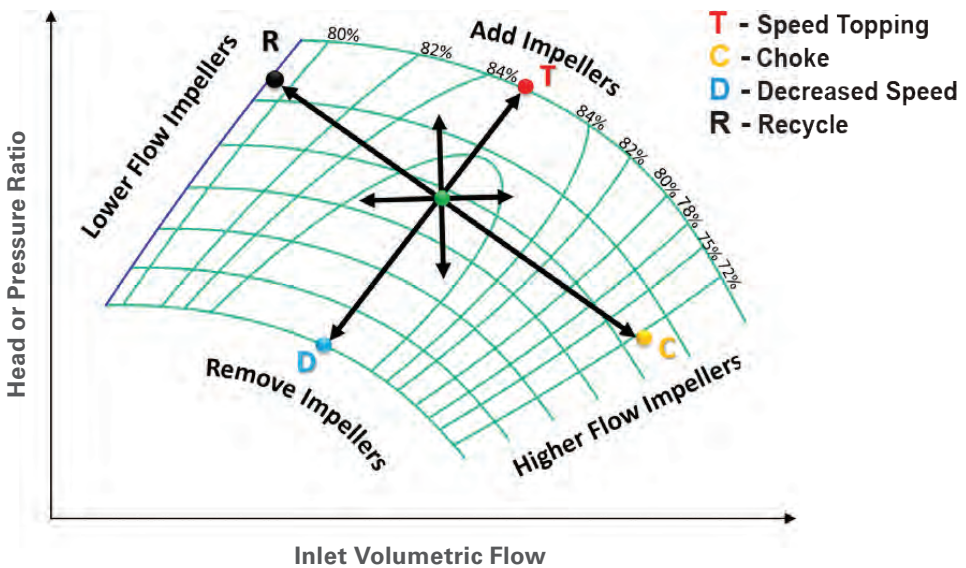


**Figure 11-8.** A typical multistage compressor flow-head map.

Essentially, six key parameters define gas compressor performance: Inlet/discharge temperature/pressure, flow, and speed for a given gas composition. Gas properties such as specific gravity, specific heat ratio, specific heat and compressibility also affect compressor performance. Changes of the above mentioned parameters may require speed and power changes.

$$H_{isen} = \frac{29.27}{SG} \times \frac{k}{k-1} \times Z \times T1 \times \left[ \left( \frac{P2}{P1} \right)^{\frac{k-1}{k}} - 1 \right]$$

$$H_{actual} = Cp \times (T2 - T1)$$

$$\eta_{isen} = \frac{H_{isen}}{H_{actual}}$$

Where:

- Cp is specific heat ratio at constant pressure
- $H_{isen}$  is isentropic head
- $H_{actual}$  is actual head
- k is specific heat ratio
- P1/P2 is inlet/discharge pressure
- T1/T2 is inlet/discharge temperature
- SG is specific gravity
- Z is compressibility factor
- $\eta_{isen}$  in the above equations is isentropic efficiency

The temperature, pressure and gas properties are combined into two terms: isentropic head and isentropic efficiency as shown in the three equations above. The two combined parameters plus flow and speed are the four key parameters applicable to evaluating compressor performance, which is typically shown in a Head-Flow map (*Figure 11-8*).

The effects of temperature, pressure and gas composition mainly move the operating point in the T (speed Topping) or D (speed Decreasing) direction as these parameters mainly affect head as shown in the second equation.

When suction temperature is increased from the original design point, more head will be created for the same pressure ratio, and higher speed will be required to move the new flow point in the T direction. The temperature also changes the map slightly. Higher temperature tends to tilt the map in the counter-clockwise direction.

Suction pressure also moves the point in the T or D direction. For a typical declining gas field, the suction pressure reduces over time. To reach the same discharge pressure, a higher pressure ratio requires increased speed and more flow passing through the compressor as gas density declines. The point moves in the T direction. In cases where the suction pressure increases, the point moves in the D direction, as the required head reduces. The same principle applies to discharge pressure: when it increases, the pressure ratio increases with the same suction pressure. More head is needed, and the point moves in the T direction. If the pressure ratio decreases, the point moves in the D direction.

Gas composition typically changes over time, especially in production applications. Heavier gas (larger Specific Gravity) requires less power to reach the same pressure ratio, thus decreasing speed requirements. Since the flow does not change much, the flow

point moves down vertically. Heavier gases also tilt the map in the clockwise direction. Therefore, the flow point moves in the D direction. Lighter gas behaves oppositely, so the flow point moves in the T direction.

The flow change effect is easier to explain. If more flow is needed, the flow point moves in the C direction to the Choke side of the map. If more flow is needed at constant power consumption, the flow point moves downward to the Choke side in the C and D direction. If more flow is required at constant head, the flow point moves horizontally to the Choke side.

Compressor efficiency is mainly a function of flow. When more flow is needed, the flow point moves in the C direction, and efficiency drops fast from the best efficiency point. At lower isentropic efficiencies, the discharge temperature increases quickly at the same level of head. More power is lost due to a less-efficient compressor. If less flow is needed, the flow point moves in the R direction to the surge side of the map, where decay in efficiency is less rapid. As typical in production applications, insufficient flow may move the operating point to the left of the surge line, requiring the anti-surge valve to open in order to protect the compressor from surge. In this situation, power is wasted by recycling the gas through the compressor.

### **Gas Compressor Restage Principles & Value Proposition**

The energy balance of the whole power train from engine (or other drivers) to the compressor can be expressed in the equation 4 below. The isentropic head and efficiency, as well as the flow of the gas compressor were discussed in the above explanation. The standard flow is a function of actual flow under standard conditions.

The power needed to produce the head is also affected by the engine efficiency and mechanical efficiency. Mechanical efficiency is relatively constant and engine efficiency is mainly a function of speed.

$$Power = C \times \frac{SQ}{\eta_{isen} \eta_{mech}} H_{isen} = FuelEnergy \eta_{engine}$$

Where:

- Power is driver (engine) output power
- C is a constant
- SQ is standard flow
- $\eta_{mech}$  is mechanical efficiency
- $\eta_{engine}$  is engine efficiency

At the design point, the efficiency terms are optimized so that the compressor can produce the required flow and head with minimum power. When the flow point stays away from the design point for an extended time, the compressor or engine is running less efficiently, which requires more power. The purpose of a gas compressor restage is to reoptimize

the compressor staging in order to maximize efficiency at the new conditions, thereby minimizing the power consumption or maximizing flow, head, or both.

Increasing discharge pressure for gas injection and gas gathering for a declining field (lower suction pressure) are two typical scenarios in which the flow point moves in the T direction. The compressor has to be rotated faster to maintain the same pressure ratio until eventually the power turbine or compressor itself reaches maximum speed. This is a typical speed topping case. By adding additional stages to the compressor, the required speeds can be reduced to generate the required pressure ratio, or the speed can remain the same in order to generate a higher pressure ratio (Figure 11-9). For gas gathering in a declining field, that results in extending field life. For gas injection, higher pressure means more oil production. These are two cases where the investment for restaging can be quickly recovered. For example, if there is 8% extra power remaining due to speed topping by restaging the compressor, the site can produce 8% extra flow or 8% higher head. For a typical 12000 hp engine driven pipeline compressor, an 8% flow increase is approximately 30 mmscfd of natural gas. The incremental revenue due to restaging correlates to about \$90,000/day based on a gas price of \$3/mmbtu.

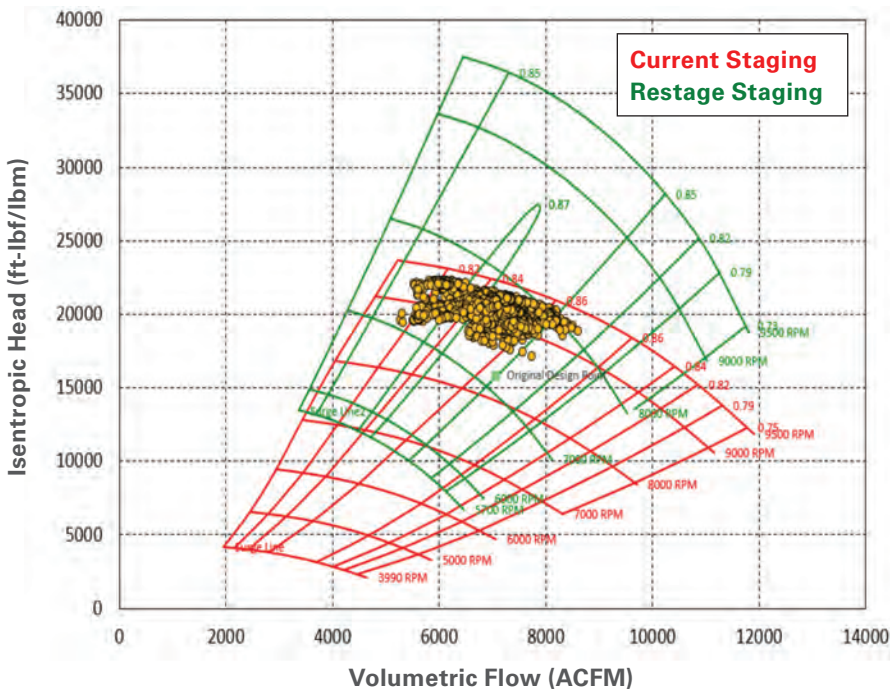


**Figure 11-9. Gas Compressor Restage Principles – Speed Topping**

When the operating point moves in the D direction, the compressor is running at much slower speeds. Normally, the compressor speed is designed to require the power turbine to run over 90% of max speed, in order to reach the highest efficiency levels. The engine efficiency drops as speed declines. When the operating point consistently requires engine speeds lower than optimum levels, removing one or two stages will increase the required compressor speed, thereby improving engine efficiency. This type of restaging reduces engine fuel consumption. By restaging the compressor, fuel savings up to 10% can be

achieved. For a 3.5MW turbine, 10% fuel saving is about \$80,000 a year by assuming a gas price of \$3/mmbtu.

During seasonal, high-flow demands, requiring maximum flow from a compressor is normal. In this scenario, the running point moves in the C direction, where efficiency drops quickly. Although the compressor may not be physically choked, the available power can limit the capacity throughput, and in some instances, a package may not be able to deliver the required flow. In this case, smaller flow stages are typically replaced by larger flow stages. *Figure 11-10* shows how restaging to larger flow stages changes the performance map (Green for restaged compressor performance map) to better match the conditions. Both compressor efficiency and flow capacity are improved. For example, if the restaging can improve the efficiency from 80% to 86% (6% improvement), the flow can be increased by 8%. This restaging is just like the speed topping case above that can increase the revenue by \$90,000 a day for a 12000 hp engine-driven compressor.

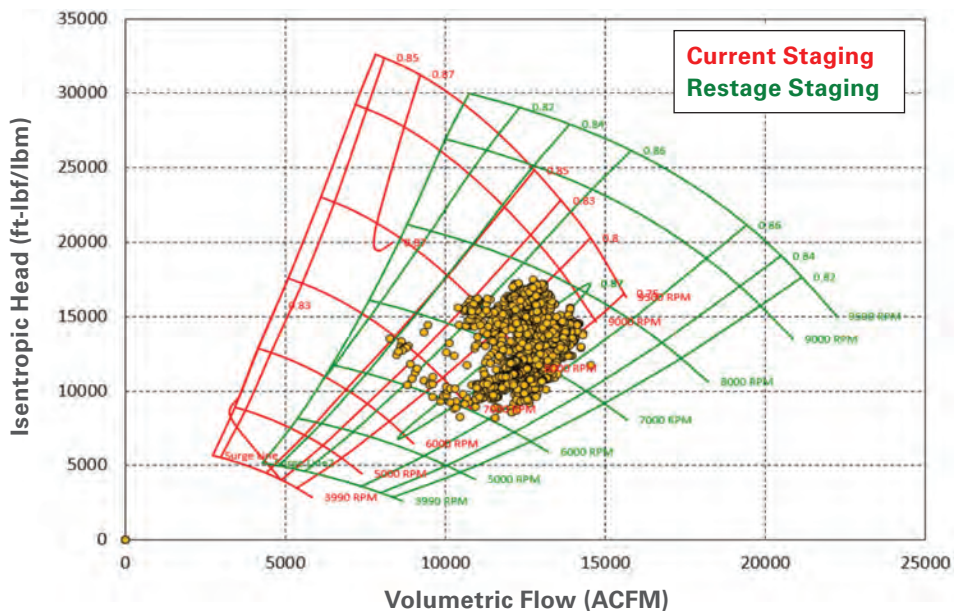


**Figure 11-10. Gas Compressor Restage Principles – Increase Capacity**

Opposite to a choke situation, when there isn't enough gas, the point moves in the R direction. When the compressor cannot produce enough flow, the anti-surge valve opens to avoid surge, and the compressor runs in recycle mode. A portion of compressed gas will be cooled to feed back to the compressor. This is the only way to keep the compressor out of surge. Surge can cause violent vibrations and catastrophic compressor damage. The energy consumed by recycling gas is wasted, and extra energy is needed at site to pump cooling water or drive fans for gas cooling. This is the equivalent of dropping compressor efficiency. Restaging can solve this problem by replacing higher flow stages with smaller stages to accommodate the lower volumetric flows (*Figure 11-11*). For a 3.5MW industrial gas turbine driving a compressor with 20% recycle flow, given a gas price of \$3.00/mmbtu and 300 days of annual operation, the potential savings can be up to \$130,000 per year. If this application involves oil production, the 20% power savings can be used to

increase head about 20%. The resulting oil-production increase could pay back the restage investment within months or even weeks.

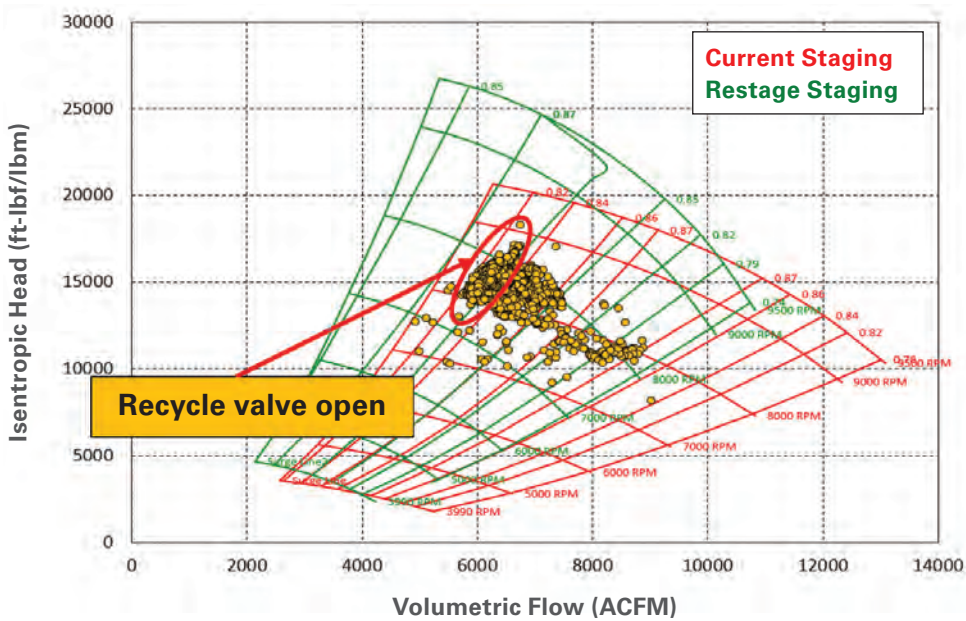


**Figure 11-11. Gas Compressor Restage Principles – Eliminate Recycle**

Besides economic reasons, running in recycle mode could cause high discharge temperatures, if insufficient cooling is supplied in deep recycle mode. Dry gas seals, balance piston babbitt and anti-surge valves can be damaged in periods of extended recycling.

In summary, the primary restaging benefits are: increased oil/gas production, lower fuel consumption and better equipment health.

### **Restage Criteria**

A restage is generally recommended at the time of the next overhaul, if the investment can be recovered within five years. If the restage investment can be recovered in less than one year, restage should be considered immediately.

The economic analysis of the payback period requires interaction between the user and the OEMs. A study based on 379 recently sold compressor restages by Solar Turbines is described below. Four parameters stood out as good indicators of beneficial restaging:

1. Inlet flow coefficient ( $\phi$ )
2. Isentropic head coefficient ( $\Psi$ ),
3. Inlet pressure ( $P_1$ )
4. Required power

The changes between the conditions before restaging and the original design were calculated. The detailed criteria for each parameter are shown in *Table 11-1* below. The <25%, 25%-50% and >50% ranges identify the percentages of the 379 compressors restaged. For example, less than 25% of compressors were restaged when Suction Pressure changed by less than 5%, but more than 50% of the compressors were restaged when suction pressure changed by 15% or more. These variation change regions thus established the “trigger points” for restage recommendations. Roughly speaking, for power, suction pressure, and head coefficient, the trigger point for restage consideration (Yellow Warning) for next overhaul is when the parameter drifted 5% to 15%. If they drifted more than 15%, that is the trigger (Red Warning) for immediate restage consideration. The flow coefficient trigger points are 25% for next overhaul and 50% for immediate consideration. If any Red Warning is triggered, the compressor should be restaged. If all four Yellow Warnings are triggered, the compressor should also be restaged.

The other general rule indicates that a compressor restage is recommended when efficiency is less than 6% of peak efficiency and power is a limiting factor. Regaining this 6% efficiency with a restage typically results in 8% or more flow gain.

Percent Change	<25%	25% - 50%	>50%
$\Phi_1$	>15%	15% - 31%	>31%
$\Psi_1$	>5%	5% - 19%	>19%
$P_1$	>5%	5% - 15%	>15%
HP	>3%	3% - 13%	>13%

**Table 11-1.** Trigger points for restage parameters.

$$\Phi_1 = \frac{Q_1}{(D_2)^3 N} \quad \text{is the inlet flow coefficient for compressors using the first inlet flow coefficient.}$$

$$\Psi_{isen} = \frac{H_{isen}}{(D_2 N)^2} \quad \text{is the isentropic head coefficient for a single body compressor.}$$

$$\Psi_{isen} = Cp \frac{T1}{(D_2 N)^2} \left[ \left( \frac{P_2}{P_1} \right)^{\frac{k-1}{k}} - 1 \right] \quad \text{for compressors using the total pressure ratio and the first compressor speed and impeller tip diameter.}$$

## CASE STUDY 11-1: EXTRA CAPACITY FOR A PIPELINE APPLICATION

This package was originally sold in 1998 for a U.S. pipeline application. The original design points are listed in the first column of *Table 11-2* below and are marked as Point 1 on the compressor maps in *Figure 11-12*. The customer wanted to relocate this package from its existing site due to increased demand. The new site conditions had lower suction and discharge pressure requirements (2.7 and 17.12% respectively), but the flow demand at the new site was 67.85% higher than current design conditions.

Column 2 shows the max flow capability of the current staging for the new site conditions at max power. The current staging could only provide 959.16 MMSCFD of flow at max power, 31.47% less than the requirement. All four key parameters were in the red zone, indicating a restage would be required to perform at the new duty point. The last column shows the delta between the Original Design Point and New Design Requirement for Original Staging. Besides all four key parameters being in the red and current staging not being able to achieve the required flow duty, the efficiency with max power and original staging would have been 46.91% lower than the original.

	Original Staging		Restaged	Delta Max Power to Design for Original Staging
	Design Point	Max Power		
Point on Map	1	2	3	
Phi	0.045	0.081	0.114	44.88%
Psi	2.043	0.747	0.644	-173.53%
P1 (PSIA)	885.00	861.77	861.77	-2.70%
HP Total (HP)	6225.00	11025.00	11080.00	43.54%
Efficiency (%)	85.50	58.20	84.50	-46.91%
P2 (PSIA)	1185.00	1011.77	1011.77	-17.12%
SQ (MMSCFD)	450.03	959.16	1399.57	53.08%
Flow (ACFM)	4490.41	10298.01	15026.39	56.40%
P2/P1	1.34	1.17	1.17	-14.05%

**Table 11-2.** Changes in operating parameters.

In 2013, the compressor was restaged to higher flow staging and the number of stages was reduced from 2 to 1 to increase speed, efficiency and flow capabilities. The new staging was 26.3% more efficient than the original staging at max power and provided a flow increase from 959.16 MMSCFD to 1399.57 MMSCFD at max power conditions. *Figure 11-12* shows the new performance map in green and the old performance map in red along with all three points from *Table 11-2*. As shown, the restage enabled the relocated compressor to have increased flow throughput, while maintaining operation in peak efficiency zones.

This is a typical pipeline application restage where increased flow demand along with maximum power consumption and efficiency gain, a compressor restage can be paid back in weeks, if not days, if the customer owns even a percentage of the gas.

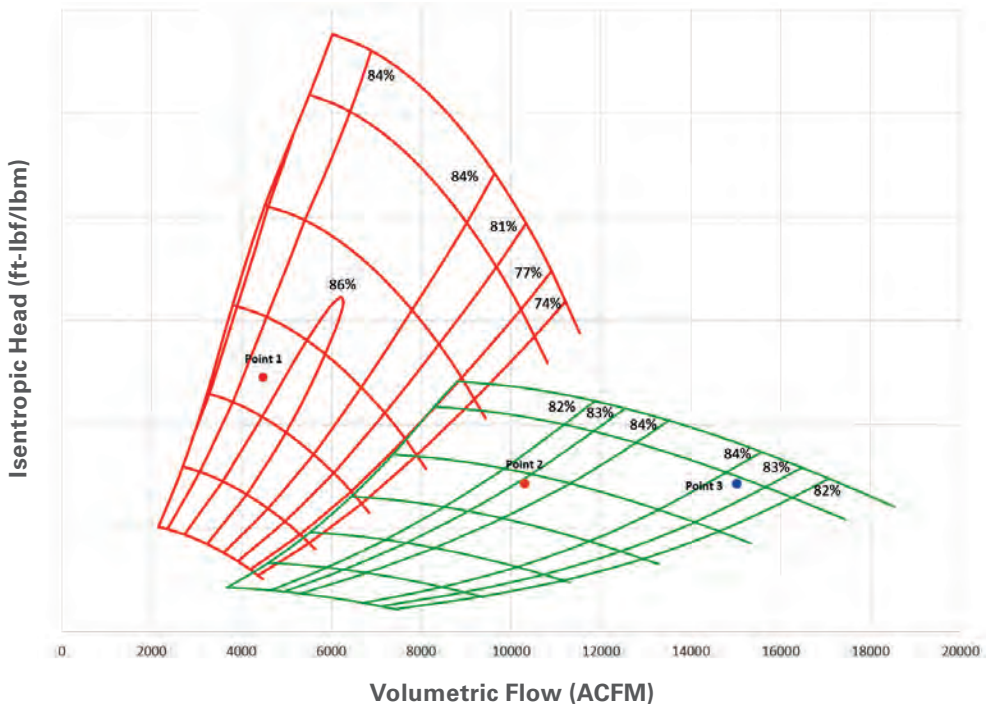


**Figure 11-12.** Existing and Restage Staging Performance Map for Case Study 11-1.

**CASE STUDY 11-2. PACKAGE RELOCATION TO INCREASE STATION CAPACITY AND DISCHARGE PRESSURE.**

In today’s evolving marketplace, the need for additional gas compression has increased. Although the purchase of new turbomachinery equipment is preferred in some instances, the reallocation of unused or standby turbomachinery packages provides opportunities to reduce capital investment, delivery schedules and sourcing activity. From an inventory management perspective, package relocation increases unit asset value, drives down operational costs and helps maintain optimum inventory levels. It also facilitates performance improvements and increased operational flexibility for either current or future conditions. In both gas gathering and transmission applications, reallocation of existing turbomachinery packages can be a very convenient and economical method to meet new site conditions, particularly increasing station discharge pressure and gas throughput. Similar to the sourcing of new equipment, close collaboration with the OEM is pivotal in ensuring that the relocated package is properly sized, upgraded accordingly, and most importantly, makes sound financial sense. This case study illustrates the significant benefits of package relocation.

In gas-gathering applications, multiple sources of gas volumes that change over time are typically involved. The addition of new wells or gas streams may sometimes be prohibited, if the available power at site is not sufficient. This particular station was designed with three stages of compression, with two primary sources of gas (Figure 11-13). Original design conditions can be seen in Table 11-3. New process conditions at site required an additional 19 MMSCFD of side stream gas flow, and an increase in station discharge

pressure to 730 PSIA. Although the existing gas compression equipment had a very wide range of operating efficiency, the combination of increased gas flow and discharge pressure was not achievable, primarily due to the available power at site. The maximum achievable flows and pressure with the existing packages can also be seen in *Table 11-3*.

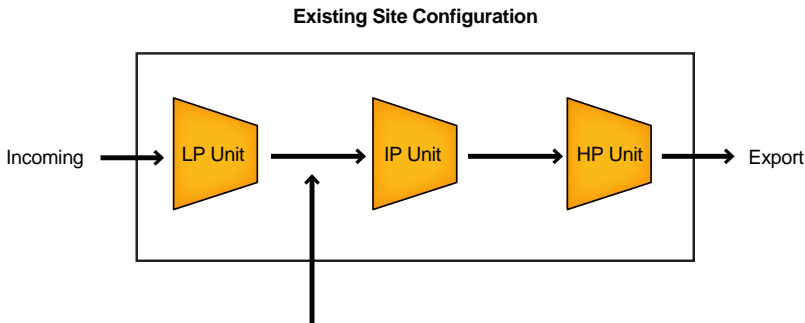


**Figure 11-13.** Existing site configuration.

			Existing Equipment	
	Design	Site Goal	Max P2	Max Flow
<b>P1</b>	36.6 PSIA	45 PSIA	45 PSIA	45 PSIA
<b>P2</b>	606.6 PSIA	730 PSIA	730 PSIA	490 PSIA
<b>SQ</b>	61 MMSCFD	80 MMSCFD	50 MMSCFD	67 MMSCFD

**Table 11-3.** Original design conditions and existing station maximum capacity.

Close coordination with the aftermarket applications team identified an existing package that could be reallocated as the 4<sup>th</sup> compression stage to increase both discharge pressure and gas flow at site, as shown in *Figure 11-14*. The addition of a 4<sup>th</sup> compression stage decreased the head requirements across the existing units, which facilitated increased gas throughput with the same available horsepower. The 4<sup>th</sup> stage would serve as a booster to meet the required station discharge pressure.

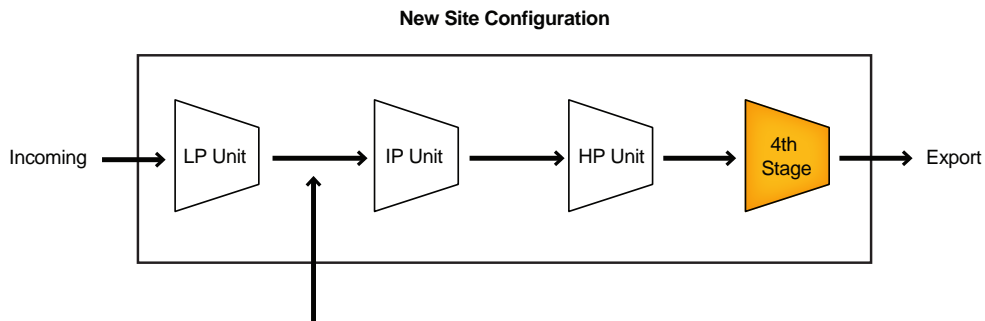


**Figure 11-14.** New site configuration.

	Goal	With 4 <sup>th</sup> Stage
<b>P1</b>	45 PSIA	45 PSIA
<b>P2</b>	730 PSIA	730 PSIA
<b>SQ</b>	80 MMSCFD	71 MMSCFD

**Table 11-4.** New station maximum capacity.

The gas compressor in the 4<sup>th</sup> stage package was originally designed for very different process conditions as shown in *Table 11-5*. The new site conditions required a much higher suction pressure, which decreased the inlet flow coefficient by 58.4%. Analysis of the existing staging showed that the 4<sup>th</sup> stage package would need to recycle 81% of the flow to maintain positive surge margin. The new design point plotted on the original performance curve can be seen far to the left of the surge line. The amount of recycling needed would increase fuel consumption and site emissions. At higher ambient temperatures, the required amount of recycling through the 4<sup>th</sup> stage package would not be possible due to limited power.

Parameter	Original	New
<b>P1 (PSIA)</b>	267	400
<b>P2 (PSIA)</b>	432	731.6
<b>Power (HP)</b>	3348	2454
<b>SQ (MMSCFD)</b>	67.86	71
<b>Inlet Flow (ACFM)</b>	4212	1680
<b>Head (FT-LBF/LBM)</b>	20204	22838

Parameter	% Change
P1	49.8%
Power	41.7%
1	58.4%
1	23.2%

**Table 11-5.** Stage package conditions.

A gas compressor restage of the 4<sup>th</sup> stage package optimized utilization of the new site conditions as can be seen in the green performance curve below in *Figure 11-15*. The selected staging increased package performance at the new conditions, and also provided enough turndown and speed margin to increase gas volumes beyond 71 MMSCFD. Additional upgrades to the IP and HP compressors enabled the customer to reach the 80 MMSCFD target. Keeping in mind the large increase in gas flow and discharge pressure at site, the limited number of package upgrades needed to meet the new conditions was very minimal. The reallocation significantly reduced the capital investment required to meet the new conditions and significantly improved the project timeline.

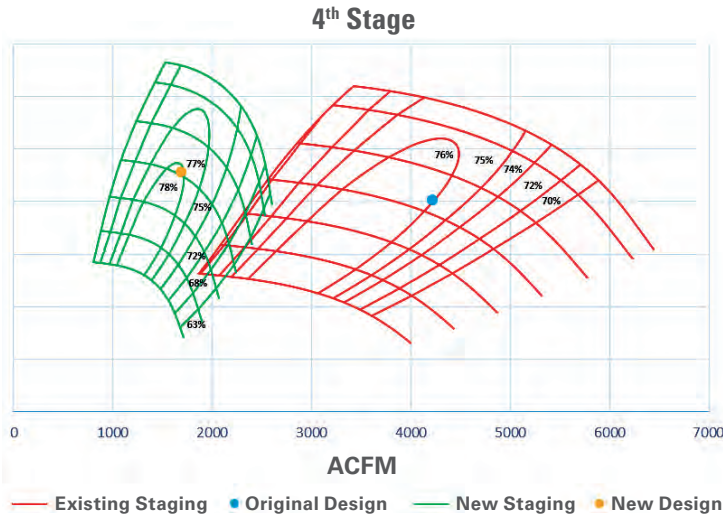


Figure 11-15. 4<sup>th</sup> stage package original vs new staging.

### CASE STUDY 11-3. LIFE CYCLE MANAGEMENT FOR DECLINING FIELD

This is another typical field-depletion case. The Indonesian offshore compressor was commissioned in 1996. After initial commissioning, the field pressure continued to decrease as shown in Table 11-6. The compressor was restaged twice, adapting to changing conditions in 2002 and 2006. Each time, the restage criteria applied well to customer requirements.

After several successful years of operation following the 2006 restage, the pressure and standard flow decreased rapidly, and the compressor could not perform with the low pressure of the well. As a result, the Anti-Surge Valve opened to increase suction pressure. To improve the conditions for the compressor, some high-pressure-side stream gas was injected to increase the suction pressure to 124.7 psi. Yet by the start of 2013, the compressor was running with the ASV approximately 80% open, resulting in 17.9 MMSCFD out of 25.9 MMSCFD throughput being recycled. The net though flow was 8 MMSCFD, or only 31% of the total flow.

Staging	1996	2002	2006	2006	2012	2002	2006	2012
Before or after restage	Design	After	After	Before	After			
Φ	0.0319	0.0488	0.0521	0.0532	0.0211	53.0%	6.8%	-60.3%
Ψ	6.93	5.8064	6.0450	4.729	7.768	-16.2%	4.1%	64.3%
P1 (psia)	350.0	285.0	84.7	124.7	124.7	-18.6%	-70.3%	0.0%
HP total (hp)	3471.5	3651.0	1836.8	2079.2	616.2	5.2%	-49.7%	-70.4%
Efficiency (%)	70.7	75.5	67.3	60.1	64.1			
P2 (psia)	1115	800	304.7	323.7	323.7	-28.3%	-61.9%	0.0%
SQ (mmscfd)	40.0	49.9	17.0	25.9	8.0	24.8%	-65.9%	-69.1%
Flow (acfm)	1218.3	1912.8	2252.4	2144.8	663.7	57.0%	17.8%	-69.1%
P2/P1	3.19	2.81	3.60	2.60	2.60	-11.9%	28.1%	0.0%

Table 11-6. Well condition variation for Case 11-3.

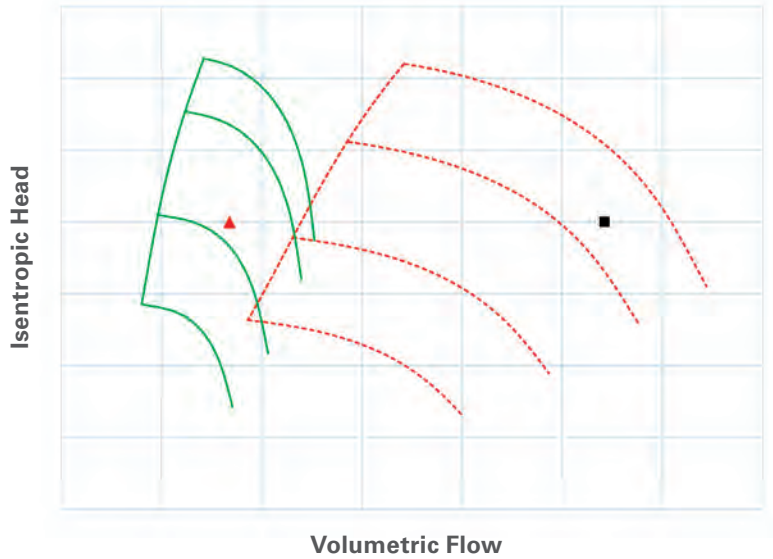


**Figure 11-17.** Restage map for Case 11-3.

The compressor was restaged in 2013 with the performance map at the new condition shown in *Figure 11-17*. The restage saved about 12.9 MMBTU/HR fuel by eliminating recycling. With the price of natural gas significantly higher in this region of the world, the payback period including fuel cost savings was nine months.

## CHAPTER 11 REFERENCES

[1] API, 2002, "Axial and Centrifugal Compressors and Expander-compressors for Petroleum, Chemical and Gas Industry Services", STD 617 7<sup>th</sup> Edition, American Petroleum Institute.

[2] Moore, J. J., Lerche, A. H., 2009, "Rotordynamic Comparison of Built-up Versus Solid Rotor Construction", GT2009-59392, Proceedings of ASME Turbo Expo 2009: Power of Land, Sea and Air, Orlando, Florida.

## REFERENCES

- ANSI/NACE MR0175, 2003, "Petroleum and Natural Gas Industries - Materials for Use in H<sub>2</sub>S-Containing Environments in Oil and Gas Production - Parts 1, 2 & 3"
- Beinecke, D., Luedtke, K., 1983, "Die Auslegung von Turboverdichtern unter Beruecksichtigung des Realen Gasverhaltens," VDI Berichte 487
- Bourn, G., Kurz, R., Clay, M., Zamotorin, R., 2018 Gas Machinery Conference, "Centrifugal Compressors in Gas Gathering"
- Brun, K., Kurz, R. (Ed.), 2018, "Compression Machinery for Oil and Gas," Elsevier, Cambridge, MA
- Brun, K., Kurz, R., Winkelmann, B., 2016, "Gas Turbine Packages and Features," 45<sup>th</sup> Turbomachinery Symposium, Houston, TX
- Giuliano, F.A., 1989, "Introduction to Oil and Gas Technology," 3rd Edition, Prentice Hall
- ISO 20765-1, 2005, "Natural Gas - Calculations of Thermodynamic Properties - Part 1"
- Kohler, Bruentrup, Key and Edvardsson, January 2014, "Hydrocarbon Processing"
- Kumar, S., Kurz, R., O'Connell, J.P., 1999, "Equations of State for Compressor Design and Testing," ASME 99-GT-12
- Kurz, R., 2004, "The Physics of Centrifugal Compressor Performance," PSIG-0408
- Kurz, R., Brun, K., 2017, "Process Control for Compression Systems," ASME 17-GT-63005
- Kurz, R., Brun, K., 2012, "Upstream and Midstream Compressor Applications - Part 1," ASME 12-GT-68005
- Kurz, R., Brun, K., 2012, "Upstream and Midstream Compressor Applications - Part 2," ASME 12-GT-68006
- Kurz, R., Brun, K., 2009, "Assessment of Compressors in Gas Storage Applications," ASME 09-GT-59258
- Kurz, R., Fozi, A.A., 2002, "Acceptance Criteria for Gas Compression Systems," ASME 02-GT-30282
- Kurz, R., Gunn, B., Brun, K., "Oil and Gas Applications for Centrifugal Compressors," ATPS 2021 [1]
- Kurz, R., Ohanian, S., Brun, K., 2010, "Compressors in High Pressure Pipeline Applications," ASME 10-GT-22018
- Kurz, R., Ohanian, S., 2003, "Modeling Turbomachinery in Pipeline Simulations," Pipeline Simulation Interest Group
- Kurz, R., Singh, A., Zamotorin, R., Lubomirsky, M., 2019, "Optimizing Compressor Stations," GMC 2019

Kurz, R., White, R.C., 2004, "Surge Avoidance in Gas Compression Systems," ASME 04-GT-53066

Kurz, R., Winkelmann, B., 2019, "Performance of Industrial Gas Turbines - Tutorial," 48<sup>th</sup> Turbomachinery Symposium, Houston, TX

Nakajama, Y., 1988, "Visualized Flow," Pergamon

Norstebo, V.S., Bakken, L.E., Dahl, H.J., 2007, "Optimum Operation of Export Compressors," ASME 07-GT-27367

Ohanian, S., Kurz, R., 2003, "Transient Simulation of the Effects of Compressor Outage," Pipeline Simulation Interest Group

Ploecker, U., Knapp, H., Prausnitz, J.M., 1978, "Calculation of High Pressure Vapor-Liquid Equilibria from a Corresponding-States Correlation with Emphasis on Asymmetric Mixtures," Ind. Eng. Chem. Process Des. Dev., Vol. 17, pp. 324-331

Poling, B.E., Prausnitz, J.M., O'Connell, J.P., 2001, "The Properties of Gases and Liquids," McGraw-Hill

Ransom, D., Podesta, L., Camatti, M., Wilcox, M., Bertoneri, M., Bigi, M., 2011, "Mechanical Performance of a Two Stage Centrifugal Compressor Under Wet Gas Conditions," 40<sup>th</sup> Turbomachinery Symposium, Houston, TX

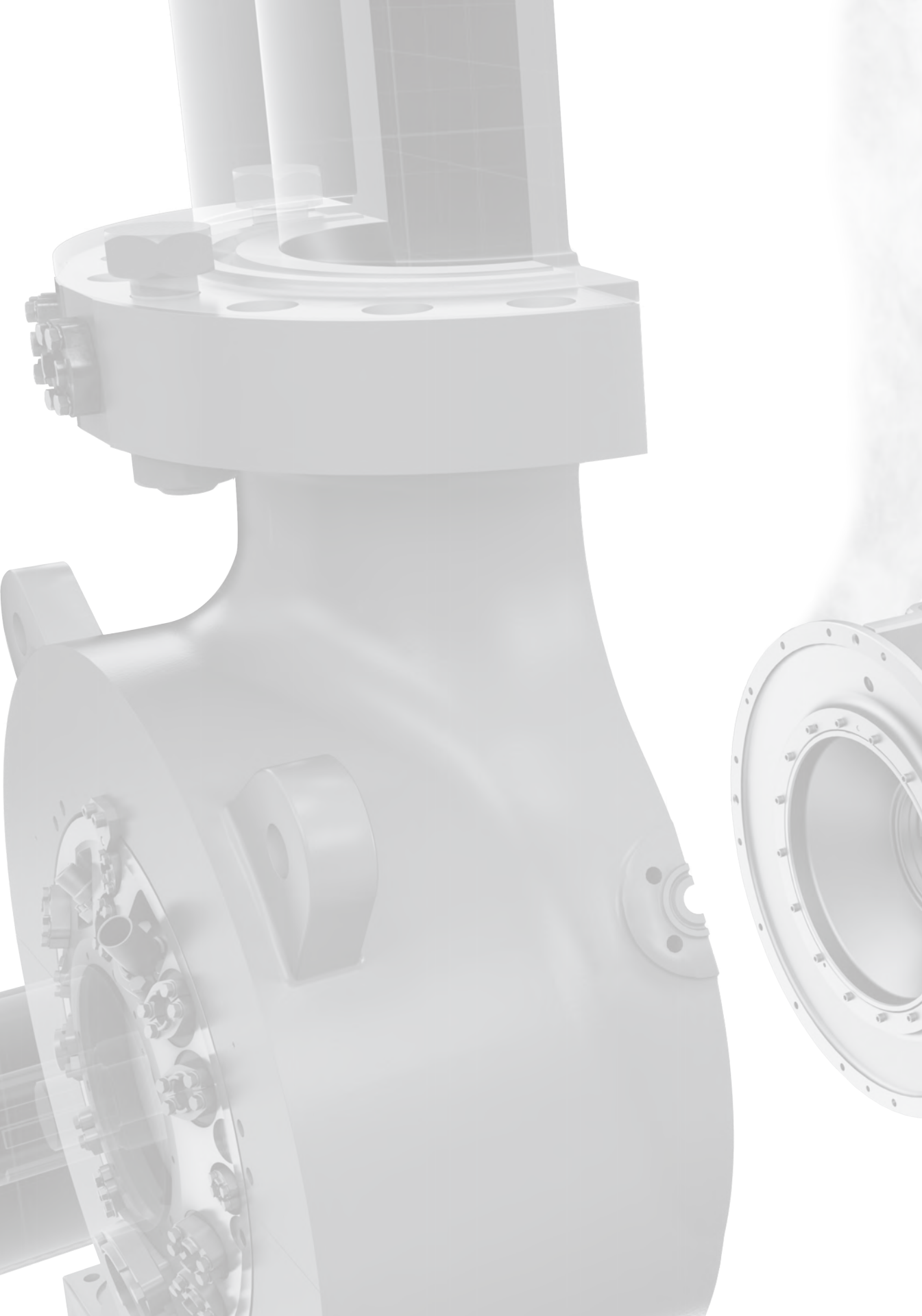
Rasmussen, P.C., Kurz, R., 2009, "Centrifugal Compressor Applications," 38<sup>th</sup> Turbomachinery Symposium, Houston, TX

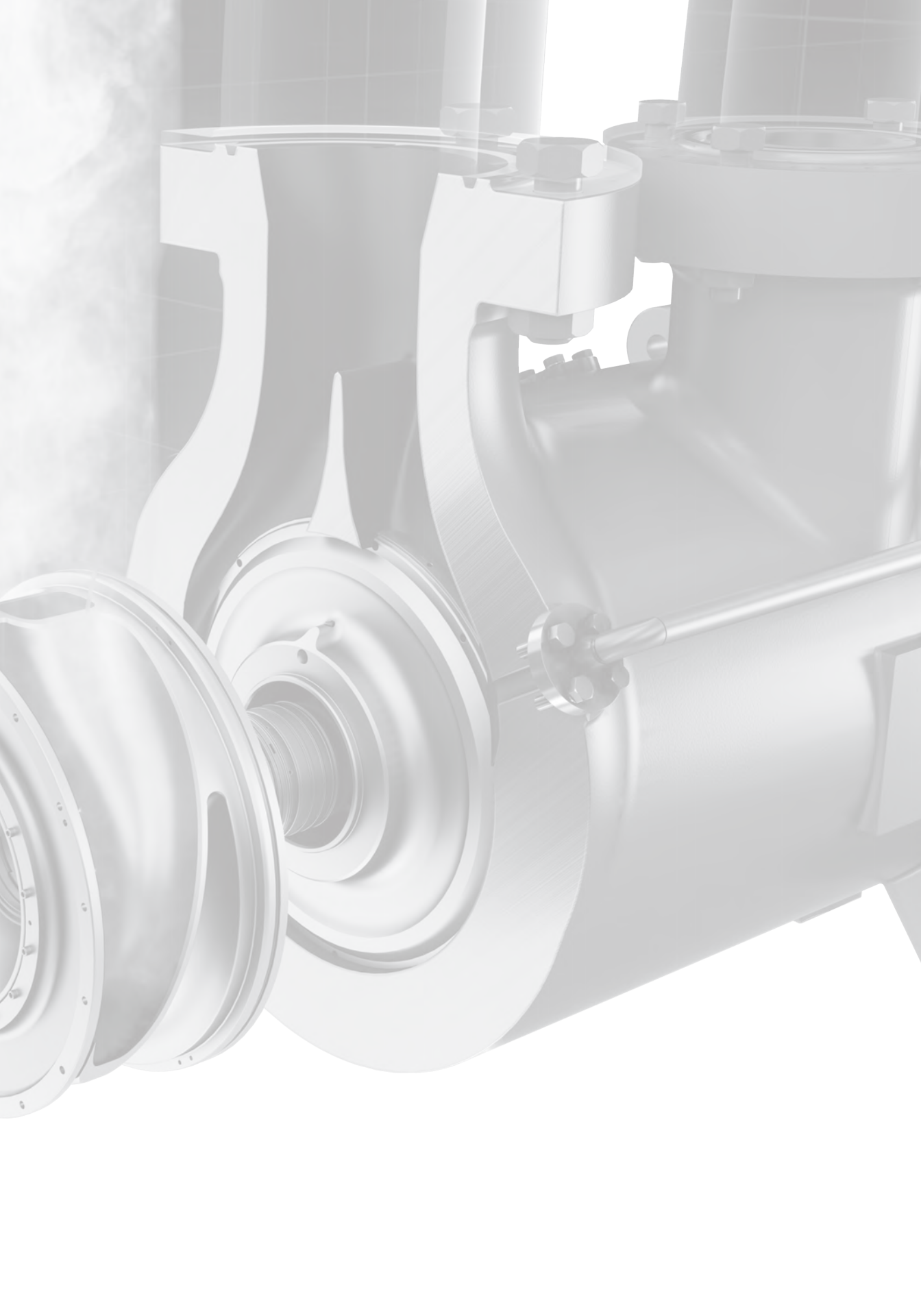
Reid, R.C., Prausnitz, J.M., Poling, B.E., 1986, "The Properties of Gases and Liquids," 4<sup>th</sup> Edition, McGraw-Hill

Starling, K.E., 1973, "Fluid Thermodynamic Properties for Light Petroleum Systems," Gulf Publishing

Venkataraman, B., Kurz, R., Gonzalez, F., Favela, B., Rajagopalan, V., Hodgson, L., 2019, "Dynamics of Modular Rotors in High-Speed Centrifugal Compressors," 48<sup>th</sup> Turbomachinery Symposium, Houston, TX







**Solar<sup>®</sup> Turbines**

*A Caterpillar Company*